Politechnika Wrocławska

DZIEDZINA: Nauki Inżynieryjno-Techniczne

DYSCYPLINA: Inżynieria Chemiczna

ROZPRAWA DOKTORSKA

Pozyskiwanie i wykorzystanie biosurfaktantów z olejów odpadowych pochodzących z przemysłu spożywczego w mikrobiologicznych ogniwach paliwowych

Mgr inż. Aleksander de Rosset

Promotor: dr hab. inż. Grzegorz Pasternak, prof. PWr

Słowa kluczowe: Mikrobiologiczne ogniwa paliwowe, Odpadowe oleje roślinne, Biosurfaktanty, Synteza bioelektrochemiczna, Waloryzacja odpadów, Optymalizacja.

WROCŁAW 2024

NARODOWE CENTRUM NAUKI

NAWA
NARODOWA AGENCJA
WYMIANY AKADEMICKIEJ

Niniejsza rozprawa doktorska została zrealizowana w ramach grantu „Polskie Powroty 2018” finansowanego przez Narodową Agencję Wymiany Akademickiej (PPN/PPO/2018/1/00038) oraz projektu NCN OPUS „Mechanizmy bioelektrochemicznej transformacji materiałów odpadowych z przemysłu naftowego do biosurfaktantów” finansowanego przez Narodowe Centrum Nauki (2019/33/B/NZ9/02774).

Spis treści

Streszczenie

Mikrobiologiczne ogniwa paliwowe (MFC) to układy bioelektrochemiczne umożliwiające konwersję materii organicznej w energię elektryczną poprzez aktywność katalityczną bakterii anodowych. Mikroorganizmy tworzące biofilm anodowy mogą jednocześnie konwertować substraty organiczne do użytecznych produktów. Ciekawą grupą syntezowanych biochemicznie związków o unikalnych właściwościach i szerokim zastosowaniu są biosurfaktanty. Jednak pomimo dużego znaczenia biosurfaktantów dla przemysłu oraz ich wpływie na zwiększanie wydajności MFC opublikowano niewiele prac, w których biosurfaktanty były celem syntezy w układach bioelektrochemicznych, a uzyskane wyniki wskazują na niewielką wydajność układu.

Głównym celem badań przedstawionych w rozprawie doktorskiej było zbadanie możliwości produkcji biosurfaktantów w MFC z odpadowego oleju roślinnego podczas produkcji energii elektrycznej i ocena możliwości wykorzystania biosurfaktantów do zwiększenia wydajności MFC. Rozwiązanie problemu niskich wydajności oraz systematyczne podejście do optymalizacji produkcji biosurfaktantów w MFC ze zużytych olejów roślinnych stanowi pierwszy krok w kierunku zwiększenia skali tego procesu w przyszłości.

Pierwsza praca dotyczy porównania dwóch różnych komercyjnie dostępnych węgli aktywnych, a także modyfikacji węgla nanocząstkami krzemionki pod kątem poprawy wydajności katod powietrznych w MFC. Prawie roczna eksploatacja materiałów różniących się powierzchnią i strukturą mikroporowatą ujawniła istotne różnice w zmianie ich wydajności w czasie trwania eksperymentu. Wyniki pokazały, że rozkład wielkości porów i wynikająca z niego podatność na zanieczyszczenia chemiczne jest kluczowym czynnikiem decydującym o utrzymaniu wysokiej wydajności układu MFC. Dowiedziono, że niemodyfikowany, tani i dostępny na rynku węgiel aktywny może być wysokowydajnym materiałem katody powietrznej, jednak jego aktywność i właściwości długoterminowe zależą od charakterystyki jego porowatości.

W kolejnym artykule zaproponowano poziomą konstrukcję MFC umożliwiającą syntezę biosurfaktantów z odpadowego oleju posmażalniczego. Porównano wydajność biosyntezy surfaktantów i produkcji prądu w MFC w układzie poziomym oraz klasycznym pionowym. Wyniki pokazały, że horyzontalny układ MFC spowodował znaczny wzrost wytwarzanej gęstości mocy oraz syntezy biosurfaktantów. Ponadto wykazano po raz pierwszy, że synteza biosurfaktantów jest bezpośrednio skorelowana z wytwarzaniem energii elektrycznej w MFC. Tym samym dowiedziono, że odpowiednio zaprojektowany układ MFC może umożliwić produkcję biosurfaktantów o dodatnim bilansie energii elektrycznej oraz monitorowanie biosyntezy środków powierzchniowo czynnych wyłącznie za pomocą sygnału elektrycznego.

W trzeciej pracy eksperymentalnej przeanalizowano wpływ stężenia źródła azotu na produkcję biosurfaktantów i prądu ze zużytego oleju posmażalniczego. Badanie

wykazało, że stężenie źródła azotu w pożywce hodowlanej jest jednym z kluczowych czynników utrzymania wysokiej wydajności degradacji zużytego oleju roślinnego, produkcji energii i jednoczesnej syntezy biosurfaktantów. Ponadto wyniki pokazały silną korelację zmian gęstości mocy i spadku napięcia powierzchniowego w funkcji stężenia azotu w pożywce, co dowodzi, że synteza biosurfaktantów i skuteczność degradacji zużytego oleju w MFC zależy bezpośrednio od stężenia źródła azotu. Jest to pierwsza praca, w której badano optymalizację azotu w celu usprawnienia syntezy biosurfaktantów i wytwarzania energii w układzie bioelektrochemicznym, co przybliża efektywną syntezę biosurfaktantów w tego typu układach do realnego zastosowania.

W ostatnim artykule zbadano membranę z nanowłókien polifluorku winylidenu (PVDF) oraz membranę PVDF modyfikowaną metodą obróbki alkalicznej i obróbki ramnolipidami wykorzystanych jako warstwy wewnętrzne separatora ceramicznego, w celu kontrolowania negatywnych skutków biofoulingu. Charakterystyka elektrochemiczna i powierzchniowa materiałów wykazała, że zastosowanie warstwy PVDF nie dało zadowalających efektów, podczas gdy PVDF modyfikowany ramnolipidami spowodował zwiększoną odporność powłoki na zanieczyszczenia. Tym samym wykazano, że produkty pochodzenia naturalnego takie jak biosurfaktanty, mogą być użyte do modyfikacji membran MFC, a także po raz pierwszy odkryto mechanizmy interakcji biosurfaktantów z membranami.

W toku pracy wykazano, że wydajna biosynteza surfaktantów w MFC ze zużytego oleju roślinnego jest możliwa dzięki zastosowaniu odpowiednio zaprojektowanego układu MFC oraz wydajnych materiałów konstrukcyjnych ogniwa. Dodatkowo zaprezentowane wyniki wykazały bezpośrednią korelację produkcji prądu i biosurfaktantów w poziomym MFC ze zużytego oleju oraz silną zależność tych parametrów od stężenia źródła azotu w pożywce. Uzyskane w pracy wyniki badań są podstawą dla rozwoju układów bioelektrochemicznych wykorzystujących odpadowe oleje roślinne pochodzące z przemysłu spożywczego w przyszłości. Ponadto wydajna synteza biosurfaktantów, wytwarzanie energii elektrycznej i jednoczesne wykorzystanie produktów odpadowych z przemysłu spożywczego idealnie wkomponowują się w cele zrównoważonego rozwoju oraz gospodarki obiegu zamkniętego. Przyszłe badania powinny skupić się na dalszej optymalizacji działania układu i materiałów konstrukcyjnych MFC pod katem produkcji biosurfaktantów i energii elektrycznej oraz na zwiększaniu skali procesu i opracowaniu tanich, szybkich i mniej inwazyjnych dla środowiska procesów separacji i oczyszczania biosurfaktantów.

Abstract

Microbial fuel cells (MFCs) are bioelectrochemical systems that enable the conversion of organic matter to electricity through the catalytic activity of anodic bacteria. Microorganisms that form anode biofilms can simultaneously convert organic substrates into useful products. Biosurfactants are an interesting group of biochemically synthesised compounds with unique properties and wide applications. However, despite the great importance of biosurfactants for the industry and their impact on increasing the efficiency of MFCs, only a few works have been published in which biosurfactants were the target of synthesis in bioelectrochemical systems, and the results obtained indicate low performance of the system.

The main objective of the research presented in the doctoral thesis was to investigate the possibilities of biosurfactants production in microbial fuel cells from waste vegetable oil during electricity production and to assess the possibility of using biosurfactants to increase the efficiency of MFCs. Solving the problem of low performance and a systematic approach to optimising the production of biosurfactants in MFCs from waste vegetable oils is the first step towards scaling up this process in the future.

The first work concerns the comparison of two different commercially available activated carbons, as well as the modification of carbon with silica nanoparticles in terms of improving the efficiency of air cathodes in MFCs. Almost a year of operation of materials with different specific surface areas and microporous structures revealed significant differences in their dynamic behaviour. The results showed that pore size distribution and the resulting susceptibility to chemical contamination is a key factor in maintaining high performance of the MFC system. It has been proven that unmodified, cheap, and commercially available activated carbon can be a high-performance air cathode material, but its activity and long-term properties depend on its porosity characteristics.

The next article proposed a horizontal MFC system enabling the synthesis of biosurfactants from waste cooking oil. The efficiency of biosurfactant production and electricity generation was compared in a horizontal and classical vertical arrangement of the MFC. The results showed that the horizontal MFC arrangement resulted in a significant increase in the power density production and biosurfactants synthesis. Furthermore, it was demonstrated for the first time that the biosurfactants synthesis is directly correlated with electricity generation in the MFC. Thus, it was proven that a properly designed MFC system can enable energy net-positive production of biosurfactants and monitoring of the biosynthesis of surfactants solely using an electrical signal.

The third experimental work analysed the influence of nitrogen source concentration on the production of biosurfactants and electricity from waste cooking oil. The study showed that the concentration of the nitrogen source in the culture medium is one of the

key factors in maintaining the high degradation efficiency of the oil substrate, energy production, and simultaneous synthesis of biosurfactants. Furthermore, the results showed a strong correlation between changes in power density and decrease in surface tension as a function of nitrogen concentration in the medium, which proves that the synthesis of biosurfactants and the degradation efficiency of waste vegetable oil in MFCs depend directly on the concentration of the nitrogen source. This is the first work in which nitrogen optimisation was studied to improve the synthesis of biosurfactants and energy production in a bioelectrochemical system, which brings the effective synthesis of biosurfactants in these types of systems closer to real application.

In the last article, a polyvinylidene fluoride (PVDF) nanofibers membrane and PVDF modified by alkaline treatment and rhamnolipids treatment were investigated as the inner layer of a ceramic membrane to control the negative effects of biofouling. The electrochemical and surface characteristics of the materials showed that the use of the PVDF layer did not give satisfactory results, while the modification of the PVDF with rhamnolipids resulted in increased resistance of the coating to contamination. Therefore, it was demonstrated that natural products such as biosurfactants can be used to modify MFC membranes, as well as, for the first time, the mechanisms of biosurfactant interaction with membranes were discovered.

The results of the performed experiments showed that efficient biosynthesis of surfactants in microbial fuel cells from waste vegetable oil is possible but requires the use of a properly designed MFC system and efficient construction materials of the MFC. Furthermore, the presented results showed a direct correlation of the electricity and biosurfactant production in horizontal MFC from waste oil and a strong dependence of these parameters on the concentration of the nitrogen source in the medium. The research results obtained in this work are the basis for the development of bioelectrochemical systems using waste vegetable oils from the food industry in the future. In addition, efficient synthesis of biosurfactants, generation of electricity, and simultaneous use of waste products from the food industry perfectly fit the goals of sustainable development and circular economy. Future research should focus on further optimisation of the system operation and MFC construction materials to produce biosurfactants and electricity, as well as scaling up the process and developing inexpensive, fast, and less environmentally invasive biosurfactant separation and purification processes.

1. Przegląd literatury

1.1. Mikrobiologiczne ogniwo paliwowe (MFC)

1.1.1. Mechanizm działania

Mikrobiologiczne ogniwa paliwowe to układy bioelektrochemiczne umożliwiające konwersję materii organicznej w energię elektryczną poprzez aktywność katalityczną bakterii anodowych [1]. Zasadę działania MFC przedstawiono szczegółowo na Rys. 1. Elektrony wytwarzane przez bakterie w procesie utleniania substratów organicznych są przekazywane do anody, a następnie przepływają do katody przez obwód zewnętrzny zawierający rezystor lub działający pod obciążeniem. Elektrony docierające do katody łączą się z protonami, które dyfundują przez membranę i tlenem - produktem jest woda. Opisane mechanizmy zewnątrzkomórkowego transferu elektronów na anodę obejmują transfer bezpośredni przez cytochromy związane z błoną komórkową oraz pośredni za pomocą mediatorów elektronowych lub wytwarzanych przez bakterie przewodzących nanowłókien białkowych (tzw. nanowire) [2]. Mediatory chemiczne (egzogenne) takie jak kwasy humusowe [3] i błękit metylenowy [4] mogą być dodawane do anolitu dla poprawy anodowego transferu elektronów. Jednak mikroorganizmy mogą same syntezować mediatory w układzie, aby umożliwić wytwarzanie energii elektrycznej. Jako nośniki elektronów mogą działać metabolity takie jak piocyjanina wytwarzana przez *Pseudomonas aeruginosa* [5] lub flawiny wytwarzane przez *Shewanella oneidensis* [6].

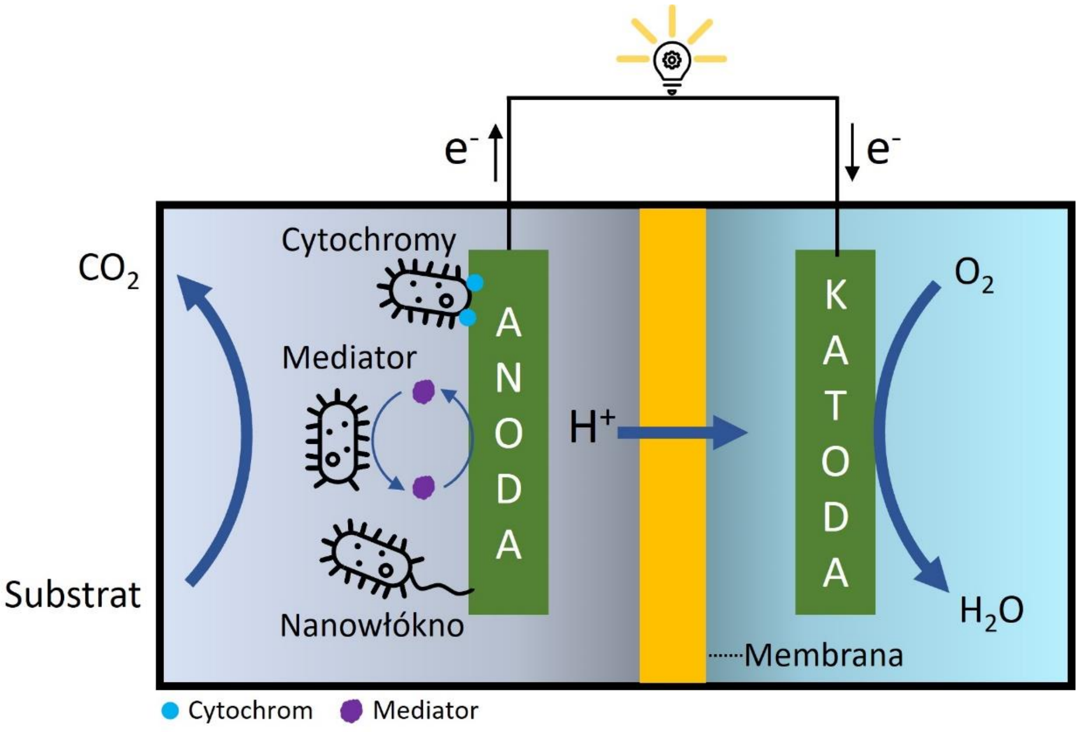

Rys. 1. Uproszczony schemat działania mikrobiologicznego ogniwa paliwowego oraz mechanizmy transportu elektronów.

1.1.2. Typy MFC

Najczęściej w badaniach laboratoryjnych wykorzystywany jest układ dwukomorowy MFC (Rys. 2a.). Składa się on z komory anodowej i katodowej oddzielonych za pomocą membrany. Główną wadą tego typu układu jest konieczność napowietrzania katolitu lub stosowanie dodatkowych utleniaczy chemicznych. Przyczynia się to do generowania dodatkowych kosztów i obniża opłacalność systemu. Kolejnym problemem układów dwukomorowych MFC jest akumulacja protonów w komorze anodowej [7]. Efektem jest niska stabilność operacyjna i wydajność wytwarzania energii elektrycznej. Jednokomorowe MFC posiada komorę anodową oraz oddzieloną membraną katodę pozostająca w bezpośrednim kontakcie z powietrzem (Rys. 2b.). Konfiguracja ta nie wymaga napowietrzania, gdyż tlen jest pasywnie dostarczany w miejsca aktywne katody. Ponadto układy jednokomorowe charakteryzują się niższymi oporami wewnętrznymi i kosztami budowy, dlatego uznawane są za bardziej efektywne finansowo. Jednak dalszy wzrost wytwarzanej mocy wymaga przeskalowania układu MFC na znacznie większe objętości. Niestety wolumetryczna gęstość wytwarzanej mocy w MFC zmniejsza się wraz ze wzrostem objętości. Wykazano, że podejście polegające na miniaturyzacji i multiplikacji jest najbardziej realną drogą do zwiększenia mocy wyjściowej MFC [8]. Dlatego aby zwiększyć skalę technologii MFC stosuje się układy modułowe, w których wiele pojedynczych ogniw tworzy stos. Układy te mogą składać się zarówno z MFC dwukomorowych, jednokomorowych jak i konfiguracji hybrydowych. MFC modułowe umożliwia kontrolowanie napięcia i natężenia prądu poprzez połączenia szeregowe lub równoległe poszczególnych MFC w układzie. W rezultacie odpowiednie ułożenie stosów może spełniać wymagania prądowe dla zasilanych urządzeń elektrycznych. Na przykład zaobserwowano, że połączenie szeregowe 8 miniaturowych MFC zwiększyło napięcie ogniwa 6-krotnie, podczas gdy połączenie równoległe tej samej ilości ogniw skutkowało około 4 razy większym natężeniem prądu [9]. W innym badaniu opracowano układ kaskadowy MFC w celu pełnego naładowania telefonów komórkowych przy użyciu czystego moczu jako paliwa [10].

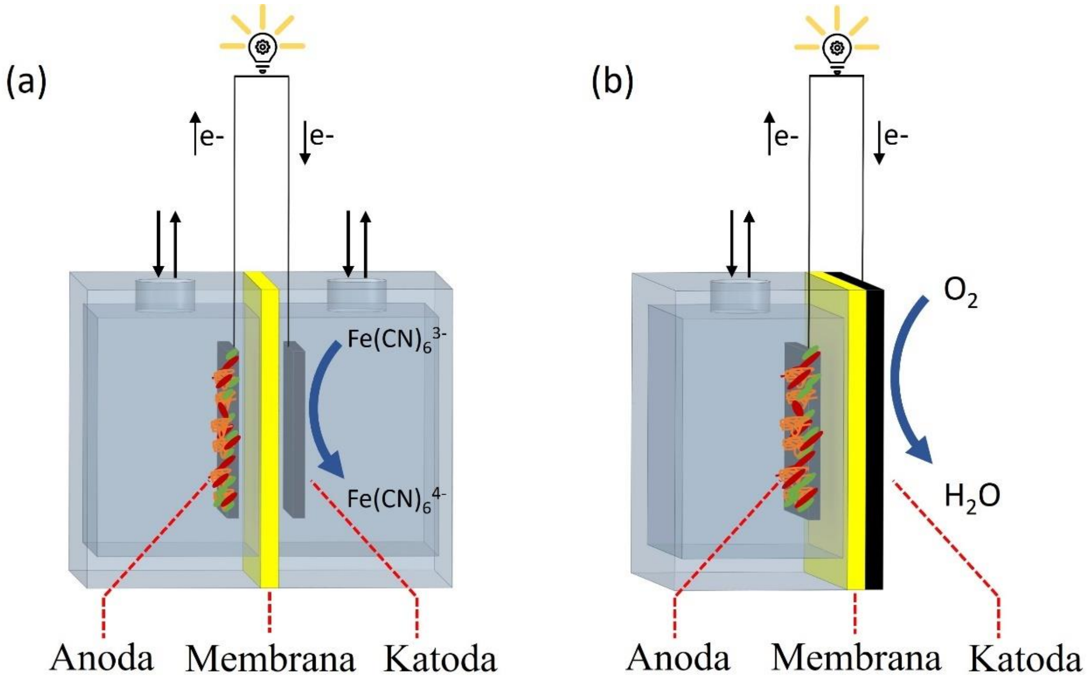

Rys. 2. Mikrobiologiczne ogniwo paliwowe: (a) dwukomorowe i (b) jednokomorowe.

1.1.3. Komponenty i materiały konstrukcyjne

Anoda

Anoda w MFC pełni funkcje zarówno siedliska dla społeczności drobnoustrojów jak i akceptora elektronów. Powinna charakteryzować się dobrą biokompatybilnością, dużą powierzchnią właściwą i wysoką przewodnością elektryczną [11]. Ponadto powinna być stabilna chemicznie i odporna na korozję bioelektrochemiczną. Doboru materiału anody do zastosowania w MFC dokonuje się przede wszystkim w oparciu o powyższe wymagania. Istnieje wiele materiałów stosowanych jako anody w MFC, które możemy sklasyfikować jako metale, polimery i materiały węglowe [12]. Wśród powyższych materiały węglowe są bardzo dobrą alternatywą ze względu na niski koszt, wysoką stabilność chemiczną oraz strukturę sprzyjająca przyłączaniu mikroorganizmów i tworzeniu biofilmu [13]. Ponadto struktura porów i powierzchni materiałów węglowych jest łatwo sterowalna w procesie wytwarzania i modyfikacji. Do powszechnie stosowanych materiałów węglowych jako anody należą tkaniny węglowe, włókniny węglowe czy pręty grafitowe. Jednak dalsze próby zwiększania mocy wyjściowej MFC wymagały zastosowania bardziej nowatorskich materiałów anodowych na bazie węgla. Na przykład zastosowanie biofilmu kompozytowego na bazie nanorurek węglowych i bakterii, dzięki unikalnej strukturze kompozytu pozwoliło na natychmiastowy dostęp bakterii do nanorurek węglowych, a tym samym pominięcie etapu tworzenia biofilmu i szybkie osiągnięcie maksymalnych mocy wyjściowych [14].

Katoda

Materiały katodowe odgrywają znaczącą rolę w pracy MFC, wpływając na parametry elektryczne ogniwa [15]. Materiały katodowe stosowane w MFC powinny być wydajne, stabilne i niedrogie. W trakcie długotrwałej pracy MFC katoda narażona jest na działanie wody, materii organicznej i nieorganicznej pochodzącej z anolitu. Dodatkowo mikroorganizmy tworzące biofilm na anodzie mogą również tworzyć biofilm na katodzie, co może prowadzić do pogorszenia kinetyki reakcji redukcji tlenu (ORR). Ponadto parametry ORR materiałów katodowych są zwykle ograniczone przez wysoką energię aktywacji oraz opory transferu elektronów i transportu masy. Materiały na bazie platyny są często stosowane w celu obniżenia energii aktywacji ORR [16]. Jednak takie rozwiązania znacząco wpływają na podwyższenie kosztów inwestycyjnych, a stosowane materiały wykazują słabą stabilność w obecności zanieczyszczeń. Równie dużym zainteresowaniem cieszą się tlenki manganu, kobaltu czy niklu jako zamienne dla platyny katalizatory ORR. Z drugiej strony metale te mogą przedostawać się do anolitu, co jest toksyczne dla mikroorganizmów [17]. W przeciwieństwie do materiałów na bazie metali, materiały węglowe, takie jak węgiel aktywny, tkaniny i włókniny węglowe oraz grafit są alternatywą bardziej stabilną i niedrogą.

Węgiel aktywny jest szeroko stosowany w MFC jako niedrogi materiał katodowy o wysokiej powierzchni właściwej [15]. Grupy funkcyjne na powierzchni węgla aktywnego, jego powierzchnia właściwa, struktura porów i obfitość miejsc aktywnych mające wpływ na zdolność katalityczną ORR są zależne od metody ich wytwarzania i prekursora [18]. Dodatkowo w celu zwiększenia wydajności ORR węgla aktywnego stosuje się obróbkę chemiczną oraz modyfikacje metalami i niemetalami [19]. Na przykład zastosowanie obróbki węgla aktywnego za pomocą H_3PO_4 spowodowało wzrost maksymalnej gęstości mocy MFC o 115% w porównaniu do MFC wyposażonego w katodę z węgla niemodyfikowanego [20]. W innej pracy wydajność katody powietrznej podniesiono przez domieszkowanie węgla aktywnego politetrafluoroetylenem (PTFE) [21]. W naszej pracy dowiedliśmy, że rozkład wielkości porów w węglu aktywnym ma kluczowe znaczenie dla zanieczyszczenia katodowego i w efekcie decyduje o utrzymaniu wysokiej wydajności długoterminowej układu MFC [22]. W związku z powyższym węgiel aktywny wydaje się odpowiednim materiałem do komercyjnego zastosowania w MFC, ze względu na jego dostępność, cenę, właściwości oraz łatwość modyfikacji.

Membrana

Membrana w większości układów MFC odgrywa kluczową rolę w transporcie jonów wodorowych oraz ogranicza przenikanie substratu i tlenu pomiędzy komorą anodową i katodową [23]. Membrana ma szczególnie duże znaczenie dla wydajności układów jednokomorowych, w których jednocześnie stanowi materiał konstrukcyjny. Właściwości membrany wpływają na efektywność usuwania zanieczyszczeń organicznych i wytwarzania energii elektrycznej w MFC. Powszechnie stosowane membrany kationowymienne, takie jak Nafion lub Ultrex znacząco podnoszą całkowity koszt budowy MFC. Co więcej, mogą być szczególnie podatne na zanieczyszczenia chemiczne i biologiczne [24].

Doskonałą alternatywę dla drogich membran jonowymiennych stanowią separatory ceramiczne ze względu na ich unikalne właściwości termiczne, chemiczne i mechaniczne. Mogą one pracować w ekstremalnie kwaśnym i zasadowym środowisku oraz w wysokim ciśnieniu roboczym [25]. Dlatego w badaniach nad zwiększeniem skali MFC zwykle stosuje się separatory ceramiczne [26]. Niestety naturalny skład materiałów ceramicznych często powoduje powstawanie ładunków ujemnych na ich powierzchniach, co zwiększa podatność na adhezję kationów z anolitu i w efekcie sprzyja biofoulingowi [24]. W efekcie wzrasta podatność na zanieczyszczenie chemiczne i biologiczne membrany, co negatywnie wpływa na transfer protonów. Skutki te można ograniczyć poprzez zwiększenie hydrofilowości, zmniejszenie chropowatości membran lub domieszkowanie biocydami [24]. Przykładowo możliwe było zwiększenie gęstości mocy MFC o ponad 60% poprzez domieszkowanie membrany ceramicznej popiołem z łusek ryżowych [27]. Polepszoną wydajność MFC przypisano zwiększonej hydrofilowości na skutek obecności nanocząstek krzemionki w materiale domieszkującym. Podobnie w innej pracy zaobserwowano, że ceramika o wyższym stężeniu krzemionki wykazywała lepszą wydajność produkcji energii elektrycznej [23]. Kolejną strategią poprawy wydajności i stabilności membran ceramicznych w MFC jest zastosowanie powłoki polimerowej o zwiększonej odporności na zanieczyszczenia. Na przykład, wykorzystując recyklingową włókninę polipropylenową jako komponent ceramicznej membrany kompozytowej, udało się zwiększyć moc MFC o 92% oraz znacząco wydłużyć żywotność membrany [28]. W naszej pracy zastosowaliśmy kompozytową membranę ceramiczną z membraną z nanowłókien PVDF modyfikowaną ramnolipidami [29]. W rezultacie uzyskano wzrost maksymalnej gęstości mocy MFC o 38% oraz znaczne polepszenie właściwości długoterminowych membrany.

Projekt MFC

Rozwiązania konstrukcyjne zastosowane przy projektowaniu MFC zależą od celu planowanych badań oraz jego skali. W badaniach MFC zwykle stosuje się reaktory o konstrukcji cylindrycznej lub sześciennej w konfiguracji jednokomorowej lub dwukomorowej wykonane ze szkła, tworzyw sztucznych, a nawet materiałów ceramicznych [1]. Na przykład Pasternak i in. [30] zastosowali materiał ceramiczny zarówno jako separator, jak i obudowę komory anodowej. Jedną ze strategii poprawy wydajności ogniwa jest optymalizacja parametrów projektowych takich jak odstępy między elektrodami, stosunek powierzchni elektrod do objętości i objętości komór [31]. Na przykład wykazano, że wolumetryczna gęstość mocy wzrosła o ponad 100%, kiedy odstęp między elektrodami został zmniejszony z 3 cm do 1 cm w warunkach ciągłego przepływu substratu przez komorę anodową [32]. W innej pracy zaobserwowano pięciokrotny wzrost gęstości mocy, gdy pole powierzchni katody zwiększono z 24 cm^2 do 96 cm^2 [33]. Podobne badanie wykazało wzrost wytwarzanej mocy w MFC o 200%, kiedy zwiększono powierzchnię geometryczną katody o 175% [34]. W naszej pracy zastosowaliśmy nowy poziomy reaktor MFC skonstruowany z komponentów wydrukowanych w technologii 3D dla poprawy biodostępności substratu olejowego [35]. Konfiguracja ta zapewniła odpowiednie warunki dla syntezy biosurfaktantów, co bezpośrednio wpłynęło na rozwój biofilmu i wydajność układu.

1.1.4. Parametry wpływające na efektywność pracy ogniwa

Temperatura

Temperatura pracy MFC ma wpływ na kinetykę reakcji elektrodowych oraz szybkość transportu masy i transferu protonów [36]. MFC zwykle testowane są w temperaturze pokojowej, choć dostępnych jest wiele prac, w których badano zmiany wydajności ogniw w znacznie niższych i wyższych temperaturach. Jak wiadomo osiągnięcie optymalnej i stabilnej wydajności MFC w niskich temperaturach zwykle będzie wymagało dłuższego czasu rozruchu. Dlatego najczęstszym rozwiązaniem umożliwiającym szybkie uzyskanie powtarzalnych cykli wytwarzania energii oraz wyższych maksymalnych mocy jest podniesienie temperatury pracy MFC [37]. Na przykład podniesienie temperatury z 20℃ do 35℃ spowodowało wzrost maksymalnej szybkości usuwania chemicznego zapotrzebowania na tlen (ChZT) o 50% oraz znacznie zwiększyło wytwarzaną moc w MFC [38]. W innym badaniu zmiana temperatury pracy jednokomorowych MFC z 20℃ na 35℃ spowodowała znaczne skrócenie czasu aklimatyzacji wymaganego do osiągnięcia napięcia w stanie ustalonym oraz o ponad 300% zwiększyła stopień usuwania ChZT [39]. Jednakże, jednocześnie stwierdzono wyższą wydajność kulombowską w MFC pracujących w 20℃. Ponadto w wyższej temperaturze (35℃) odnotowano zwiększony poziom aktywności reakcji współtowarzyszących, takich jak metanogeneza, które obniżają sprawność odzyskiwania elektronów w układzie oraz zaobserwowano słabą stabilność produkowanej mocy w zmiennych warunkach temperaturowych dla MFC aklimatyzowanych w temperaturze 35℃. Podnoszenie temperatury pracy MFC może więc być dobrym sposobem na skrócenie czasu aklimatyzacji mikroorganizmów oraz osiągnięcie wyższego stopnia usuwania ChZT. Z drugiej strony konsekwencją dojrzewania biofilmu w wyższej temperaturze może być większa wrażliwość na zmiany temperatury oraz dominacja reakcji współtowarzyszących. Dodatkowo podnoszenie temperatury pracy MFC może znacząco podwyższać koszty operacyjne.

Przewodność roztworu

Optymalne pH dla rozwoju bakterii anodowych w MFC jest najczęściej zbliżone do neutralnego [40]. Dlatego aby ułatwić transport protonów w anolicie i w efekcie obniżyć rezystancję wewnętrzną ogniwa wymagane jest zwiększenie przewodności anolitu w MFC bez zmiany pH roztworu poprzez zwiększenie siły jonowej. Wykazano, że dodanie 20 g L^{-1} NaCl do anolitu MFC zmniejszyło opór wewnętrzny o 33% [41]. Dalsze zwiększanie stężenia NaCl okazało się szkodliwe dla mikroorganizmów. Jednak najwyższą wydajność kulombowską zaobserwowano dla znacznie niższego stężenia wynoszącego 5 g L^{-1} NaCl, co sugeruje, że już niewielki wzrost zasolenia miał wpływ na działanie biofilmu anodowego.

Rezystancja zewnętrzna

Kolejnym parametrem silnie wpływającym na rozwój elektroaktywnego biofilmu na anodzie jest wartość rezystancji zewnętrznej przykładanej do obwodu elektrycznego [42]. Wykazano, że dojrzewanie biofilmu przy niższym oporze zewnętrznym skutkuje wyższą wydajnością produkcji energii elektrycznej i niższym oporem wewnętrznym MFC [30]. Ponadto zaobserwowano, że wpływ rezystancji zewnętrznej na dojrzewanie biofilmu i wydajność całego układu był nieodwracalny. Udowodniono więc, że początkowe warunki rozwoju biofilmu mają krytyczny wpływ na strukturę i skład biofilmu i tym samym długoterminową wydajność MFC. Podobnie w innej pracy odnotowano prawie dwukrotny wzrost wytwarzanej gęstości mocy gdy rezystancja zewnętrzna MFC została obniżona z 50 Ω do 10.5 Ω [43]. Zaobserwowano również zmiany w różnorodności drobnoustrojów i metabolizmie, gdy wobec MFC zastosowano różne oporności zewnętrzne.

Konsorcjum mikrobiologiczne

MFC można inokulować czystymi lub mieszanymi kulturami bakterii. Kultury mieszane są często bardziej korzystne ze względu na niższą wrażliwość na zmiany warunków środowiskowych jakich jak dostępność składników odżywczych, temperatura, pH i stężenie soli oraz wyższą zdolność adaptacji [44]. Dodatkowo zastosowanie złożonego konsorcjum bakteryjnego, takiego jak osad czynny lub gleba jest bardziej korzystne w degradacji złożonych substratów ze względu na obecność różnych rodzajów bakterii zapewniających wysoki stopień rozkładu substancji organicznych oraz dużą gęstość mocy. Osad czynny jest dobrym kandydatem do inokulacji MFC ze względu na dostępność i bardzo zróżnicowany skład bakteryjny bogaty w elektrochemicznie aktywne szczepy bakterii [45]–[47]. Ponadto, wykazano, że inokulacja tlenowym osadem czynnym pozwoliła na szybszy rozruch i lepszą wydajność wytwarzania energii elektrycznej niż osadem beztlenowy, co przypisano bardziej rozwiniętej społeczności drobnoustrojów w osadzie tlenowym. W naszej pracy wzbogacony biofilmu anodowy MFC zainokulowanego za pomocą tlenowego osadu czynnego pozwolił na konwersję odpadowego oleju roślinnego do biosurfaktantów z jednoczesną produkcją energii elektrycznej [35]. Ponadto zaobserwowana wydajność kulombowska była najwyższą wartością odnotowaną dla układu zasilanego ściekami zaolejonymi.

1.1.5. Technologie oparte na MFC

Oczyszczanie ścieków

Obecne systemy oczyszczania ścieków opierające się na wykorzystaniu osadu czynnego, są energochłonne oraz wymagają wysokich kosztów kapitałowych i operacyjnych. Konwencjonalne procesy oczyszczania ścieków wymagają bowiem napowietrzania oraz utylizacji nadmiernego osadu czynnego [48]. Ponadto podczas oczyszczania ścieków do atmosfery uwalniana jest znaczna ilość gazów cieplarnianych. Technologia MFC pozwala na jednoczesną degradację zanieczyszczeń i produkcje energii elektrycznej, może więc przekształcić oczyszczanie ścieków w proces generujący energię. MFC eliminuje konieczność napowietrzania, dzięki oczyszczaniu beztlenowemu oraz znacząco obniża ilość powstających osadów do utylizacji [49]. Jednocześnie technologia MFC umożliwia między innymi monitorowanie w czasie rzeczywistym stężenia substancji organicznych i zawartości substancji toksycznych w ściekach. Korzyści ekonomiczne i środowiskowe pokazują, że technologia MFC jest bardzo obiecującą alternatywą dla konwencjonalnych systemów oczyszczania ścieków.

Biosensory

W ciągu ostatnich lat intensywnie badano MFC pod kątem ich zastosowania jako alternatywnego źródła energii elektrycznej dla paliw kopalnych. Trwający proces wzrostu wydajności MFC związany jest z rozwojem jego elementów funkcjonalnych oraz konstrukcji reaktorów [22], [35]. Pomimo ogromnych postępów w zwiększaniu mocy wyjściowych wykorzystanie MFC jest obecnie ukierunkowane na zastosowania niskoenergetyczne [50]. Na napięcie wyjściowe MFC ma wpływ stężenie związków organicznych, temperatura, pH czy obecność substancji toksycznych. Dlatego MFC mogą być stosowane jako biosensory, czyli urządzenia analityczne zawierające biologiczny elementów czujnikowych, wytwarzający sygnał wyjściowy w odpowiedzi na zanieczyszczenia obecne w ośrodku [51] (Rys. 3.). Zapotrzebowanie na kontrolowanie zanieczyszczeń w czasie rzeczywistym, zwłaszcza w obrębie monitorowania jakości wód, stale wzrasta ze względu na rosnące obawy o środowisko. Biosensory na bazie MFC pozwalają na monitorowanie jakości strumienia zasilającego z szybką reakcją, wysoką czułością i w szerokim zakresem pomiarowym przy niewielkich kosztach operacyjnych, dzięki czemu stanowią obiecującą alternatywę dla konwencjonalnych czujników [52]. Wśród wielu typów biosensorów opartych na MFC możemy wyróżnić czujniki biochemicznego zapotrzebowania na tlen, czujniki toksyczności, czujniki pH oraz czujniki monitorowania aktywności drobnoustrojów. Na przykład opracowano pływający biosensor MFC do monitorowania jakości wody online [53]. W badaniu wykazano, że biosensor, który sam wytwarzał energie potrzebną do działania urządzenia, był w stanie wykryć mocz w słodkiej wodzie i włączyć sygnały wizualne i dźwiękowe. Ponadto zaobserwowano, że częstotliwość sygnału była proporcjonalna do stężenia moczu, co umożliwia ilościowe oznaczenie zanieczyszczeń wody na podstawie charakterystyki sygnału. W innej pracy przedstawiono biosensor MFC wyprodukowany metodą sitodruku biodegradowalnych elektrod na bazie węgla na pojedynczym arkuszu papieru i zademonstrowano jego zastosowanie jako czujnika substancji toksycznych w wodzie [54].

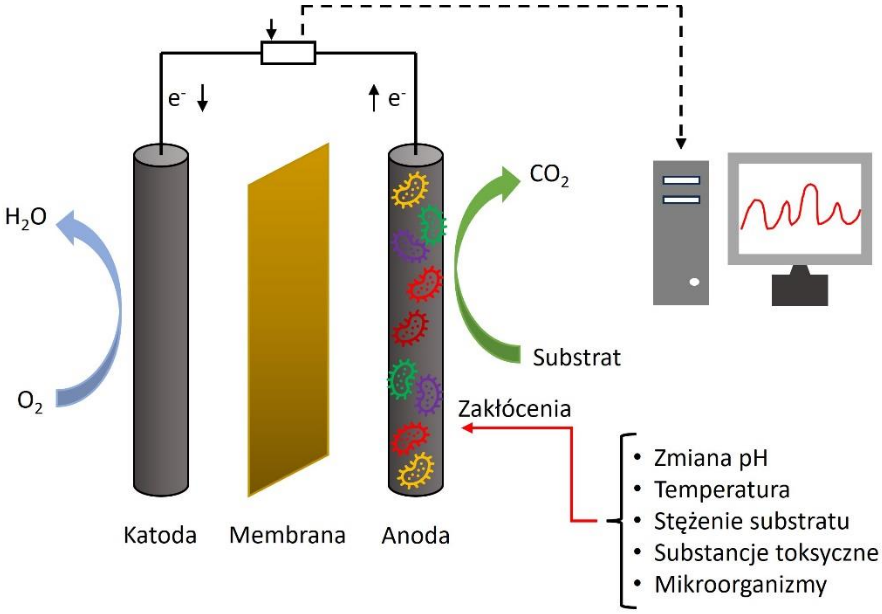

Rys. 3. Schemat działania biosensora MFC.

Bioelektrosynteza

Elektrosynteza mikrobiologiczna to obiecująca droga rozwoju układów bioelektrochemicznych umożliwiająca konwersję odpadów do cennych produktów chemicznych (Rys. 4.). Redukcja dwutlenku węgla na katodzie umożliwia zrównoważoną i ekonomiczną produkcję substancji chemicznych takich jak kwas octowy [55] czy butanol [56]. Technologia ta zyskuje na znaczeniu, dzięki możliwości wychwytywania i utylizacji dwutlenku węgla u źródła, który w przeciwnym razie byłby uwalniany do atmosfery przyczyniając się do globalnego ocieplenia. W takim układzie biofilm anodowy utlenia substancje organiczne, podczas gdy mikroorganizmy biofilmu katodowego wykorzystują elektrony do redukcji dwutlenku węgla. Zastosowanie MFC do redukcji dwutlenku węgla zapewnia wiele korzyści w porównaniu z konwencjonalnymi systemami sekwestracji CO_2. Technologia MFC może jednocześnie oczyszczać ścieki na anodzie i redukować CO_2 na katodzie obniżając koszty operacyjne systemu. Ponadto mikroorganizmy katalizujące reakcję redukcji są tanie, zdolne do samoregeneracji i pracują w stosunkowo niskiej temperaturze [57].

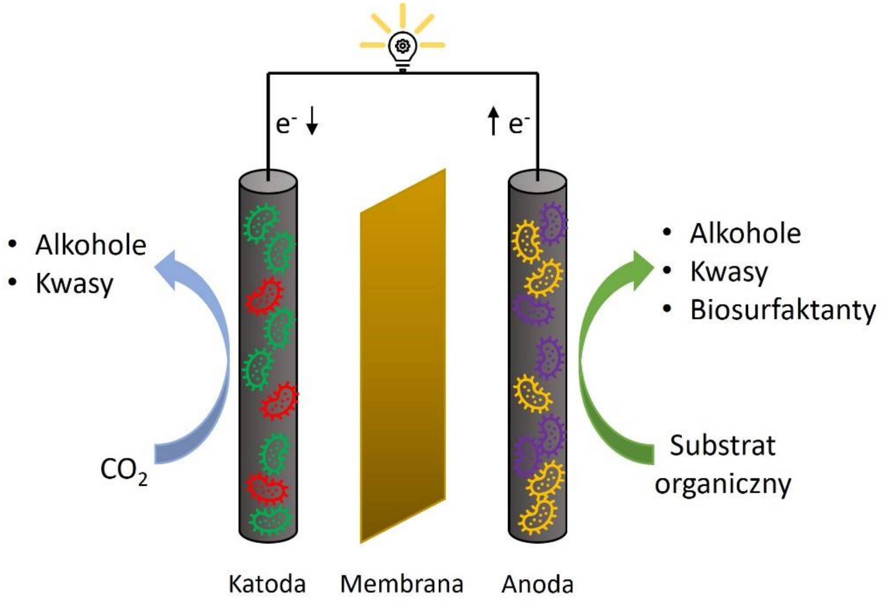

Rys. 4. Synteza związków organicznych w MFC.

Mikroorganizmy tworzące biofilm anodowy również mogą konwertować substraty organiczne do użytecznych produktów (Rys. 4.). Wysokie stężenie butanolu w anolicie wykryto dla MFC zasilanego glukozą i zainokulowanego *Clostridium acetobutylicum* [58]. Podobnie wśród metabolitów MFC zasilanych biomasą alg wykryto butanol, kwas propionowy i kwas masłowy [59]. W innej pracy opisano produkcję acetoiny z glukozy w MFC za pomocą genetycznie zmodyfikowanego szczepu *Escherichia coli* [60]. Ciekawą grupą syntezowanych biochemicznie związków o unikalnych właściwościach i szerokim zastosowaniu są biosurfaktanty. Jednak pomimo dużego znaczenia biosurfaktantów dla przemysłu oraz ich wpływie na zwiększanie wydajności MFC opublikowano niewiele prac, w których biosurfaktanty były celem syntezy w układach bioelektrochemicznych [61].

1.2. Biosurfaktanty

1.2.1. Budowa i właściwości

Biosurfaktanty to amfifilowe związki chemiczne składające się z ugrupowania hydrofilowego i hydrofobowego. Połączenie tych ugrupowań umożliwia interakcję pomiędzy cząsteczkami o różnym charakterze polarnym. Cząsteczki biosurfaktantów agregują na powierzchni międzyfazowej i w zależności od rodzaju układu, część hydrofilowa biosurfaktantu może być zwrócona w kierunku zewnętrznego lub wewnętrznego obszaru. Tym samym biosurfaktanty mogą wpływać na obniżenie napięcia powierzchniowego i międzyfazowego oraz tworzenie stabilnych emulsji. Minimalne stężenie biosurfaktantu niezbędne do maksymalnej redukcji napięcia powierzchniowego lub międzyfazowego określa się mianem krytycznego stężenia micelizacji (CMC) (Rys. 5.). Dalsze zwiększanie stężenia biosurfaktantu nie wpływa na napięcie powierzchniowe i międzyfazowe, a cząsteczki amfifilowe ulegają agregacji z częściami hydrofilowymi skierowanymi na zewnątrz cząsteczki i częściami hydrofobowymi skierowanymi do wewnątrz, tworząc micele. Większość biosurfaktantów ma niższe wartości CMC, napięcia powierzchniowego i napięcia międzyfazowego w porównaniu do ich syntetycznych odpowiedników, co czyni je bardziej wydajnymi i skutecznymi w podobnych zastosowaniach. Ponadto syntetyczne środki powierzchniowo czynne pochodzące z przemysłu petrochemicznego są toksyczne i mogą powodować szkody dla ekosystemów, a ich produkcja jest sprzeczna z celami zrównoważonego rozwoju [62]. Biosurfaktanty to produkty naturalne powstające w wyniku procesów metabolicznych mikroorganizmów. W porównaniu do syntetycznych środków powierzchniowo czynnych mają zmniejszoną toksyczność, zwiększoną tolerancję na pH, temperaturę i zasolenie oraz są biokompatybilne i biodegradowalne. Na przykład charakterystyka ramnolipidów wytworzonych przez *Pseudomonas aeruginosa* BS20 wykazała brak negatywnych skutków autoklawowania w temperaturze 121°C przez 10 minut na aktywność powierzchniową biosurfaktantu [63]. Ponadto testowany ramnolipid wykazał prawie stabilny profil aktywności powierzchniowej w zakresie pH od 2 do 13 oraz przy stężeniu chlorku sodu do 6% (w/v). Równie wysoką stabilność aktywności powierzchniowej w wysokich temperaturach i stężeniu chlorku sodu do 6% (w/v) wykazano dla surfaktyny wyprodukowanej przez *Bacillus subtilis* BS5 [64]. Dzięki tym właściwościom oraz zrównoważonym i przyjaznym dla środowiska metodom wytwarzania biosurfaktanty postrzegane są jako korzystny zamiennik surfaktantów syntetycznych.

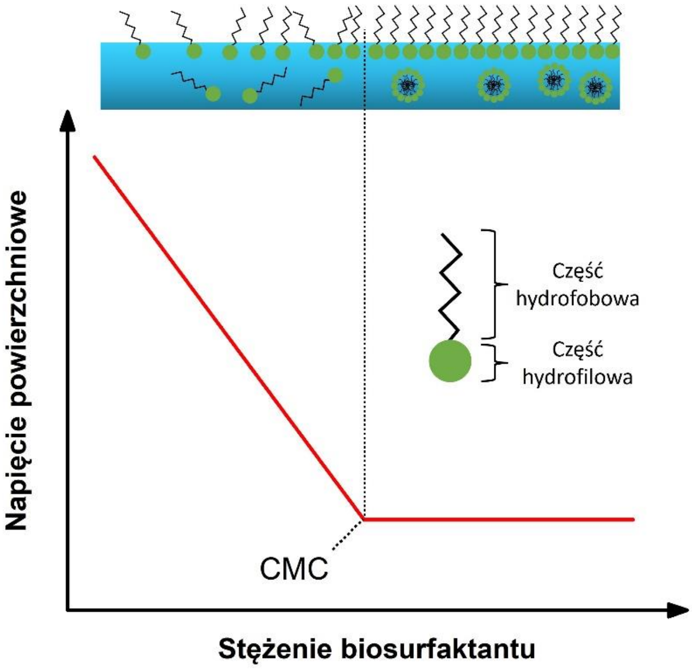

Rys. 5. Charakterystyka zmian napięcia powierzchniowego w funkcji stężenia biosurfaktantów.

Biosurfaktanty możemy podzielić pod względem masy cząsteczkowej na związki o niskiej masie cząsteczkowej oraz związki o wysokiej masie cząsteczkowej, nazywane bioemulgatorami lub biopolimerami. Bioemulgatory mogą skutecznie emulgować dwie niemieszające się ciecze, podczas gdy niskocząsteczkowe biosurfaktanty skutecznie obniżają napięcie powierzchniowe [65]. Ze względu na budowę cząsteczki biosurfaktanty dzielimy na glikolipidy, lipopeptydy, fosfolipidy, lipoproteiny i lipopolisacharydy [66]. Najszerzej zbadaną podklasą glikolipidów o bardzo korzystnych właściwościach są ramnolipidy. Związki te mogą obniżać zarówno napięcie powierzchniowe i międzyfazowe, a do ich produkcji można wykorzystać produkty odpadowe pochodzenia spożywczego [67]. Ramnolipidy zbudowane są z dwóch części: glikonowej oraz lipidowej [68]. Część glikonowa składa się z jednej cząsteczki (monoramnolipidy) lub dwóch cząsteczek (diramnolipidy) ramnozy, połączonych wiązaniem α-1,2-glikozydowym i ma charakter hydrofilowy (Rys. 6.). Ugrupowanie lipidowe ma charakter hydrofobowy i składa się z jednego lub większej liczby nasyconych/nienasyconych łańcuchów β-hydroksy kwasów tłuszczowych, połączonych wiązaniem estrowym. Wykazano, że biosurfaktant ramnolipidowy wyprodukowany przez *Pseudomonas aeruginosa* P6 był w stanie obniżyć napięcie powierzchniowe wody z 72 mN m^{-1} do 36 mN m^{-1} oraz wykazał aktywność emulgacyjną (E24) heksadekanu na poziomie 63.3%, co świadczy o szerokim spektrum możliwych zastosowań ramnolipidów [69].

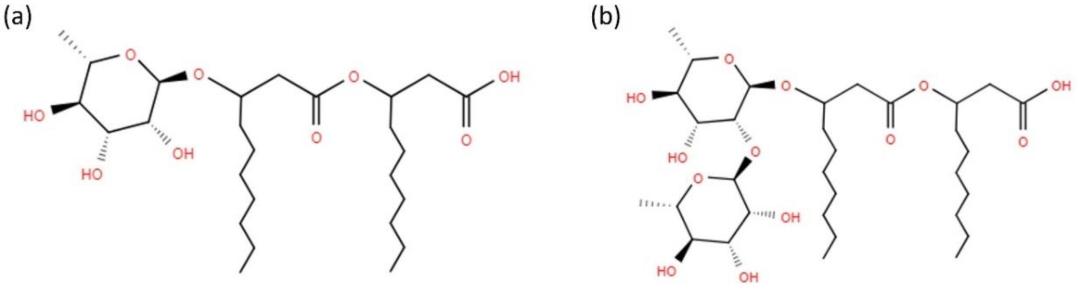

Rys. 6. Przykładowa struktura (a) monoramnolipidu i (b) diramnolipidu.

1.2.2. Zastosowania

Przemysł naftowy

Wysoka sprawność odzysku w powiązaniu z niska toksycznością i biodegradowalnością biosurfaktantów, czyni je atrakcyjną dla przemysłu i środowiska alternatywą dla syntetycznych środków powierzchniowo czynnych wykorzystywanych w odzyskiwaniu ropy naftowej z wyczerpujących się złóż [70]. W procesie tym biosurfaktanty, które mogą być wytwarzane *in-situ*, skutecznie obniżają napięcie powierzchniowe pomiędzy ropą a skałą mobilizując węglowodory uwięzione w porach skał. Przykładowo, wzrost odzysku ropy o 6% uzyskano dzięki zastosowaniu biosurfaktantu lipopeptydowego wyprodukowanego przez szczep *Bacillus mojavensis* PTCC 1696 [71]. Podobnie, zastosowanie ramnolipidu wytworzonego przez *Pseudomonas aeruginosa* zwiększyło o prawie 12% odzysk ropy naftowej ze złoża, co było wartością wyższą niż dla surfaktantów syntetycznych [72].

Bioremediacja

Biosurfaktanty są doskonałą ekologiczną alternatywą dla syntetycznych związków powierzchniowo czynnych wykorzystywanych w remediacji gleb. Najgroźniejszymi zanieczyszczeniami gleb generowanymi w przemyśle są węglowodory. Zastosowanie biosurfaktantów w remediacji węglowodorów, ma na celu zwiększenie ich biodostępności dla mikroorganizmów. Ponadto biosurfaktanty mogą być wytwarzane bezpośrednio u źródła zanieczyszczeń, co obniża koszty całego procesu. Na przykład wykazano, że biosurfaktant wytworzony przez szczep *Rhodococcus erythropolis* 3C-9 znacząco zwiększył szybkość biodegradacji n -heksadekanu przez *Alcanivorax dieselolei* i *Psychrobacter celer* [73]. Podobnie biosurfaktant wytworzony przez szczepy *Pseudomonas aeruginosa* MTCC7815 i MTCC7814 spowodował wzrost metabolizmu fenantrenu, pirenu i fluorenu [74]. W innej pracy wykazano wzrost biodegradacji wielopierścieniowych węglowodorów aromatycznych w obecności biosurfaktantu wytworzonego przez *Bacillus circulans* [75]. Yin i in. [76] zaobserwowali 23 krotny wzrost rozpuszczalności fenantrenu w obecności ramnolipidu wytworzonego przez szczep *Pseudomonas aeruginosa* S6 wyizolowany ze ścieków zawierających ropę naftową. Dodatkowo wyznaczone współczynniki solubilizacji i podziału między fazę micelarną i wodną dla wytworzonego ramnolipidu były znacznie wyższe niż dla syntetycznych środków powierzchniowo czynnych.

1.2.3. Konwencjonalne metody biosyntezy i oczyszczania

Biosurfaktanty produkowane są najczęściej na drodze fermentacji tlenowej lub beztlenowej w klasycznych hodowlach płynnych. Jednak koszt produkcji biosurfaktantów pozostaje nadal wyższy niż ich syntetycznych odpowiedników. Bardziej ekonomiczne i przyjazne dla środowiska wytwarzanie biosurfaktantów wymaga integracji i optymalizacji procesu produkcji i przetwarzania. Podstawowym kryterium wpływającym na koszt oraz wydajność biosyntezy jest surowiec. W literaturze opisano różne rodzaje substratów stosowanych w produkcji biosurfaktantów. Oprócz komercyjnych surowców do syntezy biosurfaktantów zbadano także produkty odpadowe z różnych gałęzi przemysłu, takie jak glicerol [77], odpadowe oleje roślinne [78], czy melasę [79]. Takie podejście pozwala na jednoczesną produkcje biosurfaktantów oraz waloryzacje odpadów, a proces biosyntezy czyni bardziej ekonomicznym i przyjaznym dla środowiska, stymulując przejście w stronę gospodarki o obiegu zamkniętym. Kolejnym wyzwaniem jest optymalizacja syntezy biosurfaktantów, ponieważ na wzrost i metabolizm drobnoustrojów podczas fermentacji wpływa wiele czynników biotycznych i abiotycznych (Fig. 7.). Uzyskanie optymalnej biosyntezy wymaga określenia warunków hodowli, obejmujących źródło i stężenie węgla, azotu, fosforu i mikroelementów [80], wielkość i skład inokulum oraz temperaturę, pH, napowietrzanie, prędkość mieszania [81], [82], jak i rozwiązania konstrukcyjne bioreaktora [83]. Dlatego znalezienie idealnych warunków do produkcji biosurfaktantów w klasycznej biosyntezie było przedmiotem wielu badań, wśród których obszernie omówiono optymalizację stężenia oraz źródła azotu [84][85]. Wykazano, że zastosowanie azotanu sodu przy stosunku C/N równym 10 pozwoliło na znaczne zwiększenie efektywności degradacji odpadowego oleju posmażalniczego oraz syntezy biosurfaktantów przez nowo wyizolowany szczep *Pseudomonas* SWP-4 [86]. W ostatnich latach na znaczeniu zyskuje zastosowanie inżynierii genetycznej w celu opracowania nowych mikroorganizmów dla poprawy produkcji i wydajności biosurfaktantów. Ulepszenie szczepu drobnoustroju za pomocą technologii rekombinacji DNA może zapewnić wyższą wydajność przy niższych kosztach. Ponadto biosurfaktanty uzyskane z modyfikowanych genetycznie mikroorganizmów mogą posiadać unikalne właściwości. Na przykład opracowano systematyczne podejście inżynieryjne, polegające na modyfikacji 53 genów u *Bacillus subtilis* 168 w celu poprawy biosyntezy surfaktyny [87]. W rezultacie uzyskano najwyższą w literaturze wydajność surfaktyny, co według autorów może utorować drogę do komercyjnej produkcji.

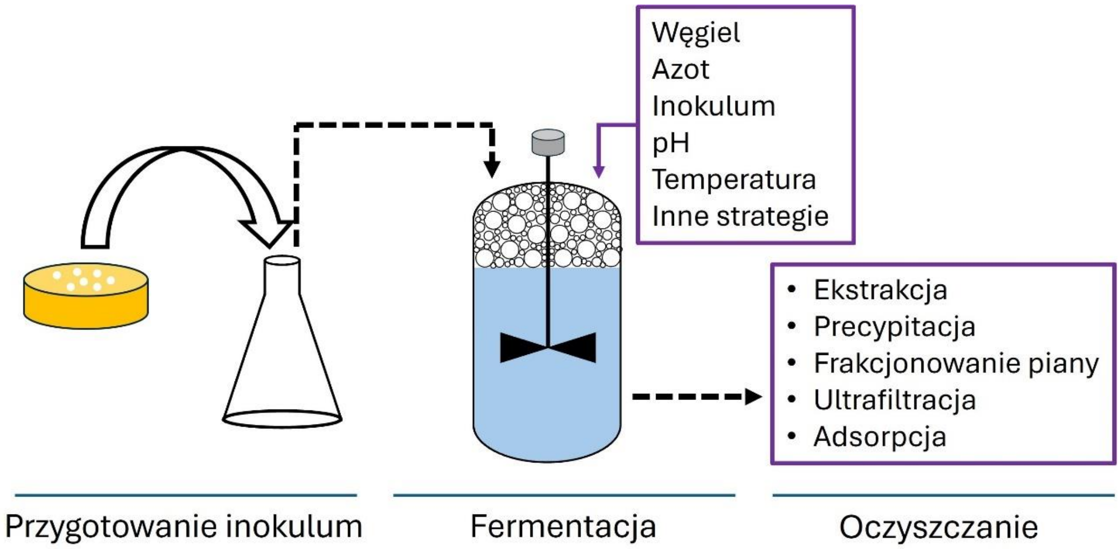

Rys. 7. Schemat ideowy konwencjonalnego procesu produkcji biosurfaktantów.

W zależności od zastosowania produktu końcowego dalsze przetwarzanie można dostosować w celu osiągnięcia pożądanej wydajności i czystości (Rys. 7.). Najczęściej stosowaną techniką separacji biosurfaktantów z hodowli mikrobiologicznej jest ekstrakcja w fazie ciekłej przy zastosowaniu różnych rozpuszczalników organicznych, takich jak chloroform, metanol, dichlorometan czy octan etylu. Metoda ta wymaga jednak zużycia dużej ilość rozpuszczalników, co wpływa na wzrost kosztów procesu oraz negatywnie oddziałuje na środowisko. W związku z tym szeroko badane są alternatywne techniki separacji biosurfaktantów, takie jak ekstrakcja do fazy stałej, frakcjonowanie piany czy ultrafiltracja. Techniki te mogą umożliwiać uzyskanie wysoce czystych biosurfaktantów mniejszym kosztem i w bardziej łagodny dla środowiska sposób. Frakcjonowanie piany jest jedną z bardzo ciekawych metod bezrozpuszczalnikowych, którą można stosować w trakcie etapu produkcyjnego. W efekcie metoda ta pomaga w ciągłym usuwaniu tworzącej się piany w trakcie procesu produkcji i zapobiega hamowaniu wzrostu biomasy i spadku wydajności procesu. Wykazano, że metoda frakcjonowania piany *in-situ* jest skutecznym narzędziem do odzysku i oczyszczania biosurfaktantów takich jak surfaktyna [88] i ramnolipidy [89]. Równie atrakcyjną metodą umożliwiającą jednoczesne zatężanie i oczyszczanie biosurfaktantów jest technika ekstrakcji do fazy stałej. Na przykład, zastosowanie ekstrakcji do fazy stałej w oczyszczaniu ramnolipidów wykazało wyższą wydajność i powtarzalność w porównaniu z metoda ekstrakcji ciecz-ciecz [90]. Podsumowując, dalsze przetwarzanie może stanowić obecnie nawet 80% całkowitego kosztu otrzymania biosurfaktantów, dlatego optymalizacja technik przetwarzania ma fundamentalne znaczenie dla ekonomiczności i konkurencyjności biosurfaktantów na rynku.

1.3. Mechanizmy działania biosurfaktantów w MFC

Tworzenie i rozwój biofilmu

Wydajna produkcja energii elektrycznej w MFC wymaga wytworzenia biofilmu elektroaktywnego na powierzchni anody. W początkowej fazie działania MFC elektroaktywny biofilm anodowy dojrzewa, tworząc bardziej równomierne pokrycie, a w efekcie obserwujemy wzrost prądu wyjściowego. W pierwszym etapie tworzenia biofilmu, adhezja mikroorganizmów do powierzchni anody znacząco wpływa na etap rozruchu MFC. Kolejno w miarę wzrostu ilości mikroorganizmów przyłączających się do anody, szybkość transferu elektronów znacznie wzrasta. Wykazano, że środki powierzchniowo czynne mogą reagować z powierzchniami materiałów anodowych zwiększając ich hydrofilowość, co jak wiadomo sprzyja tworzeniu się elektroaktywnego biofilmu [91]. Środki powierzchniowo czynne mają również zdolność zmiany struktury błon komórkowych w celu utworzenia kanałów, które skutecznie zmniejszają opór błony komórkowej, przyspieszają transport masy przez błony i zwiększają degradację substratu [92]. Na przykład, znaczne obniżenie czasu rozruchu MFC oraz wzrost maksymalnej gęstości mocy o 20%, uzyskano dzięki modyfikacji powierzchni anody z eksfoliowanego grafitu za pomocą dodecylosiarczanu sodu [93]. Ponadto środki powierzchniowo czynne mogą indukować tworzenie biofilmu w obecności substratów hydrofobowych, poprzez zwiększenie ich biodostępności [94]. Tworzenie biofilmu może więc być wywołane oraz wspomagane obecnością biosurfaktantów, które mogą być wytwarzane *in-situ* w MFC. Zhang i in. [92] zbadali mechanizm powstawania biofilmów anodowych i przenoszenia elektronów w obecności ramnolipidów podczas rozruchu i stabilnych etapów pracy MFC. Dodatek ramnolipidów w stężeniu 40 mg L^{-1} skrócił czas rozruchu MFC o 48h oraz spowodował wzrost maksymalnej gęstości mocy o ponad 43%. Dodatkowo, analiza bakterii anodowych wykazała, że ramnolipidy mają istotny wpływ na wzbogacanie biofilmu w egzoelektrogeny oraz ich skład.

Transfer elektronów

Etapem ograniczającym szybkość rozruchu MFC jest anodowy transfer elektronów z komórek mikroorganizmów do powierzchni elektrody. Środki powierzchniowo czynne mogą wpływać na przepuszczalność membrany, która jest główną przeszkodą w zewnątrzkomórkowym transferze elektronów za pomocą mediatorów [95].

W badaniach wykazano, że dodatek syntetycznych środków powierzchniowo czynnych skutecznie zwiększa generowaną moc w MFC [93], [96]. Podobnie obecność biosurfaktantów w MFC może mieć korzystny wpływ na transfer elektronów, a w efekcie spadek oporu wewnętrznego i wzrost produkowanej mocy. Wykazano, że dodatek soforolipidu zwiększył przepuszczalność membrany i produkcję piocyjaniny, a w efekcie skutecznie obniżył opór wewnętrzny MFC o 36% [97]. Podobnie w innej pracy dodatek lipidu trehalozy zmniejszył opór wewnętrzny MFC o 57%, a w efekcie prawie 6 krotnie zwiększył maksymalną gęstość mocy [98]. W naszej pracy endogennie wytwarzane biosurfaktanty ramnolipidowe w komorze anodowej MFC spowodowały spadek oporu wewnętrznego o 40% [35]. Dodatkowo w kolejnej pracy wykazaliśmy zależność między ilością produkowanego biosurfaktantu a oporami anodowymi w MFC [99]. W kolejnym badaniu zwiększona produkcja endogennych ramnolipidów w wyniku nadekspresji genu rhlA znacząco poprawiła zewnątrzkomórkowy transfer elektronów szczepu *Pseudomonas aeruginosa* poprzez zwiększenie produkcji piocyjaniny i zwiększenie przyczepienia bakterii do powierzchni anody [100]. W rezultacie wartość oporu wewnętrznego spadła o prawie 30% a gęstość mocy wzrosła o ponad 240%.

Degradacja substratów hydrofobowych

Można wyróżnić dwa główne mechanizmy rozkładu związków hydrofobowych przez mikroorganizmy w obecności biosurfaktantów w MFC (Rys. 8.). Biodegradacja hydrofobowych substancji organicznych może zachodzić poprzez solubilizację substratu polegającą na utworzenie struktury micelarnej z biosurfaktantami, w której hydrofilowe głowy są zorientowane w stronę wodnej fazy, a lipofilowe ogony są przyłączone do hydrofobowego substratu, ułatwiając adsorpcję zanieczyszczeń do komórki bakteryjnej, po której następuje wewnątrzkomórkowa degradacja. Alternatywnie, biosurfaktanty mogą oddziaływać z zewnętrznymi powierzchniami ścian komórkowych bakterii, powodując wzrost jej hydrofobowości i promując tym samym adhezję komórek bakteryjnych do związków hydrofobowych. W efekcie wzrost drobnoustrojów na powierzchni substratu umożliwia jego degradację. Na przykład wytwarzane *in situ* w MFC dwa typy biosurfaktantów pozwoliły na uzyskanie wysokiego stopnia degradacji węglowodorów pochodzących z ropy naftowej [101]. Ponadto w naszej pracy wykazaliśmy, że obecność biosurfaktantów w MFC miała wpływ na ścieżkę degradacji odpadowego oleju roślinnego [35].

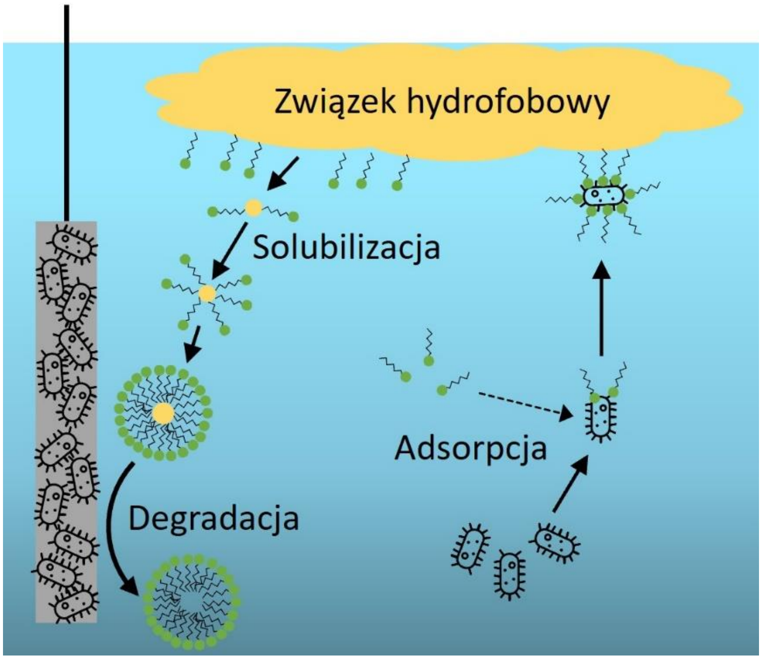

Rys. 8. Mechanizmy degradacji substratów hydrofobowych w obecności biosurfaktantów w komorze anodowej MFC.

1.4. Synteza biosurfaktantów w MFC

Surowce i rodzaje wytwarzanych biosurfaktantów

Badanie źródła węgla wykorzystywanego do syntezy biosurfaktantów jest niezwykle ważne, ponieważ substrat zastosowany do produkcji biosurfaktantów ma bezpośredni wpływ na wzrost mikroorganizmów, wydajność syntezy pożądanego produktu oraz ekonomiczność procesu. Ponadto różne substraty mogą prowadzić do powstania zróżnicowanych struktur chemicznych biosurfaktantów o odmiennych właściwościach i zastosowaniach. Biosurfaktanty można wytwarzać w MFC zarówno z prostych substratów jak i znacznie bardziej złożonych węglowodorów. W pierwszej pracy opisującej syntezę biosurfaktantów w układach bioelektrochemicznych jako źródło węgla wykorzystano octan sodu [102]. W badaniu tym wykazano, że oddziaływanie ramnolipidów i fenazyn wytwarzanych przez *Pseudomonas sp.* pozwoliło *Brevibacillus sp.* na osiągnięcie zewnątrzkomórkowego transferu elektronów. Jednak od tego czasu opublikowano niewiele prac na temat biosyntezy surfaktantów w BES [61]. Najczęściej stosowanym substratem do produkcji biosurfaktantów w MFC jest zużyty olej roślinny oraz ścieki zawierające węglowodory ropopochodne (Tab. 1.). Substraty te bogate są w źródła węgla o zróżnicowanych strukturach, które mogą być wykorzystane przez mikroorganizmy w procesie biosyntezy surfaktantów. Liu i in. [103] wykazali jednoczesną produkcję biosurfaktantu i energii elektrycznej ze zużytego oleju roślinnego w komorze anodowej MFC. W naszej pracy, wykorzystując jako substrat zużyty olej roślinny uzyskaliśmy najwyższą gęstość produkowanej mocy w MFC, w którym zachodzi synteza biosurfaktantów [99]. Ponadto analiza metabolitów wykazała obecność jedenastu związków należących do grupy mono- i di-ramnolipidów. W innej pracy wykazano jednoczesną produkcję surfaktyny i ramnolipidów oraz wysoką produkcję mocy w MFC, dzięki zastosowaniu ropy naftowej jako źródła węgla [101]. Podobnie zastosowanie oleju silnikowego jako substratu w komorze anodowej MFC pozwoliło na uzyskanie wysokiej gęstości produkowanej mocy oraz wykazano syntezę kilku biosurfaktantów lipopeptydowych [104].

Mikroorganizmy

Synteza biosurfaktantów i jednoczesne wytwarzanie energii elektrycznej wymaga inokulacji MFC za pomocą bakterii aktywnych elektrochemicznie o zdolnościach do biosyntezy, lub za pomocą mieszanego konsorcjum mikrobiologicznego, który wymaga okresu wzbogacenia w bakterie o tych zdolnościach. Wykorzystanie czystych szczepów przynosi efekty, gdy jako substrat stosujemy proste związki chemiczne o stosunkowo wysokiej czystości [100]. Trudnodegradowalne substraty będące złożoną mieszaniną węglowodorów zwykle wymagają rozbudowanego konsorcjum, aby uzyskać wysoki stopień degradacji oraz zadowalającą wydajność biosyntezy. Na przykład wykorzystanie pojedynczego szczepu *Serratia sp.* w celu degradacji zużytego oleju roślinnego nie pozwoliło na uzyskanie wysokiej wydajności generowanej gęstości mocy w MFC [103]. Podczas gdy w naszej pracy wykorzystaliśmy osad czynny, który po okresie wzbogacenia pozwolił na osiągnięcie wysokiej wydajności zarówno biosyntezy surfaktantów jak i produkcji prądu [35]. W innej pracy wysoką gęstość prądu oraz syntezę dwóch biosurfaktantów uzyskano, dzięki jednoczesnemu wykorzystaniu dwóch szczepów, *B. subtilis i P. aeruginosa*, w degradacji ropy naftowej w MFC [101]. Podobnie, efekt synergiczny *S. aureus i P. aeruginosa* pozwolił na wysokowydajna degradacje oleju silnikowego w MFC, z jednoczesną synteza kilku biosurfaktantów lipopeptydowych [104].

Strategie poprawy produkcji biosurfaktantów w MFC

Pomimo niewielu prac dotyczących syntezy biosurfaktantów w MFC zbadano kilka aspektów w celu zwiększenia wydajności i ekonomiczności produkcji tych cennych biomolekuł. Jednym z podejść do obniżenia kosztów produkcji jest wykorzystanie nieprzetworzonych substratów odpadowych w warunkach niesterylnych. Dotychczas zbadano wykorzystanie odpadowych olejów roślinnych lub ścieków zanieczyszczonych substancjami ropopochodnymi (Tab. 1.). Jednak porównanie produkcji biosurfaktantów z odpadowego oleju roślinnego w MFC i reaktorze okresowym z ciągłym mieszaniem wykazało wyższą wydajność konwencjonalnego bioreaktora w porównaniu do MFC [103]. Ponadto w badaniu uzyskano niewielką produkcję energii elektrycznej. Aby umożliwić wydajną biosyntezę i jednoczesną produkcje elektryczności wymagany jest rozwój techniczny w zakresie projektowania reaktorów, jak i optymalizacja kluczowych parametrów wpływających na procesy zachodzące w ogniwie. W naszej pracy przedstawiliśmy nową konstrukcję MFC o horyzontalnym układzie elektrod, która pozwoliła na znaczne polepszenie biodostępności substratu olejowego, i tym samym polepszenie syntezy biosurfaktantów i generowania energii elektrycznej [35]. Ponadto wykazaliśmy bezpośrednią korelację między wzrostem mocy i spadkiem napięcia powierzchniowego w MFC. W kolejnej pracy, optymalizując stężenie azotu w pożywce stosowanej jako roztwór anodowy MFC horyzontalnego uzyskaliśmy najwyższą odnotowaną wydajność produkcji energii w MFC wytwarzającym jednocześnie biosurfaktanty [99]. Kolejnym podejściem mającym na celu zwiększenie ogólnej wydajności MFC jest modyfikacja elektrod. Na przykład wykazano, że nanocząstki żelaza zastosowane jako katalizatory katodowe poprawiły produkcję energii elektrycznej w MFC zasilanym zużytym olejem roślinnym o ponad 500% i produkcję biosurfaktantów o 32% [105]. W innej pracy zastosowano modyfikację powierzchni anody nanocząstkami Fe_2O_3 w MFC zainokulowanym szczepem bakteryjnym rozkładającym węglowodory oraz produkującym biosurfaktanty [104]. W rezultacie moc MFC zasilanego olejem silnikowym wzrosła o 37%. Jedną z obiecujących dróg zwiększenia produkcji biosurfaktantów w MFC jest zastosowanie genetycznie modyfikowanych szczepów. Zastosowanie inżynierii genetycznej powinno koncentrować się na opracowaniu drobnoustrojów o wysokim poziomie aktywności metabolicznej, dzięki czemu biosurfaktanty mogłyby być wytwarzane bardziej ekonomicznie. Na przykład opracowano podejście do zwiększenia produkcji ramnolipidów w MFC polegające na nadekspresji genu rhlA szczepu *Pseudomonas aeruginosa*. W rezultacie modyfikowany szczep zapewnił produkcję ramnolipidów i energii elektrycznej o 43% i 250% większą niż szczep macierzysty [100].

Tab. 1. Produkcja biosurfaktantów w MFC.

Konstrukcja MFC	Strategia	Substrat	Inokulum	Czas pracy	Membrana	Produkt	Gęstość mocy		Bibliografia
				dni			mW m^{-3}	mW m^{-2}	
Dwukomorowa z mieszaniem	Nadekspresja genu rhlA w celu zwiększenia syntezy ramnolipidów i mocy wyjściowej MFC	Glukoza	*P. aeruginosa PAO1-rhlA*	6	PEM	Ramnolipidy	-	9.4 ± 0.6	[100]
Dwukomorowa z mieszaniem	Porównanie efektywności produkcji biosurfaktantu w MFC i bioreaktorze wsadowym z ciągłym mieszaniem	Zużyty olej roślinny	*Serratia sp.*	7	Mostek solny	Niezidentyfikowany biosurfaktant	6.33	1.13	[103]
Dwukomorowa z mieszaniem	Nanocząstki żelaza i niklu jako katalizatory katodowe mikrobiologicznego ogniwa paliwowego produkującego biosurfaktanty	Zużyty olej roślinny	*Serratia sp.*	6	CEM	Niezidentyfikowany biosurfaktant	66.4	6.64	[105]
Jednokomorowa horyzontalna	Pozioma konstrukcja MFC dla zwiększenia efektywność degradacji zużytego oleju roślinnego i syntezy biosurfaktantów	Zużyty olej roślinny	Activated sludge	50	CEM	Niezidentyfikowany biosurfaktant	6 600	146.7	[35]
Jednokomorowa horyzontalna	Optymalizacja stężenia azotu dla zwiększenia efektywności wytwarzania biosurfaktantów i energii elektrycznej w poziomych MFC	Zużyty olej roślinny	Activated sludge	215	CEM	Ramnolipidy	17 500	388.9	[99]
Jednokomorowa	Efekt synergiczny dwóch szczepów produkujących biosurfaktanty w degradacji ropy naftowej w MFC	Ropa naftowa	*B. subtilis i P. aeruginosa*	~60	IEM	Ramnolipidy i surfaktyna	6 300	525	[101]
Jednokomorowa	Modyfikacja anody nanocząstkami Fe_2O_3 w celu zwiększenia odzysku energii w MFC	Olej silnikowy	*S. aureus i P. aeruginosa*	7	-	Biosurfaktanty lipopeptydowe	10 200	-	[104]

2. Cel i zakres pracy

Głównym celem badań przedstawionych w rozprawie doktorskiej była ocena możliwości produkcji biosurfaktantów w mikrobiologicznych ogniwach paliwowych z odpadowego oleju roślinnego podczas produkcji energii elektrycznej i wykorzystania biosurfaktantów do zwiększenia wydajności mikrobiologicznych ogniw paliwowych. Planując szczegółowe cele rozprawy założono, że mikrobiologiczne ogniwa paliwowe mogą produkować biosurfaktanty z odpadowych olejów roślinnych, a wydajność wytwarzania energii elektrycznej i syntezy biosurfaktantów zależy od optymalizacji wielu czynników biotycznych i abiotycznych. Wyznaczenie optymalnych rozwiązań projektowych i parametrów procesowych może stanowić pierwszy krok w kierunku zwiększenia skali tego procesu w przyszłości.

Szczegółowe cele rozprawy doktorskiej obejmują:

1. Dobór materiałów funkcjonalnych mikrobiologicznego ogniwa paliwowego wykorzystywanego do produkcji biosurfaktantów i energii elektrycznej.

2. Opracowanie konstrukcji mikrobiologicznego ogniwa paliwowego zdolnego do wydajnej konwersji zużytego oleju roślinnego do biosurfaktantów.

3. Charakterystyka reakcji bioelektrochemicznych prowadzących do produkcji biosurfaktantów w mikrobiologicznym ogniwie paliwowym ze zużytego oleju roślinnego.

4. Optymalizacja składu pożywki zasilającej mikrobiologicznego ogniwa paliwowego pod katem produkcji biosurfaktantów i energii elektrycznej.

5. Identyfikacja i ilościowe określenie produkowanych biosurfaktantów.

6. Wykorzystanie biosurfaktantów w celu zwiększenia wydajności mikrobiologicznych ogniw paliwowych.

3. Metodologia

3.1. Projektowanie i konstruowanie ogniw

W eksperymentach wykorzystano jednokomorowe MFC z katodą powietrzną. Zaprojektowane elementy ogniw drukowano z polipropylenu z wykorzystaniem drukarki Prusa i3 MK3S (Prusa Research, Czechy) lub wycinano za pomocą lasera z płyt polimetakrylanu metylu (PMMA) o grubości 3 mm. Szczegóły projektowe dla każdego badania będącego częścią rozprawy doktorskiej przedstawiono w Tabeli 2.

Tab. 2. Budowa i eksploatacja MFC.

	Artykuł 1 (5.1.)	Artykuł 2 (5.2.)	Artykuł 3 (5.3.)	Artykuł 4 (5.4.)
Konstrukcja	Jednokomorowa drukowana z polipropylenu			Jednokomorowa z PMMA
Objętość robocza	20 mL			26 mL
Anoda	Welon węglowy o gramaturze 20 g m^{-2}			
Katoda	Węgiel aktywny CWZ-22 i CWZ-35	Węgiel aktywny CWZ-22	Węgiel aktywny CWZ-22	Węgiel aktywny CWZ-22
Membrana	Membrana kationowymienna			Membrany kompozytowe ceramiczne
Inokulum	Tlenowy osad czynny z oczyszczalni ścieków			
Substrat	Octan sodu	Zużyty olej posmażalniczy	Zużyty olej posmażalniczy	Octan sodu

3.2. Eksperymenty elektrochemiczne

3.2.1. Pomiar napięcia w czasie rzeczywistym

W każdym eksperymencie napięcie obwodu zamkniętego mierzono w czasie rzeczywistym i rejestrowano w odstępach 3 minutowych za pomocą systemu akwizycji danych KEYSIGHT DAQ970A (KEYSIGHT TECHNOLOGIES, USA) lub PicoLog 6 (Pico Technology, UK).

3.2.2. Eksperymenty polaryzacyjne

Eksperymenty polaryzacyjne przeprowadzono w układzie trójelektrodowym lub dwuelektrodowym, stosując potencjostat MultiPalmSens4 (Palmsens BV, Holandia).

W układzie trójelektrodowym anodę zastosowano jako elektrodę roboczą, katodę jako przeciwelektrodę, a nasyconą elektrodę Ag/AgCl jako elektrodę odniesienia umieszczoną w komorze anodowej. W układzie dwuelektrodowym anoda stanowiła elektrodę roboczą, podczas gdy katodę zastosowano zarówno jako przeciwelektrodę i elektrodę odniesienia.

Krzywe polaryzacji uzyskano przy użyciu techniki woltamperometrii liniowej w zakresie od potencjału obwodu otwartego do 0.0 V elektrody roboczej względem elektrody odniesienia, przy szybkości skanowania 1 mV s^{-1}. Na podstawie uzyskanych danych eksperymentalnych wyodrębniono maksymalną gęstość mocy, gęstość prądu i optymalną rezystancję, wyliczoną w punkcie mocy maksymalnej.

3.2.3. Elektrochemiczna spektroskopia impedancyjna (EIS)

Elektrochemiczną spektroskopię impedancyjną (EIS) wykorzystano do analizy wydajności poszczególnych komponentów MFC. Doświadczenia EIS przeprowadzono dla całego ogniwa, w którym anoda pełniła rolę elektrody roboczej, natomiast katoda pełniła funkcję przeciwelektrody i elektrody odniesienia. Do wykonania EIS wykorzystano potencjostat MultiPalmSens4 (Palmsens BV, Holandia). W eksperymentach zastosowano prąd przemienny o amplitudzie 10 mV i zakresie częstotliwości od 100 kHz do 10 mHz. Wszystkie widma EIS rejestrowano, gdy MFC znajdowało się w trybie napięcia obwodu otwartego.

3.3. Pomiary fizykochemiczne

3.3.1. Przewodność, stężenie tlenu, pH

Stężenie tlenu monitorowano za pomocą galwanicznego czujnika tlenu ELMETRON COG-1 (ELMETRON, Polska). Czujnik skalibrowano na 0% nasycenia tlenem w roztworze Na_2SO_3, a następnie w powietrzu na 100% nasycenia. Pomiary pH przeprowadzono za pomocą elektrody IONODE IJ44A (ELMETRON, Polska). Przewodność mediów zmierzono czujnikiem ELMETRON ECF-1.

3.3.2. Chemiczne zapotrzebowanie na tlen i wydajność kulombowska

W hodowlanym podłożu wyjściowym i po obróbce w MFC określono chemiczne zapotrzebowanie na tlen (ChZT) metodą utleniania dwuchromianem potasu, zgodnie z instrukcją producenta (Hach, USA). Zdolność usuwania ChZT obliczono jako procentowy stosunek różnicy ChZT w podłożu wyjściowym i ChZT na koniec cyklu wsadowego do ChZT w podłożu wyjściowym.

Wydajność kulombowską (CE) obliczono zgodnie z poniższym równaniem :

$$\mathrm{CE} = \frac{\mathrm{M}\int_0^{\mathrm{t}} \mathrm{Idt}}{\mathrm{FbV_{An}\Delta COD}},$$

gdzie M – masa cząsteczkowa substratu węglowego; I – natężenie prądu (A); t – długość cyklu wsadowego (s); F – stała Faradaya (96500 C/mol e^-); b – liczba wymienionych elektronów na mol tlenu; V_{An} – objętość robocza komory anodowej; ΔCOD – zmiana stężenia ChZT (mg L^{-1}).

3.3.3. Analiza sorpcji azotu

Metodę adsorpcji/desorpcji azotu w temperaturze -196°C przy użyciu sorptometru NOVA 2000 (Quantachrome Instruments, USA) wykorzystano w celu wyznaczenia powierzchni właściwej i rozkładu wielkości porów wyjściowych materiałów katodowych. Przed pomiarem próbkę odgazowano pod próżnią w temperaturze 400°C przez noc. Parametry obliczono z izoterm adsorpcji/desorpcji przy użyciu równania Brunauera-Emmetta-Tellera (BET), teorii funkcjonału gęstości (DFT) i równania Dubinina-Radushkevicha (DR).

3.4. Skaningowa mikroskopia elektronowa (SEM)

Wyjściowe materiały katodowe a także katody po okresie doświadczalnym przygotowano do analizy przy użyciu skaningowego mikroskopu elektronowego poprzez suszenie próbek w temperaturze 60°C przez jedną godzinę. Ponadto, przed analizą, materiały trzymano przez noc w temperaturze 50°C.

Membrany nowe i po działaniu w MFC przygotowano do analizy powierzchni według poniższej procedury, aby utrwalić biofilm wytworzony na powierzchni membran i umożliwić jego obserwację pod mikroskopem. W pierwszym etapie próbki zanurzono na 12 godzin w 2.5% roztworze aldehydu glutarowego w 0.1 M roztworze soli fizjologicznej buforowanej fosforanami (PBS). Następnie próbki membran przemyto trzykrotnie w 0.1 M PBS i odwodniono we wzrastającym gradiencie etanolu w wodzie. Na koniec próbki zanurzono w czystym HMDS i suszono na powietrzu przez 10 minut. Ponadto, przed analizą próbki suszono w temperaturze 50°C przez noc.

Analizy morfologii i składu powierzchni przeprowadzono za pomocą skaningowego mikroskopu elektronowego TESCAN VEGA 3 oraz Helios NanoLab™ 600i.

3.5. Pomiary aktywności biosurfaktantów

3.5.1. Napięcie powierzchniowe

Napięcie powierzchniowe anolitu mierzono za pomocą tensjometru ciśnienia pęcherzyka BPT Mobile (KRUSS, Niemcy). Urządzenie skalibrowano z nową kapilara pomiarową przed każdą serią pomiarów. Do pomiaru pobrano 1 ml anolitu z MFC i zawrócono bezpośrednio po pomiarze, aby zapobiec napowietrzaniu próbki i umożliwić lepsze jej uśrednienie.

3.5.2. Zdolność pienienia i stabilność piany

Zdolność pienienia i stabilność piany oceniono dla 20 mL odwirowanego i przefiltrowanego anolitu wytrząsając go ręcznie w probówce 50 mL przez 30 sekund. Następnie mierzono wysokość piany bezpośrednio po zakończeniu wytrząsania oraz po upływie 10 minut. Na podstawie uzyskanych wartości obliczono parametry według następujących równań:

Zdolność pienienia = $\pi \times r^2 \times h_0$,

Stabilność piany = h_{10}/h_0,

gdzie r – średnica naczynia pomiarowego; h_0 – początkowa wysokość piany; h_{10} – wysokość piany po 10 minutach.

3.5.3. Wskaźnik emulgacji (E24)

Wskaźnik emulgacji oznaczono przez dodanie 3 mL oleju roślinnego do probówki z 3 mL odwirowanego i przefiltrowanego anolitu. Mieszaninę wytrząsano energicznie przez 2 minuty i pozostawiono na 24 godziny. Wskaźnik emulgacji (E24) obliczono jako procentowy stosunek wysokości warstwy zemulgowanej do całkowitej wysokości słupa cieczy w probówce pomiarowej.

3.6. Ekstrakcja i oczyszczanie biosurfaktantów

Procedura przygotowania do izolacji biosurfaktantów polegała na odwirowaniu anolitów przez 10 minut przy prędkości 6000 obrotów na minutę. Następnie supernatant wstępnie pozbawiony mikroorganizmów filtrowano za pomocą sterylnego filtra strzykawkowego o średnicy porów 0.22 µm.

Do ekstrakcji i oczyszczenia biosurfaktantów wykorzystano metodę ekstrakcji do fazy stałej. Jako fazę stacjonarną zastosowano krzemionkę modyfikowaną grupami oktadecylowymi (CHROMABOND® C18, 3 mL, 500 mg). Procedurę rozpoczęto od kondycjonowania kolumny kolejno za pomocą 15 mL acetonitrylu, 3 mL metanolu i 3 mL wody. Następnie przez kolumnę przepuszczono próbkę, przemyto 3 ml wody i suszono kolumnę przez 10 minut w przepływie powietrza. Biosurfaktanty ekstrahowano przy użyciu 3 ml acetonitrylu. Rozpuszczalnik odparowano w temperaturze 40°C, otrzymując oczyszczone biosurfaktanty.

3.7. Chromatografia gazowa sprzężona ze spektrometrią mas (GC-MS)

Do analizy składu zużytego oleju roślinnego oraz anolitów po obróbce w MFC wykorzystano technikę GC-MS. Procedurę rozpoczęto od ekstrakcji w układzie ciecz-ciecz związków organicznych za pomocą dichlorometanu w środowisku obojętnym. Kolejno 2 µl otrzymanego ekstraktu analizowano na aparacie GC-MS (HP 6890-5973). Jako układ rozdzielający zastosowano kolumnę kapilarną HP-INNOWAX (Agilent

Technologies, USA) o średnicy wewnętrznej 0.25 mm i długości 30 m. Hel zastosowano jako gaz nośny przy natężeniu przepływu 0.7 ml min^{-1}. Program temperatury pieca ustawiono następująco: 40°C przez 5 min, następnie zwiększono do 240°C z szybkością 20°C min^{-1}, utrzymując temperaturę 240°C przez 20 min. Zakres skanowania masy cząsteczkowej ustawiono od 29 do 350 Da.

4. Bibliografia

[1] B. E. Logan *et al.*, "Microbial fuel cells: Methodology and technology," *Environ. Sci. Technol.*, vol. 40, no. 17, pp. 5181–5192, 2006, doi: 10.1021/es0605016.

[2] K. S. Aiyer, "How does electron transfer occur in microbial fuel cells?," *World J. Microbiol. Biotechnol.*, vol. 36, no. 2, pp. 1–9, 2020, doi: 10.1007/s11274-020-2801-z.

[3] L. Huang and I. Angelidaki, "Effect of humic acids on electricity generation integrated with xylose degradation in microbial fuel cells," *Biotechnol. Bioeng.*, vol. 100, no. 3, pp. 413–422, 2008, doi: 10.1002/bit.21786.

[4] M. Rahimnejad, G. D. Najafpour, A. A. Ghoreyshi, M. Shakeri, and H. Zare, "Methylene blue as electron promoters in microbial fuel cell," *Int. J. Hydrogen Energy*, vol. 36, no. 20, pp. 13335–13341, 2011, doi: 10.1016/j.ijhydene.2011.07.059.

[5] M. I. Rashid and S. Andleeb, "Pyocyanin yield improvement for enhancement of Pseudomonas aeruginosa inoculated Microbial Fuel Cell efficiency," *4th Int. Conf. Power Gener. Syst. Renew. Energy Technol. PGSRET 2018*, no. September, pp. 1–6, 2019, doi: 10.1109/PGSRET.2018.8685940.

[6] T. Lin, W. Ding, L. Sun, L. Wang, C. G. Liu, and H. Song, "Engineered Shewanella oneidensis-reduced graphene oxide biohybrid with enhanced biosynthesis and transport of flavins enabled a highest bioelectricity output in microbial fuel cells," *Nano Energy*, vol. 50, pp. 639–648, 2018, doi: 10.1016/j.nanoen.2018.05.072.

[7] W. Yang, J. Li, D. Ye, L. Zhang, X. Zhu, and Q. Liao, "A hybrid microbial fuel cell stack based on single and double chamber microbial fuel cells for self-sustaining pH control," *J. Power Sources*, vol. 306, pp. 685–691, 2016, doi: 10.1016/j.jpowsour.2015.12.073.

[8] P. Ledezma, A. Stinchcombe, J. Greenman, and I. Ieropoulos, "The first self-sustainable microbial fuel cell stack," *Phys. Chem. Chem. Phys.*, vol. 15, no. 7, pp. 2278–2281, 2013, doi: 10.1039/c2cp44548d.

[9] S. Mateo, A. Cantone, P. Cañizares, F. J. Fernández-Morales, O. Scialdone, and M. A. Rodrigo, "On the staking of miniaturized air-breathing microbial fuel cells," *Appl. Energy*, vol. 232, no. May, pp. 1–8, 2018, doi: 10.1016/j.apenergy.2018.09.213.

[10] X. A. Walter, A. Stinchcombe, J. Greenman, and I. Ieropoulos, "Urine transduction to usable energy: A modular MFC approach for smartphone and remote system charging," *Appl. Energy*, vol. 192, pp. 575–581, 2017, doi: 10.1016/j.apenergy.2016.06.006.

[11] R. Goswami and V. K. Mishra, "A review of design, operational conditions and applications of microbial fuel cells," *Biofuels*, vol. 9, no. 2, pp. 203–220, 2018, doi: 10.1080/17597269.2017.1302682.

[12] G. Palanisamy, H. Y. Jung, T. Sadhasivam, M. D. Kurkuri, S. C. Kim, and S. H. Roh, "A comprehensive review on microbial fuel cell technologies: Processes, utilization, and advanced developments in electrodes and membranes," *J. Clean. Prod.*, vol. 221, pp. 598–621, 2019, doi: 10.1016/j.jclepro.2019.02.172.

[13] X. Fan, Y. Zhou, X. Jin, R.-B. Song, Z. Li, and Q. Zhang, "Carbon material-based anodes in the microbial fuel cells," *Carbon Energy*, vol. 3, no. 3, pp. 449–472, Jul. 2021, doi: https://doi.org/10.1002/cey2.113.

[14] T. Kou, Y. Yang, B. Yao, and Y. Li, "Interpenetrated Bacteria-Carbon Nanotubes Film for Microbial Fuel Cells," *Small Methods*, vol. 2, no. 10, p. 1800152, Oct. 2018, doi: https://doi.org/10.1002/smtd.201800152.

[15] S. Qiu, Z. Guo, F. Naz, Z. Yang, and C. Yu, "An overview in the development of cathode materials for the improvement in power generation of microbial fuel cells," *Bioelectrochemistry*, vol. 141, p. 107834, 2021, doi: 10.1016/j.bioelechem.2021.107834.

[16] D. V. P. Sanchez, P. Huynh, M. E. Kozlov, R. H. Baughman, R. D. Vidic, and M. Yun, "Carbon nanotube/platinum (Pt) sheet as an improved cathode for microbial fuel cells," *Energy and Fuels*, vol. 24, no. 11, pp. 5897–5902, 2010, doi: 10.1021/ef100825h.

[17] P. Chatterjee, M. M. Ghangrekar, and D. Leech, "A brief review on recent advances in air-cathode microbial fuel cells," *Environ. Eng. Manag. J.*, vol. 17, no. 7, pp. 1531–1544, 2018, doi: 10.30638/eemj.2018.152.

[18] V. J. Watson, C. Nieto Delgado, and B. E. Logan, "Influence of Chemical and Physical Properties of Activated Carbon Powders on Oxygen Reduction and Microbial Fuel Cell Performance," *Environ. Sci. Technol.*, vol. 47, no. 12, pp. 6704–6710, Jun. 2013, doi: 10.1021/es401722j.

[19] H. Yuan, Y. Hou, I. M. Abu-Reesh, J. Chen, and Z. He, "Oxygen reduction reaction catalysts used in microbial fuel cells for energy-efficient wastewater treatment: A review," *Mater. Horizons*, vol. 3, no. 5, pp. 382–401, 2016, doi: 10.1039/c6mh00093b.

[20] Z. Wang *et al.*, "The influence and mechanism of different acid treatment to activated carbon used as air-breathing cathode catalyst of microbial fuel cell," *Electrochim. Acta*, vol. 246, pp. 830–840, 2017, doi: 10.1016/j.electacta.2017.05.086.

[21] H. Dong, H. Yu, H. Yu, N. Gao, and X. Wang, “Enhanced performance of activated carbon-polytetrafluoroethylene air-cathode by avoidance of sintering on catalyst layer in microbial fuel cells,” *J. Power Sources*, vol. 232, pp. 132–138, 2013, doi: 10.1016/j.jpowsour.2013.01.036.

[22] A. De Rosset, P. Rutkowski, and G. Pasternak, “The effect of surface and porous structure on long-term performance of carbon powder cathodes without binder , during a 300-day trial in microbial fuel cells,” *Sustain. Energy Technol. Assessments*, vol. 58, no. April, p. 103340, 2023, doi: 10.1016/j.seta.2023.103340.

[23] G. Pasternak, J. Greenman, and I. Ieropoulos, “Comprehensive Study on Ceramic Membranes for Low-Cost Microbial Fuel Cells,” *ChemSusChem*, vol. 9, no. 1, pp. 88–96, 2016, doi: 10.1002/cssc.201501320.

[24] G. Pasternak, A. de Rosset, N. Tyszkiewicz, B. Widera, J. Greenman, and I. Ieropoulos, “Prevention and removal of membrane and separator biofouling in bioelectrochemical systems: a comprehensive review,” *iScience*, vol. 25, no. 7, p. 104510, 2022, doi: 10.1016/j.isci.2022.104510.

[25] A. N. Ghadge and M. M. Ghangrekar, “Development of low cost ceramic separator using mineral cation exchanger to enhance performance of microbial fuel cells,” *Electrochim. Acta*, vol. 166, pp. 320–328, 2015, doi: 10.1016/j.electacta.2015.03.105.

[26] I. Das, M. M. Ghangrekar, R. Satyakam, P. Srivastava, S. Khan, and H. N. Pandey, “On-Site Sanitary Wastewater Treatment System Using 720-L Stacked Microbial Fuel Cell: Case Study,” *J. Hazardous, Toxic, Radioact. Waste*, vol. 24, no. 3, pp. 1–7, 2020, doi: 10.1061/(asce)hz.2153-5515.0000518.

[27] A. Raychaudhuri and M. Behera, “Ceramic membrane modified with rice husk ash for application in microbial fuel cells,” *Electrochim. Acta*, vol. 363, p. 137261, 2020, doi: 10.1016/j.electacta.2020.137261.

[28] G. Pasternak, N. Ormeno-Cano, and P. Rutkowski, “Recycled waste polypropylene composite ceramic membranes for extended lifetime of microbial fuel cells,” *Chem. Eng. J.*, p. 130707, Jun. 2021, doi: 10.1016/J.CEJ.2021.130707.

[29] A. de Rosset, F. Yalcinkaya, J. Wolska, S. Wacławek, and G. Pasternak, “Enhancing performance and durability of PVDF-ceramic composite membranes in microbial fuel cells using natural rhamnolipids,” *J. Power Sources*, vol. 621, no. January, p. 235257, Nov. 2024, doi: 10.1016/j.jpowsour.2024.235257.

[30] G. Pasternak, J. Greenman, and I. Ieropoulos, “Dynamic evolution of anodic biofilm when maturing under different external resistive loads in microbial fuel cells. Electrochemical perspective,” *J. Power Sources*, vol. 400, no. August, pp. 392–401, 2018, doi: 10.1016/j.jpowsour.2018.08.031.

[31] X. A. Walter, S. Forbes, J. Greenman, and I. A. Ieropoulos, “From single MFC to cascade configuration: The relationship between size, hydraulic retention time and power density,” *Sustain. Energy Technol. Assessments*, vol. 14, pp. 74–79, 2016, doi: 10.1016/j.seta.2016.01.006.

[32] S. Cheng, H. Liu, and B. E. Logan, “Increased Power Generation in a Continuous Flow MFC with Advective Flow through the Porous Anode and Reduced Electrode Spacing,” *Environ. Sci. Technol.*, vol. 40, no. 7, pp. 2426–2432, Apr. 2006, doi: 10.1021/es051652w.

[33] S. Cheng and B. E. Logan, “Increasing power generation for scaling up single-chamber air cathode microbial fuel cells,” *Bioresour. Technol.*, vol. 102, no. 6, pp. 4468–4473, 2011, doi: 10.1016/j.biortech.2010.12.104.

[34] S. E. Oh and B. E. Logan, “Proton exchange membrane and electrode surface areas as factors that affect power generation in microbial fuel cells,” *Appl. Microbiol. Biotechnol.*, vol. 70, no. 2, pp. 162–169, 2006, doi: 10.1007/s00253-005-0066-y.

[35] G. Pasternak, A. de Rosset, and P. Rutkowski, “Horizontal microbial fuel cell system producing biosurfactants in response to current generation from waste cooking oil as a fuel,” *Energy Convers. Manag.*, vol. 281, no. March, p. 116807, 2023, doi: 10.1016/j.enconman.2023.116807.

[36] M. Aghababaie, M. Farhadian, A. Jeihanipour, and D. Biria, “Effective factors on the performance of microbial fuel cells in wastewater treatment–a review,” *Environ. Technol. Rev.*, vol. 4, no. 1, pp. 71–89, 2015, doi: 10.1080/09593330.2015.1077896.

[37] A. Tremouli, M. Martinos, and G. Lyberatos, “The Effects of Salinity, pH and Temperature on the Performance of a Microbial Fuel Cell,” *Waste and Biomass Valorization*, vol. 8, no. 6, pp. 2037–2043, 2017, doi: 10.1007/s12649-016-9712-0.

[38] A. Larrosa-Guerrero, K. Scott, I. M. Head, F. Mateo, A. Ginesta, and C. Godinez, “Effect of temperature on the performance of microbial fuel cells,” *Fuel*, vol. 89, no. 12, pp. 3985–3994, 2010, doi: 10.1016/j.fuel.2010.06.025.

[39] I. S. Michie, J. R. Kim, R. M. Dinsdale, A. J. Guwy, and G. C. Premier, “The influence of psychrophilic and mesophilic start-up temperature on microbial fuel cell system performance,” *Energy Environ. Sci.*, vol. 4, no. 3, pp. 1011–1019, 2011, doi: 10.1039/c0ee00483a.

[40] S. Puig, M. Serra, M. Coma, M. Cabré, M. D. Balaguer, and J. Colprim, “Effect of pH on nutrient dynamics and electricity production using microbial fuel cells,” *Bioresour. Technol.*, vol. 101, no. 24, pp. 9594–9599, 2010, doi: 10.1016/j.biortech.2010.07.082.

[41] O. Lefebvre, Z. Tan, S. Kharkwal, and H. Y. Ng, “Effect of increasing anodic NaCl concentration on microbial fuel cell performance,” *Bioresour. Technol.*, vol. 112, pp. 336–340, 2012, doi: 10.1016/j.biortech.2012.02.048.

[42] L. Zhang, X. Zhu, J. Li, Q. Liao, and D. Ye, “Biofilm formation and electricity generation of a microbial fuel cell started up under different external resistances,” *J. Power Sources*, vol. 196, no. 15, pp. 6029–6035, 2011, doi: 10.1016/j.jpowsour.2011.04.013.

[43] P. Aelterman, M. Versichele, M. Marzorati, N. Boon, and W. Verstraete, "Loading rate and external resistance control the electricity generation of microbial fuel cells with different three-dimensional anodes," *Bioresour. Technol.*, vol. 99, no. 18, pp. 8895–8902, 2008, doi: 10.1016/j.biortech.2008.04.061.

[44] A. S. Mathuriya, "Inoculum selection to enhance performance of a microbial fuel cell for electricity generation during wastewater treatment," *Environ. Technol. (United Kingdom)*, vol. 34, no. 13–14, pp. 1957–1964, 2013, doi: 10.1080/09593330.2013.808674.

[45] C. Gao, A. Wang, W. M. Wu, Y. Yin, and Y. G. Zhao, "Enrichment of anodic biofilm inoculated with anaerobic or aerobic sludge in single chambered air-cathode microbial fuel cells," *Bioresour. Technol.*, vol. 167, pp. 124–132, 2014, doi: 10.1016/j.biortech.2014.05.120.

[46] S. Firdous *et al.*, "The performance of microbial fuel cells treating vegetable oil industrial wastewater," *Environ. Technol. Innov.*, vol. 10, pp. 143–151, 2018, doi: 10.1016/j.eti.2018.02.006.

[47] N. Yu *et al.*, "Electricity and methane production from soybean edible oil refinery wastewater using microbial electrochemical systems," *Int. J. Hydrogen Energy*, vol. 42, no. 1, pp. 96–102, 2017, doi: 10.1016/j.ijhydene.2016.11.116.

[48] B. Ahansazan, H. Afrashteh, N. Ahansazan, and Z. Ahansazan, "Activated Sludge Process Overview," *Int. J. Environ. Sci. Dev.*, vol. 5, no. 1, pp. 81–85, 2014, doi: 10.7763/IJESD.2014.V5.455.

[49] V. G. Gude, "Wastewater treatment in microbial fuel cells - An overview," *J. Clean. Prod.*, vol. 122, pp. 287–307, 2016, doi: 10.1016/j.jclepro.2016.02.022.

[50] A. T. Hoang *et al.*, "Microbial fuel cells for bioelectricity production from waste as sustainable prospect of future energy sector," *Chemosphere*, vol. 287, no. June 2021, 2022, doi: 10.1016/j.chemosphere.2021.132285.

[51] Y. Cui, B. Lai, and X. Tang, "Microbial fuel cell-based biosensors," *Biosensors*, vol. 9, no. 3, pp. 1–18, 2019, doi: 10.3390/bios9030092.

[52] M. H. Do *et al.*, "Microbial fuel cell-based biosensor for online monitoring wastewater quality: A critical review," *Sci. Total Environ.*, vol. 712, p. 135612, 2020, doi: 10.1016/j.scitotenv.2019.135612.

[53] G. Pasternak, J. Greenman, and I. Ieropoulos, "Self-powered, autonomous Biological Oxygen Demand biosensor for online water quality monitoring," *Sensors Actuators, B Chem.*, vol. 244, pp. 815–822, 2017, doi: 10.1016/j.snb.2017.01.019.

[54] J. Chouler, Á. Cruz-Izquierdo, S. Rengaraj, J. L. Scott, and M. Di Lorenzo, "A screen-printed paper microbial fuel cell biosensor for detection of toxic compounds in water," *Biosens. Bioelectron.*, vol. 102, no. September 2017, pp. 49–56, 2018, doi: 10.1016/j.bios.2017.11.018.

[55] K. P. Nevin *et al.*, “Electrosynthesis of organic compounds from carbon dioxide is catalyzed by a diversity of acetogenic microorganisms,” *Appl. Environ. Microbiol.*, vol. 77, no. 9, pp. 2882–2886, 2011, doi: 10.1128/AEM.02642-10.

[56] E. Blanchet, F. Duquenne, Y. Rafrafi, L. Etcheverry, B. Erable, and A. Bergel, “Importance of the hydrogen route in up-scaling electrosynthesis for microbial CO2 reduction,” *Energy Environ. Sci.*, vol. 8, no. 12, pp. 3731–3744, 2015, doi: 10.1039/c5ee03088a.

[57] S. Bajracharya, S. Srikanth, G. Mohanakrishna, R. Zacharia, D. P. Strik, and D. Pant, “Biotransformation of carbon dioxide in bioelectrochemical systems: State of the art and future prospects,” *J. Power Sources*, vol. 356, pp. 256–273, 2017, doi: 10.1016/j.jpowsour.2017.04.024.

[58] A. S. Finch, T. D. Mackie, C. J. Sund, and J. J. Sumner, “Metabolite analysis of Clostridium acetobutylicum: Fermentation in a microbial fuel cell,” *Bioresour. Technol.*, vol. 102, no. 1, pp. 312–315, 2011, doi: 10.1016/j.biortech.2010.06.149.

[59] A. M. Lakaniemi, O. H. Tuovinen, and J. A. Puhakka, “Production of electricity and butanol from microalgal biomass in microbial fuel cells,” *Bioenergy Res.*, vol. 5, no. 2, pp. 481–491, 2012, doi: 10.1007/s12155-012-9186-2.

[60] A. H. Förster, S. Beblawy, F. Golitsch, and J. Gescher, “Electrode-assisted acetoin production in a metabolically engineered Escherichia coli strain,” *Biotechnol. Biofuels*, 2017, doi: 10.1186/s13068-017-0745-9.

[61] G. Pasternak, T. D. Askitosari, and M. A. Rosenbaum, “Biosurfactants and Synthetic Surfactants in Bioelectrochemical Systems : A Mini-Review Influence on Electron Transfer,” vol. 11, no. March, pp. 1–9, 2020, doi: 10.3389/fmicb.2020.00358.

[62] S. Rebello, A. K. Asok, S. Mundayoor, and M. S. Jisha, “Surfactants: Toxicity, remediation and green surfactants,” *Environ. Chem. Lett.*, vol. 12, no. 2, pp. 275–287, 2014, doi: 10.1007/s10311-014-0466-2.

[63] A. M. Abdel-Mawgoud, M. M. Aboulwafa, and N. A. H. Hassouna, “Characterization of rhamnolipid produced by pseudomonas aeruginosa isolate Bs20,” *Appl. Biochem. Biotechnol.*, vol. 157, no. 2, pp. 329–345, 2009, doi: 10.1007/s12010-008-8285-1.

[64] A. M. Abdel-Mawgoud, M. M. Aboulwafa, and N. A. H. Hassouna, “Characterization of surfactin produced by bacillus subtilis isolate BS5,” *Appl. Biochem. Biotechnol.*, vol. 150, no. 3, pp. 289–303, 2008, doi: 10.1007/s12010-008-8153-z.

[65] C. Uzoigwe, J. G. Burgess, C. J. Ennis, and P. K. S. M. Rahman, “Bioemulsifiers are not biosurfactants and require different screening approaches,” *Front. Microbiol.*, vol. 6, no. APR, pp. 1–6, 2015, doi: 10.3389/fmicb.2015.00245.

[66] R. Hausmann and C. Syldatk, “Types and Classification of Microbial Surfactants,” in *Biosurfactants: production and utilization—processes, technologies, and economics*, CRC Press, 2014, pp. 3–19.

[67] M. M. Müller *et al.*, “Rhamnolipids-Next generation surfactants?,” *J. Biotechnol.*, vol. 162, no. 4, pp. 366–380, 2012, doi: 10.1016/j.jbiotec.2012.05.022.

[68] A. M. Abdel-Mawgoud, F. Lépine, and E. Déziel, “Rhamnolipids: Diversity of structures, microbial origins and roles,” *Appl. Microbiol. Biotechnol.*, vol. 86, no. 5, pp. 1323–1336, 2010, doi: 10.1007/s00253-010-2498-2.

[69] G. S. El-Housseiny, K. M. Aboshanab, M. M. Aboulwafa, and N. A. Hassouna, “Structural and Physicochemical Characterization of Rhamnolipids produced by Pseudomonas aeruginosa P6,” *AMB Express*, vol. 10, no. 1, 2020, doi: 10.1186/s13568-020-01141-0.

[70] R. Sen, “Biotechnology in petroleum recovery: The microbial EOR,” *Prog. Energy Combust. Sci.*, vol. 34, no. 6, pp. 714–724, 2008, doi: 10.1016/j.pecs.2008.05.001.

[71] H. Ghojavand, F. Vahabzadeh, and A. K. Shahraki, “Enhanced oil recovery from low permeability dolomite cores using biosurfactant produced by a Bacillus mojavensis (PTCC 1696) isolated from Masjed-I Soleyman field,” *J. Pet. Sci. Eng.*, vol. 81, pp. 24–30, 2012, doi: 10.1016/j.petrol.2011.12.002.

[72] J. M. D. A. Câmara, M. A. S. B. Sousa, E. L. Barros Neto, and M. C. A. Oliveira, “Application of rhamnolipid biosurfactant produced by Pseudomonas aeruginosa in microbial-enhanced oil recovery (MEOR),” *J. Pet. Explor. Prod. Technol.*, vol. 9, no. 3, pp. 2333–2341, 2019, doi: 10.1007/s13202-019-0633-x.

[73] F. Peng, Z. Liu, L. Wang, and Z. Shao, “An oil-degrading bacterium: Rhodococcus erythropolis strain 3C-9 and its biosurfactants,” *J. Appl. Microbiol.*, vol. 102, no. 6, pp. 1603–1611, 2007, doi: 10.1111/j.1365-2672.2006.03267.x.

[74] N. K. Bordoloi and B. K. Konwar, “Bacterial biosurfactant in enhancing solubility and metabolism of petroleum hydrocarbons,” *J. Hazard. Mater.*, vol. 170, no. 1, pp. 495–505, 2009, doi: 10.1016/j.jhazmat.2009.04.136.

[75] P. Das, S. Mukherjee, and R. Sen, “Improved bioavailability and biodegradation of a model polyaromatic hydrocarbon by a biosurfactant producing bacterium of marine origin,” *Chemosphere*, vol. 72, no. 9, pp. 1229–1234, 2008, doi: 10.1016/j.chemosphere.2008.05.015.

[76] H. Yin *et al.*, “Characteristics of biosurfactant produced by Pseudomonas aeruginosa S6 isolated from oil-containing wastewater,” *Process Biochem.*, vol. 44, no. 3, pp. 302–308, 2009, doi: 10.1016/j.procbio.2008.11.003.

[77] S. N. R. L. Silva, C. B. B. Farias, R. D. Rufino, J. M. Luna, and L. A. Sarubbo, “Glycerol as substrate for the production of biosurfactant by Pseudomonas aeruginosa UCP0992,” *Colloids Surfaces B Biointerfaces*, vol. 79, no. 1, pp. 174–183, 2010, doi: 10.1016/j.colsurfb.2010.03.050.

[78] S. Sharma, P. Datta, B. Kumar, P. Tiwari, and L. M. Pandey, “Production of novel rhamnolipids via biodegradation of waste cooking oil using Pseudomonas aeruginosa MTCC7815,” *Biodegradation*, vol. 30, no. 4, pp. 301–312, 2019, doi: 10.1007/s10532-019-09874-x.

[79] R. Verma, S. Sharma, L. M. Kundu, and L. M. Pandey, “Experimental investigation of molasses as a sole nutrient for the production of an alternative metabolite biosurfactant,” *J. Water Process Eng.*, vol. 38, no. July, p. 101632, 2020, doi: 10.1016/j.jwpe.2020.101632.

[80] C. Chen *et al.*, “Optimization and characterization of biosurfactant production from kitchen waste oil using Pseudomonas aeruginosa,” pp. 14934–14943, 2018.

[81] E. F. Santos, M. F. S. Teixeira, A. Converti, A. L. F. Porto, and L. A. Sarubbo, “Production of a new lipoprotein biosurfactant by Streptomyces sp. DPUA1566 isolated from lichens collected in the Brazilian Amazon using agroindustry wastes,” *Biocatal. Agric. Biotechnol.*, vol. 17, no. October 2018, pp. 142–150, 2019, doi: 10.1016/j.bcab.2018.10.014.

[82] W. Sun *et al.*, “Optimization of biosurfactant production from Pseudomonas sp. CQ2 and its application for remediation of heavy metal contaminated soil,” *Chemosphere*, vol. 265, p. 129090, 2021, doi: 10.1016/j.chemosphere.2020.129090.

[83] P. Bongartz *et al.*, “A scalable bubble-free membrane aerator for biosurfactant production,” *Biotechnol. Bioeng.*, vol. 118, no. 9, pp. 3545–3558, 2021, doi: 10.1002/bit.27822.

[84] P. L. Fernandes, E. M. Rodrigues, F. R. Paiva, B. A. L. Ayupe, M. J. McInerney, and M. R. Tótola, “Biosurfactant, solvents and polymer production by Bacillus subtilis RI4914 and their application for enhanced oil recovery,” *Fuel*, vol. 180, pp. 551–557, 2016, doi: 10.1016/j.fuel.2016.04.080.

[85] M. Ozdal, S. Gurkok, and O. G. Ozdal, “Optimization of rhamnolipid production by Pseudomonas aeruginosa OG1 using waste frying oil and chicken feather peptone,” *3 Biotech*, vol. 7, no. 2, pp. 1–8, 2017, doi: 10.1007/s13205-017-0774-x.

[86] G. Lan *et al.*, “Rhamnolipid production from waste cooking oil using Pseudomonas SWP-4,” *Biochem. Eng. J.*, vol. 101, pp. 44–54, 2015, doi: 10.1016/j.bej.2015.05.001.

[87] Q. Wu, Y. Zhi, and Y. Xu, “Systematically engineering the biosynthesis of a green biosurfactant surfactin by Bacillus subtilis 168,” *Metab. Eng.*, vol. 52, no. November 2018, pp. 87–97, 2019, doi: 10.1016/j.ymben.2018.11.004.

[88] J. Willenbacher, M. Zwick, T. Mohr, F. Schmid, C. Syldatk, and R. Hausmann, “Evaluation of different Bacillus strains in respect of their ability to produce Surfactin in a model fermentation process with integrated foam fractionation,” *Appl. Microbiol. Biotechnol.*, vol. 98, no. 23, pp. 9623–9632, 2014, doi: 10.1007/s00253-014-6010-2.

[89] J. Beuker, A. Steier, A. Wittgens, F. Rosenau, M. Henkel, and R. Hausmann, "Integrated foam fractionation for heterologous rhamnolipid production with recombinant Pseudomonas putida in a bioreactor," *AMB Express*, vol. 6, no. 1, pp. 1–10, 2016, doi: 10.1186/s13568-016-0183-2.

[90] B. Behrens, J. Engelen, T. Tiso, L. M. Blank, and H. Hayen, "Characterization of rhamnolipids by liquid chromatography/mass spectrometry after solid-phase extraction," *Anal. Bioanal. Chem.*, vol. 408, no. 10, pp. 2505–2514, 2016, doi: 10.1007/s00216-016-9353-y.

[91] K. Guo *et al.*, "Effects of Surface Charge and Hydrophobicity on Anodic Biofilm Formation, Community Composition, and Current Generation in Bioelectrochemical Systems," *Environ. Sci. Technol.*, vol. 47, no. 13, pp. 7563–7570, Jul. 2013, doi: 10.1021/es400901u.

[92] Y. Zhang *et al.*, "Accelerating anodic biofilms formation and electron transfer in microbial fuel cells: Role of anionic biosurfactants and mechanism," *Bioelectrochemistry*, vol. 117, pp. 48–56, 2017, doi: 10.1016/j.bioelechem.2017.06.002.

[93] Y.-C. Song, D.-S. Kim, J.-H. Woo, B. Subha, S.-H. Jang, and S. Sivakumar, "Effect of surface modification of anode with surfactant on the performance of microbial fuel cell," *Int. J. Energy Res.*, vol. 39, no. 6, pp. 860–868, May 2015, doi: https://doi.org/10.1002/er.3284.

[94] C. Sánchez, "A review of the role of biosurfactants in the biodegradation of hydrophobic organopollutants: production, mode of action, biosynthesis and applications," *World J. Microbiol. Biotechnol.*, vol. 38, no. 11, pp. 1–24, 2022, doi: 10.1007/s11274-022-03401-6.

[95] R. Kumar, L. Singh, and A. W. Zularisam, "Exoelectrogens: Recent advances in molecular drivers involved in extracellular electron transfer and strategies used to improve it for microbial fuel cell applications," *Renew. Sustain. Energy Rev.*, vol. 56, pp. 1322–1336, 2016, doi: 10.1016/j.rser.2015.12.029.

[96] L. Ren, J. C. Tokash, J. M. Regan, and B. E. Logan, "Current generation in microbial electrolysis cells with addition of amorphous ferric hydroxide, Tween 80, or DNA," *Int. J. Hydrogen Energy*, vol. 37, no. 22, pp. 16943–16950, 2012, doi: 10.1016/j.ijhydene.2012.08.119.

[97] H. B. Shen *et al.*, "Enhanced bioelectricity generation by improving pyocyanin production and membrane permeability through sophorolipid addition in pseudomonas aeruginosa-inoculated microbial fuel cells," *Bioresour. Technol.*, vol. 167, pp. 490–494, 2014, doi: 10.1016/j.biortech.2014.05.093.

[98] P. Cheng, R. Shan, H.-R. Yuan, G. Dong, L. Deng, and Y. Chen, "Improved performance of microbial fuel cells through addition of trehalose lipids," *bioRxiv*, p. 339267, Jan. 2018, doi: 10.1101/339267.

[99] A. de Rosset *et al.*, "Bioelectrochemical synthesis of rhamnolipids and energy production and its correlation with nitrogen in air-cathode microbial fuel cells," *J. Environ. Manage.*, vol. 365, no. February, 2024, doi: 10.1016/j.jenvman.2024.121514.

[100] T. Zheng *et al.*, “Endogenously enhanced biosurfactant production promotes electricity generation from microbial fuel cells,” *Bioresour. Technol.*, vol. 197, pp. 416–421, 2015, doi: 10.1016/j.biortech.2015.08.136.

[101] K. Sharma, V. Singh, S. Pandit, B. Sen Thapa, K. Pant, and T. R. Tusher, “Isolation of Biosurfactant-Producing Bacteria and Their Co-Culture Application in Microbial Fuel Cell for Simultaneous Hydrocarbon Degradation and Power Generation,” *Sustain.*, vol. 14, no. 23, 2022, doi: 10.3390/su142315638.

[102] T. H. Pham *et al.*, “Metabolites produced by Pseudomonas sp. enable a Gram-positive bacterium to achieve extracellular electron transfer,” *Appl. Microbiol. Biotechnol.*, vol. 77, no. 5, pp. 1119–1129, 2008, doi: 10.1007/s00253-007-1248-6.

[103] J. Liu, C. Vipulanandan, and M. Yang, “Biosurfactant Production from Used Vegetable Oil in the Anode Chamber of a Microbial Electrosynthesizing Fuel Cell,” *Waste and Biomass Valorization*, vol. 10, no. 10, pp. 2925–2931, 2019, doi: 10.1007/s12649-018-0331-9.

[104] T. Naaz *et al.*, “Bioremediation of hydrocarbon by co-culturing of biosurfactant-producing bacteria in microbial fuel cell with Fe2O3-modified anode,” *J. Environ. Manage.*, vol. 351, no. December 2023, p. 119768, 2024, doi: 10.1016/j.jenvman.2023.119768.

[105] J. Liu and C. Vipulanandan, “Effects of Fe, Ni, and Fe/Ni metallic nanoparticles on power production and biosurfactant production from used vegetable oil in the anode chamber of a microbial fuel cell,” *Waste Manag.*, vol. 66, pp. 169–177, 2017, doi: 10.1016/j.wasman.2017.04.004.

5. Publikacje będące wynikiem pracy doktorskiej

5.1. The effect of surface and porous structure on long-term performance of carbon powder cathodes without binder, during a 300-day trial in microbial fuel cells

5.1.1. Omówienie publikacji

Materiał katody jest kluczowym czynnikiem ograniczającym wydajność większości konfiguracji MFC z katoda powietrzną. Składnikiem zmniejszającym energię aktywacji ORR w najbardziej wydajnych katodach jest platyna. Jednak jej wysoki koszt w połączeniu ze słabą stabilnością w obecności zanieczyszczeń w ściekach spowodowały, że opracowano nowe katalizatory katodowe zastępujące platynę, wśród których uwagę stale przyciąga węgiel aktywny ze względu na niski koszt, dużą powierzchnię właściwą, dobre właściwości katalityczne i łatwość modyfikacji. Ponadto węgiel aktywny można otrzymać z wielu prekursorów, w tym z odpadów spożywczych i poprzemysłowych. Dotychczas wielokrotnie opisywano zastosowanie węgli aktywnych jako materiałów katodowych w MFC oraz kilka podejść do jego modyfikacji, jednak pełne zrozumienie wpływu powierzchni węgla aktywnego na długoterminową aktywność ORR wymaga dokładnej charakterystyki jego porowatości.

W badaniu oceniono działanie dwóch różnych typów węgli aktywnych jako materiałów katody powietrznej w MFC i wpływ modyfikacji nanocząsteczkami krzemionki na właściwości długoterminowe, oraz skorelowano wyniki eksperymentalne z charakterystyką powierzchni zastosowanych materiałów.

W pracy zastosowano MFC z katodą powietrzną wydrukowane w 3D z polipropylenu. Katody wykonano z trzech rodzajów materiałów węglowych: dostępnych komercyjnie węgli aktywnych CWZ-22 i CWZ-35 oraz CWZ-22 modyfikowanego poprzez zmieszanie z mikroemulsją silanowo-siloksanową do osiągnięcia 1.8% (w/w). Wszystkie MFC zainokulowano osadem czynnym z komory tlenowej oczyszczalni ścieków. Po okresie inokulacji komorę anodową MFC zasilano w systemie wsadowym pożywką zawierającą octan sodu jako źródło węgla dla mikroorganizmów. W prawie rocznej eksploatacji skuteczność i stabilność materiałów katodowych oceniono za pomocą badań elektrochemicznych, charakterystyki właściwości powierzchniowych i strukturalnych oraz analizy termograwimetrycznej, dostarczając informacji na temat długotrwałego działania i zanieczyszczenia tanich, dostępnych na rynku materiałów katodowych do MFC.

Monitorowanie wydajności produkcji energii elektrycznej w MFC wykazało, że węgiel aktywny CWZ-35 o najwyższej w tym zestawieniu powierzchni właściwej uzyskał najbardziej intensywny wzrost produkowanej gęstości mocy w ciągu pierwszych 3 miesięcy działania. Jednak w kolejnym okresie odnotowano spadek wydajności prądowej i trend ten utrzymywał się już do końca trwania eksperymentu.

W przeciwieństwie do tych wyników CWZ-22 o niższej powierzchni właściwej, ale jednocześnie węższym zakresie porów i dominacji porów o średnicy poniżej 1 nm wykazał najwyższa w tym doświadczeniu maksymalną gęstość mocy (30.7 W m^{-3}) oraz wysoce stabilną wydajność produkowanej energii elektrycznej do końca trwania eksperymentu. Pomimo zbliżonej wydajności i stabilności CWZ-22/Si, analiza krzywych polaryzacji nie wykazała pozytywnego wpływu domieszkowania nanocząsteczkami krzemionki na wydajność mocy i jej właściwości długoterminowe. Ponadto analiza elektrochemicznej spektroskopii impedancyjnej oraz ocena zanieczyszczenia materiałów katodowych solami nieorganicznymi wykazała, że elektroosmoza umiarkowanej ilości soli z anolitu do katody miała pozytywny wpływ na wydajność katod CWZ-22 i CWZ-22/Si. Natomiast doprowadziła do szybkiego wzrostu rezystancji katody CWZ-35.

Podsumowując, w badaniu wykazano, że niemodyfikowany, tani i dostępny w handlu węgiel aktywny CWZ-22 bez spoiwa jest lepszym wyborem pod względem długotrwałej eksploatacji niż silnie porowaty i droższy węgiel aktywny CWZ-35. Wyniki pokazały, że rozkład wielkości porów i wynikająca z niego podatność na zanieczyszczenia chemiczne jest kluczowym czynnikiem decydującym o utrzymaniu wysokiej wydajności układu MFC, który ma być eksploatowany przez lata.

5.1.2. Publikacja

Sustainable Energy Technologies and Assessments 58 (2023) 103340

Contents lists available at ScienceDirect

Sustainable Energy Technologies and Assessments

journal homepage: www.elsevier.com/locate/seta

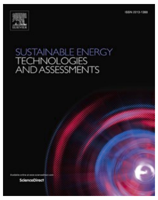

The effect of surface and porous structure on long-term performance of carbon powder cathodes without binder, during a 300-day trial in microbial fuel cells

Aleksander de Rosset [1], Piotr Rutkowski, Grzegorz Pasternak [*], [1]

Department of Process Engineering and Technology of Polymer and Carbon Materials, Faculty of Chemistry, Wroclaw University of Science and Technology, Wroclaw 50-370, Poland

ARTICLE INFO

Keywords:
Microbial fuel cell
Activated carbon
Cathode
Long-term
Porosity

ABSTRACT

The performance of microbial fuel cell (MFC) highly depends on the selection of appropriate electrode materials, in particular – cathodes. Herein, two different activated carbons (CWZ-22 and CWZ-35) without binder, as well as the activated carbon modified with silica nanoparticles (CWZ-22/Si), were used to improve the performance of air cathodes. Nearly one year of operation of materials varying in surface area and microporous structure revealed significant differences in their dynamic behaviour. CWZ-22 with lower surface area and a smaller micropore size, reached an internal resistance (R_{int}) of 162 Ω, and a maximum power density of 23.3 W m^{-3}. CWZ-22/Si, coated with silane-siloxane-based silicone microemulsion displayed a drop of maximum power generation by 10%. CWZ-35, with higher surface area, but also higher micropore size, displayed 22.8 W m^{-3} and R_{int} of 159 Ω. The monitoring of electrochemical and performance parameters indicated an improved long-term behaviour of the cathodes in the following order: CWZ-22 > CWZ-22/Si > CWZ-35. This is the first work in which the pore size distribution and surface area are demonstrated to have a long-term impact on cathodic fouling, and, depending on these properties, this impact may be either positive or negative on MFC performance.

Introduction

The perspective of fossil fuel consumption in the world and the impact of its use on the environment, human health, and life safety force the search for alternative energy sources [1]. In recent years, the growing role of renewable energy has become one of the key factors for the sustainable development of society [2]. Therefore, greener and more economical renewable energy sources have received additional attention. Another problem resulting from rapid industrialisation and the development of advanced technologies is the pollution of the environment, especially water [3].

The microbial fuel cell (MFC) is a bioelectrochemical reactor in which organic matter is oxidised by electroactive bacteria and converted to electricity [4]. The typical MFC design comprises anode and cathode compartments, while more practical MFC designs use an air–cathode instead of a cathodic chamber. The air–cathode MFC consists of an anode chamber, separator, and cathode material in direct contact with air [5]. The advantages of MFC technology compared to fossil fuels are the direct conversion of organic matter into electricity, the possibility of using a wide range of organic substrates [6], and the adaptability to complex matrices such as soil [7]. In addition, the efficiency of bioenergy recovery from wastewater in MFCs can reach values greater than 80%, which is impossible to achieve with fossil fuel combustion [8]. Furthermore, MFC technology allows the simultaneous treatment of wastewater and generation of electricity, which brings both economic and environmental benefits [9].

In recent years, multiple pilot studies have emerged, in which MFCs were tested to treat urine [10], domestic [11], swine [12] and brewery [13] wastewater. In many cases, these studies were carried out over a short-term period of days rather than months. However, some examples of long-term studies have also been reported. Long-term operation usually shows deterioration of the performance in time, such as reported by Liang et al. [14] (from 125 to 50 W/m^3, over one year period). This performance drop is associated with multiple factors, among which fouling and biofouling of the cathode is probably the most impactful. It may lead to such a serious deterioration of the performance as more than

---

[*] Corresponding author.
E-mail address: grzegorz.pasternak@pwr.edu.pl (G. Pasternak).

[1] www.gplab.eu - Laboratory of Microbial Electrochemical Systems.

https://doi.org/10.1016/j.seta.2023.103340
Received 14 April 2023; Received in revised form 13 June 2023; Accepted 16 June 2023

90% in long-term operation leading to undertaking an adequate measures that have to be taken to regenerate the power performance [15]. This can be also associated to the salt accumulation, such as carbonates within the cathode structure [16]. Nevertheless, this often likely to be a synergistic effect of both, the biofilm, and chemicals. Various strategies can be implemented to limit the deteriorating effect of undesirable biofilm over the surface of functional MFC materials. These strategies have been recently reviewed by Pasternak et al. [17].

The cathode material is, in most configurations with an air–cathode, the key limiting factor in MFC performance. The component that decreases the activation energy of oxygen reduction reaction (ORR) in the most efficient cathodes is platinum. However, its high cost, combined with poor stability in the presence of contaminants in wastewater, resulted in the development of new cathode catalysts to replace platinum [18]. Among various cathodic catalysts, activated carbon (AC) is constantly attracting attention due to its low cost, large surface area, good catalytic properties, and ease of modification [19]. Furthermore, AC can be obtained from many precursors, including food and post-industrial wastes [20,21]. The use of AC as a cathode material and several approaches of modifications were described so far. The abundance of active sites for the ORR is a key parameter that affects the cathode efficiency. One solution to improve the MFC performance is to increase the size of the cathode [22]. As an example, Oh and Logan showed that a 200% increase in power could be obtained by increasing the cathode geometric surface by 175% [23]. Another way to improve the performance of the AC cathode is to modify its catalytic activity, for example, by increasing the specific surface area of AC. However, a full understanding of the effect of the AC surface on ORR activity requires study of the specific surface area and pore size distribution. These are one of the key parameters that also affect the performance of other functional elements of MFCs such as membranes and anodes [17,24]. As previously shown in short-term operation, the content of micropores in AC has a key impact on ORR activity [25,26]. However, this impact was not studied during long-term operation, with the exception of work described by An et al. [27].

Another method to improve the performance of the AC cathode is the use of dispersed materials, coatings, and binders that change the properties of the cathode materials. The most commonly used binder is PTFE [28,29]. Nevertheless, PTFE is an expensive material, and more cost-effective solutions should be searched continuously. Recently, it has been shown that the presence of silica in a ceramic separator significantly improved proton transfer [30]. Pasternak et al. drew a similar conclusion, when the highest energy efficiency was obtained for the MFC equipped with a ceramic membrane with the highest silica concentration [24]. Therefore, Si-based coatings could be a promising and cost-effective alternative for PTFE binders. Commercial low-cost coatings such as silane/siloxane dispersions were often used for applications such as improving the durability of ceramic materials and the hydrophobisation of textiles [31,32]. Thus, due to their properties, Si-based coatings may also prevent the cathodic material from biofouling.

Overall, the cost-effective ACs for MFCs were studied in long-term in only a few, individual works. To the best of our knowledge only 3 works are available, where the performance of AC cathodes for more than 6 months was investigated [33–35]. Long-term studies of the cathodes must be undertaken prior to large-scale applications because the cost of the ORR catalyst significantly contributes to the overall revenue of the technology.

Therefore, the aim of this work was to investigate the long-term effect of the carbon surface properties, as well as the modification of the carbon surface with a silane/siloxane-based nanoparticle coating on the MFC performance. The study focused on commercially available activated carbons as the cathodes. Their efficiency and stability were assessed by electrochemical studies, surface and structural properties, and thermogravimetric analysis, providing insights into long-term operation and fouling of low-cost, commercially available materials for MFCs. This will help to provide indications for selecting the appropriate materials for upscaling projects.

Materials and methods

Cathodes materials and module preparation

The cathodes were made of three types of carbon materials: activated carbons CWZ-22 and CWZ-35 (Grand Activated, Poland), produced by gas-steam activation of charcoal and CWZ-22 modified by mixing with silane-siloxane microemulsion (SILRES® BS 290, Wacker, Germany) to achieve 1.8% (w/w) of final silicates concentration. This modified cathode was labelled within this manuscript as CWZ-22/Si. The prepared AC materials, wetted with distilled water, were mechanically pressed into a cathode spacer which contained a stainless steel mesh, acting as a current collector (Fig. S1). Furthermore, a carbon veil was placed on the outer side as a diffusion and protective layer. The geometric surface area of the cathode was equal to 9 cm^2. Finally, the cathodes were air-dried overnight before assembling.

Construction and operation of the MFC

This study used a single-chamber air–cathode MFC, described in an earlier work [36]. The working volume was 20 cm^3 and the anode chamber was separated from the cathode by a cation exchange membrane (CMI-7000, USA). A square-shaped anode was prepared from carbon veil (PRF Composite Materials, Dorset, UK) with 316LSi steel wire. The geometric surface area of the anode was equal to 9 cm^2. Between the anode chamber and the prepared cathode module, a rubber seal was used. The elements were connected with screws. Each cathode was tested in triplicate. The MFCs were inoculated with a mixture (1:1) of two activated sludge collected from the aerobic chambers of the wastewater treatment plant (Ścinawka, Poland; Kudowa, Poland). After 5 days of inoculation, the activated sludge was replaced with a mineral salt medium (MSM) with the same composition and preparation method as in the previous study [36]. Sodium acetate at a concentration of 0.82 g L^{-1} was used as the sole carbon source. The MFCs were fed a fresh portion of MSM medium daily (HRT = 23.09 ± 1.92 h). All MFCs were operated at 25 °C, with a starting external load of 2 kΩ. Previous studies have shown that the best operating conditions of the cell were obtained when the external resistance (R_{ext}) of the MFC was set close to the internal resistance (R_{int}) [37,38]. Therefore, after each polarisation experiment, the optimal resistance calculated at the maximum power point was applied to each MFC individually.

Real time temporal monitoring and electrochemical experiments

Closed circuit voltage (CCV) was measured in real time and recorded with 3 min interval by a KEYSIGHT DAQ970A data acquisition system (KEYSIGHT TECHNOLOGIES, USA). Polarisation experiments were performed in three-electrode mode using a MultiPalmSens4 potentiostat (Palmsens BV, Netherlands). The anode was used as working electrode (WE), the cathode as counter electrode and the saturated Ag/AgCl electrode as reference electrode, placed in the anode chamber. Power and polarisation curves were obtained using the linear sweep voltammetry (LSV) technique in the potential range from open circuit potential to 0.0 V WE vs Ag/AgCl, at a scan rate of 1 mV s^{-1}. Based on the obtained experimental data, the maximum power density, current density, and optimal resistance were extracted.

Electrochemical impedance spectroscopy (EIS) was used to analyse the internal resistance of MFCs equipped with different cathode materials. The EIS experiments were carried out for the whole cell with the anode as a working electrode, while the cathode served as a counter and reference electrode. MultiPalmSens4 potentiostat (Palmsens BV, Netherlands) was used to perform the EIS. The applied alternating current with an amplitude of 10 mV had a frequency range of 100 kHz to 10 mHz. All EIS spectra were recorded when the MFC was in open circuit voltage (OCV) mode.

Performance of MFC

COD removal and coulombic efficiency

The chemical oxygen demand (COD) was measured using the potassium dichromate oxidation method, according to the manufacturer's instructions (Hach, USA). The COD removal efficiency was calculated using the following equation:

$$\Delta \mathrm{COD} = \frac{\mathrm{COD}_0 - \mathrm{COD}_t}{\mathrm{COD}_0},$$

where COD_0 – initial COD of fresh medium in anode chamber (mg L^{-1}); COD_t – COD of the anode solution after the 't' time (mg L^{-1}).

The Coulombic Efficiency (CE) was determined for the batch system according to [5]:

$$\mathrm{CE} = \frac{M\int_0^t I\,dt}{F b V_{An} \Delta \mathrm{COD}},$$

where M – molecular weight of carbon substrate (g mol^{-1}); I – current (A); t – time of operation (s); F – Faraday's constant (96, 500 C/mol e^-); b – number of electrons exchanges per mole of oxygen; V_{An} – working volume of the anode chamber (L); ΔCOD – change in COD concentration (g L^{-1}).

Energy production and efficiency

The electricity produced in the operating period was calculated as the product of the average power generated by the MFC and the working time of the MFC:

$$\mathrm{EP} = \frac{\int_0^t P dt}{V},$$

where P – power (kW); t – operating time (h); V – working volume of the MFC (m^3).

The energy efficiency was calculated as the ratio of the energy recovered in the system to the energy of the starting material, according to the formula:

$$\eta_{MFC} = \frac{\int_0^t P dt}{\Delta H \times n_s},$$

where P – power (W); t – operating time (s); ΔH – heat of combustion (J/mol); n_s – amount (mole) of added substrate during operation time.

Characterization of cathode materials

Surface area and pore size distribution

The specific surface area and pore size distribution of activated carbons were characterised by nitrogen adsorption/desorption at −196 °C using a NOVA 2000 Sorptometer (Quantachrome Instruments, USA). Before the measurement, the sample was degassed under vacuum at 400 °C overnight. The AC parameters were calculated from the adsorption/desorption isotherms using the Brunauer–Emmett–Teller (BET), Density Functional Theory (DFT) and Dubinin-Radushkevich (DR) equations.

Scanning electron microscope (SEM)

Analysis of the morphology and surface composition of cathode materials was assessed using a scanning electron microscope with an EDS attachment (Helios NanoLab™ 600i). The pristine materials, as well as the cathodes after the experimental period, were dried at 60 °C for one hour. Furthermore, the materials were kept at 50 °C overnight prior to analysis.

Thermogravimetric analysis (TGA)

For cathodes analysis, PerkinElmer TGA8000 thermogravimetric analyser (PerkinElmer, USA) was used. Sample weight and temperature were recorded digitally throughout the whole TGA measurement and analysed with the Pyris 1 TGA software. For each material, measurements were performed in an oxygen atmosphere with a flow rate of 20 mL min^{-1}. The temperature programme was set as follows: 30 °C for 5 min, then 105 °C for 30 min, successively increase the temperature to 900 °C at a rate of 7 °C min^{-1}, keep the temperature at 900 °C for 1 min.

Data processing

The experimental data were analysed and visualised graphically using OriginLab 2019. Current, power, and internal resistance were calculated according to Ohm's law.

$$R = \frac{U}{I}(\Omega),$$

$$P = U \times I(W),$$

where U – voltage (V); I – current (A); P – power (W); R – resistance (Ω).

Results and discussion

Real-time monitoring of MFC power performance

The MFC was supplied with three different carbon cathode materials. During nearly one-year operation of the microbial fuel cells, the power density output was monitored in real time. Fig. 1a shows the real time data of the highest performing MFCs for each cathode type. In this initial stage of operation, biofilm growth is a process that limits the efficiency of the MFC [37]. Therefore, the power density during the first month of operation did not show significant differences in power performance. Afterwards, a more rapid increase of power was observed for MFCs equipped with the CWZ-35 cathode. Previous studies reported that functional MFC elements such as membranes or electrode materials play a crucial role in the development of well-established biofilm [39,40]. The highest power density of 18.8 W m^{-3} (377 μW) was recorded for CWZ-35 after 100 days of operation and resulted from the ongoing biofilm development due to the increased cathode performance. This was later proven through polarisation experiments. From this moment, a gradual decrease in the output power of MFCs with the CWZ-35 cathode was observed. In contrast to these results, a further increase in the power density of MFCs was observed for CWZ-22 and CWZ-22/Si, modified with silica nanoparticles. The highest power density obtained after 197 days of operation for CWZ-22 was equal to 27.8 W m^{-3} (557 μW) (Fig. 1b.), while the modified CWZ-22/Si showed a maximum real-time power density lower by 22% after 183 days (when compared to CWZ-22). In the 7th month of operation, a significant decrease in the power of CWZ-22/Si was observed. In contrast, the CWZ-22 retained the highest power efficiency throughout the entire period of operation, while similar studies showed a regular decrease in power output during long-term operation [27,33].

Electrochemical characteristics

Long-term efficiency

Polarisation experiments were carried out throughout the study in a three-electrode mode to characterise the dynamic changes in the MFCs performance. Fig. 1c. shows the values of the maximum power densities extracted from the LSV data. After 105 days of operation, CWZ-35 reached the highest power density of 22.8 ± 2.2 W m^{-3}. This trend was reversed in the following period and a significant decrease in power efficiency was observed. Furthermore, the power density of one of the

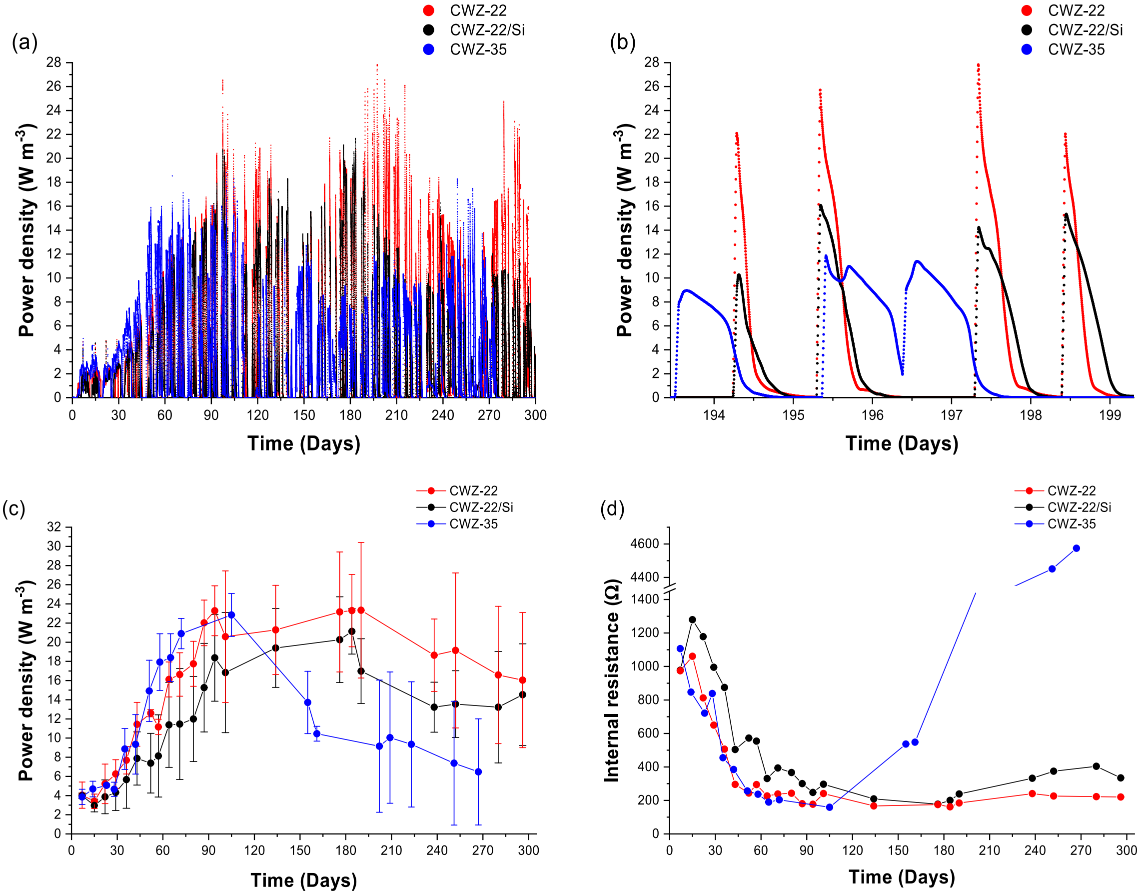

Fig. 1. Real-time temporal power density output (a) and the characteristics of exemplary feeding cycles (b). Graph of the changes in: power density (c) and internal resistance (d) during operation. For clarity, the error bars were removed from the plot (d).

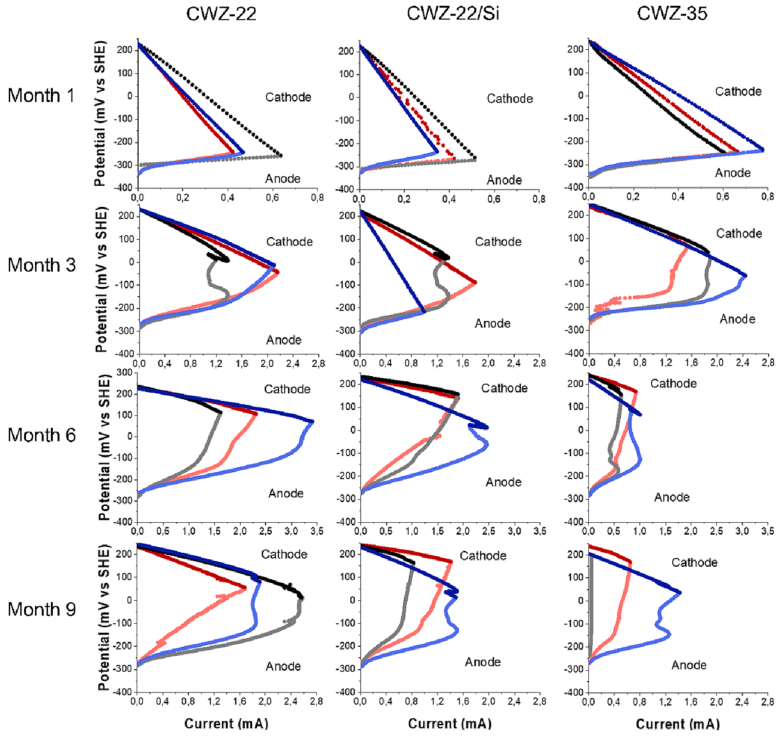

Fig. 2. Polarisation curves of anodes and cathodes for all of the MFCs along the operational period. Each plot represents individual replicates.

CWZ-35 replicates has decreased rapidly by more, starting with the 50% drop compared to the previous measurement. In contrary to CWZ-35, CWZ-22 and CWZ-22/Si were displayed by a relatively high power density from day 90 to the end of the experiment. On day 190, CWZ-22 reached a maximum power density of 23.3 ± 7.1 W m^{-3}. Furthermore, one of its replicates achieved a power density of 30.7 W m^{-3}. Overall, this material has shown a reduction in the maximum power density of 31% during the 300-day test, which was the lowest value compared to the materials available in the literature, at a similar operating time [33,35]. Modifying CWZ-22 with silica nanoparticles did not improve maximum power density but maintained high long-term performance. Moreover, an increasing trend of CWZ-22/Si performance was observed in the last stage of the experimental period, while the nonmodified CWZ-22 displayed a decreasing trend. CWZ-22/Si reached a maximum power density of 21.1 ± 2.4 W m^{-3} after 184 days of operation.

A similar tendency can be observed for internal resistance (Fig. 1d). The internal resistance (R_{int}) values of all MFCs decreased at a similar rate until day 70, and then stabilised. For CWZ-35, only a short period of stable internal resistance was observed up to day 105, and then a significant increase in R_{int} was noted. The lowest R_{int} value for CWZ-35 was 159.3 ± 35.5 Ω on day 105. After 184 days of operation, the minimal R_{int} observed for CWZ-22 was 162.3 ± 42 Ω, while CWZ-22/Si achieved an internal resistance value higher by 10%.

The cathode and anode polarisation curves were obtained by the three-electrode polarisation tests (Fig. 2.). The open circuit potential of the anode (OCP_{anode}) in the first month of biofilm maturation reached values of −323.9 ± 22.1 V, −317 ± 9.2 V and −345.8 ± 8.1 V for CWZ-22, CWZ-22/Si and CWZ-35, respectively. Afterwards, the OCP_{anode} in all MFCs evolved to a more positive, possibly due to biofilm buildup, which negatively affects electron transfer resistance and substrate diffusion rate [41]. This effect was the most prevalent for CWZ-35. The cathode open circuit potential ($OCP_{cathode}$) was similar for all MFCs in the first month of operation. Afterwards, a slight increase in the $OCP_{cathode}$ was observed for CWZ-22 and CWZ-22/Si. On the contrary, the CWZ-35 during the 9 months of operation showed a decrease in $OCP_{cathode}$ by almost 9%.

When analysing the curves obtained for all materials in the first month, it was observed that the high R_{int} (Fig. 1d.) was caused by the ohmic resistance of the cathodes (Fig. 2.). In the third month, CWZ-22 and CWZ-35 were limited by anode mass transfer, while the overall performance of CWZ-22/Si was further limited by cathode ohmic resistance. The average current observed for CWZ-35 was 1.96 ± 0.45 mA. It should be noted that from the sixth month of operation, the cathode polarisation curves for all MFCs showed a positive potential at maximum currents. Thus, the overall efficiency of all MFCs were limited by the anode operation, which was probably affected by the incapability of the cathode to accept electrons to the active sites. Nevertheless, CWZ-22/Si had a lower rate of cathodic voltage drop, compared to CWZ-22, starting from the sixth month of operation until the end of the experiment. The average currents for CWZ-22 and CWZ-22/Si were 2.44 ± 0.90 mA and 1.97 ± 0.13 mA, respectively, in the sixth month of work. At month 9, the analysis of the polarisation curves showed a deterioration in the performance of all MFCs due to a significant increase in the anode mass transfer losses and the cathode ohmic resistance. Furthermore, from the sixth month of operation, a strong overshoot phenomenon was observed on the polarisation curves of the CWZ-22/Si and CWZ-35. This phenomenon was probably caused by the blockage of the pores by ions diffusing into the cathode, dominated by sodium and calcium (Tab. S2.), which hindered the access of oxygen to the active sites and slowed down the flow of electrons [42]. For the CWZ-22, only a slight overshoot phenomenon was observed, proving a well-established MFC system. A possible reason for the increase in losses may be the build-up of a thick biofilm layer on the anode, which limits the diffusion of the substrate, causing a negative gradient towards deeper layers [41], accompanied by the membrane biofouling phenomenon, which limits proton transfer [17,43].

Electrochemical impedance spectroscopy

The experimental data acquired by EIS experiments was fitted to the equivalent circuit model according to [44], where the circuit element R_A corresponded to the anode, R_C to the cathode, and R_{M+E} corresponded to the resistance of the membrane and electrolyte. Constant phase element (CPE) imitate the capacitive behaviour of the electrical double layer due to several factors such as: electrode surface roughness and porosity, the presence of biofilm, and the changes in the biofilm thickness [44]. Additionally, at the end of the equivalent circuit model, a Finite Length Warburg element marked as W_S was applied [45]. The Nyquist plots obtained with the EIS in the successive stages of operation are shown in Fig. 3a. The acquired EIS spectra of the MFCs showed three semicircles. Fig. 3b. presents the results of the analysis of individual impedance components using an equivalent circuit model [46,43]. The EIS experiment in 3 months of operation showed that CWZ-35 and CWZ-22 indicated a similar sum of impedances of 78.6 ± 17.3 Ω and 70.1 ± 16.2 Ω, respectively, while the lowest R_C was detected in CWZ-35. CWZ-22/Si exhibited the highest anode and cathode impedance in this period. A different trend was observed in the 6th month, when CWZ-35 showed the highest sum of impedances, the main component of which was R_C. During this period, a decrease in R_C and R_{M+E} were observed for CWZ-22 and CWZ-22/Si. The sum of the CWZ-22 resistance was of 58.2 Ω and was almost 30% lower than for the CWZ-22/Si. The EIS data for month 9 showed an increase of internal resistance for each MFC, with the highest values observed for CWZ-35.

The internal resistance as determined by the EIS of CWZ-22 and CWZ-22/Si decreased by 6 months of operation. It is known, that R_A decreases with the development of the anode biofilm [37]. Commonly, the cathode deterioration is associated to the chemical fouling caused by electro-osmotic drag and consequent biofilm formation [15,16]. Nevertheless, here we are showing that a certain level of chemical fouling is beneficial for the MFC operation. Similar results were shown by Cheng et al. [47] who investigated ion precipitation through the real-time *in situ* method. The reduction of R_{M+E} could have resulted from multiple factors including improved release of electron shuttles to the electrolyte [48]. In contrast to these results, the internal resistance of CWZ-35 increased with each successive measurement due to increases in R_A, R_C and R_{M+E}. The data displayed on Fig. 3, showed that the R_C and R_{M+E} had the highest effect on the MFC efficiency deterioration and its correspondence with the outer cathode surfaces and salt accumulation. In the third month of operation, small amounts of precipitated salts were observed only for the CWZ-22 cathodes. However, in the sixth month, a similar degree of (visual) inorganic fouling was observed for all MFCs, which was accompanied by the lowest internal resistance values of CWZ-22 and CWZ-22/Si. Therefore, we conclude that electroosmosis of salts to the cathode had a positive effect on the efficiency of CWZ-22 and CWZ-22/Si materials. In contrast, it led to a rapid increase in the CWZ-35 R_C, which was also revealed in polarisation experiments. In the second half of the experimental period, despite the increase in cathode coverage by salts, the CWZ-22 and CWZ-22/Si efficiencies were not limited by the cathode resistance.

Coulombic and energy efficiency

The efficiency of the substrate degradation was evaluated by determining the COD removal ability and the coulombic efficiency of the MFCs (Fig. 4a.). The COD concentration of fresh MSM was of 489 mg L^{-1}, while the COD after treatment was equal to 90.7 ± 15.1 mg L^{-1}, 81.8 ± 2.1 mg L^{-1} and 114.8 mg L^{-1} for CWZ-22, CWZ-22/Si and CWZ-35, respectively. Thus, the COD removal values were similar for CWZ-22 and CWZ-22/Si and amounted to 81.46 ± 3.80% and 83.27 ± 0.52%, respectively. However, the Coulombic Efficiency (CE) of CWZ-22 was 63.63 ± 8.74% and was 19% higher than for the Si-modified variant. The average COD and CE removal values for CWZ-35 were of 76.52% and 56.45%, respectively. It should be mentioned that for one of the CWZ-35 replicates, the COD removal and CE values were close to zero

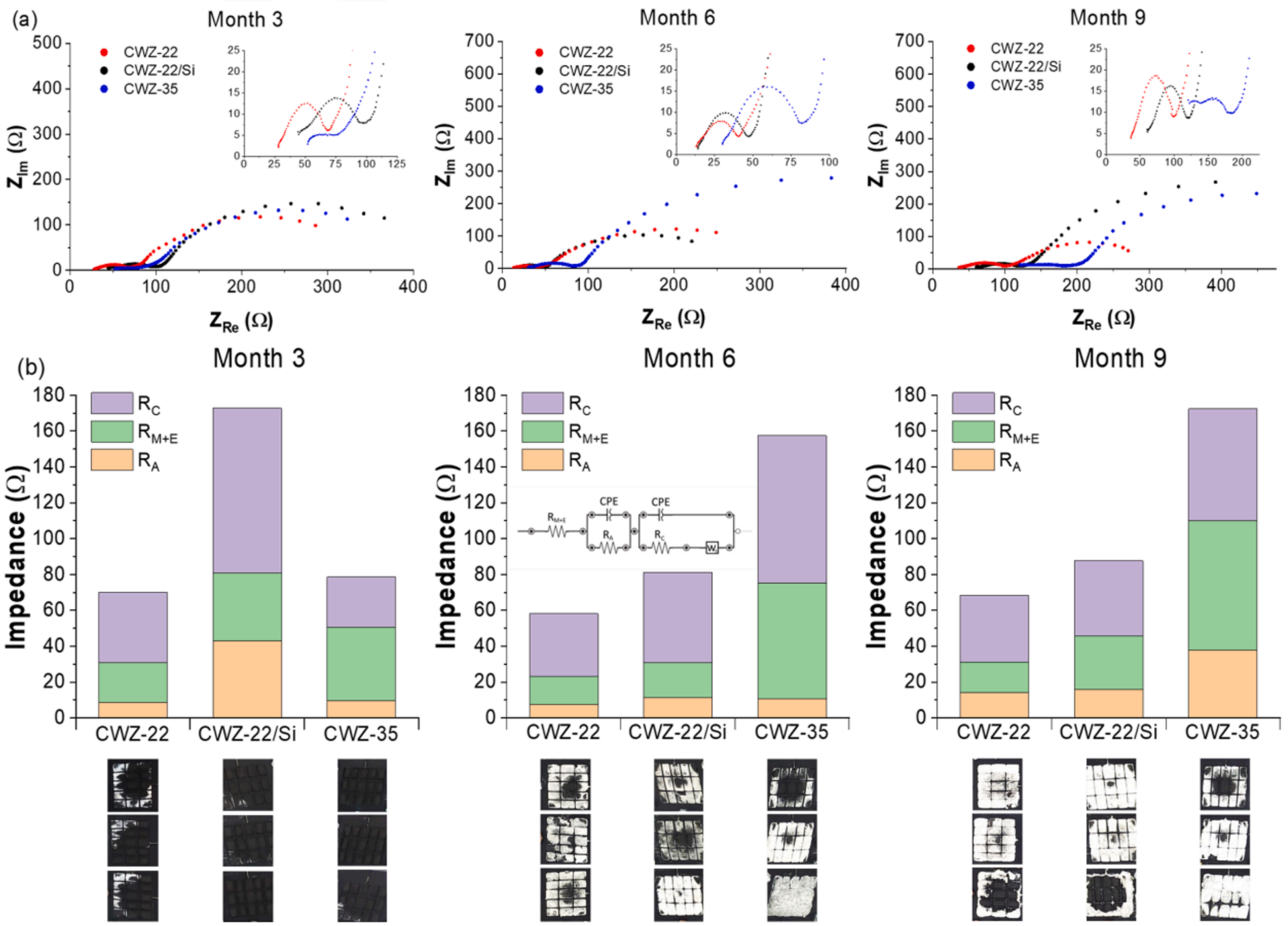

Fig. 3. Nyquist plots (a) and EIS data analysis using the equivalent circuit model (b), the model is presented in the middle plot of the figure. The photographs below each bar display the intensity of the chemical fouling on the outer surface of the cathode. The white colour intensity correlates with the amount of salt precipitated over the cathode (black) surface. A bigger scale pictures have been included in Fig. S3.

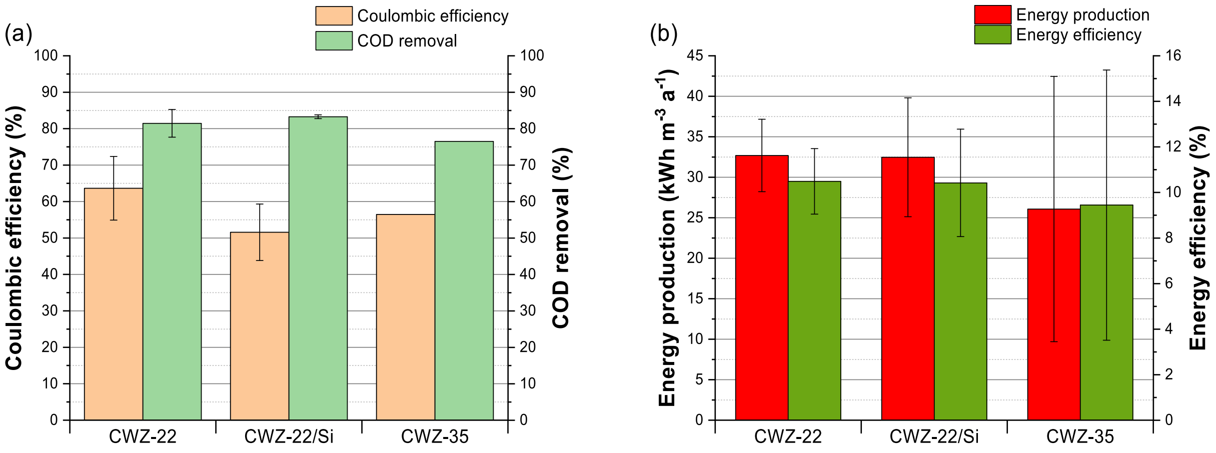

Fig. 4. COD removal and coulombic efficiency calculated after 280 days of operation (a) and energy production and energy efficiency approximated to one year (b).

and were rejected from the data presented in the Fig. 4a. Despite the lower currents of CWZ-35 obtained during CE measurement compared to CWZ-22/Si, the CE value of CWZ-35 was higher due to the longer batch cycle (Fig. 1b). The COD removal is affected by the design of the MFC and the operating conditions of the bioreactor [49]. In the present study we used an MFC design with a large volume of the anode chamber without agitation, which increased the diffusion resistances, limited the performance of the MFC system, and affected the COD removal.

Furthermore, the total energy production (EP) and energy efficiency (EE) over the entire period of operation were calculated and approximated to one-year operation (Fig. 4b.). The MFC with the CWZ-22 and CWZ-22/Si cathode produced 32.69 ± 4.47 kWh m^{-3} a^{-1} and 32.47 ±

7.34 kWh m^{-3} a^{-1}, respectively. The slight difference for these parameters for CWZ-22 and CWZ-22/Si, was caused by the shorter period of stable currents in CWZ-22 batch cycles. On the other hand, the lowest EP and EE values recorded for CWZ-35 resulted from weak long-term performance.

Table 1 summarises the MFCs efficiencies recorded for this study. The highest values were observed for MFCs equipped with CWZ-22 cathodes. Therefore, this material is revealed to be the most attractive and cost-effective to produce a high-performance cathode in MFCs with good long-term properties. Additionally, the results suggest that the use of silica nanoparticles as a low-cost additive to improve the long-term cathodic performance is not an appropriate strategy. In contrast, the CWZ-35 showed the highest power and current densities in the short-term period, while the poorest long-term performance among all tested materials.

Characterization of the carbon cathode materials

Pore size distribution and surface area analysis

The pore size distribution obtained from the N_2 adsorption–desorption curve for the cathode materials tested is shown in Fig. 5. Micropores (0 to 2 nm diameter) provide active sites for the oxygen reduction reaction (ORR), while mesopores (2–50 nm) and macropores (>50 nm) are used as transport channels for oxygen molecules to the active sites [26]. Fig. 5a,b. shows that CWZ-22 and CWZ-22/Si materials are dominated by micropores with a diameter of 0.65 to 1.45 nm (over 50% contribution). For CWZ-35, a narrower pore size range was observed (Fig. 5c). Pores with a diameter of 1.25 to 1.45 nm accounted for over 50% of the total pore volume. The results of surface and porosity measurements are summarised in the Tab. S1. Micropore volumes and specific surface areas were of 0.38 cm^3 g^{-1} and 971.7 m^2 g^{-1}, 0.35 cm^3 g^{-1} and 948.3 m^2 g^{-1}, and 0.48 cm^3 g^{-1} and 1272.5 m^2 g^{-1} for CWZ-22, CWZ-22/Si and CWZ-35, respectively. Previous studies reported that the increase in micropore abundance of the AC cathode results in an improvement of power density, which stands in line with our findings for the initial period for CWZ-35. On the other hand, the increased performance of cathodes and thus MFCs may lead to a stronger electroosmosis phenomenon, where the ions pass from the analyte towards the cathode. Therefore, a sudden decrease in ORR efficiency after 3 months of CWZ-35 operation can be attributed to blocking of ORR active sites by diffusing ions. This long-term performance drop was not observed for CWZ-22 and CWZ-22/Si, which reached a similar level of power compared to CWZ-35 at a comparable time. It may be considered that the predominance of pore sizes below 1 nm prevented deactivation of active sites, maintaining the high ORR activity despite the high coverage of cathodes by inorganic salts. One of such possible mechanisms of pore protection could have resulted from a possible effect of a molecular sieve, which prevented the ion salts to precipitate and accumulate in deeper layers. The above results indicate that the higher specific surface area, and thus the total volume of micropores of CWZ-35, resulted in a faster increase of power output over the 3-month period of operation. However, the high micropore content below 1 nm observed for CWZ-22 and CWZ-22/Si positively affected the long-term properties of these cathodes. Although the Si-modification of CWZ-22 resulted in higher total pore volume, a reduction of the micropore volume was observed for this material when compared to a nonmodified one. Thus, a slightly lower efficiency throughout the experiment was a result of micropore content, while the overall long-term characteristics of these two materials were comparable due to similar pore size distribution.

Scanning electron microscopy

The catalyst for each cathode material was collected after the experimental period to investigate its surface morphology and perform an X-ray microanalysis studies (SEM-EDS). SEM micrograph analysis (Fig. 6.) showed that the modification of activated carbon CWZ-22 by silica nanoparticles resulted in regular deposition of typical spherical structures [51] over the surface of activated carbon. After the experimental period, the concentration of precipitated salts around the spherical silica structures was observed. This phenomenon was caused by the ability of silica nanoparticles to control nucleation of the crystallization as it was previously described in the literature [50]. The results of X-ray microanalysis are summarised in the Tab. S2. After the experimental period, all cathode materials revealed contamination with inorganic salts, as shown on Fig. 6, mainly by sodium oxide (Fig. S2.), but the level of chemical fouling varied, as determined by EDS (Tab. S2). The CWZ-22 cathode displayed the lowest sodium content on the surface, while CWZ-35 revealed more than three times higher amounts of this element. In addition, an increase in the content of copper and manganese was observed in all materials. Oxides of these metals have the ability to catalyse the ORR reaction [51], therefore, it is suspected that their presence could be another reason for the dynamic improvement of cathodic performance. Compositional analysis also revealed a reduction in silicon content in the CWZ-22 modified with silica after the experiment. It is possible that the silica particles covered with precipitated salts were not detected in the analysis. More detailed studies of the dynamic elemental composition during chemical fouling of the cathodes could provide a new insights into their operation.

Thermogravimetric analysis

All of the cathode materials were analysed for their thermal behaviour once the operational period has been completed. The differential curves were also displayed to highlight the temperature changes (Fig. 7.). The mass changes and rates have provided insights into their

Table 1
Electrical power generation in MFCs. Data represent average values ± SD.

		References					
		This work	This work	This work	[27]	[33]	[35]
Type of MFC		Single chamber MFC					
Cathode catalyst		AC CWZ-22	AC CWZ-22/Si	AC CWZ-35	AC + PTFE	AC + PTFE	AC + PTFE
Power density	W m^{-3}	23.3 ± 3.8	21.1 ± 2.4	22.8 ± 2.2	22.5 ± 0.5	56,2 ± 3.6	30.3 ± 3.1
	mW m^{-2}	517.8 ± 84.4	468.9 ± 53.3	506.7 ± 48.9	1286 ± 30	1722 ± 110	1214 ± 123
R_{int}	Ω	162.3 ± 42.0	178.0 ± 7.0	159.3 ± 35.5	n.r.	n.r.	n.r.
Current density	A m^{-3}	122.0 ± 45.0	98.5 ± 6.5	98.0 ± 22.5	approx. 85.7	approx. 258.1	approx. 187.5
	A m^{-2}	2.7 ± 1.0	2.2 ± 0.14	2.2 ± 0.5	approx. 4.9*	approx. 7.9*	approx. 7.5*
CE	%	63.6 ± 8.7	51.6 ± 7.7	56.5	45.4 ± 2.7	n.r.	33
EP	kWh m^{-3} a^{-1}	32.7 ± 4.5	32.5 ± 7.3	26.07 ± 16.4	n.r.	n.r.	n.r.
EE	%	10.5 ± 1.4	10.4 ± 2.3	9.4 ± 5.9	n.r.	n.r.	n.r.
Price	€ m^{-2}	4.7	5.0	5.6	n.r.	54.9	n.r.
Operation time	month	10	10	10	6	12	14
Power reduction	%	31	31	72	36	55	40
Volume	mL	20	20	20	28	60	28

CE – coulombic efficiency; EP – energy production; EE – energy efficiency; *data taken from the plots, not available in the referenced text; n.r. – not reported.

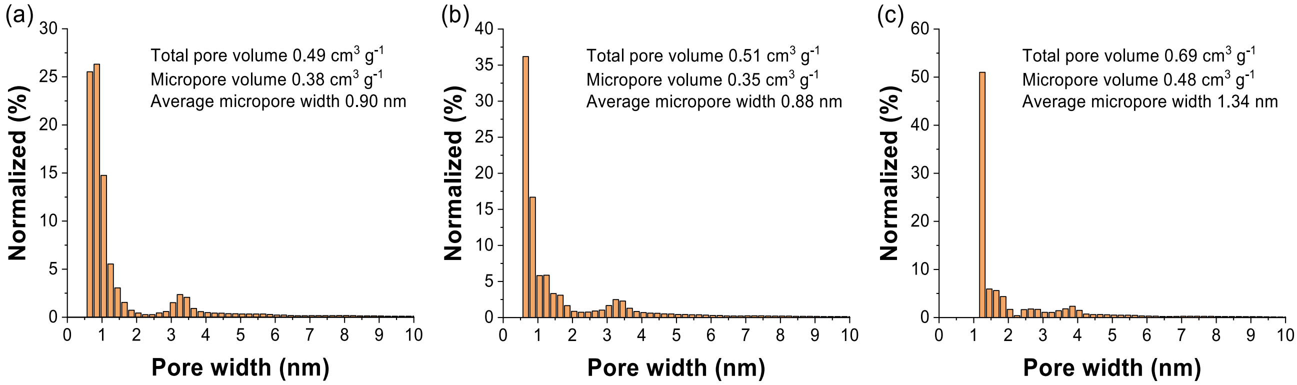

Fig. 5. DFT pore size distribution plots of CWZ-22 AC (a), CWZ-22/Si modified AC (b), and CWZ-35 AC (c).

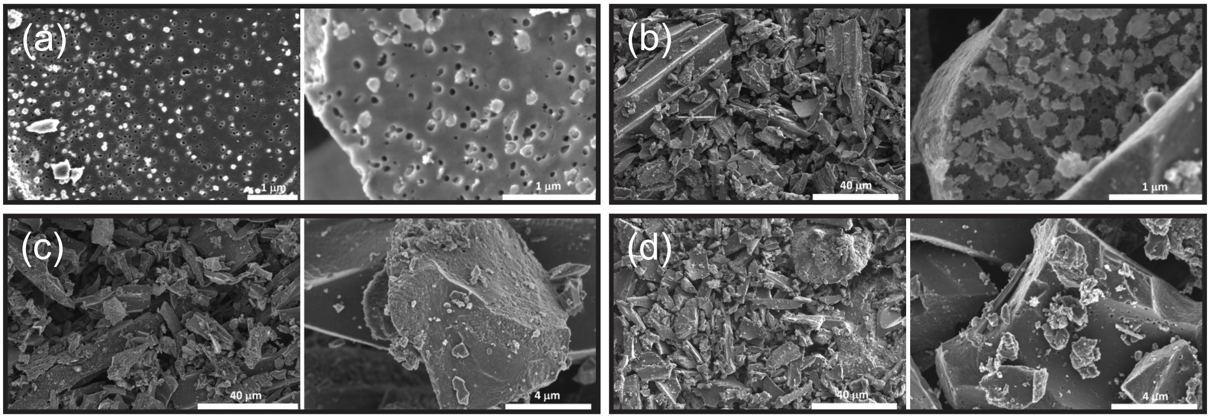

Fig. 6. Scanning Electron Microscopy images. CWZ-22/Si before operation (a), CWZ-22/Si cathode after operation (b), CWZ-22 cathode after operation (c), and CWZ-35 cathode after operation (d). Each group represent two different magnifications of the same material.

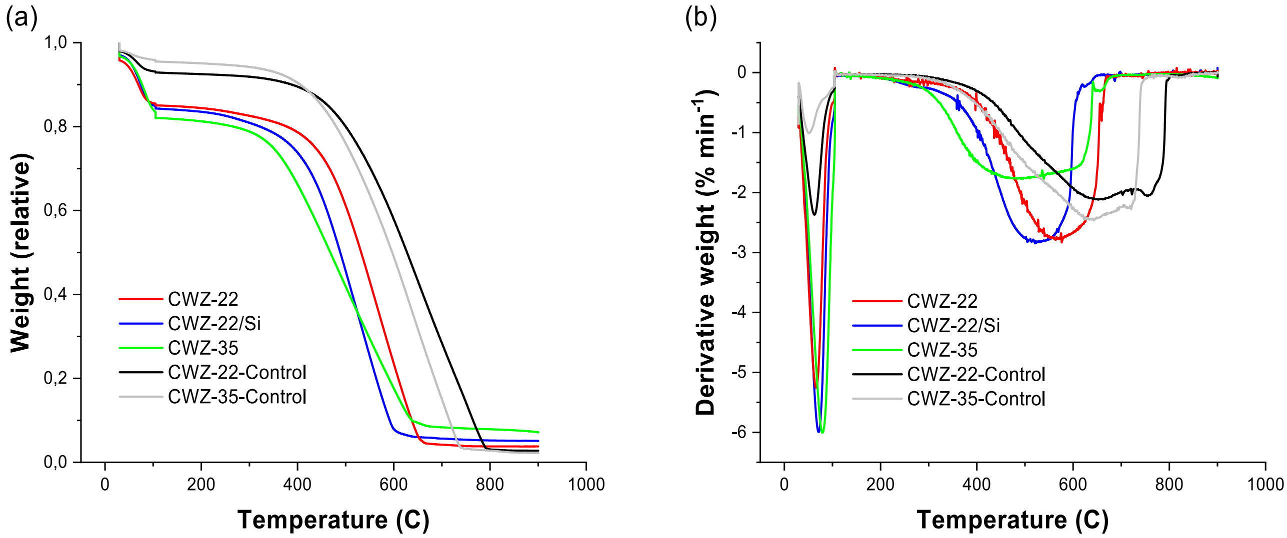

Fig. 7. Results of thermogravimetric analysis in the oxygen atmosphere of carbon cathode samples after use in MFCs: relative mass changes (a) and derivative weight (b).

properties. The use of the cathodes in MFCs has significantly reduced their most dominant oxidation temperatures. While 655 °C was recorded for CWZ-22 control, the same material after use displayed peaks of 530 °C and 570 °C for CWZ-22/Si and CWZ-22 respectively. The CWZ-35 control displayed prevalent temperature at 635 °C and 478 °C after use. Therefore, it is expected that the ionic transfer and accumulation of cations during long-term operation was the highest for CWZ-35, moderate for CWZ-22/Si, and the lowest for CWZ-22. In particular, copper, manganese, and magnesium could have the most significant effect on catalytic oxidation of carbon by lowering the oxidation temperatures. These results were in line with the residual ash content, as shown in Fig. 7. The ash content for the investigated cathodes was equal to 2.8, 3,8 and 5.1% for CWZ-22 before, after use, and Si-modified, respectively, while for CWZ-35 2.2% (control) and 7.2% (after use) were recorded. The oxidation of Si-modified CWZ-22 has also been shifted due to the protective layer formed over the carbon surface. This data is consistent with the long-term behaviour of the electrochemical and performance parameters of the MFCs. Therefore, such results indicate that excessive electroosmotic drag recorded during initial phase of MFC operation results in long-term performance deterioration, while moderate ionic transfer to the cathode may induce the oxygen reduction reaction as it was recorded for the non-modified CWZ-22.

Conclusions

The performance of the two different types of activated carbons as the air–cathode materials for MFCs and the effect of modification with silica nanoparticles on long-term properties were evaluated in a 300-day trial. The results indicated the highest performance of the MFC equipped with the CWZ-35 cathodes in the initial period. The nitrogen physisorption analysis showed that CWZ-35 is a more microporous material than CWZ-22, which was the reason for the high efficiency at the beginning of the study. However, the period of stable power generation for CWZ-35 was the shortest among all the tested materials. In contrast to these results, CWZ-22 and CWZ-22/Si showed good stability and satisfactory power output throughout the experiment. It can be assumed that the pore size distribution of CWZ-22, with a dominance of pores below 1 nm, was one of the reasons for the lower susceptibility to deactivation of active sites. Despite the slight differences in the generated CWZ-22 and CWZ-22/Si power densities, the analysis of the polarisation curves showed no positive effects of doping with silica nanoparticles on power performance and its long-term properties.

According to the above results, it has been shown that an unmodified, cheap, and commercially available activated carbon CWZ-22 without binder is a better choice in terms of long-term operation than highly porous and more expensive CWZ-35 activated carbon. The results show that the pore size distribution and resulting vulnerability to chemical fouling is the crucial decisive factor to maintain the high performance of the MFC setup aimed to be operated in years.

Funding

This work was financed by the Polish National Agency for Academic Exchange – Polish Returns grant (PPN/PPO/2018/1/00038) and National Science Centre (Poland) OPUS grant (2019/33/B/NZ9/02774), as well as by the Faculty of Chemistry of Wrocław University of Science and Technology.

CRediT authorship contribution statement

Aleksander de Rosset: Investigation, Methodology, Resources, Visualization, Formal analysis, Writing – original draft. **Piotr Rutkowski:** Supervision, Writing – review & editing. **Grzegorz Pasternak:** Conceptualization, Funding acquisition, Methodology, Project administration, Formal analysis, Writing – review & editing, Writing – original draft.

Declaration of Competing Interest

The authors declare that they have no known competing financial interests or personal relationships that could have appeared to influence the work reported in this paper.

Data availability

Data will be made available on request.

Appendix A. Supplementary data

Supplementary data to this article can be found online at https://doi.org/10.1016/j.seta.2023.103340.

References

[1] Zhukovskiy YL, Batueva DE, Buldysko AD, Gil B, Starshaia VV. Fossil energy in the framework of sustainable development: Analysis of prospects and development of forecast scenarios. Energies 2021;14(17):1–28. https://doi.org/10.3390/en14175268.

[2] Buonocore JJ, Choma E, Villavicencio AH, Spengler JD, Koehler DA, Evans JS, et al. Metrics for the sustainable development goals: renewable energy and transportation. Palgrave Commun 2019;5(1). https://doi.org/10.1057/s41599-019-0336-4.

[3] Y. Wen, G. Schoups, and N. Van De Giesen, “Organic pollution of rivers: Combined threats of urbanization, livestock farming and global climate change,” *Sci. Rep.*, vol. 7, no. September 2016, pp. 1–9, 2017, doi: 10.1038/srep43289.

[4] Zhou M, Chi M, Luo J, He H, Jin T. An overview of electrode materials in microbial fuel cells. J Power Sources 2011;196(10):4427–35. https://doi.org/10.1016/j.jpowsour.2011.01.012.

[5] Logan BE, et al. Microbial fuel cells: Methodology and technology. Environ Sci Technol 2006;40(17):5181–92. https://doi.org/10.1021/es0605016.

[6] Kumar SS, Kumar V, Malyan SK, Sharma J, Mathimani T, Maskarenj MS, et al. Microbial fuel cells (MFCs) for bioelectrochemical treatment of different wastewater streams. Fuel 2019;254:115526.

[7] Dziegielowski J, Mascia M, Metcalfe B, Di Lorenzo M. Voltage evolution and electrochemical behaviour of Soil microbial fuel cells operated in different quality soils. Sustain Energy Technol Assessments 2023;56:103071. https://doi.org/10.1016/j.seta.2023.103071.

[8] Zhang F, Saito T, Cheng S, Hickner MA, Logan BE. Microbial fuel cell cathodes with poly(dimethylsiloxane) diffusion layers constructed around stainless steel mesh current collectors. ACS Natl Meet B Abstr 2010;44(4):1490–5.

[9] Nasrabadi AM, Moghimi M. 4E analysis of stacked microbial fuel cell as a component in power plants for power generation and water treatment; with a cost-benefit perspective. Sustain Energy Technol Assessments 2022;vol. 53, no. PD: 102742. https://doi.org/10.1016/j.seta.2022.102742.

[10] Ieropoulos IA, Stinchcombe A, Gajda I, Forbes S, Merino-Jimenez I, Pasternak G, et al. Pee power urinal-microbial fuel cell technology field trials in the context of sanitation. Environ Sci Water Res Technol 2016;2(2):336–43.

[11] Suransh J, Jadhav DA, Nguyen DD, Mungray AK. Scalable architecture of low-cost household microbial fuel cell for domestic wastewater treatment and simultaneous energy recovery. Sci Total Environ 2023;857:159671.

[12] Babanova S, Santoro C, Jones J, Phan T, Serov A, Atanassov P, et al. Practical demonstration of applicability and efficiency of platinum group metal-free based catalysts in microbial fuel cells for wastewater treatment. J Power Sources 2021;491:229582.

[13] Dong Y, Qu Y, He W, Du Y, Liu J, Han X, et al. A 90-liter stackable baffled microbial fuel cell for brewery wastewater treatment based on energy self-sufficient mode. Bioresour Technol 2015;195:66–72.

[14] Liang P, Duan R, Jiang Y, Zhang X, Qiu Y, Huang X. One-year operation of 1000-L modularized microbial fuel cell for municipal wastewater treatment. Water Res 2018;141:1–8. https://doi.org/10.1016/j.watres.2018.04.066.

[15] Pasternak G, Greenman J, Ieropoulos I. Regeneration of the power performance of cathodes affected by biofouling. Appl Energy 2016;173:431–7. https://doi.org/10.1016/j.apenergy.2016.04.009.

[16] Santini M, Guilizzoni M, Lorenzi M, Atanassov P, Marsili E, Fest-Santini S, et al. Three-dimensional X-ray microcomputed tomography of carbonates and biofilm on operated cathode in single chamber microbial fuel cell. Biointerphases 2015;10(3):031009.

[17] Pasternak G, de Rosset A, Tyszkiewicz N, Widera B, Greenman J, Ieropoulos I. Prevention and removal of membrane and separator biofouling in bioelectrochemical systems: a comprehensive review. iScience 2022;25(7):104510. https://doi.org/10.1016/j.isci.2022.104510.

[18] Santoro C, Stadlhofer A, Hacker V, Squadrito G, Schröder U, Li B. Activated carbon nanofibers (ACNF) as cathode for single chamber microbial fuel cells (SCMFCs). J Power Sources 2013;243:499–507. https://doi.org/10.1016/j.jpowsour.2013.06.061.

[19] Santoro C, Artyushkova K, Babanova S, Atanassov P, Ieropoulos I, Grattieri M, et al. Parameters characterization and optimization of activated carbon (AC) cathodes for microbial fuel cell application. Bioresour Technol 2014;163:54–63.

[20] Liu Yi, Zhao Y, Li K, Wang Z, Tian P, Liu Di, et al. Activated carbon derived from chitosan as air cathode catalyst for high performance in microbial fuel cells. J Power Sources 2018;378:1–9.

[21] Bose D, Sridharan S, Dhawan H, Vijay P, Gopinath M. Biomass derived activated carbon cathode performance for sustainable power generation from Microbial Fuel Cells. Fuel 2019;236:325–37.

[22] Oh S, Min B, Logan BE. Cathode performance as a factor in electricity generation in microbial fuel cells. Environ Sci Technol 2004;38(18):4900–4. https://doi.org/10.1021/es049422p.

[23] Oh SE, Logan BE. Proton exchange membrane and electrode surface areas as factors that affect power generation in microbial fuel cells. Appl Microbiol Biotechnol 2006;70(2):162–9. https://doi.org/10.1007/s00253-005-0066-y.

[24] Pasternak G, Greenman J, Ieropoulos I. Comprehensive Study on Ceramic Membranes for Low-Cost Microbial Fuel Cells. ChemSusChem 2016;9(1):88–96. https://doi.org/10.1002/cssc.201501320.

[25] Wang X, Gao N, Zhou Q, Dong H, Yu H, Feng Y. Acidic and alkaline pretreatments of activated carbon and their effects on the performance of air-cathodes in microbial fuel cells. Bioresour Technol 2013;144:632–6. https://doi.org/10.1016/j.biortech.2013.07.022.

[26] Eom H, Jwa E, Jeung Y-C, Hwang KS, Jeong N, Mok YS, et al. Surface modification of carbon catalysts for efficient production of H 2 O 2 in bioelectrochemical systems. Environ Sci Water Res Technol 2022;8(10):2304–13.

[27] An J, Li N, Wan L, Zhou L, Du Q, Li T, et al. Electric field induced salt precipitation into activated carbon air-cathode causes power decay in microbial fuel cells. Water Res 2017;123:369–77.

[28] Dong H, Yu H, Yu H, Gao N, Wang X. Enhanced performance of activated carbon-polytetrafluoroethylene air-cathode by avoidance of sintering on catalyst layer in microbial fuel cells. J Power Sources 2013;232:132–8. https://doi.org/10.1016/j.jpowsour.2013.01.036.

[29] Cheng S, Wu J. Air-cathode preparation with activated carbon as catalyst, PTFE as binder and nickel foam as current collector for microbial fuel cells. Bioelectrochemistry 2013;92:22–6. https://doi.org/10.1016/j.bioelechem.2013.03.001.

[30] Raychaudhuri A, Sahoo RN, Behera M. Application of clayware ceramic separator modified with silica in microbial fuel cell for bioelectricity generation during rice mill wastewater treatment. Water Sci Technol 2021;84(1):66–76. https://doi.org/10.2166/wst.2021.213.

[31] González-Coneo J, Zarzuela R, Elhaddad F, Carrascosa LM, Gil MLA, Mosquera MJ. Alkylsiloxane/alkoxysilane sols as hydrophobic treatments for concrete: A comparative study of bulk vs surface application. J Build Eng 2021;46(November): 2022. https://doi.org/10.1016/j.jobe.2021.103729.

[32] Aslanidou D, Karapanagiotis I, Panayiotou C. Superhydrophobic, superoleophobic coatings for the protection of silk textiles. Prog Org Coatings 2016;97:44–52. https://doi.org/10.1016/j.porgcoat.2016.03.013.

[33] Zhang E, Wang F, Yu Q, Scott K, Wang X, Diao G. Durability and regeneration of activated carbon air-cathodes in long-term operated microbial fuel cells. J Power Sources 2017;360:21–7. https://doi.org/10.1016/j.jpowsour.2017.05.119.

[34] Zhang X, Pant D, Zhang F, Liu J, He W, Logan BE. Long-Term Performance of Chemically and Physically Modified Activated Carbons in Air Cathodes of Microbial Fuel Cells. ChemElectroChem 2014;1(11):1859–66. https://doi.org/10.1002/celc.201402123.

[35] Zhang F, Pant D, Logan BE. Long-term performance of activated carbon air cathodes with different diffusion layer porosities in microbial fuel cells. Biosens Bioelectron 2011;30(1):49–55. https://doi.org/10.1016/j.bios.2011.08.025.

[36] Pasternak G, de Rosset A, Rutkowski P. Horizontal microbial fuel cell system producing biosurfactants in response to current generation from waste cooking oil as a fuel. Energ Conver Manage 2023;281:116807.

[37] Pasternak G, Greenman J, Ieropoulos I. Dynamic evolution of anodic biofilm when maturing under different external resistive loads in microbial fuel cells. Electrochemical perspective. J Power Sources 2018;400(August):392–401. https://doi.org/10.1016/j.jpowsour.2018.08.031.

[38] Aelterman P, Versichele M, Marzorati M, Boon N, Verstraete W. Loading rate and external resistance control the electricity generation of microbial fuel cells with different three-dimensional anodes. Bioresour Technol 2008;99(18):8895–902. https://doi.org/10.1016/j.biortech.2008.04.061.

[39] L. Szydlowski, J. Ehlich, I. Goryanin, and G. Pasternak, “High-throughput 96-well bioelectrochemical platform for screening of electroactive microbial consortia,” *Chem. Eng. J.*, vol. 427, no. April 2021, p. 131692, 2022, doi: 10.1016/j.cej.2021.131692.

[40] Baranitharan E, Khan MR, Prasad DMR, Teo WFA, Tan GYA, Jose R. Effect of biofilm formation on the performance of microbial fuel cell for the treatment of palm oil mill effluent. Bioprocess Biosyst Eng 2015;38(1):15–24. https://doi.org/10.1007/s00449-014-1239-9.

[41] Greenman J, Gajda I, You J, Mendis BA, Obata O, Pasternak G, et al. Microbial fuel cells and their electrified biofilms. Biofilm 2021;3:100057.

[42] Kulikovsky AA, Kucernak A, Kornyshev AA. Feeding PEM fuel cells. Electrochim Acta Jan. 2005;50(6):1323–33. https://doi.org/10.1016/J.ELECTACTA.2004.08.023.

[43] Pasternak G, Ormeno-Cano N, Rutkowski P. Recycled waste polypropylene composite ceramic membranes for extended lifetime of microbial fuel cells. Chem Eng J 2021;425:130707.

[44] N. Sekar and R. P. Ramasamy, “Electrochemical impedance spectroscopy for microbial fuel cell characterization,” *J. Microb. Biochem. Technol.*, vol. 5, no. SPECIALISSUE.2, 2013, doi: 10.4172/1948-5948.s6-004.

[45] Lepage G, Albernaz FO, Perrier G, Merlin G. Characterization of a microbial fuel cell with reticulated carbon foam electrodes. Bioresour Technol 2012;124: 199–207. https://doi.org/10.1016/j.biortech.2012.07.067.

[46] Borole AP, Aaron D, Hamilton CY, Tsouris C. Understanding long-term changes in microbial fuel cell performance using electrochemical impedance spectroscopy. Environ Sci Technol 2010;44(7):2740–5. https://doi.org/10.1021/es9032937.

[47] Cheng Z, Jiang X, Cui Z, Jia H, Wang J. The characteristic of electrode of degradation of bio-electrochemical system based on in-situ ultrasonic monitoring: Biofilm and ion precipitation. Sci Total Environ 2021;789:147987. https://doi.org/10.1016/j.scitotenv.2021.147987.

[48] Velasquez-Orta SB, Head IM, Curtis TP, Scott K, Lloyd JR, Von Canstein H. The effect of flavin electron shuttles in microbial fuel cells current production. Appl Microbiol Biotechnol 2010;85(5):1373–81. https://doi.org/10.1007/s00253-009-2172-8.

[49] Zhang X, He W, Ren L, Stager J, Evans PJ, Logan BE. COD removal characteristics in air-cathode microbial fuel cells. Bioresour Technol 2015;176:23–31. https://doi.org/10.1016/j.biortech.2014.11.001.

[50] Al Nasser WN, Shah UV, Nikiforou K, Petrou P, Heng JYY. Effect of silica nanoparticles to prevent calcium carbonate scaling using an in situ turbidimetre. Chem Eng Res Des 2016;110:98–107. https://doi.org/10.1016/j.cherd.2015.12.006.

[51] Goswami C, Hazarika KK, Bharali P. Transition metal oxide nanocatalysts for oxygen reduction reaction. Mater Sci Energy Technol 2018;1(2):117–28. https://doi.org/10.1016/j.mset.2018.06.005.

SUPPORTING INFORMATION

The effect of surface and porous structure on long-term performance of carbon powder cathodes without binder, during a 300-day trial in microbial fuel cells

Aleksander de Rosset, Piotr Rutkowski, Grzegorz Pasternak*

Department of Process Engineering and Technology of Polymer and Carbon Materials,
Faculty of Chemistry, Wroclaw University of Science and Technology, Wroclaw 50-370,
Poland.

*Corresponding author: grzegorz.pasternak@pwr.edu.pl

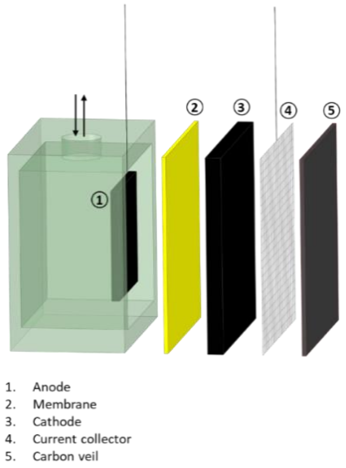

Fig. S1. Structure of the cathode module

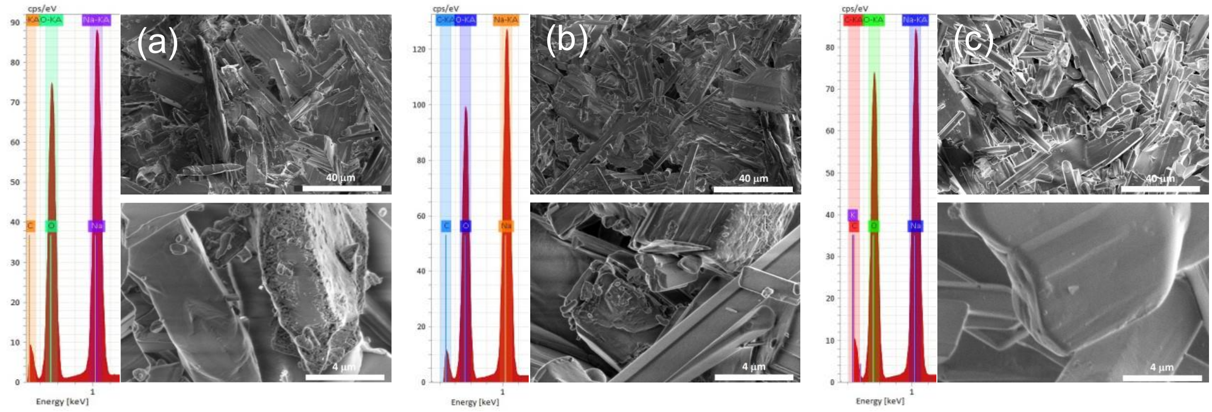

Fig. S2. Scanning Electron Microscopy images of salts collected from the air-side of the cathode. CWZ-22 (a), CWZ-22/Si (b), and CWZ-35 (c).

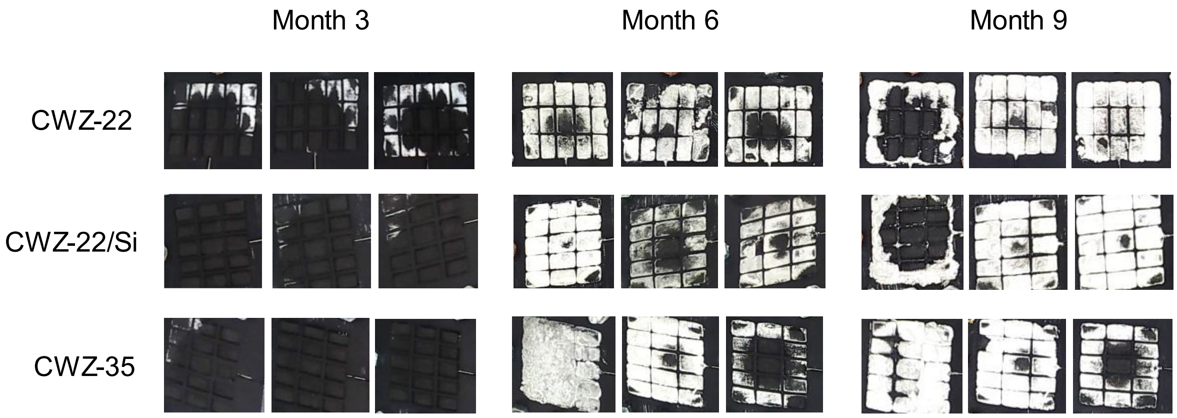

Fig. S3. Images of the chemical fouling on the outer surface of the cathode.

Tab. S1. Physical parameters of activated carbons.

	CWZ-22	CWZ-22/Si	CWZ-35
BET surface area [$m^2\ g^{-1}$]	971.7	948.3	1272.5
Total pore volume [$cm^3\ g^{-1}$]	0.49	0.51	0.69
Average pore width [nm][a]	1.20	1.04	1.32
Micropore volume [$cm^3\ g^{-1}$][a]	0.38	0.35	0.48

[a] – calculated with DR method

Tab. S2. Composition of the cathodes before and after use in MFCs.

Element	Mass [%]					
	CWZ-22		CWZ-22/Si		CWZ-35	
	before	after	before	after	before	after
Carbon	80,43	89,12	88,50	83,34	81,47	80,24
Oxygen	11,36	6,31	6,78	10,16	10,59	11,71
Sodium	ND	1,49	0,16	3,70	ND	5,04
Silicon	ND	0,25	0,90	0,16	0,13	ND
Potassium	3,16	0,35	0,96	0,40	2,17	0,60
Calcium	3,02	1,07	2,32	0,91	2,97	1,13
Copper	0,41	0,56	ND	0,58	0,23	0,40
Manganese	0,12	0,43	ND	0,30	0,18	0,43
Magnesium	ND	0,43	0,38	0,44	1,17	0,45

5.2. Horizontal microbial fuel cell system producing biosurfactants in response to current generation from waste cooking oil as a fuel

5.2.1. Omówienie publikacji

Głównym wyzwaniem dla przemysłowego wykorzystania biosurfaktantów są wysokie koszty produkcji, związane z niską wydajnością ich wytwarzania oraz wysokimi kosztami surowców i oczyszczania. Jednym z możliwych rozwiązań jest wykorzystanie MFC zasilanych olejami odpadowymi z przemysłu spożywczego do syntezy mikrobiologicznych surfaktantów i jednoczesnej produkcji energii elektrycznej. Takie rozwiązanie pomogłoby zmniejszyć problem związany z odpadami i zwiększyć ekonomiczność i konkurencyjność procesu produkcji biosurfaktantów. Jednak dotychczas w literaturze opisanych zostało niewiele badań dotyczących wykorzystania odpadowych olejów roślinnych w układach bioelektrochemicznych, a uzyskane wyniki wskazują na niewielką wydajność układu, ze względu na mocno hydrofobowy charakter substratu.

Dlatego celem tej pracy było zbadanie wpływu konstrukcji MFC na produkcję biosurfaktantów i energii elektrycznej, ustalenie dodatniego wyniku energetycznego procesu bioelektrochemicznej syntezy biosurfaktantów z odpadowego oleju rzepakowego oraz określenie roli wytwarzania energii elektrycznej w syntezie jako możliwej metody monitorowania stężenia biosurfaktantów za pomocą napięcia wyjściowego.

W badaniu zastosowano MFC z katodą powietrzną w pełni wydrukowane w 3D z polipropylenu. W pierwszym etapie eksperymentu wszystkie MFC zostały zainokulowane osadem czynnym z oczyszczalni ścieków, a następnie były zasilane przez 8 tygodni w trybie wsadowym pożywką zawierającą octan sodu jako źródło węgla w celu utworzenia stabilnego biofilmu na anodzie. Drugi etap rozpoczął się po osiągnięciu powtarzalnych gęstości mocy w eksperymentach polaryzacyjnych. W drugim etapie octan sodu zastąpiono odpadowym olejem posmażalniczym o stężeniu 0.1% (v/v). Początkowo wszystkie MFC pracowały jako układy pionowe z mieszaniem, ale nie odnotowano znaczącym zmian wytwarzanej energii elektrycznej oraz zaobserwowano akumulację substratu olejowego na powierzchni cieczy, dlatego 3 ogniwa zmodyfikowano, aby pracowały pasywnie w ułożeniu poziomym.

Testy polaryzacyjne oraz rzeczywiste wartości mocy wyjściowych wykazały, że konsorcjum mikrobiologiczne cechowało się wyższą zdolnością adaptacyjną do konwersji zużytego oleju roślinnego w poziomej konstrukcji MFC, ze względu na pożądane rozmieszczenie substratu w komorze anodowej i na powierzchni anodowego biofilmu. W rezultacie poziome MFC wykazały wyższy wzrost wydajności oraz spadek rezystancji wewnętrznej, w porównaniu do pionowego MFC, co przypisano bardziej intensywnemu rozwojowi biofilmu na poziomej anodzie wskutek korzystniejszego rozprowadzenia substratu wewnątrz układu. Maksymalna uzyskana gęstość mocy MFC poziomego była o ponad 100% wyższa niż MFC pionowego z mieszaniem. Podobnie zaobserwowano znaczący wpływ orientacji elektrod na syntezę biosurfaktantów z odpadowego oleju roślinnego w MFC. Minimalna wartość napięcia powierzchniowego uzyskana w poziomym MFC wyniosła 45.4 mN m^{-1}, podczas gdy w anolicie pionowego MFC zaobserwowano jedynie nieznaczny spadek napięcia powierzchniowego. Ponadto odnotowano bezpośrednią korelację pomiędzy wytwarzaną mocą a napięciem powierzchniowym anolitu poziomego MFC. Pomiary degradacji substratu oraz wyliczona wydajność kulombowska również wykazały, że zmieniając orientację anody na poziomą, wydajność odzyskiwania energii została zwiększona ponad 8-krotnie, zmniejszając straty wydajności na konkurencyjnych ścieżkach degradacji odpadowego oleju.

Przedstawione badanie wykazało, że efektywność degradacji zużytego oleju roślinnego można znacząco zwiększyć poprzez zmianę orientacji elektrod. Produkcja energii i wydajność kulombowska poziomego MFC były znacznie wyższe niż pionowego MFC z mieszaniem. Co więcej, produkcję biosurfaktantów zaobserwowano jedynie w poziomych MFC i wykazano, że ich obecność jest bezpośrednio skorelowana z wytwarzaniem energii, co może dodatkowo pozwolić na proste i bezkosztowe monitorowanie syntezy bioelektrochemicznej w dobrze ugruntowanym systemie.

5.2.2. Publikacja

Energy Conversion and Management 281 (2023) 116807

Contents lists available at ScienceDirect

Energy Conversion and Management

journal homepage: www.elsevier.com/locate/enconman

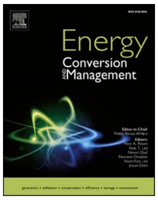

Horizontal microbial fuel cell system producing biosurfactants in response to current generation from waste cooking oil as a fuel

Grzegorz Pasternak [*], Aleksander de Rosset, Piotr Rutkowski

Department of Process Engineering and Technology of Polymer and Carbon Materials, Faculty of Chemistry, Wroclaw University of Science and Technology, Wroclaw 50-370, Poland

A R T I C L E I N F O

Keywords:
MFC
Biosurfactant
Electrofermentation
Design
Bioelectrochemical synthesis

A B S T R A C T

Microbial fuel cells (MFCs) are recognised as a platform technology, where several processes take place at the same time, including electricity generation. In this study, for the first time, the horizontal MFC system is proposed, capable of synthesizing biosurfactants, where their quantity is directly correlated with the power production. Waste rapeseed oil was used as a sustainable fuel to drive both processes. Initially, all tested MFCs worked as vertical systems where only negligible power generation was noted. Therefore, the MFCs were reconfigured to work as passive, horizontally-aligned system while vertical, agitated control was also investigated. Only a slight reduction of surface tension, resulted from biosurfactant synthesis, was observed in the anolyte in an agitated vertical MFC system, which produced a maximum power density of 2.37 W m^{-3}. The horizontal MFC system led to an increase in electricity production of 104.7 % to 4.84 W m^{-3}. Furthermore, an increase in current generation was accompanied by an increase in biosurfactant production which was observed by the drop of surface tension in anodic chamber to 50.7 mN m^{-1}. Significant, direct correlation (r = -0.77) between power and biosurfactant generation was noted. The results showed that it is possible to establish the energy net positive production of biosurfactants, through an appropriately designed MFC system, and provided the first evidence, that the biosynthesis process is a direct response of current generation. These results represent a novel approach in monitoring of the biosynthesis of surfactants solely through the use of electrical signal and design of bioelectrochemical systems. This process occurs through electrofermentative pathways, assisted with the extracellular electron transport.

1. Introduction

Microbial fuel cell (MFC) is a bioelectrochemical reactor in which organic matter is oxidized by electroactive bacteria and converted into electricity [1,2]. The typical MFC design comprises of anode and cathode compartments, while more practical MFC designs use an air–cathode instead of a cathodic chamber [3]. Several derivatives of these systems have been established for various processes. Since bioelectrochemical systems offer a unique ability to generate electricity in parallel with other processes, one of their promising applications is microbial electrosynthesis. In this process, autotrophic electroactive microorganisms interact with a cathode as an electron donor to reduce a specific substrates such as CO_2. This leads to the biosynthesis of specific, potentially valuable products [4]. Interest in this technology has grown rapidly in recent years, with several ongoing R&D projects around the world [5]. Examples of cathode electrosynthesis processes are acetate production from carbon dioxide (CO_2) [6] or conversion of fumarate to succinate [7]. On the other hand, microorganisms at the anode can convert the organic substrate into butanol [8], ethanol [9] or acetoin [10]. The anodic and cathodic processes, where the electrode with its potential acts as the electron source or sink to drive unbalanced fermentation and synthesis from organic waste, are referred as electrofermentation [5,11].

These approaches can be used to enhance the spectrum of possible by-products of electricity production from waste in MFCs. An interesting group of biochemically synthesised, but complex compounds is biosurfactants (BSFs). BSFs are microbial-derived amphiphilic compounds which contain hydrophilic and hydrophobic groups that can reduce surface and interfacial tension [12]. These compounds are mainly produced by various bacterial genera (such as *Pseudomonas, Rhodococcus,*

The preproof version of this article is available at https://doi.org/10.2139/ssrn.4196412.

[*] Corresponding author.

E-mail address: grzegorz.pasternak@pwr.edu.pl (G. Pasternak).

https://doi.org/10.1016/j.enconman.2023.116807
Received 1 December 2022; Received in revised form 19 January 2023; Accepted 10 February 2023

Streptomyces, Bacillus, Serratia) and fungal species, and posess large variety of structures and properties. The most commonly described groups and examples (in brackets) of biosurfactants consist of glycolipids (rhamnolipids), phospholipids (phosphatidylethanolamine) and lipopeptides (surfactin) [13]. Biosurfactants can be used as food additives, detergents, bioremediation agents, and have prospective applications in the crude oil extraction industry, pharmaceutical industry and environmental protection [14,15,16,17]. Compared to chemically synthesized surfactants, biosurfactants have advantages in biodegradability, biocompatibility, lower toxicity, and higher stability at extreme temperatures, pH and salinity [18,19]. Regardless of the importance of such useful compounds, a scarce number of reports have been published in this field where biosurfactants have been the target of electrochemically-driven biosynthesis, although these compounds can be directly used to improve the performance of bioelectrochemical systems [20,21].

The synthesis of biosurfactants in BES was reported in 2008, and it has been shown, that the interaction of rhamnolipids produced by *Pseudomonas spp*. with phenazines allowed *Brevibacillus* sp. to achieve extracellular electron transfer [22]. Since then, according to the recent review by Pasternak *et al.* [20], there have been only individual studies, where biosurfactants were investigated in BES and these studies reported some unique characteristics of biosurfactants. When present in bioelectrochemical systems, these compounds may contribute significantly to the operation and efficiency of MFC by improving its power output [20] and can be further applied in microscale systems to improve their possible issues caused by low power output [24]. Their presence improves the bioavailability of hydrophobic substrates [25] and increases the hydrophilicity of the electrode surface, leading to improved biofilm formation [26]. Furthermore, biosurfactants have a significant impact on exoelectrogen biodiversity and therefore facilitate their enrichment in anodic bacterial communities [26]. These studies show the importance of these amphiphilic compounds in the startup and operation of bioelectrochemical systems. Nevertheless, the synthesis of such valuable compounds is full of challenges, one of which is the oxygen-limiting conditions. One of the approaches to combat the low-yield synthesis can be synthetic biology. Such an approach was reported for the overexpression (where genetically modified organisms overproduce specific compound) systems in *Pseudomonas aeruginosa and P. putida* species [27,28]. None of the above-mentioned studies have reported the correlation of the synthesis process with the production of electricity, and mainly the synthetic substrates such as LB (Lysogeny Broth) or acetate were used to induce the production.

On the industrial scale, the main challenge for the use of biosurfactants is high production costs, therefore, cheaper and more efficient synthesis processes must be developed [29]. The use of waste products can help solve this challenge. Therefore, the aim of this work was to establish the net positive energy process of bioelectrochemical synthesis of biosurfactants from waste rapeseed oil, investigate the effects of MFC design on biosurfactant and electricity production, and determine the role of electricity generation in the synthesis as a possible, real-time monitoring method. Such an approach for real-time monitoring of the surfactant biosynthesis through electrical signal may be a significant breakthrough for low-cost process monitoring.

2. Materials and methods

2.1. Construction and operation of MFC

In this study, a single-chamber air–cathode microbial fuel cell was used. The MFC assembly was constructed of components printed in 3D technology from polypropylene (Fiberlogy, Poland). The outer dimensions of the cell were 8 cm in width, 5 cm in height, and 5 cm in length, and the working volume was of 20 cm^3. The square-shaped anode with a geometric area of 9 cm^2 was prepared from carbon veil (PRF Composite Materials, Dorset, UK) with 308LSi steel wire. The cathode was made of CWZ-22 activated carbon (850 m^2 g^{-1}). The cathode materials were pressed into a cathode spacer with a stainless-steel mesh placed inside the cathode as a current collector. The total surface area of the cathode was equal to 9 cm^2. In addition, on the air side, a carbon veil was placed as a diffusion and protective layer. The anode chamber was separated from the cathode by a cation exchange membrane (CMI-7000, USA). A rubber seal was used between the anode chamber and the cathode module, and the elements were connected with screws. The distance between anode and cathode was set as 7 mm. All MFCs were operated at room temperature, with a starting external load (R_{ext}) of 2 kΩ. Earlier studies have shown that the best results were obtained when MFCs were operated under R_{ext} closer to internal resistance (R_{int}) [30,31]. Therefore, after each measurement of the polarization curves, the optimal resistance was calculated at maximum power point, and the value of the external resistor was adjusted. Since the experiment was aimed at a net positive energy process, it consisted of three horizontal MFCs and a single vertical MFC control with agitation as a reference model (Fig. 1). During the operation of the vertical control MFC, the anode solution was stirred with a magnetic stirrer at a speed of 160 rpm. Fluidic conditions in horizontal MFCs remained passive throughout the experiment.

2.2. Culture conditions

The composition of the mineral salt medium (MSM) used in the anode chamber was as follows (g L $^{-1}$): NH_4Cl (Chempur, Poland) 1.5; Na_2HPO_4 (POCH, Poland) 0.6; KCl (POCH, Poland) 0.1; $NaHCO_3$ (Chempur, Poland) 2.5; trace element solution of 10 ml L^{-1} and a carbon source $CH_3COOH{\cdot}3H_2O$ (Chempur, Poland) 0.82 g L $^{-1}$. The pH of the MSM was equal to 8.5. All solutions were prepared with Milli-Q water and autoclaved prior to use (121 °C, 20 min.).

In the first stage of the experiment, all MFCs were inoculated with activated sludge from the aerobic chamber of the wastewater treatment plant (Ścinawka, Poland). After 3 days, the activated sludge was removed and replaced with MSM using $CH_3COOH{\cdot}3H_2O$ as the carbon source at a concentration of 0.82 g L^{-1}. The feed solution (MSM/acetate) was then changed daily for 8 weeks to form stable biofilms on the anode (HRT = 25.0 ± 2.7 h). The second stage started when the repeatable power densities were achieved. In the second stage, sodium acetate was replaced with waste vegetable oil at a concentration of 0.1 % (v/v). The density of the oil was of 0.905 g cm^{-3}. The waste cooking oil was consequently used as a fuel for the next 8 weeks, until the end of the experimental period. The medium with waste vegetable oil was replaced every 1–2 days (HRT = 32.6 ± 16.4 h). During the entire experiment, the evaporated anolyte was resubstituted daily with sterile Milli-Q water.

2.3. Electrochemical experiments and real time temporal monitoring

Closed circuit voltage (CCV) was measured and recorded in real time with 3 min interval using KEYSIGHT DAQ970A data acquisition system (KEYSIGHT TECHNOLOGIES, USA). The electrochemical characteristics of the cell were tested in a three-electrode system using a Multi-PalmSens4 potentiostat (Palmsens BV, Netherlands), with the anode as working electrode (WE), the cathode serving as the counter electrode and the saturated Ag/AgCl electrode as the reference electrode. Polarization and power curves were obtained using the linear sweep voltammetry (LSV) technique in the potential range from open circuit potential to 0.0 V WE vs Ag/AgCl, at the scan rate of 1 mV s^{-1}. On the basis of the experimental data obtained, the maximum power density, current density, and internal resistance were determined. Cyclic voltammetry measurements were performed in the potential range of −0.7 V to 0.5 V WE vs Ag/AgCl with a scan rate of 15 mV s^{-1}.

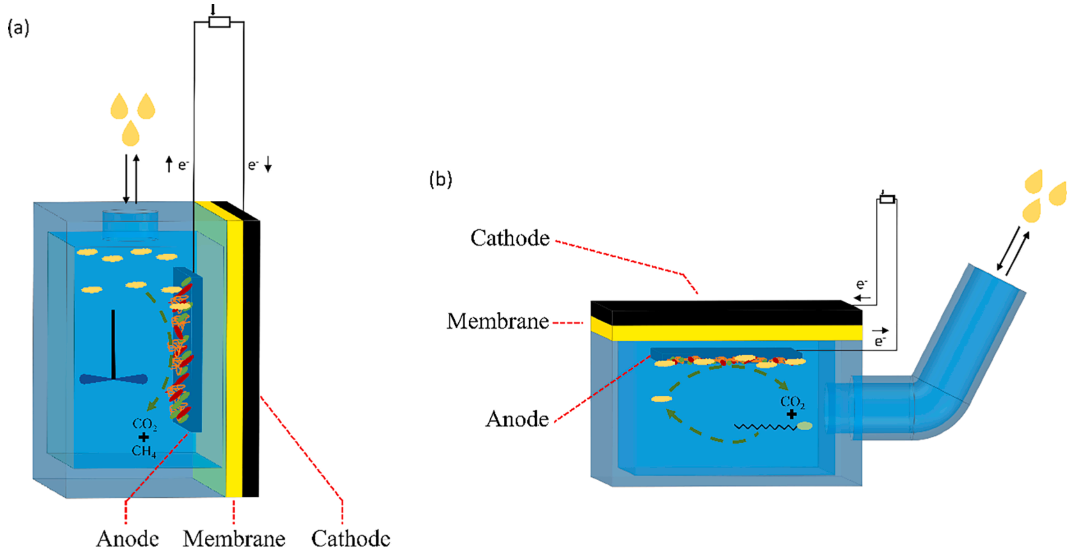

Fig. 1. Process of bioelectrochemical conversion of waste cooking oil to biosurfactants investigated in: vertical (a) and horizontal (b) MFC design.

2.4. Monitoring of biosurfactants

2.4.1. Surface tension measurement

The surface tension (SFT) of the anolyte was measured with a BPT mobile bubble pressure tensiometer (KRUSS, Germany). The device was calibrated before each series of measurements. For SFT measurements, 1 ml of the anolyte from the MFC was sampled and analyzed. Subsequently, the sample was returned to the anodic chamber. Such an approach allowed us to prevent the anolyte aeration and enabled better averaging of the sample. The surface tension was monitored at one-hour interval, until the minimum value was reached. Afterwards, the sampling frequency was reduced as displayed on Figs. 4 and 5. The abiotic control was also monitored as the reference to underline the surface tension properties of produced biosurfactants.

2.4.2. Foaming activities

Foaming ability and foam stability were measured and calculated according to the following equations:

$$Foaming\ ability = \pi \times r^2 \times h_0,$$

$$Foam\ stability = \frac{h_{10}}{h_0},$$

where r – diameter of measuring vessel; h_0 – initial foam height; h_{10} – foam height after 10 min.

2.4.3. Emulsification index (E24)

To determine E24, 3 mL of vegetable oil and 3 mL of supernatant were transferred to a tube, mixed with the vortex for 2 min and leaved to stand for 24 h. The emulsification index (E24) is given as a percentage of height of emulsified layer divided by total high of the liquid column [12].

2.5. Coulombic efficiency and COD removal

The chemical oxygen demand (COD) of the fresh medium, as well as the medium after MFC treatment, was determined by the potassium dichromate oxidation method, according to the manufacturer’s instructions (Hach, USA). COD removal efficiency was calculated using the following equation:

$$COD\ removal = \frac{COD_0 - COD_t}{COD_0},$$

where COD_0 – initial COD of the fresh medium (mg L^{-1}); COD_t – COD of the anolyte after “t” time (mg L^{-1}).

Coulombic efficiency (CE) was calculated for the complex substrate in the batch system according to [32]:

$$CE = \frac{8\int_0^t Idt}{FV_{An}\Delta COD},$$

where 8 – constant, based on molecular weight of oxygen and number of electrons exchanged per mole of oxygen; I – current (A); t – time of operation (s); F – Faraday’s constant (96500C/mol e^-); V_{An} – working volume of anode chamber; ΔCOD – change in COD concentration (mg L^{-1}).

2.6. Data processing

The experimental data were processed and visualized graphically using OriginLab 2019. The current and power were calculated according to Ohm’s law:

$I = \frac{U}{R}$(Ampere),

$P = U \times I$(Watt),

where U – voltage (V); R – resistance (Ω); P – power (W); I – current (A).

2.7. Physicochemical measurements

Oxygen concentration was monitored by the galvanic oxygen sensor ELMETRON COG-1 (ELMETRON, Poland). The sensor was calibrated for 0 % oxygen saturation in Na_2SO_3 solution and in the air, corresponding to 100 % saturation. pH of the MSM was measured using the IONODE IJ44A electrode (ELMETRON, Poland).

2.8. Analysis of waste cooking oil and its degradation products

Gas chromatography coupled with mass spectrometry was used to analyse organic compounds. The procedure started with a preliminary liquid–liquid extraction with CH_2Cl_2 in an inert environment. Then, 2 µl of the extract obtained was analysed on a GC–MS instrument (HP 6890–5973). The HP-INNOWAX capillary column (Agilent Technologies, USA) with an internal diameter of 0.25 mm and a length of 30 m was used as the separation system. High purity He was used as the carrier gas at a flow rate of 0.7 ml/min. The oven temperature program

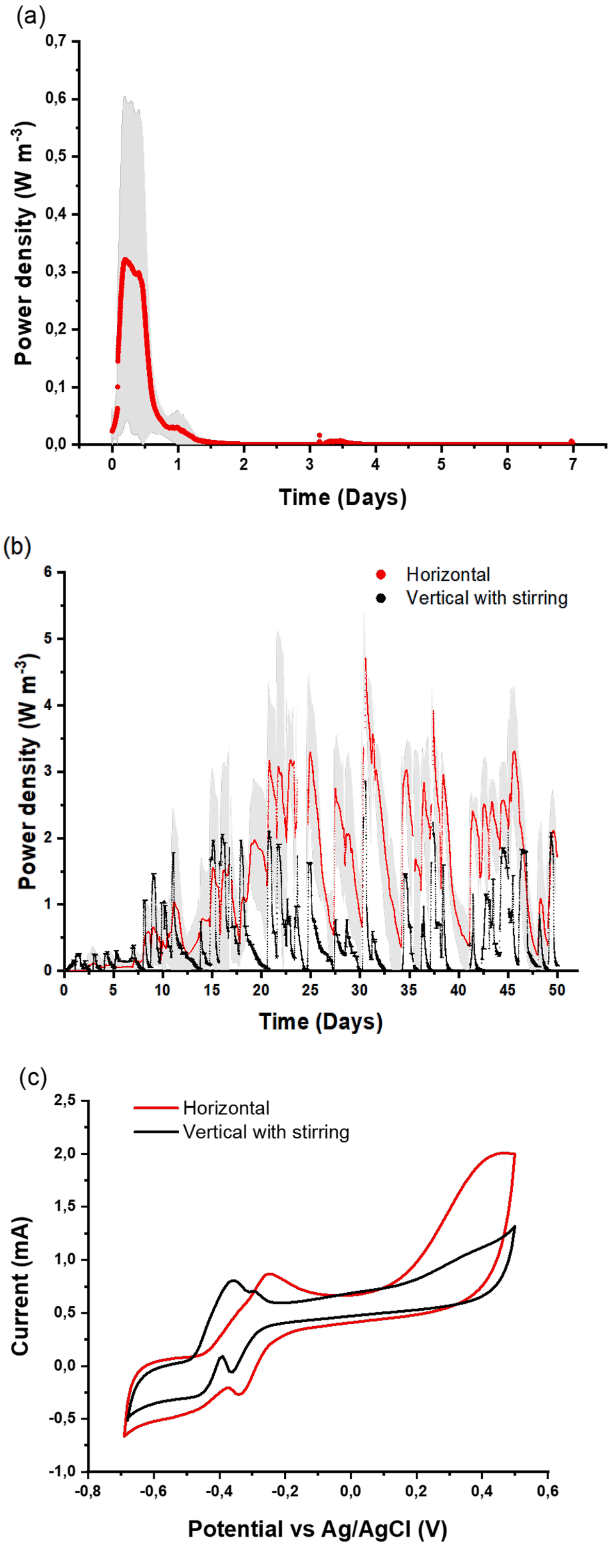

Fig. 2. Real time temporal performance of all MFCs operating in vertical configuration without mixing during the first 7 days of operation (a) and after reconfiguration for the entire experiment with waste vegetable oil as a substrate (b), as well as cyclic voltammetry curves (c) carried out after 46 days of operation.

was set as follows: 40 °C for 5 min, then increased to 240 °C at a rate of 20 °C/min, keeping the temperature at 240 °C for 20 min. The molecular weight scan range was set from 29 to 350 Da.

3. Results and discussion

3.1. Electricity generation

In the first stage of the experiment, all MFCs were operated in the vertical position without agitation, and sodium acetate was used as the carbon source. After 8 weeks of operation, stable power and similar performance were achieved for all MFCs. At the beginning of the second stage of the experiment, all MFCs were left in a vertical position without agitation and fed with waste vegetable oil. In the initial MFC configuration, no current response was observed in the first 7 days of operation following the substrate change (Fig. 2a.). Moreover, the waste oil accumulation over the surface of the anolyte was noticed. Due to the limited bioavailability of the waste vegetable oil for microorganisms on the anode, a reconfiguration was made and the electricity production efficiency of the horizontal MFC was assessed and compared to the performance of vertical MFC with stirring. The recorded real-time power performance showed that all MFCs achieved similar values after 10 days of adaptation to the new substrate (Fig. 2b.). At a later stage however, an intensive increase in the power density output of the horizontal MFCs was observed, while no significant changes in the power efficiency of the vertical MFC with mixing were noticed. In the third week, the power density of horizontal MFCs was around twice as high as vertical MFC, and this trend continued until the end of the experiment. The maximum average power density of horizontal MFCs (4.71 ± 0.62 W m^{-3}) was observed on 31 day of operation and was 68 % higher than for vertical MFC with agitation. Previous studies have reported that after the time of adaptation to the new, yet simple substrate, it is possible to generate electrical power similar to the value observed for the original substrate [33]. However, the complex composition and hydrophobic nature of the waste vegetable oil is more challenging in terms of microbial adaptation in a microaerobic environment. The results obtained from real-time measurements indicated that the microbial consortium revealed improved adaptation to the conversion of waste vegetable oil within the horizontal MFC design, most likely due to the desirable distribution of the substrate within the anode chamber and anodic biofilm surface.

The cyclic voltammogram of horizontal MFC indicated the existence of two redox systems involved in the transfer of electrons to the anode (Fig. 2c.). The oxidation–reduction couples occurred at formal potentials of −0.293 V and −0.370 V vs Ag/AgCl for horizontal MFCs, implying the presence of a similar microbial consortium on the anodes, capable of electrofermentation of the waste oil substrate. Such potentials indicate that the biofilm created may be dominated with *Geobacter sulfurreducens* and *Pseudomonas aeruginosa* [34,35]. The cyclic voltammogram of the vertical MFC also showed the existence of two redox systems involved in the transfer of electrons to the anode. However, the oxidation–reduction peaks occurred at different formal potentials of −0.330 V and −0.409 V vs Ag/AgCl, suggesting a different redox pathways of the biofilm.

To characterize the dynamic changes in performance of both MFC designs, polarisation experiments were carried out throughout the experiment. Fig. 3a. shows the values of the maximum power densities extracted from the polarisation data. After 31 days of operation on waste vegetable oil, the horizontal MFC reached the highest power density of 4.84 ± 1.5 W m^{-3}. At the same time, the vertical MFC achieved a power density of 2.37 W m^{-3}. Therefore, the horizontal positioning of the anode resulted in a 104.7 % improvement in power density, compared to the typical vertical design with agitation. The electrical power generated in the vertical MFC with mixing was comparable to the literature data, while the power density obtained in the horizontal setup have outreached the values obtained by MFCs with a similar configuration and fed with waste vegetable oils reported in the literature [36,37,38].

Fig. 3c and 3d show the polarization and power curves obtained on

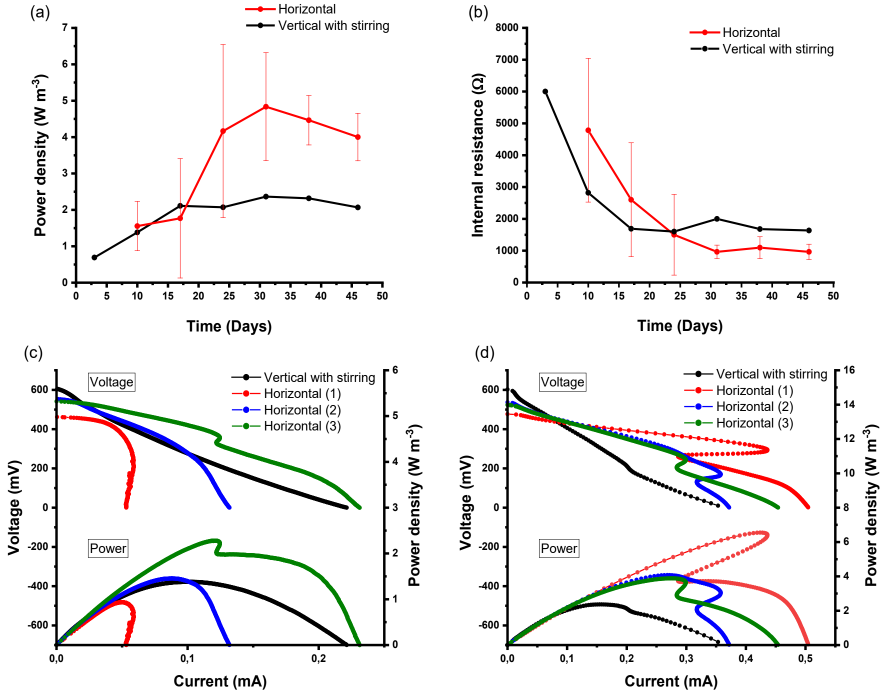

Fig. 3. Graph of changes in: power density (a) and internal resistance (b) as a function of operating time, as well as polarization and power curves for: 10 (c) and 31 (d) days of operation.

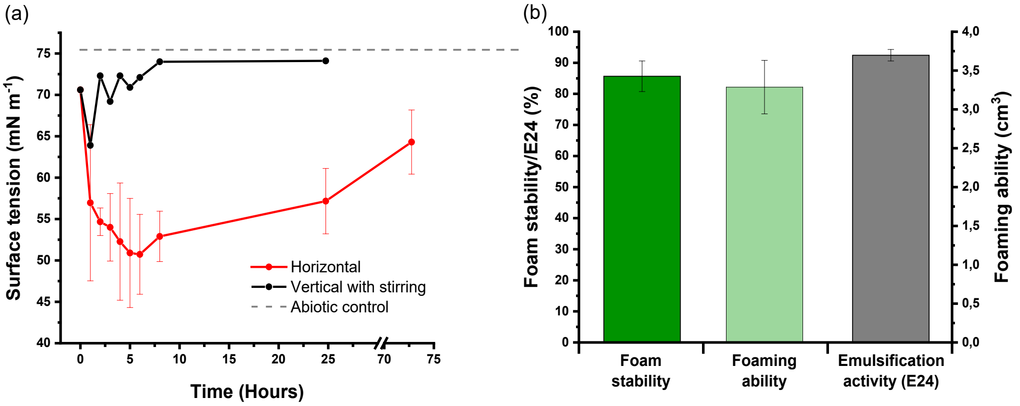

Fig. 4. Comparison of changes of surface tension during the degradation of the waste vegetable oil of vertical and horizontal MFCS (a), as well as foaming and emulsification properties of anolyte of the horizontal MFCs (b). The horizontal dashed line represents the average value of the surface tension of the medium measured at the same frequency (abiotic control), equal to 75.5 ± 0.4 mN m^{-1}.

the 10th and 31st days of operation. The open circuit voltage (OCV) ranged from 0.47 V to 0.61 V for all MFCs. The highest OCV value obtained for the vertical MFC (0.61 V), was probably caused by the improved ion transfer associated with mixing the anolyte [32]. The shape of the polarization curves can generally be divided into three sections of the potential losses: the initial voltage drop due to electrode reaction overpotentials (activation losses), followed by a relatively linear potential drop, where the ohmic losses (associated *i.a.* to the MFC design or electrolyte and biofilm properties) dominate, and finally the usually sharp potential drop at higher current, for which concentration losses are responsible (mass transfer effects) [32]. By analysing the polarization curves acquired from the 10th day (Fig. 3c), it was observed that the low power density recorded for MFCs was caused mainly by ohmic losses. A different trend was observed on the 31st day of operation with the waste vegetable oil substrate. As shown in Fig. 3d, the power of the horizontal MFCs was limited by mass transfer effects, while the overall performance of the agitated vertical MFC was limited by high activation and still by ohmic resistances. Furthermore, in the polarization curves of all horizontal MFCs, a strong overshoot phenomenon was observed. The complexity of the waste cooking oil as a substrate causes an overshoot phenomenon at higher currents because the bacteria at the anode cannot sustain the increasing demand for electrons [39,40]. The maximum current observed for horizontal MFCs on the 31st day of operation was 0.44 ± 0.07 mA, while the maximum current of vertical agitated MFC was 20 % lower (0.35 mA). The adaptation of MFC to the new substrate (waste oil), the shape of the polarization curves was similar for all MFCs. However, after a month of operation, the horizontal MFC showed a significant increase in efficiency compared to the vertical

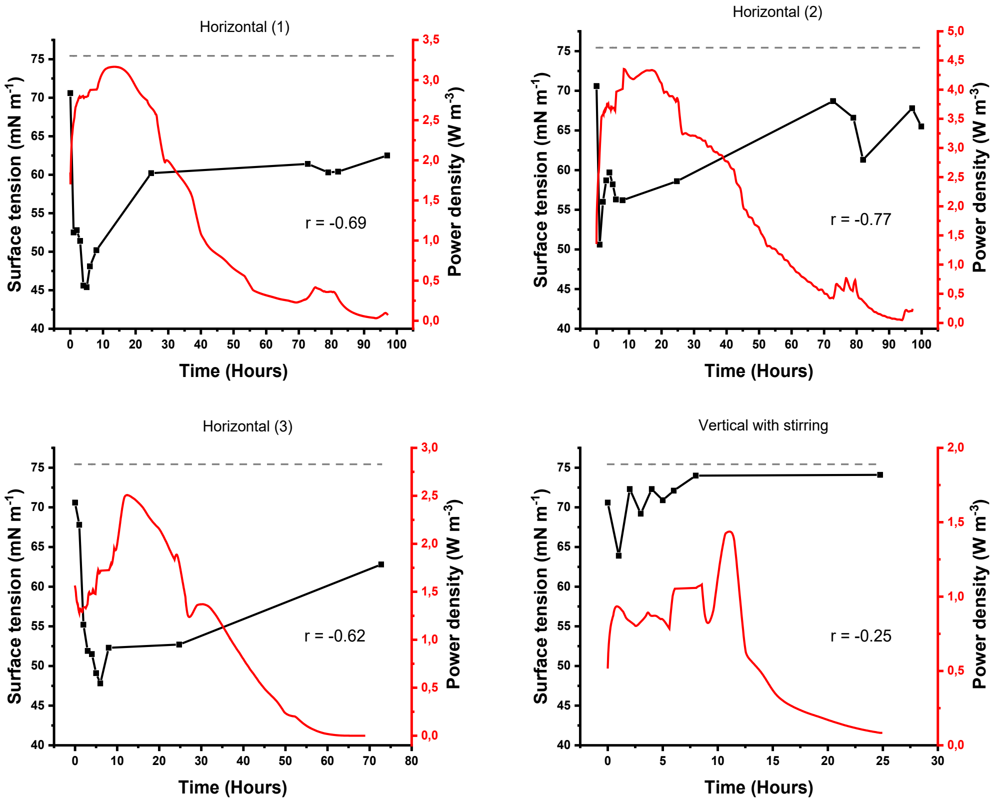

Fig. 5. Changes in power density and surface tension during the degradation of waste vegetable oil in all MFCs. The horizontal dashed line represents the average value of the surface tension of the medium measured at the same frequency (abiotic control). The Pearson's correlation coefficients (r) between power and surface tension are given on each plot.

MFC. The decrease in internal resistance was attributed to the improved development of the biofilm on the horizontal MFC anode, which is directly related to a better distribution of the substrate inside the horizontal system. The internal MFC environment has a crucial role in developing well established biofilm, as it was reported previously for functional MFC elements such as membranes, external load, or presence of biosurfactants [26,31,41].

A similar trend can be observed in Fig. 3b, which presents changes of the internal resistance. The R_{int} values in both MFC designs decreased at a similar rate in the first 3 weeks of adaptation to the oil substrate. After 24 days of operation, a similar values of internal resistance for the vertical and horizontal MFCs was reached (Fig. 3b.). Subsequently, the internal resistance of the horizontal MFC continued to decrease. On the contrary to these results, the R_{int} of the vertical MFC stabilised, reaching an average value of 1730 Ω. The R_{int} of horizontal MFCs stabilised after 5 weeks of operation at an average value of 1010 Ω. By changing the orientation of the electrodes to horizontal, the internal resistance of the MFC was reduced by 40 %. Overall, in the first weeks , the internal resistance of the MFCs decreased along with the ongoing adaptation of the biofilm to the new substrate. Thus, the lower internal resistance of the horizontal MFCs suggests improved development of the biofilm, capable of metabolising waste vegetable oil.

3.2. *Electrochemical activity of microorganisms coupled with the synthesis of biosurfactants*

Real-time monitoring of surface tension was used for detecting biosurfactants in the anolyte. The decrease in anolyte surface tension is a consequence of the biosynthesis of surfactants by microorganisms. The surface tension of the surfactant solution decreases linearly with the increase in the concentration of surfactant molecules in the system, until the critical micelle concentration (CMC) is reached [42,43]. After 46 days of using waste cooking oil fuel, changes in surface tension were monitored during the entire feeding cycle. The results of surface tension monitoring are shown in Fig. 4a. After 6 h of the newly started batch cycle, the horizontal MFCs have reached the lowest surface tension of 50.7 ± 4.8 mN m^{-1}. It should be noted that the minimum value of surface tension achieved in the horizontal MFC throughout the study was equal to 45.4 mN m^{-1}. In the vertical MFC anolyte, only a slight decrease in surface tension to 63.9 mN m^{-1} was observed. Additionally, to characterize the properties of the biosurfactant, the foaming ability, foam stability and emulsification index (E24) were determined for the anolyte of horizontal MFC. A foaming ability of 3.3 ± 0.3 cm^3 (per 20 cm^3 of anolyte), foam stability of 85.7 ± 4.9 %, and E24 of 92.4 ± 1.8 % were obtained (Fig. 4b.).

Depending on the environmental condition in the bioreactor, the production of biosurfactants by microorganisms can take place aerobically, microaerobically or anaerobically. The oxygen concentration in the horizontal MFC was equal to 7.2 %. Thus, the microaerobic pathway of surfactant biosynthesis is presumed as the predominant in this study. Such conditions are sufficient to initiate the biosynthesis process by several microbial species such as *Pseudomonas, Bacillus*, *Clostridium*, *Desulfovibrio*, and *Geobacillus* [44]. Moreover, in our other experiment with an identical method of inoculation, construction and working conditions, one of the dominant strains was *Pseudomonas Aeruginosa*, which indicates the biosynthesis of rhamnolipids in this system. While considering the low coulombic efficiency and the lack of biosurfactant presence in vertical system it can be concluded, that biosurfactants are produced during in electrofermentative pathways, assisted by the extracellular electron transport.

For the first time, a direct relationship between the power generated and the surface tension of the anolyte was observed. The determined correlation coefficients (r) showed a strong negative correlation ($r = (-0.62 \div -0.77)$) for the horizontal MFC, while for the vertical MFC this relationship was weak ($r = -0.25$). Real-time power density changes and surface tension changes plots for each MFC are shown in Fig. 5. In the initial phase of batch-cycle, a sharp decrease in surface tension was observed, and the minimum SFT values were reached during the highest power production by electroactive microorganisms. Such a behaviour suggests a direct correlation of the biosynthesis process with the utilisation and conversion of the fuel into electricity. The limited substrate availability for bacteria was the main factor which initiated the biosurfactant synthesis. There are two main mechanisms of biosurfactant activity that increase the degradation of hydrophobic compounds by microorganisms [45,46]. They can increase the solubility of hydrophobic compounds in water by creating micellar structures, thereby increasing the bioavailability of the substrate for microorganisms. Another way is that biosurfactant molecules adsorb on the surface of cells, increasing their hydrophobicity and thus facilitating the contact of the insoluble substrate with microbial cells. Therefore, when the biosynthesis process is initiated, as a consequence of the increasing amount of biosurfactants in the system, the amount of bioavailable substrate increases and thus the amount of generated electrical power. We presume that a further increase of surface tension results from two ongoing processes. The catabolism of biosurfactants in the system results in further power generation, and the interactions of biosurfactants with the substrate molecules lead to a depletion of biosurfactants at the water/air interface. This could explain the shift in the observed minimal value of the surface tension at the maximum value of the power performance. A similar phenomenon was observed in conventional batch culture, where no electricity was generated [47]. The results indicate that it is possible to monitor the synthesis of biosurfactants using the output voltage of the microbial fuel cells in an established and well characterised, stable system.

The above results indicate that changing the electrode orientation can lead mutual benefits for both energy efficiency and surfactant biosynthesis. Furthermore, the horizontal design made it possible for the first time to monitor biosurfactant synthesis using the voltage output of microbial fuel cells. Table 1 summarizes the results of this experiment and compares them with data from the literature recorded for vegetable oils. The volumetric power density obtained in horizontal MFC is one of the highest values in this comparison and the highest value recorded for the process where both electricity and biosurfactant synthesis takes place. In addition, in these works the higher-range power densities obtained in the MFCs fed with oily wastewater required an increase in the operating temperature or the use of platinum as a component of the cation exchange membrane [48,49]. The simultaneous synthesis of biosurfactants increases the importance of the horizontal alignment of the electrodes in MFC fed with waste vegetable oil.

3.3. MFC performance

The biodegradation efficiency of the oil substrate was assessed by

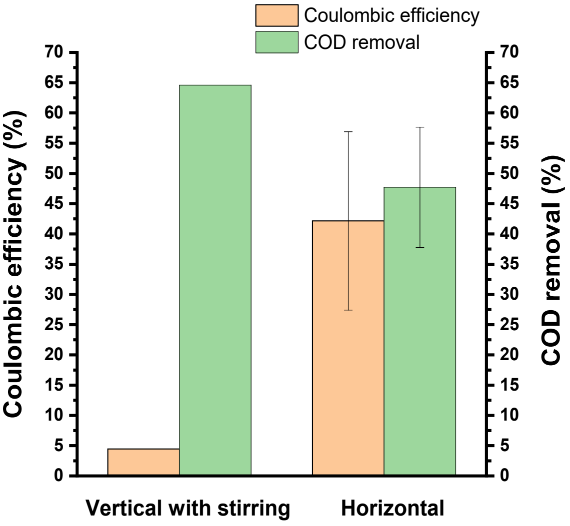

Fig. 6. COD removal performance and coulombic efficiency.

Table 1
Summary of the experiment results and comparison with the literature data.

Type	Operation mode	Fuel	Inoculum	Separator	Electron acceptor	Maximum power density		Product/-s	Reference
						mW m^{-2}	mW m^{-3}(−|-)		
DCMFC (H-type) Stirring	Batch	Used vegetable oil	*Serratia* sp.	Agar salt bridge	None (aeration)	1,13	6,33	Biosurfactant electricity	[37]
UML-MFC	Continous (HRT = 24 h)	POME	Activated sludge	None	None (aeration)	44,6$_{C}$	28,35	Electricity	[50]
DCMFC (H-type) Stirring	Batch	Used vegetable oil	*Serratia* sp.	CEM	None (aeration)	6,64	66,4	Biosurfactant electricity	[36]
SCMFC	Batch (35 °C)	Soybean oil rafinery wastewater	Activated sludge	CEM	None	746	24 100	Electricity	[48]
SCMFC	Batch	OMW	Activated sludge	Nafion + Pt	None	207	12 100	Electricity	[49]
DCMFC	Batch	POME	Anaerobic sludge	Nafion 117	$KMnO_4$	22	320	Electricity	[38]
DCMFC	Batch (35 °C)	Vegetable oil industrial wastewater	Activated sludge	CEM	$KMnO_4$	6119	–	Electricity	[51]
SCMFC Vertical	**Batch**	**waste vegetable oil**	**Activated sludge**	**CEM**	**None**	**52,56**	**2 365**	**Electricity**	**This study**
SCMFC Horizontal	**Batch**	**waste vegetable oil**	**Activated sludge**	**CEM**	**None**	**146,67**	**6 600**	**Biosurfactant electricity**	**This study**

DCMFC – Dual Chamber Microbial Fuel Cell; SCMFC – Single Chamber Microbial Fuel Cell; POME – Palm Oil Mill Effluent; OMW – Olive Mill Wastewater; CEM – Cation Exchange Membrane.

determining the COD removal ability and the coulombic efficiency of the MFCs (Fig. 6.). The COD concentration of the fresh medium was 1840 mg L^{-1}, while the final COD concentration of the anolyte were 565 mg L^{-1} and 899 ± 160 mg L^{-1} for vertical and horizontal MFC, respectively. The low coulombic efficiency accompanied by a high degree of COD removal by vertical MFC was, most likely, the result of the dominance of competitive degradation pathways such as fermentation. Furthermore, the agitation performed in the vertical MFC had an impact on the increase in gas diffusion through the CEM and 3-D printed MFC assembly. On the contrary, the high coulombic efficiency of the horizontal MFCs indicates a good development of the biofilm, which was revealed in polarisation experiments. Thus, it was a result of improved contact of the oil substrate with the electrode, and a biofilm surface was reached in this MFC design. The lower degree of COD removal is presumably the result of the accumulation of biosurfactants in the anode chamber, which remained as a part of COD. By changing the anode orientation to horizontal, the efficiency of electricity recovery has been significantly improved, reducing the efficiency losses on competitive degradation pathways. Furthermore, the lack of agitation led to reducing of the diffusion of oxygen into the anode chamber, which is one of the reasons for the increase in Coulombic efficiency. These results showed that, by using a horizontal MFC design, waste vegetable oil can be used as the sole carbon source for efficient conversion into electricity and biosurfactants simultaneously. The observed coulombic efficiency values were more than 15 % higher than those reported in earlier studies [48,51].

3.4. Analysis of waste cooking oil degradation residues

Changes in the composition of the anolyte were analysed using the GC–MS technique. Fig. 7a. shows the results of the GC–MS analysis of the biotic control sample. The main components of the oil were linoleic acid (9,12-octadecadienoic acid, C18:2), palmitic acid (Hexadecanoic acid, C16:0) and oleic acid (9-octadecenoic acid, C18:1), accounting for 7.63 %, 17.04 % and 50.05 % respectively. As shown in Fig. 7b., a higher oil degradation ratio was observed for vertical MFC, corresponding to the results of COD removal.

Relative changes in the components of waste vegetable oil after the degradation process in microbial fuel cells are shown in Fig. 8a and 8b. The values were normalised to the control samples in such a way that the 0 value on the y-axis for each compound corresponds to the biotic control value. The results showed that most of the fatty acids were completely degraded in both MFC designs; only palmitic acid was difficult to metabolize by bacteria. Furthermore, the quantitative analysis showed that the horizontal MFC degraded 86.4 ± 5.2 % of palmitic acid, while the vertical design provided 61.8 % degradation. Different trends were observed for C12-C26 aliphatic hydrocarbons. The degradation ratio of these components in the vertical MFC increased with the elongation of the carbon chain, except for C13, while in the horizontal MFC an increase in the content of aliphatic hydrocarbons, especially C12-C18, was observed.

In conclusion, in both types of MFC designs, we were able to completely break down the saturated and unsaturated acids in the range C14-C18, except of the palmitic acid. However, a higher degree of palmitic acid degradation was found in horizontal MFC. The difference in relative changes in the components C12-C26 indicates that different pathways of fatty acid conversion were involved in metabolism in vertical and horizontal MFC designs. The vertical construction ensured a high degree of fatty acid degradation and a decrease in the content of almost all aliphatic hydrocarbons. However, the vertical MFC showed very low coulombic efficiency and no biosurfactant synthesis was observed, which brings this system closer to the conventional fermenters. The inverted electrode system ensured the degradation of fatty acids to a higher degree. The relative increase in the content of aliphatic hydrocarbons can be explained by the reduction of fatty acids by carboxylic acid reductase (CAR) enzymes to the corresponding aldehydes and then aldehyde decarbonylase enzymes to alkanes [52,53].

4. Conclusions

The effectiveness of two microbial fuel cell designs powered by waste vegetable oil in the production of electricity and the biosynthesis of surfactants was compared. The observed power density, current, and internal resistance indicated an improved efficiency of the MFC in a horizontal setup by 104.7 %, 25.7 % and 40 % correspondingly, when compared to the vertical system supplied with agitation of the anolyte. The horizontal configuration improved the distribution of the oil substrate inside the anode chamber, increasing the bioavailability of the oil to microorganisms, which directly influenced the biofilm development and subsequent oil degradation. Moreover, a decrease in surface tension to 50.7 ± 4.8 mN m^{-1}, indicating the presence of biosurfactants, was observed only in the horizontal MFC. Therefore, it has been shown that the efficiency of the degradation of waste vegetable oil can be significantly increased by changing the orientation of the electrode. The power production and Coulombic efficiency of the horizontal MFC was significantly higher than that of the vertical MFC with agitation. Most importantly, the production of biosurfactants was observed only in horizontal MFCs and we have demonstrated that their presence is

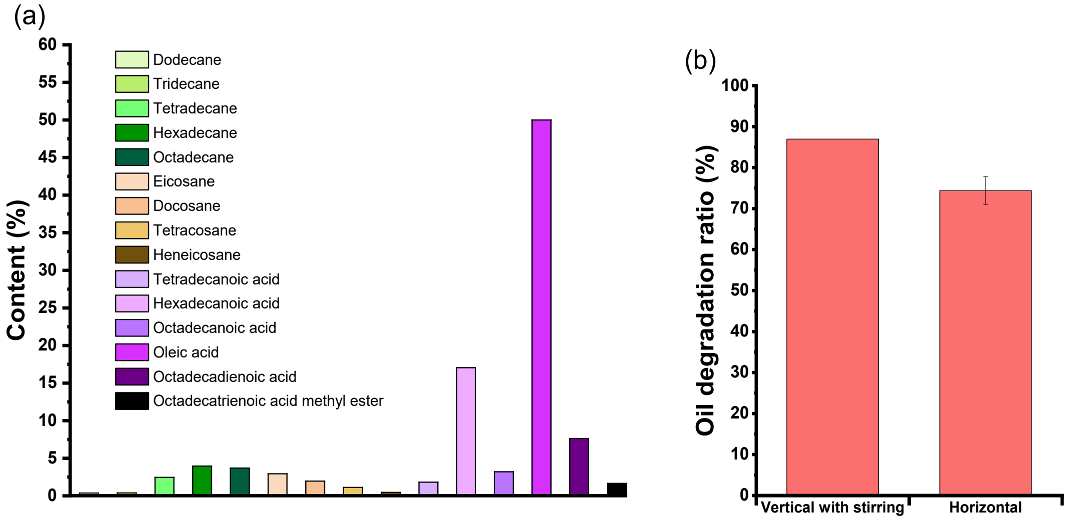

Fig. 7. Composition of the biotic control (a) and the oil degradation ratio in MFCs (b).

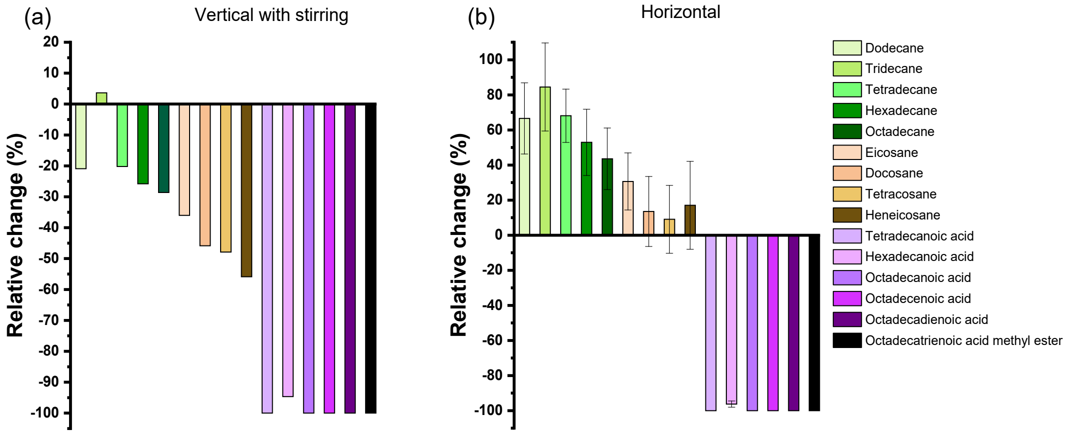

Fig. 8. Relative change in the content of organic components after the treatment in vertical (a) and horizontal (b) MFC.

directly correlated (r ranging from −0.62 to −0.77) to power generation, which may further allow for simple and costless monitoring of biosurfactant synthesis in well-established bioelectrochemical synthesis setup.

CRediT authorship contribution statement

Grzegorz Pasternak: Conceptualization, Methodology, Formal analysis, Resources, Supervision, Funding acquisition, Project administration, Writing – original draft, Writing – review & editing. **Aleksander de Rosset:** Investigation, Visualization, Formal analysis, Writing – original draft. **Piotr Rutkowski:** Methodology, Supervision, Writing – review & editing.

Declaration of Competing Interest

The authors declare that they have no known competing financial interests or personal relationships that could have appeared to influence the work reported in this paper: [Grzegorz Pasternak reports financial support was provided by National Science Centre Poland. Grzegorz Pasternak reports financial support was provided by National Agency for Academic Exchange].

Data availability

Data will be made available on request.

Acknowledgements

This work was financed by the Polish National Agency for Academic Exchange – Polish Returns grant (PPN/PPO/2018/1/00038) and National Science Centre (Poland) OPUS grant (2019/33/B/NZ9/02774), as well as by the Faculty of Chemistry of Wrocław University of Science and Technology.

References

[1] Bennett H.P, Stirling J.L, B. Group, Anodic reactions in microbial fuel cells, XXV (n. d.) 559–568.
[2] Santoro C, Arbizzani C, Erable B, Ieropoulos I. Microbial fuel cells : From fundamentals to applications. a review. J Power Sources 2017;356:225–44. https://doi.org/10.1016/j.jpowsour.2017.03.109.
[3] Zhang F, Pant D, Logan BE. Long-term performance of activated carbon air cathodes with different diffusion layer porosities in microbial fuel cells. Biosens Bioelectron 2011;30:49–55. https://doi.org/10.1016/j.bios.2011.08.025.
[4] Rabaey K, Rozendal RA. Microbial electrosynthesis - revisiting the electrical route for microbial production. Nat Rev Microbiol 2010;8:706–16. https://doi.org/10.1038/nrmicro2422.
[5] Roy M, Aryal N, Zhang Y, Patil SA, Pant D. Technological progress and readiness level of microbial electrosynthesis and electrofermentation for carbon dioxide and organic wastes valorization. Curr Opin Green Sustain Chem 2022;35:100605. https://doi.org/10.1016/j.cogsc.2022.100605.
[6] Nevin KP, Hensley SA, Franks AE, Summers ZM, Ou J, Woodard TL, et al. Electrosynthesis of organic compounds from carbon dioxide is catalyzed by a diversity of acetogenic microorganisms. Appl Environ Microbiol 2011;77:2882–6. https://doi.org/10.1128/AEM.02642-10.
[7] Park DH, Laivenieks M, Guettler MV, Jain MK, Zeikus JG. Microbial utilization of electrically reduced neutral red as the sole electron donor for growth and metabolite production. Appl Environ Microbiol 1999;65:2912–7. https://doi.org/10.1128/aem.65.7.2912-2917.1999.
[8] Lakaniemi AM, Tuovinen OH, Puhakka JA. Production of electricity and butanol from microalgal biomass in microbial fuel cells. Bioenergy Res 2012;5:481–91. https://doi.org/10.1007/s12155-012-9186-2.
[9] Flynn JM, Ross DE, Hunt KA, Bond DR, Gralnick JA. Enabling unbalanced fermentations by using engineered electrode- interfaced bacteria. MBio 2010;1. https://doi.org/10.1128/mBio.00190-10.
[10] Förster AH, Beblawy S, Golitsch F, Gescher J. Electrode-assisted acetoin production in a metabolically engineered Escherichia coli strain. Biotechnol Biofuels 2017. https://doi.org/10.1186/s13068-017-0745-9.
[11] Moscoviz R, Toledo-Alarcón J, Trably E, Bernet N. Electro-Fermentation: How To Drive Fermentation Using Electrochemical Systems. Trends Biotechnol 2016;34: 856–65. https://doi.org/10.1016/j.tibtech.2016.04.009.
[12] Chen C, Sun N, Li D, Long S, Tang X, Xiao G, et al. Optimization and characterization of biosurfactant production from kitchen waste oil using Pseudomonas aeruginosa 2018:14934–43.
[13] Hausmann R, Syldatk C, Types and Classification of Microbial Surfactants, in: Biosurfactants Prod. Util. Technol. Econ., CRC Press, 2014: pp. 3–19.
[14] Campos JM, Montenegro Stamford TL, Sarubbo LA, de Luna JM, Rufino RD, Banat IM. Microbial biosurfactants as additives for food industries. Biotechnol Prog 2013;29:1097–108. https://doi.org/10.1002/btpr.1796.
[15] Marchant R, Banat IM. Biosurfactants: A sustainable replacement for chemical surfactants? Biotechnol Lett 2012;34:1597–605. https://doi.org/10.1007/s10529-012-0956-x.
[16] Mishra S, Lin Z, Pang S, Zhang Y, Bhatt P, Chen S. Biosurfactant is a powerful tool for the bioremediation of heavy metals from contaminated soils. J Hazard Mater 2021;418:126253. https://doi.org/10.1016/j.jhazmat.2021.126253.
[17] Gudiña EJ, Rangarajan V, Sen R, Rodrigues LR. Potential therapeutic applications of biosurfactants. Trends Pharmacol Sci 2013;34:667–75. https://doi.org/10.1016/j.tips.2013.10.002.
[18] Zhang L, Veres-Schalnat TA, Somogyi A, Pemberton JE, Maiera RM. Fatty acid cosubstrates provide β-oxidation precursors for rhamnolipid biosynthesis in pseudomonas aeruginosa, as evidenced by isotope tracing and gene expression assays. Appl Environ Microbiol 2012;78:8611–22. https://doi.org/10.1128/AEM.02111-12.
[19] Banat IM, Makkar RS, Cameotra SS. Potential commercial applications of microbial surfactants. Appl Microbiol Biotechnol 2000;53:495–508. https://doi.org/10.1007/s002530051648.
[20] Pasternak G, Askitosari TD, Rosenbaum MA. Biosurfactants and Synthetic Surfactants in Bioelectrochemical Systems : A Mini-Review Influence on Electron Transfer 2020;11:1–9. https://doi.org/10.3389/fmicb.2020.00358.
[21] Pasternak G, de Rosset A, Tyszkiewicz N, Widera B, Greenman J, Ieropoulos I. Prevention and removal of membrane and separator biofouling in bioelectrochemical systems: a comprehensive review. IScience 2022;25:104510. https://doi.org/10.1016/j.isci.2022.104510.
[22] Pham TH, Boon N, Aelterman P, Clauwaert P, De Schamphelaire L, Vanhaecke L, et al. Metabolites produced by Pseudomonas sp. enable a Gram-positive bacterium to achieve extracellular electron transfer. Appl Microbiol Biotechnol 2008;77: 1119–29. https://doi.org/10.1007/s00253-007-1248-6.
[24] Szydlowski L, Ehlich J, Goryanin I, Pasternak G. High-throughput 96-well bioelectrochemical platform for screening of electroactive microbial consortia. Chem Eng J 2022;427:131692. https://doi.org/10.1016/j.cej.2021.131692.

[25] Hwang JH, Kim KY, Resurreccion EP, Lee WH. Surfactant addition to enhance bioavailability of bilge water in single chamber microbial fuel cells (MFCs). J Hazard Mater 2019;368:732–8. https://doi.org/10.1016/j.jhazmat.2019.02.007.

[26] Zhang Y, Jiang J, Zhao Q, Gao YZ, Wang K, Ding J, et al. Accelerating anodic biofilms formation and electron transfer in microbial fuel cells: role of anionic biosurfactants and mechanism. Bioelectrochemistry 2017;117:48–56. https://doi.org/10.1016/j.bioelechem.2017.06.002.

[27] Zheng T, Xu YS, Yong XY, Li B, Yin D, Cheng QW, et al. Endogenously enhanced biosurfactant production promotes electricity generation from microbial fuel cells. Bioresour Technol 2015;197:416–21. https://doi.org/10.1016/j.biortech.2015.08.136.

[28] Askitosari TD, Berger C, Tiso T, Harnisch F, Blank LM, Rosenbaum MA. Coupling an Electroactive Pseudomonas putida KT2440 with Bioelectrochemical Rhamnolipid Production. Microorganisms 2020;8:1959. https://doi.org/10.3390/microorganisms8121959.

[29] Moya Ramírez I, Tsaousi K, Rudden M, Marchant R, Jurado Alameda E, García Román M, et al. Rhamnolipid and surfactin production from olive oil mill waste as sole carbon source. Bioresour Technol 2015;198:231–6. https://doi.org/10.1016/j.biortech.2015.09.012.

[30] Aelterman P, Versichele M, Marzorati M, Boon N, Verstraete W. Loading rate and external resistance control the electricity generation of microbial fuel cells with different three-dimensional anodes. Bioresour Technol 2008;99:8895–902. https://doi.org/10.1016/j.biortech.2008.04.061.

[31] Pasternak G, Greenman J, Ieropoulos I. Dynamic evolution of anodic biofilm when maturing under different external resistive loads in microbial fuel cells. electrochemical perspective. J Power Sources 2018;400:392–401. https://doi.org/10.1016/j.jpowsour.2018.08.031.

[32] Logan BE, Hamelers B, Rozendal R, Schröder U, Keller J, Freguia S, et al. Microbial fuel cells: Methodology and technology. Environ Sci Tech 2006;40:5181–92. https://doi.org/10.1021/es0605016.

[33] Catal T, Li K, Bermek H, Liu H. Electricity production from twelve monosaccharides using microbial fuel cells. J Power Sources 2008;175:196–200. https://doi.org/10.1016/j.jpowsour.2007.09.083.

[34] Yong YC, Yu YY, Li CM, Zhong JJ, Song H. Bioelectricity enhancement via overexpression of quorum sensing system in Pseudomonas aeruginosa-inoculated microbial fuel cells. Biosens Bioelectron 2011;30:87–92. https://doi.org/10.1016/j.bios.2011.08.032.

[35] Fricke K, Harnisch F, Schröder U. On the use of cyclic voltammetry for the study of anodic electron transfer in microbial fuel cells. Energ Environ Sci 2008;1:144–7. https://doi.org/10.1039/b802363h.

[36] Liu J, Vipulanandan C. Effects of Fe, Ni, and Fe/Ni metallic nanoparticles on power production and biosurfactant production from used vegetable oil in the anode chamber of a microbial fuel cell. Waste Manag 2017;66:169–77. https://doi.org/10.1016/j.wasman.2017.04.004.

[37] Liu J, Vipulanandan C, Yang M. Biosurfactant production from used vegetable oil in the anode chamber of a microbial electrosynthesizing fuel cell. Waste Biomass Valoriz 2019;10:2925–31. https://doi.org/10.1007/s12649-018-0331-9.

[38] Baranitharan E, Khan MR, Prasad DMR, Teo WFA, Tan GYA, Jose R. Effect of biofilm formation on the performance of microbial fuel cell for the treatment of palm oil mill effluent. Bioprocess Biosyst Eng 2015;38:15–24. https://doi.org/10.1007/s00449-014-1239-9.

[39] Winfield J, Ieropoulos I, Greenman J, Dennis J. The overshoot phenomenon as a function of internal resistance in microbial fuel cells. Bioelectrochemistry 2011;81:22–7. https://doi.org/10.1016/j.bioelechem.2011.01.001.

[40] Watson VJ, Logan BE. Analysis of polarization methods for elimination of power overshoot in microbial fuel cells. Electrochem Commun 2011;13:54–6. https://doi.org/10.1016/j.elecom.2010.11.011.

[41] Pasternak G, Ormeno-Cano N, Rutkowski P. Recycled waste polypropylene composite ceramic membranes for extended lifetime of microbial fuel cells. Chem Eng J 2021:130707. https://doi.org/10.1016/J.CEJ.2021.130707.

[42] Youssef NH, Duncan KE, Nagle DP, Savage KN, Knapp RM, McInerney MJ. Comparison of methods to detect biosurfactant production by diverse microorganisms. J Microbiol Methods 2004;56:339–47. https://doi.org/10.1016/j.mimet.2003.11.001.

[43] Burlatsky SF, Atrazhev VV, Dmitriev DV, Sultanov VI, Timokhina EN, Ugolkova EA, et al. Surface tension model for surfactant solutions at the critical micelle concentration. J Colloid Interface Sci 2013;393:151–60. https://doi.org/10.1016/j.jcis.2012.10.020.

[44] Domingues PM, Almeida A, Serafim Leal L, Gomes NCM, Cunha Â. Bacterial production of biosurfactants under microaerobic and anaerobic conditions. Rev Environ Sci Biotechnol 2017;16:239–72. https://doi.org/10.1007/s11157-017-9429-y.

[45] Shao B, Liu Z, Zhong H, Zeng G, Liu G, Yu M, et al. Effects of rhamnolipids on microorganism characteristics and applications in composting: a review. Microbiol Res 2017;200:33–44. https://doi.org/10.1016/j.micres.2017.04.005.

[46] Al-Tahhan RA, Sandrin TR, Bodour AA, Maier RM. Rhamnolipid-induced removal of lipopolysaccharide from Pseudomonas aeruginosa: effect on cell surface properties and interaction with hydrophobic substrates. Appl Environ Microbiol 2000;66:3262–8. https://doi.org/10.1128/AEM.66.8.3262-3268.2000.

[47] Pasternak G, Kołwzan B. Surface tension and toxicity changes during biodegradation of carbazole by newly isolated methylotrophic strain Methylobacterium sp. GPE1. Int Biodeter Biodegr 2013;84. https://doi.org/10.1016/j.ibiod.2012.07.021.

[48] Yu N, Xing D, Li W, Yang Y, Li Z, Li Y, et al. Electricity and methane production from soybean edible oil refinery wastewater using microbial electrochemical systems. Int J Hydrogen Energy 2017;42:96–102. https://doi.org/10.1016/j.ijhydene.2016.11.116.

[49] Bermek H, Catal T, Akan SS, Ulutaş MS, Kumru M, Özgüven M, et al. Olive mill wastewater treatment in single-chamber air-cathode microbial fuel cells. World J Microbiol Biotechnol 2014;30:1177–85. https://doi.org/10.1007/s11274-013-1541-8.

[50] Cheng J, Zhu X, Ni J, Borthwick A. Palm oil mill effluent treatment using a two-stage microbial fuel cells system integrated with immobilized biological aerated filters. Bioresour Technol 2010;101:2729–34. https://doi.org/10.1016/j.biortech.2009.12.017.

[51] Firdous S, Jin W, Shahid N, Bhatti ZA, Iqbal A, Abbasi U, et al. The performance of microbial fuel cells treating vegetable oil industrial wastewater. Environ Technol Innov 2018;10:143–51. https://doi.org/10.1016/j.eti.2018.02.006.

[52] Venkitasubramanian P, Daniels L, Rosazza JPN. Reduction of carboxylic acids by Nocardia aldehyde oxidoreductase requires a phosphopantetheinylated enzyme. J Biol Chem 2007;282:478–85. https://doi.org/10.1074/jbc.M607980200.

[53] Kalim Akhtara M, Turner NJ, Jones PR. Carboxylic acid reductase is a versatile enzyme for the conversion of fatty acids into fuels and chemical commodities. PNAS 2013;110:87–92. https://doi.org/10.1073/pnas.1216516110.

5.3. Bioelectrochemical synthesis of rhamnolipids and power generation and its correlation with nitrogen in air-cathode microbial fuel cells

5.3.1. Omówienie publikacji

Osiągnięcie wysokiej wydajności syntezy biosurfaktantów w klasycznych hodowlach płynnych wymaga optymalizacji źródła węgla, źródła i stężenia składników odżywczych pożywki, takich jak azot czy fosfor, a także pH, napowietrzenia i zasolenia podłoża. Oprócz składu pożywki fermentacyjnej duże znaczenie dla wydajności biosyntezy mają warunki pracy bioreaktora, takie jak temperatura, mieszanie czy rozwiązania projektowe reaktora. Znalezienie idealnych warunków do produkcji biosurfaktantów w klasycznym podejściu do biosyntezy było przedmiotem wielu badań, wśród których szeroko omawiano optymalizację źródła i stężenia azotu. Azot jest niezbędnym do życia składnikiem dla mikroorganizmów i ma istotny wpływ na zawartość węglowodanów, białek, kwasów nukleinowych i ATP w biofilmie, oraz odgrywa kluczową rolę w regulacji genów biorących udział w produkcji biosurfaktantów. Niemniej jednak dotychczas nie zbadano wpływu tego parametru na syntezę biosurfaktantów w nowych warunkach procesu, takich jak elektrofermentacja.

Celem pracy „Bioelectrochemical synthesis of rhamnolipids and power generation and its correlation with nitrogen in air-cathode microbial fuel cells" było zbadanie wpływu stężenia azotu w elektrolicie na efektywność syntezy biosurfaktantów i wytwarzania energii elektrycznej z odpadowego oleju roślinnego w MFC, a także określenie optymalnego stosunku molowego węgiel/azot i struktury chemicznej wytworzonych produktów biosyntezy.

W badaniu wykorzystano horyzontalne MFC z katodą powietrzną wydrukowane w 3D z polipropylenu. Wszystkie MFC zainokulowano osadem czynnym z komory tlenowej oczyszczalni ścieków. Po okresie inokulacji komorę anodową zasilano pożywką mikrobiologiczną w trybie wsadowym, w której stężenie NH_4Cl wahało się od 0 do 1 g L^{-1}, a jako jedyne źródło węgla dla mikroorganizmów użyto oleju posmażalniczego. W pracy oceniono wpływ stężenia azotu w pożywce na wydajność produkcji energii elektrycznej i syntezy biosurfaktantów za pomocą charakterystyki elektrochemicznej ogniw, pomiarów aktywności biosurfaktantów w anolicie oraz pomiarów wydajności degradacji substratu. Ponadto wykonano analizę społeczności drobnoustrojów tworzących biofilm anodowy oraz określono strukturę chemiczną wytworzonych biosurfaktantów.

Obserwowana gęstość produkowanej mocy wskazywała na poprawę wydajności wraz ze wzrostem stężenia NH_4Cl w anolicie, aż do osiągnięcia maksymalnej wartości dla 0.5 g L^{-1}. Dla tego stężenia zaobserwowano również największy spadek napięcia powierzchniowego, świadczący o syntezie biosurfaktantów. Co więcej, wyniki pokazały silną korelację zmian gęstości mocy i spadku napięcia powierzchniowego w funkcji stężenia azotu w pożywce, co udowadnia, że synteza biosurfaktantów i skuteczność degradacji zużytego oleju w MFC zależy bezpośrednio od stężenia źródła azotu. Podobną tendencję zaobserwowano w pomiarach EIS. Przeprowadzony eksperyment EIS wykazał spadek sumy impedancji i impedancji anody wraz ze wzrostem stężenia NH_4Cl w pożywce, aż do osiągnięcia wartości minimalnej dla 0.5 g L^{-1}. Wnioskujemy zatem, że najniższa wartość oporów wewnętrznych MFC, najwyższa wydajność produkcji energii elektrycznej oraz syntezy biosurfaktantów dla 0.5 g L^{-1} była wynikiem wydajniejszego rozwoju biofilmu na anodach, a także efektów przypisywanych syntezie biosurfaktantów i ich wpływowi na działanie innych komponentów MFC. Analiza społeczności drobnoustrojów wykazała obecność dominującego szczepu wytwarzającego biosurfaktanty - *Pseudomonas aeruginosa*, a także innych gatunków elektroaktywnych mogących brać udział w biodegradacji substratu olejowego i biosyntezie. Ich aktywność doprowadziła do biosyntezy jedenastu typów mono- i di-ramnolipidów.

W badaniu udowodniono, że stężenie źródła azotu w pożywce hodowlanej jest jednym z kluczowych czynników utrzymania wysokiej wydajności degradacji zużytego oleju roślinnego, produkcji energii i jednoczesnej syntezy biosurfaktantów. Ponadto jest to pierwsze badanie, w którym zoptymalizowano stężenie azotu w celu poprawy syntezy biosurfaktantów i wytwarzania energii w układzie bioelektrochemicznym, co przybliża o krok wydajną syntezę biosurfaktantów w tego typu układach do implementacji.

5.3.2. Publikacja

Journal of Environmental Management 365 (2024) 121514

Contents lists available at ScienceDirect

Journal of Environmental Management

journal homepage: www.elsevier.com/locate/jenvman

Research article

Bioelectrochemical synthesis of rhamnolipids and energy production and its correlation with nitrogen in air-cathode microbial fuel cells

Aleksander de Rosset [a,1], Natalia Tyszkiewicz [a,b,1], Jerzy Wiśniewski [b], Natalia Pudełko-Malik [b], Piotr Rutkowski [a], Piotr Młynarz [b], Grzegorz Pasternak [a,*,1]

[a] Department of Process Engineering and Technology of Polymer and Carbon Materials, Faculty of Chemistry, Wroclaw University of Science and Technology, Wroclaw, 50-370, Poland
[b] Department of Biochemistry, Molecular Biology and Biotechnology, Faculty of Chemistry, Wroclaw University of Science and Technology, Wroclaw, 50-370, Poland

ARTICLE INFO

Keywords:
MFC
Rhamnolipids
Waste vegetable oil
Waste valorisation
Bioelectrochemical synthesis
Optimisation

ABSTRACT

Microbial fuel cells (MFCs) have been recently proven to synthesise biosurfactants from waste products. In classic bioreactors, the efficiency of biosynthesis process can be controlled by the concentration of nitrogen content in the electrolyte. However, it was not known whether a similar control mechanism could be applied in current-generating conditions. In this work, the effect of nitrogen concentration on biosurfactant production from waste cooking oil was investigated. The concentration of NH_4Cl in the electrolyte ranged from 0 to 1 g L^{-1}. The maximum power density equal to 17.5 W m^{-3} was achieved at a concentration of 0.5 g L^{-1} (C/N = 2.32) and was accompanied by the highest surface tension decrease (to 54.6 mN m^{-1}) and an emulsification activity index of 95.4%. Characterisation of the biosurfactants produced by the LC-MS/MS method showed the presence of eleven compounds belonging to the mono- and di-rhamnolipids group, most likely produced by *P. aeruginosa*, which was the most abundant (19.6%) in the community. Importantly, we have found a strong correlation ($R = -0.96$) of power and biosurfactant activity in response to C/N ratio. This study shows that nitrogen plays an important role in the current-generating metabolism of waste cooking oil. To the best of our knowledge, this is the first study where the nitrogen optimisation was investigated to improve the synthesis of biosurfactants and power generation in a bioelectrochemical system.

1. Introduction

Microbial fuel cells (MFCs) are recognised as devices capable of degrading many types of organic pollutants and simultaneously recovering energy from the substrate (Logan et al., 2006). Such process can be carried out both various groups of microorganisms and novel applications are emerging due to recent discoveries of electroactive extremophilic microorganisms (Edel et al., 2022), while the most commonly investigated comprise of *Geobacter and Shewanella* species. The use of MFCs as an alternative energy source is currently aimed at low-energy applications, while each year of their research and development increases their power performance (Hoang et al., 2022). The ongoing process of MFC performance growth is related to the development of its functional elements (Rosset et al., 2023; Vázquez et al., 2023). Multiple efforts have been made to develop alternative bioelectrochemical systems (BESs) such as microbial electrolysis cells and microbial desalination cells, as well as the processes of microbial electrosynthesis and electrobioremediation (Chen et al., 2019). One of the promising directions for BES development is microbial electrofermentation, where the electrode with its potential acts as a source or sink of electrons to drive the conversion of organic waste (Moscoviz et al., 2016). In the anodic process, multiple products can be produced, such as butanol (Finch et al., 2011), ethanol (Yuan et al., 2022), acetoin (Förster et al., 2017), and even more complex, biosurfactants (Pham et al., 2008). The latter have a wide range of applications and high production costs using current classical bioreactor methods (Marchant and Banat, 2012b), while material and metabolic engineering can be successfully applied to further enhance their efficiency (Klein et al., 2023).

Biosurfactants (BSFs) are microbial-derived amphiphilic compounds that can reduce surface/interfacial tension (Pasternak et al., 2020). The main advantage of BSFs over synthetic surfactants is lower toxicity and greater biodegradability, selectivity, and stability (Marchant and Banat,

---

* Corresponding author.
E-mail address: grzegorz.pasternak@pwr.edu.pl (G. Pasternak).
[1] website: www.gplab.eu.

https://doi.org/10.1016/j.jenvman.2024.121514
Received 6 February 2024; Received in revised form 17 May 2024; Accepted 16 June 2024

2012a). BSFs can be used in the pharmaceutical, food, and cosmetic industries, as well as in bioremediation and environmental protection (Sarubbo et al., 2022). These compounds, which possess a wide variety of structures and properties, are mainly produced by different bacterial genera, such as *Pseudomonas, Rhodococcus, Streptomyces, Bacillus,* and *Serratia*. The most frequently described groups of BSFs consist of glycolipids, phospholipids, and lipopeptides. The biggest challenge in the production of BSFs, on an industrial scale, is the high cost of their production. Therefore, BESs, with their ability to generate electricity from waste substances, such as waste vegetable oil, can be a promising alternative.

Biosurfactants may contribute significantly to the operation and performance of MFC by increasing the bioavailability of hydrophobic substrates (Kaczorek et al., 2018) and improving the hydrophilicity of the electrode surface (Gomaa et al., 2021), leading to better biofilm formation. However, there are few studies to date where BSFs have been studied in BESs (Pasternak et al., 2020), and only three works are available, where BSFs have been synthesised from waste vegetable oil bioconversion in MFC. Two of these studies used dual chamber MFCs with large volumes that require anolyte mixing and generate high power losses (Liu et al., 2019; Liu and Vipulanandan, 2017), while Pasternak et al. (2023) investigated a new MFC design with a horizontal electrode arrangement. This allowed to achieve a high BSF activity and the highest power production. In such a way, BSFs and electricity were generated simultaneously. In addition, the authors showed for the first time a direct correlation between the synthesis of BSFs and the energy production in MFCs.

Biosurfactants produced by microorganisms in the classical biosynthesis approach are excreted into the solution or adhere to the cells. One of the roles of BSFs in the metabolism of a hydrophobic substrate is to increase bioavailability or to enable the growth of microbial cells on the substrate surface by reducing interfacial tension (Sharma and Pandey, 2020). To achieve the high performance of BSFs synthesis in classical liquid cultures, many studies have been carried out to optimise the carbon source (Jain et al., 2013), the source and concentration of electrolyte components such as nitrogen (Chen et al., 2018) or phosphorus (Priya and Usharani, 2009), as well as the pH, aeration and salinity of the medium (E. F. Santos et al., 2019). In addition to the nutrient composition of fermentative media, the influence of bioreactor operating conditions such as temperature, mixing (Sun et al., 2021) or reactor design solutions (Bongartz et al., 2021) has been examined. The industrial approach to increase the efficiency of BSFs production may also comprise the utilisation of high-yielding genetically modified strains. For example, modification of 53 genes in a non-producing strain of *B. subtilis* allowed a surfactin production efficiency of 12.8 g L^{-1} (Wu et al., 2019). Finding ideal conditions to produce BSFs in the classical biosynthesis approach has been the subject of many studies, among which optimisation of the nitrogen source and concentration has been extensively discussed (Abdel-Mawgoud et al., 2008; Abouseoud et al., 2008; Fernandes et al., 2016; Ozdal et al., 2017).

Simple inorganic compounds such as ammonium or nitrate salts, as well as urea, yeast extract, and peptone were tested as a nitrogen source in classic liquid cultures producing BSFs (Onwosi and Odibo, 2012; Zhao et al., 2016). Nitrate sources most often allow for higher yields of BSFs production in the classical biosynthesis approach (Zhao et al., 2016). However, another study showed that the use of various nitrogen sources in production affects similarly the efficiency and structure of BSFs (A. S. Santos et al., 2002). It was shown that the use of ammonium nitrogen favoured the production of monorhamnolipids, while nitrate nitrogen favoured the production of dirhamnolipids. Therefore, the selection of the nitrogen source should be dictated by the yield of BSF, as well as in terms of the usability of the obtained products. Ammonium nitrogen for MFC medium supplementation is more suitable. Nitrate ions can reduce the efficiency of MFCs due to competition between the processes of electricity generation and denitrification (Sukkasem et al., 2008). Moreover, nitrogen in wastewater occurs mainly in the ammonium form, which brings the experimental conditions closer to real applications.

Table 1
Characterisation of the MFC power performance, electrolyte properties, as well as the properties of BSFs produced in the anolyte. The data of MFC performance and BSFs properties represent average values of two replicates.

		NH_4Cl (g L^{-1})				
		0	0.05	0.2	0.5	1
C/N molar ratio		–	23.16	5.79	2.32	1.16
pH		8.609	8.612	8.489	8.320	8.155
Conductivity	mS cm^{-1}	8.143	8.370	9.024	10.500	12.544
Power density	W m^{-3}	7.3	8.0	10.7	12.4	9.9
	mW m^{-2}	162.2	177.8	237.8	275.6	220.0
Current density	A m^{-3}	27.0	35.1	48.3	57.5	35.1
	A m^{-2}	0.6	0.8	1.1	1.3	0.8
Surface tension	mN m^{-1}	62.2	61	55.9	54.6	56.2
Emulsification index	%	52.8	89.8	94.4	95.4	88.9
Coulombic efficiency	%	34.0	42.1	52.1	44.7	27.4
COD removal	%	93.5	94.9	95.0	95.0	95.5

Nitrogen is an essential ingredient for microorganisms to create proteins, cell wall components, and nucleic acids (Thompson et al., 2006). Ramos et al. (2023) investigated the effect of the C/N molar ratio on the formation and performance of the biofilm created by *Pseudomonas aeruginosa*. The study showed that the C/N conditions had a significant effect on the content of carbohydrates, proteins, nucleic acids, and ATP in the biofilm and therefore played a key role in the removal of COD from wastewater. Furthermore, the influence of C/N on the induction ratio of N-acetyl-L-homoserine lactone (AHL), a biomolecule responsible for biofilm formation and regulation of genes involved in BSFs production, was revealed. Nevertheless, it is not known how this parameter affects a novel process condition such as electrofermentation, proposed herein.

Therefore, the aim of this work was to investigate the influence of nitrogen concentration in the electrolyte on the efficiency of BSFs synthesis and electricity generation in MFC, as well as to determine the optimal carbon/nitrogen (C/N) molar ratio, and chemical structure of the produced BSFs. The efficiency of the production of electricity and BSFs was assessed using electrochemical tests, surface activity measurements, and substrate degradation measurements, providing information on the impact of the C/N ratio on the start-up and operation of the MFC fed with waste vegetable oil. Moreover, the produced BSFs were characterised by the LC-MS/MS technique. This work describes the first step in optimising the synthesis of BSFs by combining the classic and electrochemical methods to boost their quantity.

2. Materials and methods

2.1. Construction and operation of MFC

This work used a horizontal air-cathode microbial fuel cell, manufactured as described in the previous work (Pasternak et al., 2023). In brief, the square-shaped anode was prepared from carbon veil (PRF Composite Materials, Dorset, UK) and 316LSi steel wire. The cathode was made of activated carbon CWZ-22 (972 m^2 g^{-1}). The cathode material was pressed into the cathode module with stainless steel mesh placed inside as a current collector, according to the previous study (Rosset et al., 2023). The geometric surface area of the anode and cathode was equal to 9 cm^2. The anode chamber was separated from the cathode module by a cation exchange membrane (CMI-7000, USA). The total displacement volume was equal to 20 mL. All MFCs were operated at 25 °C, with a starting external load (R_{ext}) of 2 kΩ. After each measurement of the polarisation curves, the optimal resistance (R_{int}) was calculated and the external resistor setting was adjusted (Aelterman et al., 2008).

2.2. Biosynthesis conditions

The composition of the mineral salt medium (MSM) was as follows (g L^{-1}): Na_2HPO_4 (POCH, Poland) 0.6; KCl (POCH, Poland) 0.1; $NaHCO_3$ (Chempur, Poland) 2.5; trace element solution of 10 mL L^{-1} and NH_4Cl (Chempur, Poland) ranged from 0 g L^{-1} to 1 g L^{-1}. The concentration of NH_4Cl, pH, and conductivity of individual MSM are summarised in Table 1. The pH of MSM for all MFC decreased to ~ 6.5 during the process. Therefore, the pH throughout the batch cycle remained within the optimal range for the anodic MFC biofilm (Puig et al., 2010). Each MSM was tested in triplicate. All graphs in this study show the average value of the two repetitions with the highest power and BSFs production efficiencies. The solutions were prepared with Milli-Q water and autoclaved prior to use (121 °*C*, 20 min.). Waste vegetable oil ($\rho = 0.905$ g cm^{-3}) at a concentration of 0.1% (v/v), was used as a sole carbon source. All MFCs were inoculated with a mixture (1:1) of two activated sludges collected from the aerobic chambers of the wastewater treatment plant (Ścinawka, Kudowa, Poland). After 6 days of inoculation, the activated sludge was removed and replaced with adequate MSM. The medium was then changed every 1–2 days (HRT = 39.1 ± 13.8 h). Evaporation of the anolyte was supplemented daily with sterile Milli-Q water.

2.3. Electrochemical measurements

Closed circuit voltage (CCV) was recorded with a 3 min interval using a KEYSIGHT DAQ970A data acquisition system (KEYSIGHT TECHNOLOGIES, USA). Linear sweep voltammetry (LSV) was performed using a MultiPalmSens4 potentiostat (Palmsens BV, The Netherlands) in a three-electrode mode, with the anode as the working electrode, the cathode as the counter electrode, and the saturated Ag/AgCl electrode as the reference electrode, placed in the anode chamber. The power and polarisation curves were obtained in the potential range from open circuit potential (OCP) to 0.0 V WE vs Ag/AgCl, at a scan rate of 1 mV s^{-1}.

Electrochemical impedance spectroscopy (EIS) for the whole cell was performed with the anode as the working electrode and the cathode as the counter and reference electrode. EIS spectra were obtained using a MultiPalmSens4 potentiostat (Palmsens BV, The Netherlands). An alternating current with an amplitude of 10 mV and a frequency range from 100 kHz to 10 mHz was applied. All EIS measurements were performed in the OCV mode and analysed with the EC-Lab V10.40 software.

2.4. Analysis of biosurfactant activity

2.4.1. Surface tension measurement

The BPT mobile bubble pressure tensiometer (KRUSS, Germany) was used to determine the surface tension (SFT) of the anolyte. The device was calibrated before each series of measurements. To prevent sample aeration and enable better sample averaging, 1 mL of MFC anolyte was taken to measure the SFT and returned after the measurement. Surface tension was monitored with a 1-h interval until reaching the minimum value, then the sampling frequency was reduced, as presented in Fig. 4.

2.4.2. Emulsification activity index (E24)

The 3 mL of vegetable oil and 3 mL of the centrifuged and filtered anolyte were mixed for 2 min in a 15 mL tube and left for 24 h. The emulsification index (E24) is defined as a percentage of the height of the emulsified layer in relation to the total high of the liquid column (Chen et al., 2018).

2.4.3. Foaming activity

Foaming activity was measured for 20 mL of anolyte in a 50 mL tube by shaking the sample manually for 30 s. Foaming ability and foam stability were calculated according to equations (1) and (2).

$$\text{Foaming ability} = \pi \times r^2 \times h_0 \tag{1}$$

$$\text{Foam stability} = \frac{h_{10}}{h_0} \tag{2}$$

where r – diameter of the measuring vessel; h_0 – initial foam height; h_{10} – foam height after 10 min.

2.5. Chemical oxygen demand and coulombic efficiency

For fresh medium and anolyte after MFC treatment, the chemical oxygen demand (COD) was determined by the potassium dichromate oxidation method, according to the manufacturer's instructions (Hach, USA). The COD removal efficiency was calculated using equation (3).

$$\Delta COD = \frac{COD_0 - COD_t}{COD_0} \tag{3}$$

where COD_0 – initial COD of the fresh medium; COD_t – COD of the anolyte after 't' time.

Coulombic efficiency (CE) was determined for the batch system and the complex substrate according to equation (4) (Logan et al., 2006).

$$CE = \frac{8\int_0^t I\,dt}{FV_{An}\Delta COD} \tag{4}$$

where 8 – constant, based on molecular weight of oxygen and number of electrons exchanged per mole of oxygen; I – current (A); t – time of operation (s); F – Faraday's constant (96,500 C/mol e^-); V_{An} – working volume of anode chamber (L); ΔCOD – change in COD concentration (mg L^{-1}).

2.6. Microbial community analysis

2.6.1. DNA isolation

The microbial biomass was collected from the anolyte. DNA extraction was performed using Bead-Beat Micro AX Gravity kit (A&A BIOTECHNOLOGY, Warszawa, Poland). The quality and quantity of DNA extracts were assessed spectrophotometrically using NanoDrop™ 2000/2000c (ThermoFisher Scientific, USA).

2.6.2. 16S rRNA

Microbial diversity was determined using targeted sequencing of the V3–V4 region within the 16S rRNA gene. The 16S rRNA primers, namely 341F and 785R were used for amplification and subsequent library preparation (Klindworth et al., 2013). The amplification process was conducted by utilising the Q5 Hot Start High-Fidelity 2X Master Mix, with adherence to reaction conditions described by the manufacturer. Paired-end sequencing was conducted using the Illumina v3 kit on the MiSeq device, resulting in read lengths of 2 × 300 nucleotides. The bioinformatic analysis was carried out through the QIIME 2 platform (Bolyen et al., 2019), in combination with the DADA2 package (Callahan et al., 2016). The initial bioinformatic analysis covered quality control and sequence preprocessing. For quality control, dynamic control parameters were generated based on the error model specific to each sample using the FIGARO tool. Moreover, quality control measures were taken to ensure that each sample's maximum expected error rates were within acceptable limits. The obtained sequences have been subjected to preprocessing using the Cutadapt tool. Taxonomic classification of Amplicon Sequence Variants (ASVs) representative sequences was performed using the Silva 138 reference database with a two-step hybrid approach. First, an exact matching of reads to the reference database was carried out using vsearch (Rognes et al., 2016). Any reads that were not matched in the previous step were classified using a sklearn method available in the q2-feature-classifier module of QIIME (Bokulich et al., 2018).

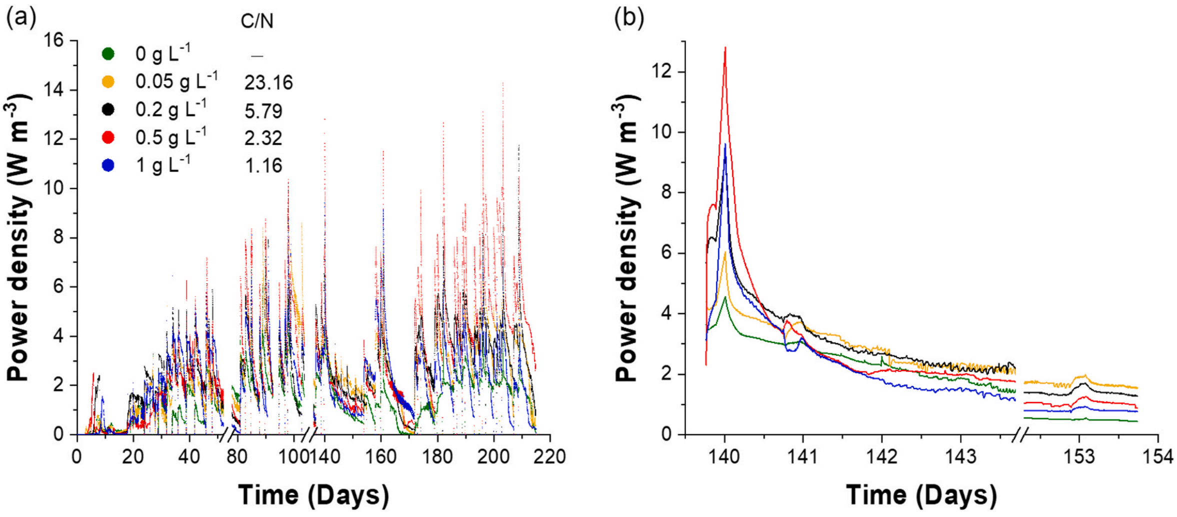

Fig. 1. (a) Real-time temporal power performance and (b) characteristic of the exemplary feeding cycle.

2.7. *Biosurfactant analysis*

2.7.1. *Solid phase extraction*

Analytes were collected during the stationary phase of growth, when the surface tension value was the lowest, indicating the highest concentration of BSFs. The culture broth was centrifuged for 10 min at 6000 rpm and then the supernatant was filtrated using a 0.22 μm sterile syringe filter to remove cells. The solid phase extraction (SPE) method was used for the extraction and purification of BSFs. For this purpose, C18 cartridges (CHROMABOND; 3 mL volume; 500 mg adsorbent weight) were used. Column was conditioned with 15 mL of acetonitrile and 3 mL of methanol and equilibrated with 3 mL of water. Then 130 mL of sample was loaded into column, followed by washing step with 3 mL of water. Column was dried for 10 min and the BSFs were extracted using 3 mL of acetonitrile. Solvent was evaporated in 40 °C to obtain crude BSFs.

2.7.2. *LC-MS/MS analysis*

The crude BSFs were dissolved in 150 μL aqueous 5 mM ammonium formate buffer/acetonitrile 60/40 (v/v). The sample was then diluted 100 times and analysed using the LC-MS/MS approach. BSFs characterisation was carried out using a Synapt G2 Si Q-TOF MS equipped with an electrospray ion source (ESI) combined with the Acquity UPLC I-class chromatographic system (Waters, USA). For compound separation, reversed-phase chromatography on a ACQUITY UPLC® BEH Shield RP18 1.7 μm (2.1 × 100 mm) column was used. Mobile phases were composed of 10 mM ammonium formate in 5:95 can:water (A) and 10 mM ammonium formate in 95:5 ACN:water (B). The flow rate was set to 0.300 mL min^{-1} with a total run time of 6.5 min. Linear elution was carried out as follows: 1.00 min–20% B, 2.50 min–90% B, 4.50 min–90% B, 4.60 min–20% B, 6.50 min–20% B. The sample and column temperatures were set at 10 °C and 45 °C, respectively. The injection volume was set at 2.00 μL. Data acquisition was performed using MassLynx software (version 4.1, SCN932, Waters, USA). Samples were investigated using negative ion mode. The MS ion source parameters were set as follows: the capillary voltages, 2.50 kV; sampling cone, 40 V; source temperature, 130 °C; desolvation temperature, 450 °C; desolvation gas flow, 800 L h^{-1} and cone gas flow, 60 L h^{-1}.

2.7.3. *TLC analysis*

For analysis, TLC Silica gel 60 F254 plates (Merck, Germany) were used. TLC analysis was performed to detect different classes of BSFs: glycolipids, lipopeptides, and lipids. For sugars detection (hexoses and pentoses) orcinol approach was used according to Laabei et al. (2014). To visualise peptides and free amino acids used ninhydrin test (Das et al., 2008) and for lipids identification used iodine staining. BSFs were extracted using the SPE approach and then diluted in pure methanol for TLC analysis.

2.8. *Analysis of waste cooking oil degradation*

Gas chromatography coupled with mass spectrometry (GC-MS) was used to analyse organic compounds in the fresh anolyte, as well as the MFC-treated. In the first stage, liquid-liquid extraction with CH_2Cl_2 was performed in an inert environment. Then, 2 μl of the extract achieved was analysed on a GC-MS instrument (HP 6890-5973). The HP-INNOWAX capillary column (Agilent Technologies, USA) with an internal diameter of 0.25 mm and a length of 30 m was used as a separation system. High purity He was used as the carrier gas at a flow rate of 0.7 mL min^{-1}. The oven temperature program was set according to the previous work (Pasternak et al., 2023).

2.9. *pH, conductivity and oxygen concentration*

The galvanic oxygen sensor ELMETRON COG-1 (ELMETRON, Poland) was used to monitor the oxygen concentration in the anolyte. The sensor was calibrated in Na_2SO_3 solution (0% oxygen saturation) and then in the air (corresponding to 100% oxygen saturation in the liquid phase). The pH of the medium was determined using the IONODE IJ44A electrode (ELMETRON, Poland). The conductivity of the MSM was measured using the ELMETRON ECF-1 conductivity sensor.

2.10. *Data processing*

All data were processed and visualised graphically using OriginPro software (OriginPro 2019). Current and power were calculated according to the Ohm's law (Equation (5) and (6)).

$$I = \frac{U}{R}\ [A] \tag{5}$$

$$P = U \times I\ [W] \tag{6}$$

where U – voltage (V); R – resistance (Ω); P – power (W); I – current (A)

3. Results and discussion

3.1. *Electrochemical characteristics*

3.1.1. *Real-time temporal monitoring*

During 7 months of MFCs operation, the power density output was monitored in real time. Fig. 1 shows real time data from the most

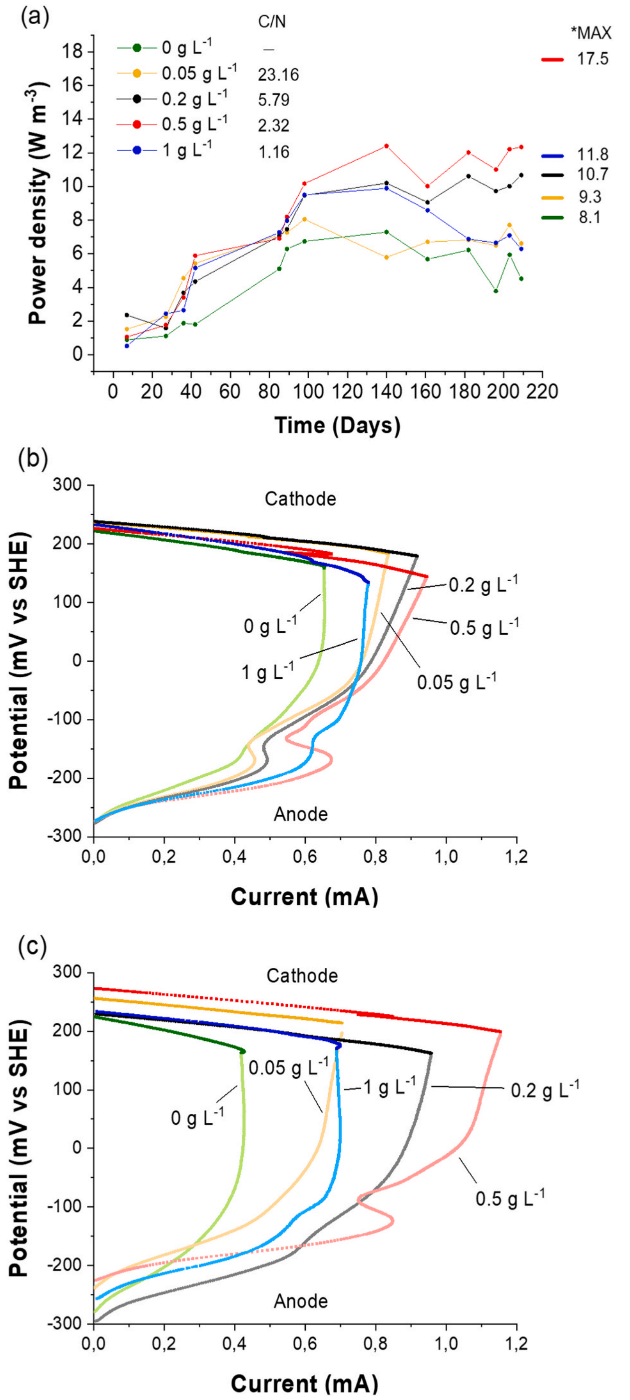

Fig. 2. (a) Power density changes, as well as polarisation curves for (b) 98th and (c) 182nd day of operation. The data on the plot (a) represents average values of two replicates. *MAX – maximal values observed for an individual replicate.

efficient MFCs (out of the three replicates) for each concentration of NH_4Cl in MSM. The recorded power density output revealed that all MFCs did not show a significant increase in efficiency in the first 3 weeks of operation. During this period, the biofilm was enriched with microorganisms capable of metabolising waste vegetable oil. As shown on Fig. 1a, from 20th to 90th day of operation, a similar increase in power density was observed for all MFCs except of 0.0 g L^{-1}. As is known, in the initial stage of operation, biofilm growth is the limiting process of MFC efficiency (Pasternak et al., 2018) and nitrogen plays a key role in the growth of stable biofilms on the anode (Fernandes et al., 2016). Therefore, the power efficiency for MFC without a nitrogen source in MSM (0.0 g L^{-1}) differed from the remaining MFCs (0.05–1 g L^{-1}). In the later stage, an increasing trend in power density was observed only for 0.5 g L^{-1}. For the remaining concentrations, a stable phase of power density was observed. On the 204th day the maximum power density output in this experiment was reached for 0.5 g L^{-1} (14.3 W m^{-3}). For the remaining variants, the maximum power densities were lower by 19%, 34%, 41% and 50% for 0.2 g L^{-1}, 1 g L^{-1}, 0.05 g L^{-1}, and 0 g L^{-1}, respectively. An example of these individual differences is shown on Fig. 1b for the individual batch cycle. Therefore, it may be concluded that the composition of the biofilm created at a concentration of 0.5 g L^{-1} NH_4Cl (C/N = 2.32) allowed for the effective degradation of waste cooking oil. Furthermore, the high and stable power densities for 0.5 g L^{-1} indicated low degradative activity of planktonic bacteria, which is confirmed by the high CE value (Fig. 5).

3.1.2. *Long-term electrochemical behaviour*

Polarisation experiments were carried out throughout the experiment to characterise long-term dynamic changes in the MFC power performance. Fig. 2a shows the values of the maximum power densities extracted from the polarisation experiments, as well as the highest power densities achieved in this study, recorded for the best-performing replicate. Until day 90, all MFCs obtained similar power density, except for 0 g L^{-1}. In the following period, an intensive increase was observed only for 0.5 g L^{-1}, while 0 g L^{-1}, 0.2 g L^{-1} and 1 g L^{-1} stabilised, and a decrease in power efficiency was observed for 0.05 g L^{-1}. After 140 days of operation, 0.5 g L^{-1} reached the highest power density of 12.4 W m^{-3}. It is worth noting that the power density for one of the 0.5 g L^{-1} replicates reached as high as 17.5 W m^{-3}. This value is the highest recorded for an MFC fed with oily wastewater and operating under similar conditions (Bermek et al., 2014). The only study where the higher power density was recorded is the work of Yu et al. (2017), who conducted their studies at 35 $^{\circ}C$, which is 10 $^{\circ}C$ higher when compared to our study. The maximum power densities obtained in this study for 0 g L^{-1}, 0.05 g L^{-1}, 0.2 g L^{-1} and 1 g L^{-1} were lower by 58%, 54%, 39% and 43%, respectively. In terms of performance degradation, after 140 days, a stable power density was observed for 0.05 g L^{-1}, 0.2 g L^{-1} and 0.5 g L^{-1}, while for boundary conditions of 0 g L^{-1} and 1 g L^{-1} a decrease in power efficiency by 38% and 36% was recorded at the end of the experiment. During the first 3 months of biofilm maturation, only MFC fed with 0 g L^{-1} showed significant differences in power performance, due to the lack of a basic component for the growth of microorganisms and biofilm construction (Thompson et al., 2006). Afterwards, the different MFCs power outputs were probably caused by distinctions in the biofilm composition caused by metabolic changes at different C/N ratio in the medium.

Fig. 2b and c shows the polarisation curves obtained from polarisation experiments performed at 98 and 182 days of operation. The open circuit potential of the anode (OCP_A) at the 98th day was congruous for all the MFCs (−274.1 ± 1.6 mV). Similarly, the cathode open circuit potential (OCP_C) was uniform in this period (230.9 ± 7.0 mV). Afterwards, the OCP_A for 0.05 g L^{-1}, 0.5 g L^{-1} and 1 g L^{-1} evolved towards a more positive potential due to the biofilm overgrown, which reduced substrate diffusion rate into deeper biofilm layers (Greenman et al., 2021). Only for 0.2 g L^{-1} the OCP_A has changed towards the negative potential. It is suspected that the biofilm efficiency of these MFCs developed further during this period. The OCP_C changed significantly only for 0.05 g L^{-1} and 0.5 g L^{-1}. The OCP_C evolved toward a more positive potential due to salt electroosmosis from the anolyte to the cathode surface (Rosset et al., 2023). The shape of the polarisation curves from the 98th day showed that the performance of all MFCs was mainly limited by concentration losses at the anode, which are recorded at the higher current range on the plot. In this period, the lowest anodic losses were observed at 0.5 g L^{-1}. Furthermore, the overshoot phenomenon was observed for MFCs. The complexity of the waste cooking oil as a substrate and the immaturity of the biofilm can caused an

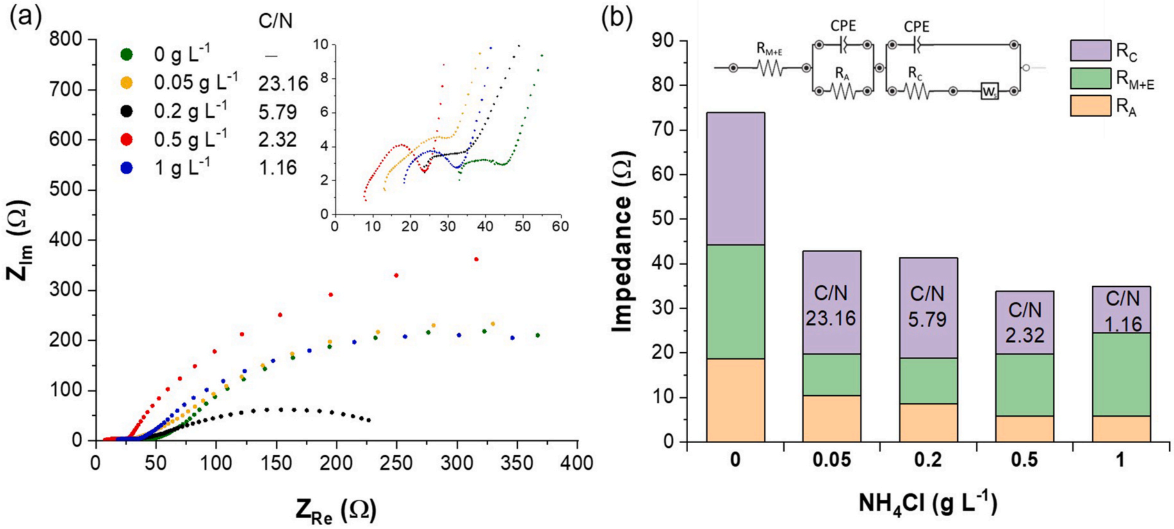

Fig. 3. (a) Nyquist plots and (b) EIS data analysis using the equivalent circuit model presented in the middle of the graph obtained after 182 days of operation.

overshoot phenomenon at higher currents, because the bacteria at the anode cannot sustain the increasing demand for electrons (Watson and Logan, 2011; Winfield et al., 2011). Significant differences in the polarisation curves were observed on the 182nd day of operation. As shown on Fig. 2c a decrease in ohmic (middle range of current) and concentration losses was observed for 0.2 g L^{-1} and 0.5 g L^{-1}, while for the other MFCs these losses increased. The maximum current achieved for 0.5 g L^{-1} on the 182nd day was 1.15 mA, while for 0 g L^{-1}, 0.05 g L^{-1}, 0.2 g L^{-1} and 1 g L^{-1} the maximum current values were lower by 63%, 39%, 16% and 39%, respectively. Polarisation data from the 182nd day revealed dominant concentration losses for each of the MFCs. The observed further decrease of internal resistance in time for 0.2 g L^{-1} and 0.5 g L^{-1} could be attributed to a better biofilm development and bioavailability of the substrate due to BSFs production. Furthermore, the increase in NH_4Cl concentration has affected the conductivity of the electrolyte.

3.1.3. Electrochemical impedance spectroscopy

The EIS experimental data were fitted to an equivalent circuit model (ECM) according to (Sekar and Ramasamy, 2013). The circuit element R_A corresponded to the anode, R_C to the cathode, and R_{M+E} to the ohmic resistances, mainly caused by the membrane and electrolyte resistance. Constant phase element (CPE) was used in the ECM, which corresponds to the capacitive behaviour of the electrical double layer due to the roughness and porosity of the electrode surface, with the presence of biofilm and changes in biofilm thickness (Sekar and Ramasamy, 2013). At the end of the ECM, a Finite length Warburg element designated as W_S was used (Lepage et al., 2012). The Nyquist plots obtained with the EIS are shown in Fig. 3a. The results of the analysis of individual impedance components using the ECM are presented on Fig. 3b. (Borole et al., 2010; Pasternak et al., 2021). The EIS experiment after 182 days of operation showed a decrease in the sum of impedances with increasing concentration of NH_4Cl in the MSM, until it reached the minimum value for 0.5 g L^{-1}. The sum of the impedances for 0.5 g L^{-1} was equal to 33.9 Ω, while the values for 0 g L^{-1}, 0.05 g L^{-1}, 0.2 g L-1 and 1 g L^{-1} were higher by 118%, 27%, 22% and 3% respectively. The same trend was observed for the R_A. Anode impedance for 0.5 g L^{-1} was 5.9 Ω. It is known that R_A decreases with biofilm maturation (Pasternak et al., 2018). Therefore, we conclude that the lowest R_A value for 0.5 g L^{-1} was the result of improved biofilm development on the anodes, as well as the effects attributed to BSFs synthesis. Previous studies have shown that rhamnolipids can lead to improved biofilm formation at the anode (Pasternak et al., 2020; Y. Zhang et al., 2017). The observed decrease in R_C with increasing NH_4Cl concentration was attributed to the beneficial effect of salts precipitation on the CWZ-22 activated carbon cathode (Rosset et al., 2023). However, despite the higher conductivity for 0.5 g L^{-1} and 1 g L^{-1} (Table 1.), it is suspected that the increase in R_{M+E} was the result of membrane biofouling caused by more efficient growth of microorganisms at higher nitrogen concentrations in the anolyte. Furthermore, the R_{M+E} values were related to the presence of BSFs as detected by surface tension measurements. It is known that surfactants can influence the permeability of the cell membrane (Sotirova et al., 2008), which is necessary for the movement of electrons in the mediated electron transfer process, as well as we believe that rhamnolipids can improve the antifouling properties of membranes.

3.2. Biosurfactant synthesis

Biosurfactant synthesis was monitored by measuring the surface tension (SFT) of the anolytes. The drop of the SFT is caused by the presence and increased concentration of BSFs in the medium. On the 98th day of operation, changes in SFT were measured for all MFC anolytes throughout the feeding cycle (Fig. 4a.). The microaerophilic conditions (oxygen concentration = 7.2%) in anodic chamber were sufficient for the enriched biofilm to synthesise BSFs. Furthermore, significant changes occurred in the production of BSFs, depending on the concentration of NH_4Cl. One hour after the feeding cycle was initiated, the lowest SFT values equal to 62.2 mN m^{-1} and 56.2 mN m^{-1}, were reached for 0 g L^{-1} and 1 g L^{-1}, respectively. For the remaining MFCs, a further drop in SFT was observed. In the second hour of the batch cycle, the minimum SFT value was reached for 0.2 g L^{-1}, equal to 55.9 mN m^{-1}. Afterwards (4th hour), the SFT values equal to 54.6 mN m^{-1} and 61.0 mN m^{-1} were recorded for 0.5 g L^{-1} and 0.05 g L^{-1}, respectively. In the last phase, the SFT of the anolytes increased due to the catabolism of the BSFs and/or the interactions of the BSFs with the substrate molecules, as previously indicated (Pasternak et al., 2023). The observed changes in SFT relative to nitrogen content were consistent with previous research. Other authors indicated that the production of BSFs in conventional liquid cultures showed that microbial metabolic disorders can be caused by an excessive nitrogen load in the reactor and thus limit the synthesis of BSFs (Lan et al., 2015). On the other hand, the absence of a nitrogen source in MSM results in a serious limitation of biomass production. Another study identified a significant effect of the C/N ratio on the regulation of genes involved in the production of BSFs by *Pseudomonas aeruginosa* (Ramos et al., 2023). Fig. 4b shows the relationship between the minimum SFT and the maximum power density measured

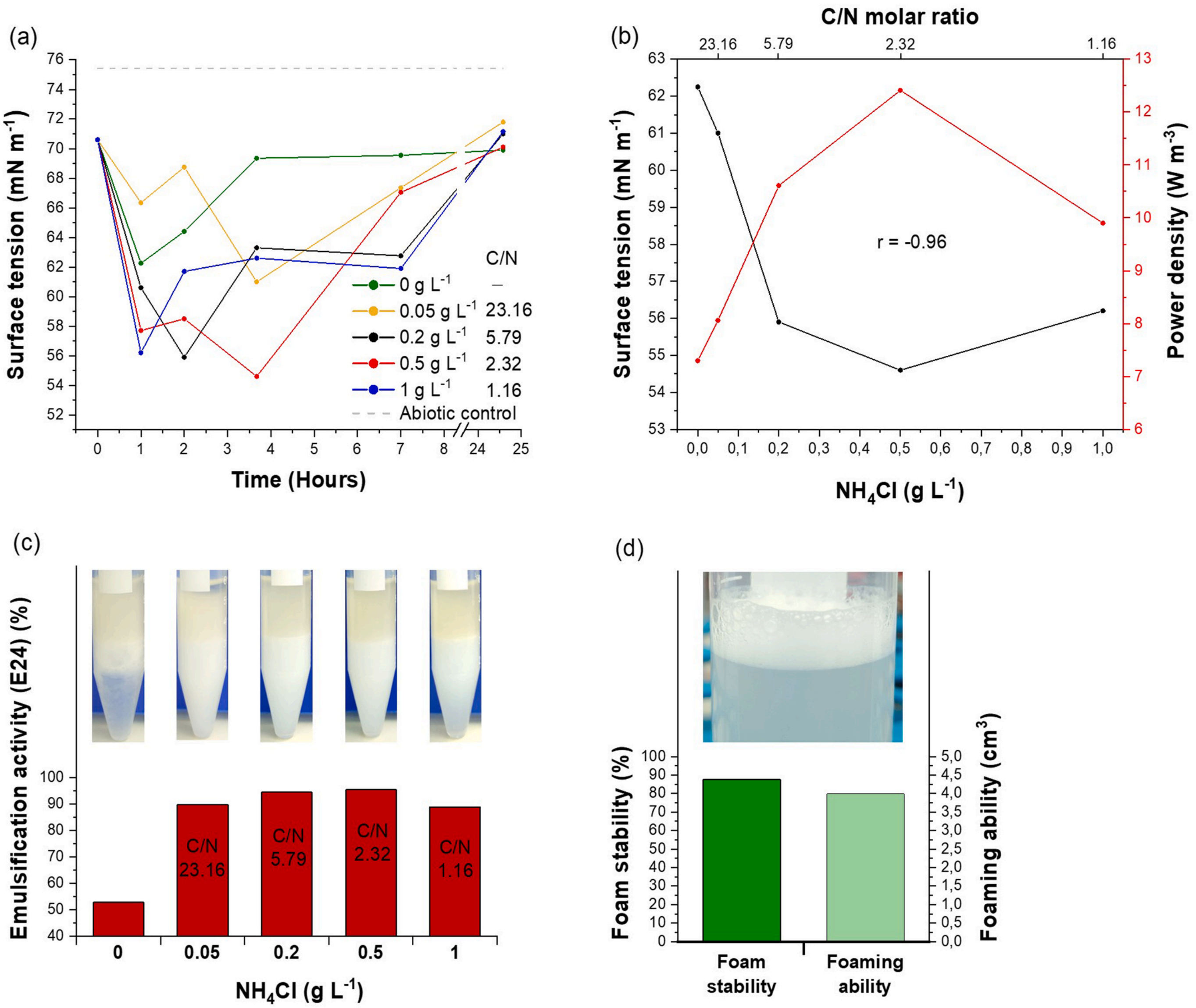

Fig. 4. (a) Changes in surface tension during the degradation of the waste cooking oil. The horizontal dashed line represents the average value of the medium SFT measured at the same frequency (abiotic control). (b) Minimum SFT and maximum power density obtained during one batch cycle as a function of NH_4Cl concentration. (c) Emulsification properties for MFC anolytes and (d) foaming properties for 0.5 g L^{-1} anolyte. All measurements were made on the 98th day of operation. Data represent the average values of two replicates.

in the same batch cycle as a function of the NH_4Cl concentration in the MSM. The determined Pearson's correlation coefficient (r) showed a strong negative correlation (r = −0.96). It can be concluded that the concentration of NH_4Cl had the same effect on power production and conversion of the waste cooking oil to BSFs, which further indicates direct relationship between power production and BSFs synthesis. Our previous work demonstrated a strong correlation between electricity production and BSFs synthesis in the horizontal MFC design (Pasternak et al., 2023), while herein an additional effect of nitrogen content on these parameters was revealed. To characterise the properties of the BSFs produced, the emulsification activity index (E24) was determined for the anolytes of all MFCs (Fig. 4c.). The highest E24 was noted for 0.5 g L^{-1} equal to 95.4%, while the lowest E24 in the study was observed for 0 g L^{-1} equal to 52.8%. For the remaining MFCs, the values were similar (88.3 ± 3.8%). Furthermore, the foaming ability and foam stability were determined for the anolyte of 0.5 g L^{-1} (Fig. 4d.). The foaming ability equal to 4.0 cm^3 (per 20 cm^3 of anolyte) and the foam stability equal to 87.5% were obtained.

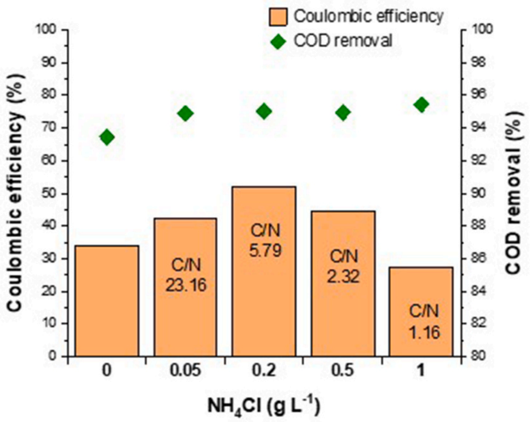

Fig. 5. COD removal and coulombic efficiency calculated after 140 days of operation. Data represent the average values of two replicates.

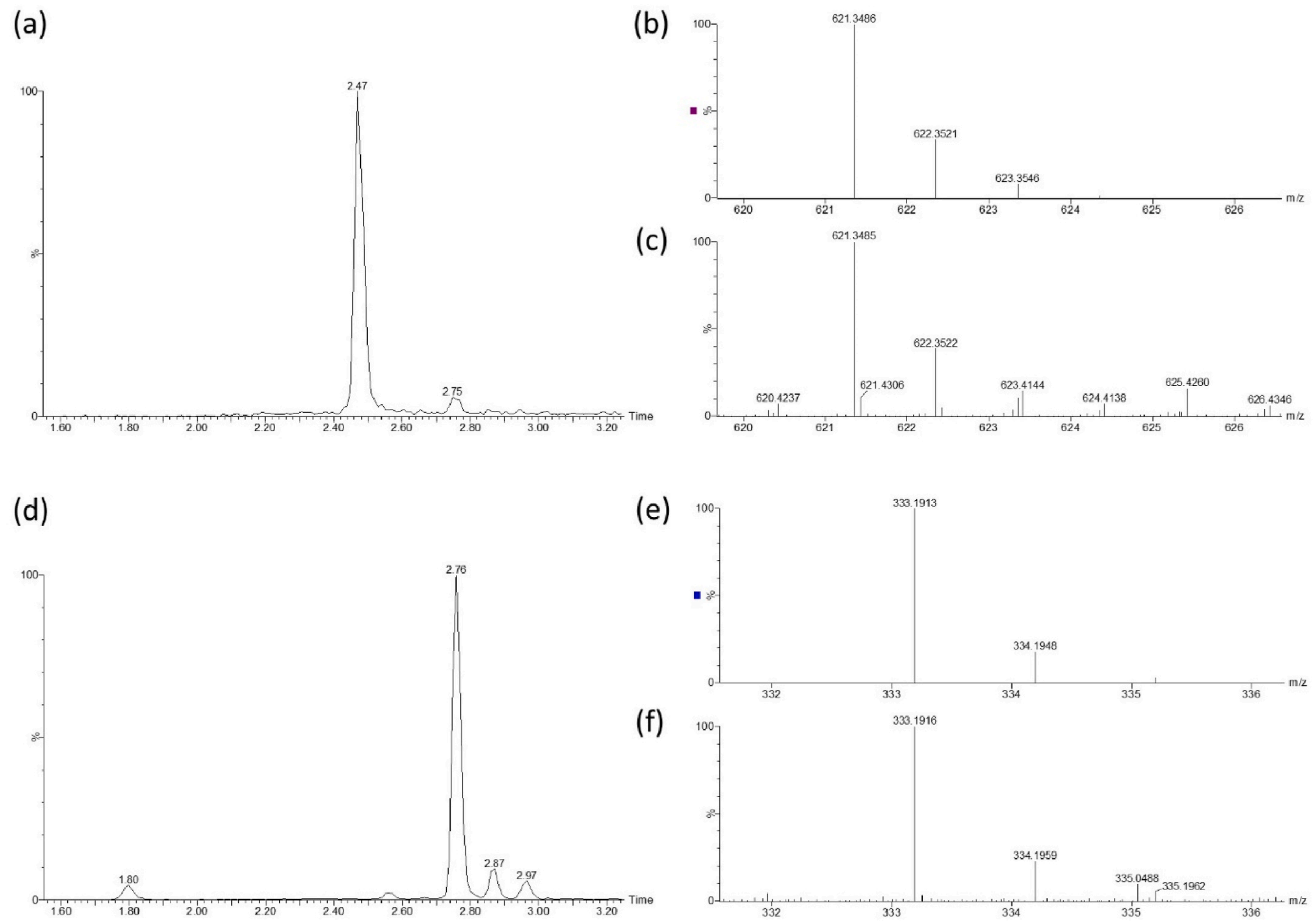

Fig. 6. (a) Extracted ion chromatogram (EIC) for Rha-C10 from monorhamnolipid group, (b) model mass spectrum, (c) experimental mass spectrum for Rha-C10, (d) extracted ion chromatogram (EIC) for Rha-Rha-C10-C8/Rha-Rha-C8-C10 from dirhamnolipid group, (e) model mass spectrum, and (f) experimental mass spectrum for Rha-Rha-C10-C8/Rha-Rha-C8-C10.

3.3. Coulombic efficiency and COD removal

The effect of NH_4Cl concentration in culture medium on waste vegetable oil degradation was assessed by determining the COD removal and the coulombic efficiency (CE) of the MFCs (Fig. 5). The COD concentration of the fresh MSM with the oil substrate was of 2822 mg L^{-1}, while after MFC treatment the COD was equal to 184 mg L^{-1}, 143 mg L^{-1}, 141 mg L^{-1}, 142 mg L^{-1} and 128 mg L^{-1} for 0 g L^{-1}, 0.05 g L^{-1}, 0.2 g L^{-1}, 0.5 g L^{-1} and 1 g L^{-1}, respectively. Thus, the COD removal values were similar for all MFCs (94.8 ± 0.7%). The highest CE value was recorded for 0.2 g L^{-1} (52.1%), while for 0.5 g L^{-1}, 0.05 g L^{-1}, 0 g L^{-1} and 1 g L^{-1} the CE values were lower by 14%, 19%, 35% and 47%, respectively. Despite the lower maximum current obtained at 0.2 g L^{-1} (in comparison to 0.5 g L^{-1}) during the CE measurement, the CE value was higher for 0.2 g L^{-1} (C/N = 5.79) due to the higher average current obtained throughout the batch cycle (Fig. 1b.). The COD removal is highly affected by the design of the MFC and the operating conditions of the bioreactor (Zhang et al., 2015). In this study, we used the same design for all MFCs, operated at the same temperature, therefore, we did not expect a significant difference of the COD removal in the given, relatively long batch cycle. However, a significant effect of NH_4Cl concentration in the culture medium on the CE value was recorded. As previously reported, the development of stable biofilms and substrate metabolism is correlated with the concentration of the nitrogen source in the culture medium (Rochex and Lebeault, 2007). Therefore, the lowest CE value observed for 1 g L^{-1} was the result of the non-optimal structure and composition of the biofilm, which may limit the substrate diffusion rate (Greenman et al., 2021; Pasternak et al., 2018), and was indicated by the high R_A values (Fig. 3.). Furthermore, it is known that nitrogen-induced logarithmic growth of microorganisms in the anolyte may affect the predominance of the competitive to current generation, degradation pathways (Chen et al., 2018). The CE value for 0.2 g L^{-1} is higher by over 40% than obtained for MFCs fed with oily wastewater (Baranitharan et al., 2015; Firdous et al., 2018).

3.4. Microbial community and biosurfactants analysis

Biomass and anolyte from the most efficient MFCs (0.5 g L^{-1}) were collected for analysis of the microbial community and BSFs. Microbial community analysis demonstrates the most abundant phyla as *Proteobacteria* (68.53%), *Bacteroidota* (18.28%) and *Firmicutes* (7.57%) (Fig. 7a). Other studies confirm the dominance of these phyla in the bacterial communities responsible for electricity generation (Guo et al., 2020; Hassan et al., 2018). At the genus level *Azospira* (23.6%), *Pseudomonas* (22.71%), *Dysgonomonas* (16.73%) and *Aeromonas* (6.61%) were identified. Microorganisms belonging to the *Azospira* genus are known for denitrification capabilities under anaerobic conditions and may demonstrate ability to use the electrode as an electron acceptor (Borole et al., 2009; Yang et al., 2022). Members of *Pseudomonas* genera have been reported to produce secondary metabolites such as phenazines and BSFs. First group of metabolites act as redox mediators in MFC systems (Ilamathi et al., 2019), while BSFs facilitate biodegradation of

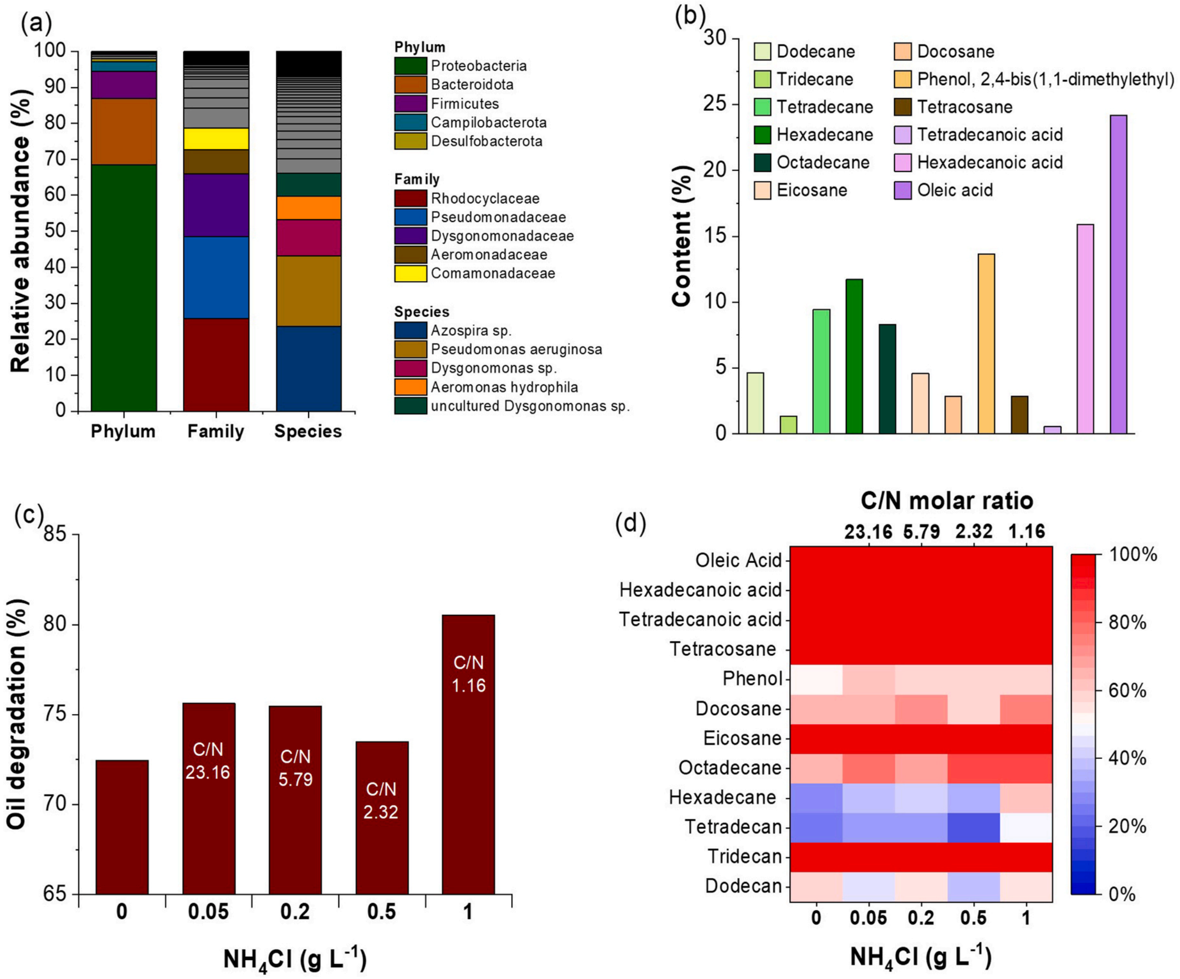

Fig. 7. (a) Microbial community analysis by the most abundant phyla, genera, and species in sample, (b) composition of the biotic control, (c) oil degradation ratio, and (d) degradation ratio of individual waste oil components. Data represents average values of two replicates.

hydrophobic compounds (Pasternak et al., 2020). Both play a crucial role in quorum sensing processes. In another study, it was observed that the presence of *Dysgonomonas* genus increased the power generated by the MFC, indicating its role in the flow of electrons to the anode (Watanabe et al., 2011). Microbial community analysis at species level revealed domination of *Pseudomonas aeruginosa* in relative frequency of 19.60%. It is known that strain is a main producer of rhamnolipids (Soberón-Chávez et al., 2005; Zhao et al., 2021), what is confirmed in this work by LC-MS/MS analysis. Eleven types of rhamnolipids were identified and classified as mono- and dirhamnolipids. In the monorhamnolipid group Rha-C10, Rha-C10-C10, Rha-C8-C10/Rha-C10-C8, Rha-C10-C12/Rha-C12-C10, Rha-C8:1-C10/Rha-C10-C8:1 and Rha-C10 -C12:1/Rha-C12:1-C10 were detected. A representative spectrum for one compound (Rha-C10) in this group is shown in Fig. 6. In dirhamnolipids group, we have observed: Rha-Rha-C10, Rha-Rha-C10-C8/Rha-Rha-C8-C10, Rha-Rha-C10-C10/Rha-Rha-C10-C10, Rha-Rha-C10-C12:1/Rha-Rha-C12:1-C10 and Rha-Rha-C10-C12/Rha-Rha-C12-C10. An example spectrum for Rha-Rha-C10-C8/Rha-Rha-C8-C10 is shown in Fig. 6. Detailed data about m/z values and retention time can be found in Table S1 in Supplementary data. A similar characterisation of rhamnolipids produced by *P. aeruginosa* using frying oil as the sole carbon source was achieved in the previous study by Sun et al. (Sun et al., 2021). TLC analysis with orcinol assay additionally confirms the glycolipid composition of the produced BSFs. The results reported herein represent variety of rhamnolipid types produced by electroactive consortium, while previously available research for BES reported these groups of compounds, only when dedicated pure cultures known to synthesise these groups, as well genetically modified microorganisms were used as the inoculates (Askitosari et al., 2020; Harnisch et al., 2024; Zheng et al., 2015). Furthermore, to the best of our knowledge, this is the first work where a wild type communities were investigated to identify the produced types of biosurfactants.

3.5. Analysis of waste cooking oil and its degradation residues

Composition of the anolytes after MFC treatment was analysed using the GC-MS method. The GC-MS analysis of the biotic control sample is shown on Fig. 7b. The main components of the waste cooking oil were oleic acid (9-octadecenoic acid, C18:1), palmitic acid (Hexadecanoic acid, C16:0) and phenol (2,4-bis(1,1-dimethylethyl)), accounting for 24%, 16% and 14% respectively. Moreover, in the composition of the waste vegetable oil a high total amount of aliphatic hydrocarbons equal to 43% was observed. As shown in Fig. 7c., the oil degradation ratio was similar for all MFCs (74.2 ± 1.5%) except for 1 g L^{-1} (80.5%).

The degradation ratio of individual waste oil components in the MFC is shown in Fig. 7d. The results showed that all MFCs completely degraded the fatty acids, tetracosane, eicosane, and tridecane. However, a difference in the degradation of the remaining components depending on the concentration of NH_4Cl in the culture medium was observed. Quantitative analysis showed the least phenol degraded for 0 g L^{-1}, while for the other MFCs a similar degradation of this component was noted. Furthermore, an improvement in the degradation of two main aliphatic hydrocarbons, hexadecane and tetradecane, was observed with an increasing concentration of NH_4Cl in MSM, except for 0.5 g L^{-1}. It is assumed that the lower degradation of aliphatic hydrocarbons for 0.5 g L^{-1} was the result of the reduction of fatty acids by carboxylic acid reductase (CAR) enzymes to the corresponding aldehydes and then to alkanes by aldehyde decarbonylase enzymes (Kalim Akhtara et al., 2013; Venkitasubramanian et al., 2007). Similar results were shown by Pasternak et al. (2023). In conclusion, all MFCs were able to completely degrade saturated and unsaturated fatty acids and three aliphatic hydrocarbons (C_{24}, C20, and C_{13}). The differences in the degradation ratio of the remaining components support our previous remarks that the different pathways of fatty acid metabolism were revealed, depending on the nitrogen concentration in the anolyte. The lowest degradation of the majority of the waste oil components, observed for 0 g L^{-1}, was the result of weak biofilm performance. On the other hand, 1 g L^{-1} (C/N = 1.16) provided the highest degradation of all waste oil components, but showed the lowest CE value in this study, which corresponds to our conclusions from the COD removal. The data from the GC/MS analysis correspond to the MFC performance indicators such as the mentioned COD, CE as well as power performance and impedance parameters.

4. Conclusions

The effect of nitrogen source concentration in the culture medium on the efficiency of biosurfactant and electricity production in horizontal microbial fuel cells was assessed. The observed power production indicated an improvement in efficiency corresponding to the increase in the concentration of NH_4Cl in the medium, and the maximum power density (12.4 W m^{-3}) was recorded for 0.5 g L^{-1} (C/N = 2.32). Similarly, the highest decrease in surface tension to 54.6 mN m^{-1}, which indicated the synthesis of biosurfactants, was also observed for this concentration. Importantly, we have shown a strong negative correlation ($r = -0.96$) of changes in power density and decrease in surface tension as a function of NH_4Cl concentration. Therefore, we prove that the biosurfactant synthesis and degradation efficiency of the waste cooking oil is directly dependent on the concentration of the nitrogen source. Other parameters such as COD, CE, compounds biotransformation, and MFC impedance elements also corresponded to the nitrogen concentration. The 16S biodiversity analysis indicated the presence of biosurfactant-producing dominant strain of *P. aeruginosa*, along with other biodegradative, electroactive and biosynthesising species. Their activity resulted in biosynthesis of eleven types of mono- and di-rhamnolipids as detected by the metabolomic approach. These results show that the concentration of the nitrogen source in the culture medium is one of the crucial factors to maintain high efficiency of waste vegetable oil degradation, power production and simultaneous biosurfactant synthesis and brings the efficient synthesis of biosurfactants in bioelectrochemical systems, one step closer to the application.

CRediT authorship contribution statement

Aleksander de Rosset: Writing – original draft, Visualization, Methodology, Investigation, Formal analysis. **Natalia Tyszkiewicz:** Writing – original draft, Visualization, Methodology, Investigation, Formal analysis. **Jerzy Wiśniewski:** Writing – review & editing, Methodology, Formal analysis. **Natalia Pudełko-Malik:** Writing – review & editing, Methodology, Formal analysis. **Piotr Rutkowski:** Writing – review & editing, Supervision. **Piotr Młynarz:** Writing – review & editing, Supervision. **Grzegorz Pasternak:** Writing – review & editing, Resources, Project administration, Methodology, Funding acquisition, Formal analysis, Conceptualization.

Declaration of competing interest

The authors declare that they have no known competing financial interests or personal relationships that could have appeared to influence the work reported in this paper.

Data availability

Data will be made available on request.

Acknowledgements

This work was financed by the Polish National Agency for Academic Exchange – Polish Returns grant (PPN/PPO/2018/1/00038) and the National Science Centre (Poland) OPUS grant (2019/33/B/NZ9/02774).

Appendix A. Supplementary data

Supplementary data to this article can be found online at https://doi.org/10.1016/j.jenvman.2024.121514.

References

Abdel-Mawgoud, A.M., Aboulwafa, M.M., Hassouna, N.A.H., 2008. Optimization of surfactin production by bacillus subtilis isolate BS5. Appl. Biochem. Biotechnol. 150 (3), 305–325. https://doi.org/10.1007/s12010-008-8155-x.

Abouseoud, M., Maachi, R., Amrane, A., Boudergua, S., Nabi, A., 2008. Evaluation of different carbon and nitrogen sources in production of biosurfactant by Pseudomonas fluorescens. Desalination 223 (1–3), 143–151. https://doi.org/10.1016/j.desal.2007.01.198.

Aelterman, P., Versichele, M., Marzorati, M., Boon, N., Verstraete, W., 2008. Loading rate and external resistance control the electricity generation of microbial fuel cells with different three-dimensional anodes. Bioresour. Technol. 99 (18), 8895–8902. https://doi.org/10.1016/j.biortech.2008.04.061.

Askitosari, T.D., Berger, C., Tiso, T., Harnisch, F., Blank, L.M., Rosenbaum, M.A., 2020. Coupling an electroactive Pseudomonas putida KT2440 with bioelectrochemical rhamnolipid production. Microorganisms 8 (12), 1959. https://doi.org/10.3390/microorganisms8121959.

Baranitharan, E., Khan, M.R., Prasad, D.M.R., Teo, W.F.A., Tan, G.Y.A., Jose, R., 2015. Effect of biofilm formation on the performance of microbial fuel cell for the treatment of palm oil mill effluent. Bioproc. Biosyst. Eng. 38 (1), 15–24. https://doi.org/10.1007/s00449-014-1239-9.

Bermek, H., Catal, T., Akan, S.S., Ulutaş, M.S., Kumru, M., Özgüven, M., Liu, H., Özçelik, B., Akarsubaşı, A.T., 2014. Olive mill wastewater treatment in single-chamber air-cathode microbial fuel cells. World J. Microbiol. Biotechnol. 30 (4), 1177–1185. https://doi.org/10.1007/s11274-013-1541-8.

Bokulich, N.A., Kaehler, B.D., Rideout, J.R., Dillon, M., Bolyen, E., Knight, R., Huttley, G. A., Gregory Caporaso, J., 2018. Optimizing taxonomic classification of marker-gene amplicon sequences with QIIME 2's q2-feature-classifier plugin. Microbiome 6 (1), 1–17. https://doi.org/10.1186/s40168-018-0470-z.

Bolyen, E., Rideout, J.R., Dillon, M.R., Bokulich, N.A., Abnet, C.C., Al-Ghalith, G.A., Alexander, H., Alm, E.J., Arumugam, M., Asnicar, F., Bai, Y., Bisanz, J.E., Bittinger, K., Brejnrod, A., Brislawn, C.J., Brown, C.T., Callahan, B.J., Caraballo-Rodríguez, A.M., Chase, J., et al., 2019. Reproducible, interactive, scalable and extensible microbiome data science using QIIME 2. Nat. Biotechnol. 37 (8), 852–857. https://doi.org/10.1038/s41587-019-0209-9.

Bongartz, P., Bator, I., Baitalow, K., Keller, R., Tiso, T., Blank, L.M., Wessling, M., 2021. A scalable bubble-free membrane aerator for biosurfactant production. Biotechnol. Bioeng. 118 (9), 3545–3558. https://doi.org/10.1002/bit.27822.

Borole, A.P., Aaron, D., Hamilton, C.Y., Tsouris, C., 2010. Understanding long-term changes in microbial fuel cell performance using electrochemical impedance spectroscopy. Environ. Sci. Technol. 44 (7), 2740–2745. https://doi.org/10.1021/es9032937.

Borole, A.P., Hamilton, C.Y., Vishnivetskaya, T., Leak, D., Andras, C., 2009. Improving power production in acetate-fed microbial fuel cells via enrichment of exoelectrogenic organisms in flow-through systems. Biochem. Eng. J. 48 (1), 71–80. https://doi.org/10.1016/j.bej.2009.08.008.

Callahan, B.J., McMurdie, P.J., Rosen, M.J., Han, A.W., Johnson, A.J.A., Holmes, S.P., 2016. DADA2: high-resolution sample inference from Illumina amplicon data. Nat. Methods 13 (7), 581–583. https://doi.org/10.1038/nmeth.3869.

Chen, C., Sun, N., Li, D., Long, S., Tang, X., Xiao, G., Wang, L., 2018. Optimization and Characterization of Biosurfactant Production from Kitchen Waste Oil Using Pseudomonas aeruginosa, pp. 14934–14943.

Chen, S., Patil, S.A., Brown, R.K., Schröder, U., 2019. Strategies for optimizing the power output of microbial fuel cells: transitioning from fundamental studies to practical implementation. Appl. Energy 233–234 (October 2018), 15–28. https://doi.org/10.1016/j.apenergy.2018.10.015.

Das, P., Mukherjee, S., Sen, R., 2008. Antimicrobial potential of a lipopeptide biosurfactant derived from a marine Bacillus circulans. J. Appl. Microbiol. 104 (6), 1675–1684. https://doi.org/10.1111/j.1365-2672.2007.03701.x.

Edel, M., Philipp, L.A., Lapp, J., Reiner, J., Gescher, J., 2022. Electron transfer of extremophiles in bioelectrochemical systems. Extremophiles 26 (3), 1–12. https://doi.org/10.1007/s00792-022-01279-8.

Fernandes, P.L., Rodrigues, E.M., Paiva, F.R., Ayupe, B.A.L., McInerney, M.J., Tótola, M. R., 2016. Biosurfactant, solvents and polymer production by Bacillus subtilis RI4914 and their application for enhanced oil recovery. Fuel 180, 551–557. https://doi.org/10.1016/j.fuel.2016.04.080.

Finch, A.S., Mackie, T.D., Sund, C.J., Sumner, J.J., 2011. Metabolite analysis of Clostridium acetobutylicum: fermentation in a microbial fuel cell. Bioresour. Technol. 102 (1), 312–315. https://doi.org/10.1016/j.biortech.2010.06.149.

Firdous, S., Jin, W., Shahid, N., Bhatti, Z.A., Iqbal, A., Abbasi, U., Mahmood, Q., Ali, A., 2018. The performance of microbial fuel cells treating vegetable oil industrial wastewater. Environ. Technol. Innovat. 10, 143–151. https://doi.org/10.1016/j.eti.2018.02.006.

Förster, A.H., Beblawy, S., Golitsch, F., Gescher, J., 2017. Electrode-assisted acetoin production in a metabolically engineered Escherichia coli strain. Biotechnol. Biofuels. https://doi.org/10.1186/s13068-017-0745-9.

Gomaa, O.M., Selim, N., Fathy, R., Maghrawy, H.H., Gamal, M., El Kareem, H.A., Kyazze, G., Keshavarz, T., 2021. Characterization of a biosurfactant producing electroactive Bacillus sp. for enhanced Microbial Fuel Cell dye decolourisation. Enzym. Microb. Technol. 147, 109767 https://doi.org/10.1016/j.enzmictec.2021.109767. September 2020.

Greenman, J., Gajda, I., You, J., Mendis, B.A., Obata, O., Pasternak, G., Ieropoulos, I., 2021. Microbial fuel cells and their electrified biofilms. Biofilm 3 (July), 100057. https://doi.org/10.1016/j.bioflm.2021.100057.

Guo, H., Tang, S., Xie, S., Wang, P., Huang, C., Geng, X., Jia, X., Huo, H., Li, X., Zhang, J., Zhang, Z., Fang, J., 2020. The oil removal and the characteristics of changes in the composition of bacteria based on the oily sludge bioelectrochemical system. Sci. Rep. 10 (1), 1–10. https://doi.org/10.1038/s41598-020-72405-9.

Harnisch, F., Deutzmann, J.S., Boto, S.T., Rosenbaum, M.A., 2024. Microbial electrosynthesis: opportunities for microbial pure cultures. Trends Biotechnol. xx (xx), 1–13. https://doi.org/10.1016/j.tibtech.2024.02.004.

Hassan, H., Jin, B., Donner, E., Vasileiadis, S., Saint, C., Dai, S., 2018. Microbial community and bioelectrochemical activities in MFC for degrading phenol and producing electricity: microbial consortia could make differences. Chem. Eng. J. 332 (June 2017), 647–657. https://doi.org/10.1016/j.cej.2017.09.114.

Hoang, A.T., Nižetić, S., Ng, K.H., Papadopoulos, A.M., Le, A.T., Kumar, S., Hadiyanto, H., Pham, V.V., 2022. Microbial fuel cells for bioelectricity production from waste as sustainable prospect of future energy sector. Chemosphere 287 (June 2021). https://doi.org/10.1016/j.chemosphere.2021.132285.

Ilamathi, R., Merline Sheela, A., Nagendra Gandhi, N., 2019. Comparative evaluation of Pseudomonas species in single chamber microbial fuel cell with manganese coated cathode for reactive azo dye removal. Int. Biodeterior. Biodegrad. 144 (March), 104744 https://doi.org/10.1016/j.ibiod.2019.104744.

Jain, R.M., Mody, K., Joshi, N., Mishra, A., Jha, B., 2013. Production and structural characterization of biosurfactant produced by an alkaliphilic bacterium, Klebsiella sp.: evaluation of different carbon sources. Colloids Surf. B Biointerfaces 108, 199–204. https://doi.org/10.1016/j.colsurfb.2013.03.002.

Kaczorek, E., Pacholak, A., Zdarta, A., Smułek, W., 2018. The impact of biosurfactants on microbial cell properties leading to hydrocarbon bioavailability increase. Colloids and Interfaces 2 (3). https://doi.org/10.3390/colloids2030035.

Kalim Akhtara, M., Turner, N.J., Jones, P.R., 2013. Carboxylic acid reductase is a versatile enzyme for the conversion of fatty acids into fuels and chemical commodities. Proc. Natl. Acad. Sci. U.S.A. 110 (1), 87–92. https://doi.org/10.1073/pnas.1216516110.

Klein, E.M., Knoll, M.T., Gescher, J., 2023. Microbe–Anode Interactions: comparing the impact of genetic and material engineering approaches to improve the performance of microbial electrochemical systems (MES). Microb. Biotechnol. 16 (6), 1179–1202. https://doi.org/10.1111/1751-7915.14236.

Klindworth, A., Pruesse, E., Schweer, T., Peplies, J., Quast, C., Horn, M., Glöckner, F.O., 2013. Evaluation of general 16S ribosomal RNA gene PCR primers for classical and next-generation sequencing-based diversity studies. Nucleic Acids Res. 41 (1), 1–11. https://doi.org/10.1093/nar/gks808.

Laabei, M., Jamieson, W.D., Lewis, S.E., Diggle, S.P., Jenkins, A.T.A., 2014. A new assay for rhamnolipid detection - important virulence factors of Pseudomonas aeruginosa. Appl. Microbiol. Biotechnol. 98 (16), 7199–7209. https://doi.org/10.1007/s00253-014-5904-3.

Lan, G., Fan, Q., Liu, Y., Chen, C., Li, G., Liu, Y., Yin, X., 2015. Rhamnolipid production from waste cooking oil using Pseudomonas SWP-4. Biochem. Eng. J. 101, 44–54. https://doi.org/10.1016/j.bej.2015.05.001.

Lepage, G., Albernaz, F.O., Perrier, G., Merlin, G., 2012. Characterization of a microbial fuel cell with reticulated carbon foam electrodes. Bioresour. Technol. 124, 199–207. https://doi.org/10.1016/j.biortech.2012.07.067.

Liu, J., Vipulanandan, C., 2017. Effects of Fe, Ni, and Fe/Ni metallic nanoparticles on power production and biosurfactant production from used vegetable oil in the anode chamber of a microbial fuel cell. Waste Manag. 66, 169–177. https://doi.org/10.1016/j.wasman.2017.04.004.

Liu, J., Vipulanandan, C., Yang, M., 2019. Biosurfactant production from used vegetable oil in the anode chamber of a microbial electrosynthesizing fuel cell. Waste and Biomass Valorization 10 (10), 2925–2931. https://doi.org/10.1007/s12649-018-0331-9.

Logan, B.E., Hamelers, B., Rozendal, R., Schröder, U., Keller, J., Freguia, S., Aelterman, P., Verstraete, W., Rabaey, K., 2006. Microbial fuel cells: Methodology and technology. Environ. Sci. Technol. 40 (17), 5181–5192. https://doi.org/10.1021/es0605016.

Marchant, R., Banat, I.M., 2012a. Biosurfactants: a sustainable replacement for chemical surfactants? Biotechnol. Lett. 34 (9), 1597–1605. https://doi.org/10.1007/s10529-012-0956-x.

Marchant, R., Banat, I.M., 2012b. Microbial biosurfactants: challenges and opportunities for future exploitation. Trends Biotechnol. 30 (11), 558–565. https://doi.org/10.1016/j.tibtech.2012.07.003.

Moscoviz, R., Toledo-Alarcón, J., Trably, E., Bernet, N., 2016. Electro-fermentation: how to drive fermentation using electrochemical systems. Trends Biotechnol. 34 (11), 856–865. https://doi.org/10.1016/j.tibtech.2016.04.009.

Onwosi, C.O., Odibo, F.J.C., 2012. Effects of carbon and nitrogen sources on rhamnolipid biosurfactant production by Pseudomonas nitroreducens isolated from soil. World J. Microbiol. Biotechnol. 28 (3), 937–942. https://doi.org/10.1007/s11274-011-0891-3.

OriginPro, Version 2019. OriginLab Corporation, Northampton, MA, USA.

Ozdal, M., Gurkok, S., Ozdal, O.G., 2017. Optimization of rhamnolipid production by Pseudomonas aeruginosa OG1 using waste frying oil and chicken feather peptone. 3 Biotech 7 (2), 1–8. https://doi.org/10.1007/s13205-017-0774-x.

Pasternak, G., Askitosari, T.D., Rosenbaum, M.A., 2020. Biosurfactants and Synthetic Surfactants in Bioelectrochemical Systems : A Mini-Review Influence on Electron Transfer 11, 1–9. https://doi.org/10.3389/fmicb.2020.00358. March.

Pasternak, G., de Rosset, A., Rutkowski, P., 2023. Horizontal microbial fuel cell system producing biosurfactants in response to current generation from waste cooking oil as a fuel. Energy Convers. Manag. 281 (March), 116807 https://doi.org/10.1016/j.enconman.2023.116807.

Pasternak, G., Greenman, J., Ieropoulos, I., 2018. Dynamic evolution of anodic biofilm when maturing under different external resistive loads in microbial fuel cells. Electrochemical perspective. J. Power Sources 400 (August), 392–401. https://doi.org/10.1016/j.jpowsour.2018.08.031.

Pasternak, G., Ormeno-Cano, N., Rutkowski, P., 2021. Recycled waste polypropylene composite ceramic membranes for extended lifetime of microbial fuel cells. Chem. Eng. J. 130707 https://doi.org/10.1016/J.CEJ.2021.130707.

Pham, T.H., Boon, N., Aelterman, P., Clauwaert, P., De Schamphelaire, L., Vanhaecke, L., De Maeyer, K., Höfte, M., Verstraete, W., Rabaey, K., 2008. Metabolites produced by Pseudomonas sp. enable a Gram-positive bacterium to achieve extracellular electron transfer. Appl. Microbiol. Biotechnol. 77 (5), 1119–1129. https://doi.org/10.1007/s00253-007-1248-6.

Priya, T., Usharani, G., 2009. Comparative study for biosurfactant production by using Bacillus subtilis and Pseudomonas aeruginosa, 2 (4), 284–287.

Puig, S., Serra, M., Coma, M., Cabré, M., Balaguer, M.D., Colprim, J., 2010. Effect of pH on nutrient dynamics and electricity production using microbial fuel cells. Bioresour. Technol. 101 (24), 9594–9599. https://doi.org/10.1016/j.biortech.2010.07.082.

Ramos, P., Honda, R., Hoek, E.M.V., Mahendra, S., 2023. Carbon/nitrogen ratios determine biofilm formation and characteristics in model microbial cultures. Chemosphere 313 (December 2022), 137628. https://doi.org/10.1016/j.chemosphere.2022.137628.

Rochex, A., Lebeault, J.M., 2007. Effects of nutrients on biofilm formation and detachment of a Pseudomonas putida strain isolated from a paper machine. Water Res. 41 (13), 2885–2892. https://doi.org/10.1016/j.watres.2007.03.041.

Rognes, T., Flouri, T., Nichols, B., Quince, C., Mahé, F., 2016. VSEARCH: a versatile open source tool for metagenomics. PeerJ 2016 (10), 1–22. https://doi.org/10.7717/peerj.2584.

Rosset, A. De, Rutkowski, P., Pasternak, G., 2023. The effect of surface and porous structure on long-term performance of carbon powder cathodes without binder , during a 300-day trial in microbial fuel cells. Sustain. Energy Technol. Assessments 58 (April), 103340. https://doi.org/10.1016/j.seta.2023.103340.

Santos, A.S., Sampaio, A.P.W., Vasquez, G.S., Anna, L.M.S., Pereira, N., Freire, D.M.G., 2002. Evaluation of different carbon and nitrogen sources. In: Finkelstein, M., McMillan, J.D., Davison, B.H. (Eds.), Production of Rhamnolipids by a Strain of Pseudomonas aeruginosa BT - Biotechnology for Fuels and Chemicals: the Twenty–Third Symposium. Humana Press, pp. 1025–1035. https://doi.org/10.1007/978-1-4612-0119-9_83.

Santos, E.F., Teixeira, M.F.S., Converti, A., Porto, A.L.F., Sarubbo, L.A., 2019. Production of a new lipoprotein biosurfactant by Streptomyces sp. DPUA1566 isolated from lichens collected in the Brazilian Amazon using agroindustry wastes. Biocatal. Agric. Biotechnol. 17 (October 2018), 142–150. https://doi.org/10.1016/j.bcab.2018.10.014.

Sarubbo, L.A., Silva, M. da G.C., Durval, I.J.B., Bezerra, K.G.O., Ribeiro, B.G., Silva, I.A., Twigg, M.S., Banat, I.M., 2022. Biosurfactants: production, properties, applications, trends, and general perspectives. Biochem. Eng. J. 181 https://doi.org/10.1016/j.bej.2022.108377. November 2021.

Sekar, N., Ramasamy, R.P., 2013. Electrochemical impedance spectroscopy for microbial fuel cell characterization. J. Microb. Biochem. Technol. 5 (SPECIALISSUE.2) https://doi.org/10.4172/1948-5948.s6-004.

Sharma, S., Pandey, L.M., 2020. Production of biosurfactant by Bacillus subtilis RSL-2 isolated from sludge and biosurfactant mediated degradation of oil. Bioresour. Technol. 307 (February), 123261 https://doi.org/10.1016/j.biortech.2020.123261.

Soberón-Chávez, G., Lépine, F., Déziel, E., 2005. Production of rhamnolipids by Pseudomonas aeruginosa. Appl. Microbiol. Biotechnol. 68 (6), 718–725. https://doi.org/10.1007/s00253-005-0150-3.

Sotirova, A.V., Spasova, D.I., Galabova, D.N., Karpenko, E., Shulga, A., 2008. Rhamnolipid-biosurfactant permeabilizing effects on gram-positive and gram-negative bacterial strains. Curr. Microbiol. 56 (6), 639–644. https://doi.org/10.1007/s00284-008-9139-3.

Sukkasem, C., Xu, S., Park, S., Boonsawang, P., Liu, H., 2008. Effect of nitrate on the performance of single chamber air cathode microbial fuel cells. Water Res. 42 (19), 4743–4750. https://doi.org/10.1016/j.watres.2008.08.029.

Sun, H., Wang, L., Nie, H., Diwu, Z., Nie, M., Zhang, B., 2021. Optimization and characterization of rhamnolipid production by Pseudomonas aeruginosa NY3 using waste frying oil as the sole carbon. Biotechnol. Prog. 37 (4), 1–11. https://doi.org/10.1002/btpr.3155.

Sun, W., Zhu, B., Yang, F., Dai, M., Sehar, S., Peng, C., Ali, I., Naz, I., 2021. Optimization of biosurfactant production from Pseudomonas sp. CQ2 and its application for remediation of heavy metal contaminated soil. Chemosphere 265, 129090. https://doi.org/10.1016/j.chemosphere.2020.129090.

Thompson, L.J., Gray, V., Lindsay, D., Von Holy, A., 2006. Carbon:nitrogen:phosphorus ratios influence biofilm formation by Enterobacter cloacae and Citrobacter freundii. J. Appl. Microbiol. 101 (5), 1105–1113. https://doi.org/10.1111/j.1365-2672.2006.03003.x.

Vázquez, I., Kerzenmacher, S., Santiago, Ó., 2023. Stainless steel wool as novel bioanode for microbial electrolysis cells: a systematic study of materials. Front. Energy Res. 11 (February), 1–13. https://doi.org/10.3389/fenrg.2023.1119090.

Venkitasubramanian, P., Daniels, L., Rosazza, J.P.N., 2007. Reduction of carboxylic acids by Nocardia aldehyde oxidoreductase requires a phosphopantetheinylated enzyme. J. Biol. Chem. 282 (1), 478–485. https://doi.org/10.1074/jbc.M607980200.

Watanabe, K., Miyahara, M., Shimoyama, T., Hashimoto, K., 2011. Population dynamics and current-generation mechanisms in cassette-electrode microbial fuel cells. Appl. Microbiol. Biotechnol. 92 (6), 1307–1314. https://doi.org/10.1007/s00253-011-3598-3.

Watson, V.J., Logan, B.E., 2011. Analysis of polarization methods for elimination of power overshoot in microbial fuel cells. Electrochem. Commun. 13 (1), 54–56. https://doi.org/10.1016/j.elecom.2010.11.011.

Winfield, J., Ieropoulos, I., Greenman, J., Dennis, J., 2011. The overshoot phenomenon as a function of internal resistance in microbial fuel cells. Bioelectrochemistry 81 (1), 22–27. https://doi.org/10.1016/j.bioelechem.2011.01.001.

Wu, Q., Zhi, Y., Xu, Y., 2019. Systematically engineering the biosynthesis of a green biosurfactant surfactin by Bacillus subtilis 168. Metab. Eng. 52, 87–97. https://doi.org/10.1016/j.ymben.2018.11.004. November 2018.

Yang, Z., Li, H., Li, N., Sardar, M.F., Song, T., Zhu, H., Xing, X., Zhu, C., 2022. Dynamics of a bacterial community in the anode and cathode of microbial fuel cells under sulfadiazine pressure. Int. J. Environ. Res. Publ. Health 19 (10). https://doi.org/10.3390/ijerph19106253.

Yu, N., Xing, D., Li, W., Yang, Y., Li, Z., Li, Y., Ren, N., 2017. Electricity and methane production from soybean edible oil refinery wastewater using microbial electrochemical systems. Int. J. Hydrogen Energy 42 (1), 96–102. https://doi.org/10.1016/j.ijhydene.2016.11.116.

Yuan, J., Huang, H., Chatterjee, S.G., Wang, Z., Wang, S., 2022. Effective factors for the performance of a co-generation system for bioethanol and electricity production via microbial fuel cell technology. Biochem. Eng. J. 178 (December 2021), 108309 https://doi.org/10.1016/j.bej.2021.108309.

Zhang, X., He, W., Ren, L., Stager, J., Evans, P.J., Logan, B.E., 2015. COD removal characteristics in air-cathode microbial fuel cells. Bioresour. Technol. 176, 23–31. https://doi.org/10.1016/j.biortech.2014.11.001.

Zhang, Y., Jiang, J., Zhao, Q., Gao, Y.Z., Wang, K., Ding, J., Yu, H., Yao, Y., 2017. Accelerating anodic biofilms formation and electron transfer in microbial fuel cells: role of anionic biosurfactants and mechanism. Bioelectrochemistry 117, 48–56. https://doi.org/10.1016/j.bioelechem.2017.06.002.

Zhao, F., Wang, Q., Zhang, Y., Lei, L., 2021. Anaerobic biosynthesis of rhamnolipids by Pseudomonas aeruginosa: performance, mechanism and its application potential for enhanced oil recovery. Microb. Cell Factories 20 (1), 1–12. https://doi.org/10.1186/s12934-021-01593-4.

Zhao, F., Zhou, J., Han, S., Ma, F., Zhang, Y., Zhang, J., 2016. Medium factors on anaerobic production of rhamnolipids by Pseudomonas aeruginosa SG and a simplifying medium for in situ microbial enhanced oil recovery applications. World J. Microbiol. Biotechnol. 32 (4), 1–11. https://doi.org/10.1007/s11274-016-2020-9.

Zheng, T., Xu, Y.S., Yong, X.Y., Li, B., Yin, D., Cheng, Q.W., Yuan, H.R., Yong, Y.C., 2015. Endogenously enhanced biosurfactant production promotes electricity generation from microbial fuel cells. Bioresour. Technol. 197, 416–421. https://doi.org/10.1016/j.biortech.2015.08.136.

SUPPORTING INFORMATION

Bioelectrochemical synthesis of rhamnolipids and energy production and its correlation with nitrogen in air-cathode microbial fuel cells

Aleksander de Rosset[1,a], Natalia Tyszkiewicz[1,2,a], Jerzy Wiśniewski[2], Natalia Pudełko-Malik[2], Piotr Rutkowski[1], Piotr Młynarz[2], Grzegorz Pasternak[1,*,a]

[1]Department of Process Engineering and Technology of Polymer and Carbon Materials, Faculty of Chemistry, Wroclaw University of Science and Technology, Wroclaw 50-370, Poland.

[2]Department of Biochemistry, Molecular Biology and Biotechnology, Faculty of Chemistry, Wroclaw University of Science and Technology, Wroclaw 50-370, Poland.

*Corresponding author: grzegorz.pasternak@pwr.edu.pl

[a]website: www.gplab.eu

Tab. S1. Summary of LC-MS/MS analysis for detected biosurfactants.

No.	m/z	Rhamnolipids	Molecular formula	Retention time [min]	Lipidmaps ID
1	333,1915	Rha-C10	$C_{16}H_{30}O_7$	1,80	LMFA13030003
2	475,2907	Rha-C8-C10/Rha-C10-C8	$C_{24}H_{44}O_9$	2,56	LMFA130300
3	473,2802	Rha-C8:1-C10/Rha-C10-C8:1	$C_{24}H_{42}O_9$	2,55	-
4	503,3220	Rha-C10-C10	$C_{26}H_{48}O_9$	2,76	LMFA13030001
5	529,3376	Rha-C10-C12:1/Rha-C12:1-C10	$C_{28}H_{50}O_9$	2,87	LMFA13030016
6	531,3521	Rha-C10-C12/Rha-C12-C10	$C_{28}H_{52}O_9$	2,97	LMFA13030013
7	479,2492	Rha-Rha-C10	$C_{22}H_{40}O_{11}$	1,72	LMFA13030006
8	621,3485	Rha-Rha-C10-C8/Rha-Rha-C8-C10	$C_{30}H_{54}O_{13}$	2,47	-
9	649,3799	Rha-Rha-C10-C10	$C_{32}H_{58}O_{13}$	2,65	LMFA13030005
10	675,3937	Rha-Rha-C10-C12:1/Rha-Rha-C12:1-C10	$C_{34}H_{60}O_{13}$	2,76	-
11	677,4112	Rha-Rha-C10-C12/Rha-Rha-C12-C10	$C_{34}H_{62}O_{13}$	2,85	-

5.4. Enhancing performance and durability of PVDF-ceramic composite membranes in microbial fuel cells using natural rhamnolipids

5.4.1. Omówienie publikacji

Separatory ceramiczne stanowią obiecującą alternatywę dla drogich membran jonowymiennych ze względu na niski koszt produkcji, dobrą stabilność, wysoką trwałość i dostępność. Ze względu na te zalety w większości badań nad zwiększaniem skali MFC stosuje się membrany ceramiczne. Jednak skład materiałów ceramicznych najczęściej powoduje powstawanie ładunków ujemnych na powierzchni materiału, co sprzyja adhezji kationów z anolitu i zmniejsza szybkość przenoszenia protonów. Dodatkowo porowata struktura membran ceramicznych sprzyja przenikaniu substratu i tlenu pomiędzy komorami. Dlatego ograniczenie skutków chemicznego i biologicznego zanieczyszczenia membran wymaga zwiększenia hydrofilowości, zmniejszenia chropowatości membrany lub domieszkowanie biocydami. Stosunkowo nową strategią poprawy wydajności i stabilności membran ceramicznych w MFC jest zastosowanie powłoki polimerowej o zwiększonej odporności na zanieczyszczenia. Membrana z nanowłókien PVDF może być dobrym komponentem kompozytowej membrany ceramicznej, ze względu na wysoką powierzchnię właściwą, ekstremalnie porowatą strukturę i wąski rozmiar porów. Ponadto wytwarzanie tego materiału techniką elektroprzędzenia pozwala kontrolować morfologię powierzchni nanowłókien, a wytworzony materiał jest łatwy do funkcjonalizacji.

W artykule przedstawiono nowatorską kompozytową membranę ceramiczną z powłoką z nanowłókien PVDF. Dodatkowo po raz pierwszy zastosowano modyfikację membrany ramnolipidami w celu zwiększenia wydajności MFC oraz wyjaśniono w jaki sposób interakcje molekularne między cząsteczkami ramnolipidu i modyfikowanej i niemodyfikowanej membrany z nanowłókien PVDF mogły wpłynąć na obserwowaną wydajność mocy.

W badaniu wykorzystano jednokomorowe MFC z katodą powietrzną skonstruowane z elementów wyciętych laserowo z arkuszy PMMA o grubości 3 mm. Jako wewnętrzną warstwę kompozytowej membrany ceramicznej zbadano membranę z nanowłókien PVDF wytworzoną technika elektroprzędzenia, a także PVDF o modyfikowanej powierzchni metodą obróbki alkalicznej (PVDF-OH), obróbki ramnolipidami (PVDF/BS) i kombinacji obu podejść (PVDF-OH/BS). Korzystając z charakterystyki elektrochemicznej, fizykochemicznej i powierzchniowej, oceniono skuteczność modyfikacji oraz zbadano długoterminową eksploatację kompozytowych membran ceramicznych.

Membrana wyjściowa z nanowłókien PVDF i po obróbce alkalicznej (PVDF-OH) wykazały najwyższe właściwości hydrofobowe, które były stabilne w czasie, podczas gdy najbardziej hydrofilowe właściwości wykazała membrana modyfikowana dwustopniowo (PVDF-OH/BS). Tym samym największą zmianę właściwości powierzchniowych uzyskano modyfikując membranę za pomocą obróbki alkalicznej i biosurfaktantami, natomiast modyfikacja biosurfaktantami bez wcześniejszej obróbki -OH ujawniła umiarkowane zmiany właściwości powierzchniowych membrany. W rezultacie zastosowanie warstwy PVDF jako komponentu membrany ceramicznej w MFC nie dało zadowalających efektów. Charakterystyka elektrochemiczna i powierzchniowa ujawniła największą podatność na zanieczyszczenia biologiczne i chemiczne dla membrany Ceramic+PVDF. Membrana PVDF modyfikowana grupami -OH zwiększyła maksymalną moc MFC, jednak jej właściwości długoterminowe okazały się najsłabsze w całym zestawieniu. Natomiast modyfikacja nanowłókien PVDF biosurfaktantami (Ceramic+PVDF/BS i Ceramic+PVDF-OH/BS) znacząco poprawiła hydrofilowość membran, tworząc warstwę półprzepuszczalną o właściwościach przeciwbiofoulingowych. Najwyższą w badaniu gęstość mocy oraz najlepsze właściwości przeciwbiofoulingowe uzyskało MFC wyposażone w membranę kompozytową Ceramic+PVDF-OH/BS.

Uzyskane wyniki udowodniły, że naturalnie wytwarzane ramnolipidy mogą oddziaływać z membranami polimerowymi w MFC. Zastosowana modyfikacja komponentu polimerowego kompozytowej membrany ceramicznej za pomocą biosurfaktantów ograniczyła negatywne skutki biofoulingu i tym samym poprawiła długoterminową wydajność energetyczną i trwałość membran. W badaniu po raz pierwszy wykazano, że zrównoważone produkty ekologiczne, takie jak biosurfaktanty, mogą stanowić metodę modyfikacji membran MFC i po raz pierwszy ujawniono mechanizmy interakcji biosurfaktantów z membranami.

5.4.2. Publikacja

Journal of Power Sources 621 (2024) 235257

Contents lists available at ScienceDirect

Journal of Power Sources

journal homepage: www.elsevier.com/locate/jpowsour

Enhancing performance and durability of PVDF-ceramic composite membranes in microbial fuel cells using natural rhamnolipids

Aleksander de Rosset [a], Fatma Yalcinkaya [b], Joanna Wolska [a], Stanisław Wacławek [b], Grzegorz Pasternak [a,*]

[a] Department of Process Engineering and Technology of Polymer and Carbon Materials, Faculty of Chemistry, Wroclaw University of Science and Technology, Wroclaw, 50-370, Poland
[b] Centre for Nanomaterials, Advanced Technology and Innovation, Technical University of Liberec, Studentska 1402/2, 46117, Czech Republic

HIGHLIGHTS

- The first use of biosurfactants for the modification of MFC membranes.
- Rhamnolipid-modified PVDF improved long-term performance of ceramic membranes.
- The PVDF layer limited the access of microorganisms to the ceramic element.
- Insights into the molecular mechanisms of biosurfactants interaction with membranes.
- Good long-term durability of the membrane related to the limited fouling effects.

GRAPHICAL ABSTRACT

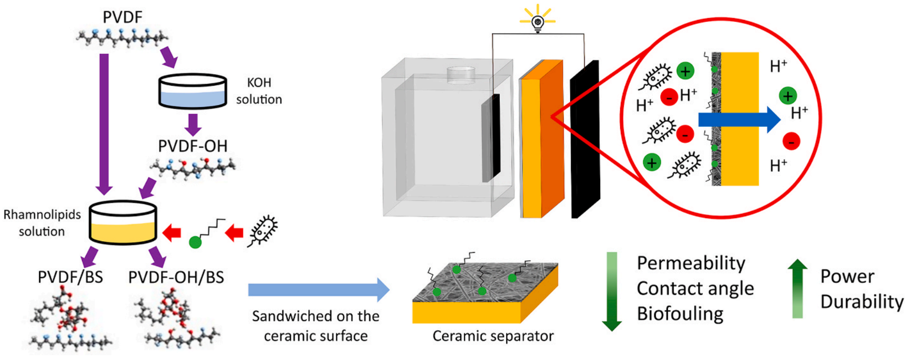

ARTICLE INFO

Keywords:
MFC
Ceramic
PVDF
Composite
Biofouling

ABSTRACT

Ceramic membranes are widely used in microbial fuel cells (MFCs) owing to their cost-effectiveness and availability. However, these membranes often face challenges such as biofouling and negative mass-transfer effects. This study explored the use of a polymer layer to mitigate these issues, focusing on a polyvinylidene fluoride (PVDF) nanofibre membrane with various surface modifications. The modifications included alkaline treatment (PVDF-OH), rhamnolipids treatment (PVDF/BS), and a combination of both (PVDF-OH/BS). The ceramic membrane integrated with PVDF-OH/BS achieved the highest power density of 13.8 W m^{-3}, which was 38 % higher than that of the unmodified ceramic membrane. Additionally, during the long-term study (days 90–101), the Ceramic + PVDF-OH/BS maintained a 64 % higher power performance compared to the unmodified ceramic membrane, indicating superior antifouling properties. Electrochemical and surface characterisation revealed that rhamnolipid-modified PVDF nanofibers enhanced fouling resistance. The findings demonstrate that natural biosurfactants which can be produced *in situ* within MFCs, can form a protective layer over membranes and significantly enhance their long-term power performance. This study represents the first instance of using natural microbial biosurfactants to improve membrane efficiency in a bioelectrochemical system.

---

[*] Corresponding author.
E-mail address: grzegorz.pasternak@pwr.edu.pl (G. Pasternak).

https://doi.org/10.1016/j.jpowsour.2024.235257
Received 23 January 2024; Received in revised form 9 August 2024; Accepted 13 August 2024

1. Introduction

Recent years have seen an increased interest in substituting fossil fuels with renewable energy sources. Microbial fuel cell (MFC) technology has emerged as a promising environmentally sustainable solution, effectively removing organic contaminants from wastewater while generating bioelectricity [1]. MFCs are sophisticated bioelectrochemical systems that utilise bacteria to oxidise organic matter, thereby producing electricity.

Despite significant advancements, commercialisation of the MFC technology remains challenging due to various technological, economic, electrochemical, and microbiological barriers that hinder scalability [2]. Typically, MFC designs feature an anode and cathode chamber separated by a proton-exchange membrane. These membranes are crucial for transporting hydrogen ions from the anolyte to the cathode while preventing substrate and oxygen crossover between the chambers [3]. Their role is vital for both efficient organic pollutant removal and electricity generation in MFC systems. Moreover, membranes can account for approximately half of the total MFC construction cost, especially when using standard cation exchange membranes (CEMs) such as Nafion or Ultrex [4]. CEMs are particularly vulnerable to chemical and biological fouling, which often necessitates membrane replacement or regeneration to restore efficiency [5]. Consequently, recent research has focused on the development and modification of new, durable, and cost-effective materials for MFC separators. Significant efforts have been made to create membranes from porous fabrics [6], polymers [7], ceramics [8], composites [9], and numerous modification approaches [10–12].

Ceramic separators are promising alternatives to expensive ion-exchange membranes because of their low production cost, good stability, high durability, and availability [13]. Given these advantages, many scaled-up studies on MFCs have employed ceramic membranes. For instance, Das et al. assessed the long-term efficiency of MFCs used for real wastewater treatment in a system with a total working volume of 720 L, utilising a ceramic separator [14]. However, the inherent composition of ceramic materials often results in the formation of negative charges on their surfaces, which can attract cations from the anolyte and decrease the proton transfer rate. Additionally, the porous nature of ceramic membranes can facilitate the unwanted penetration of substrate and oxygen between the chambers [15]. Therefore, modification approaches for ceramic membranes are desirable to achieve satisfactory performance and long-term operational stability.

To mitigate issues such as biofouling and chemical contamination, several strategies have been explored, including increasing hydrophilicity, reducing membrane roughness, and doping with biocides [5]. For example, hydrophilicity can be improved by incorporating graphene oxide (GO) into the ceramic matrix, resulting in an approximate 18 % increase in Coulombic efficiency [16]. In another study, ceramic membranes composed of barium, cerium, and gadolinium oxides doped with cobalt demonstrated enhanced biofouling resistance compared to Nafion 117 [8]. Despite these advancements, some of these materials may not be cost-effective for large-scale applications.

An effective strategy for enhancing the performance and stability of ceramic membranes in MFCs involves the application of a polymer coating to improve fouling resistance. Although there have been limited studies on polymer-ceramic composite membranes, recent advancements show promising results. For instance, Pasternak et al. utilised recycled polypropylene nonwoven fabric in a ceramic composite membrane, which resulted in a 92 % increase in power output from the MFC and a 600 % improvement in performance at the end of a long-term study period [17].

A relatively novel approach involves the use of a polyvinylidene fluoride (PVDF) nanofibres membranes [18]. Studies have demonstrated that MFCs equipped with composite membranes of PVDF nanofibres and Nafion exhibit higher power generation and Coulombic efficiency compared to those with pristine Nafion membranes [19]. Similarly, a composite membrane made from PVDF nanofibres and perfluorinated sulfuric acid ionomer (PFSA) showed superior power production compared to commercial Nafion membranes [20]. PVDF nanofibres offer significant advantages due to their high specific surface area, highly porous structure, and precise pore size control. Additionally, the electrospinning technique used to produce these nanofibres allows for controlled surface morphology and easy functionalisation [21,22].

Biosurfactants (BSFs) are surface-active compounds produced through microbiological processes. They exhibit properties similar to synthetic surfactants but are generally less toxic and more stable under extreme conditions of temperature, pH, and salinity [23]. In bioelectrochemical systems, BSFs can enhance efficiency by improving the bioavailability of hydrophobic substrates [24], increasing the hydrophilicity of electrode surfaces [25], influencing electron transfer mechanisms, and inducing biofilm formation and stability [26].

Herein, we present a novel composite ceramic membrane incorporating PVDF nanofibres. Furthermore, this is the first instance of membrane modification with rhamnolipids aimed at enhancing MFC performance. A PVDF nanofibers membrane produced by electrospinning technique, as well as surface modified PVDF by alkaline treatment, rhamnolipids treatment and a combination of both approaches were tested as the inner layer of the composite ceramic membrane. The effectiveness of these modifications in terms of long-term operation in air-cathode microbial fuel cells was assessed using electrochemical characteristic. Furthermore, physicochemical, and surface characterisations revealed the mechanism of changes in membrane stability under the influence of the applied modifications. Additionally, we explored how the molecular interactions between rhamnolipids and PVDF, both modified and unmodified, may have influenced the observed power performance.

2. Materials and methods

2.1. Preparation and modification of PVDF nanofiber membranes

Polyvinylidene fluoride (PVDF) nanofibre membranes were prepared using an NS 1S500U Nanospider machine (Elmarco, Liberec, Czech Republic) as previously reported [27]. The nanofibers density was measured to be 3 g m^{-2}, with each layer having a thickness of 0.28 mm. To enhance the mechanical properties of the PVDF nanofibers, the nanofiber web was laminated with an additional 100 g m^{-2} polyethylene terephthalate nonwoven support (from Mogul Nonwovens, Gaziantep, Turkey) for 3 min at 130 °C and 75 kN pressure. The surface of the PVDF membrane was chemically modified through alkaline treatment as described previously [28]. A 10 % (w/v) KOH solution in isopropyl alcohol was prepared at 50 °C and then cooled to room temperature. The PVDF membranes were immersed in this alkaline solution for 15 min. After treatment, the membranes were rinsed with Milli-Q water and subsequently soaked in a solution containing 0.5 g of rhamnolipids (AGAE Technologies) in 100 mL of Milli-Q water for 1 h. The modified membranes were then washed three times with distilled water to remove any excess solvent and allowed to air dry.

2.2. Preparation of ceramic separators

Ceramic separators were prepared from white clay (Goerg & Schneider no. 468, Siershahn, Germany) as previously described [17]. The clay was manually pressed into a mould and sintered at 1000 °C for 90 min, with a heating rate of 4 °C min^{-1}. The membranes were produced with dimensions of 4 cm × 4 cm and a thickness of 3.5 mm. Composite membranes were created by assembling a PVDF nanofibrous membrane with a ceramic membrane in a sandwich configuration. The active area of the MFC membranes was 12.25 cm^2.

2.3. Microbial fuel cell construction and operation

In this study, a single-chamber air-cathode microbial fuel cell (MFC) was employed. The MFC design featured laser-cut components from 3 mm-thick PMMA sheets, with a working volume of 26 cm^3. The anode, with a geometric area of 9 cm^2, was constructed from a carbon veil (PRF Composite Materials, Dorset, UK) and connected to the external circuit via a 316LSi steel wire. The cathode comprised activated carbon CWZ-22, with specific surface area of 972 $m^2\ g^{-1}$, according to a previous study [29]. The cathode material was pressed into the cathode module, with a stainless-steel mesh incorporated as a current collector. Additionally, a carbon veil was placed on the air side of the cathode to serve as a diffusion and protective layer. The active surface area of the cathode was also 9 cm^2. The membranes prepared were used as separators between the anode and cathode chambers, with an anode-cathode distance of 9 mm. All experiments were conducted at 25 °C, starting with an external load (R_{ext}) of 2 kΩ. Subsequently, the optimal resistance (R_{int}) was calculated, and R_{ext} was adjusted to match it after each polarisation experiment [30].

The MFCs were inoculated with a mixture of two activated sludges from the wastewater treatment plant (Kudowa, Ścinawka, Poland). After 2 days of inoculation, the activated sludge was replaced with a mineral salt medium (MSM/acetate) with the following composition (g L^{-1}): NH_4Cl (Chempur, Poland) 1.5, Na_2HPO_4 (POCH, Poland) 0.6, KCl (POCH, Poland) 0.1, $NaHCO_3$ (Chempur, Poland) 2.5, a trace element solution of 10 ml L^{-1} and $CH_3COOH{\cdot}3H_2O$ (Chempur, Poland) 0.82. The feed solution (MSM/acetate) was changed daily throughout the entire experiment (HRT = 23.3 ± 3.7 h). The pH of the medium was maintained at 8.5. All solutions were prepared with Milli-Q water and autoclaved prior to use (121 °C, 20 min).

2.4. Electrochemical experiments

Real-time data acquisition was conducted using a KEYSIGHT DAQ970A system (Keysight Technologies, USA) with a 3-min interval. Electrochemical characteristics were assessed with a MultiPalmSens4 potentiostat (Palmsens BV, Netherlands). Linear sweep voltammetry (LSV) measurements were performed using a three-electrode setup: the anode served as the working electrode (WE), the cathode acted as the counter electrode, and a saturated Ag/AgCl electrode was used as the reference electrode, placed in the anode chamber. Power and polarisation curves were recorded over a potential range from the open-circuit potential to 0.0 V WE vs Ag/AgCl at a scan rate of 1 mV s^{-1}.

Electrochemical impedance spectroscopy (EIS) experiments were conducted in a two-electrode configuration, with the anode acting as the working electrode and the cathode as both the counter and reference electrodes. An alternating current (AC) with an amplitude of 10 mV was applied over a frequency range of 100 kHz to 10 mHz. All EIS spectra were recorded in open-circuit voltage (OCV) mode and analysed using EC-Lab V10.40 software.

2.5. Chemical oxygen demand and coulombic efficiency

The chemical oxygen demand (COD) was measured using the potassium dichromate oxidation method, following the manufacturer's instructions (Hach, USA). COD values were determined for the fresh medium and for the anolyte collected at the end of the feeding batch cycle. COD removal efficiency was calculated as the ratio of the reduction in anolyte COD during MFC operation to the COD of the fresh medium.

Coulombic Efficiency (CE) was determined according to the following formula:

$$\mathrm{CE} = \frac{\mathrm{M}\int_0^t \mathrm{I\,dt}}{\mathrm{FbV_{An}\Delta COD}},$$

where M – molecular weight of carbon substrate (g mol^{-1}); I – current (A); t – time of operation (s); F – Faraday's constant (96500 C/mol e^-); b – number of electrons exchanges per mole of oxygen; V_{An} – working volume of the anode chamber (L); Δ*COD* – change in COD concentration (mg L^{-1}).

2.6. Physicochemical measurements

2.6.1. Conductivity and pH

An IONODE IJ44A electrode (ELMETRON, Poland) was used to monitor the solution pH. The conductivity of MSM was measured using an ELMETRON ECF-1 conductivity sensor.

2.6.2. Contact angle

The hydrophilicity of the membranes was determined by measuring the dynamic contact angle of deionised water using a PG-X goniometer (Fibro Systems). At least three membrane sections from different areas were analysed to ensure accuracy.

In addition to the contact angle measurements, the water spreading area (WSA) was evaluated to examine the membrane's wettability. For the WSA analysis, a single drop of distilled water (20 μL) was carefully placed on the membrane surface. Subsequently, the resulting spreading area image was quantified using ImageJ software.

2.6.3. Fourier-transform infrared spectroscopy (FT-IR)

To characterise the functionalisation of PVDF nanofibers, middle infrared (4000–400 cm^{-1}) spectra were obtained using a Fourier-transform infrared spectrometer (Jasco FT/IR-4700). The sample was placed on the diamond crystal of an attenuated total reflectance device. Spectral data were recorded at a resolution of 4 cm^{-1} by performing 64 scans. The collected data were analysed using Jasco Spectra Manager software.

2.6.4. Biosurfactants release tests

To evaluate the binding strength of rhamnolipids to the membrane surface, biosurfactant release tests were conducted on the two modified membranes, PVDF/BS and PVDF-OH/BS. The membranes, previously modified with biosurfactants, were immersed in Milli-Q water at 25 °C. Water samples were collected at specific time intervals to measure surface tension using a mobile bubble pressure tensiometer (KRUSS, Germany) and were analysed using a spectrophotometer (Unicam Helios Alpha, USA).

2.7. Evaluation of cathodic biofouling

Cathodic biofouling, which is often linked to electro-osmotic drag and indicates high power efficiency in MFCs, was evaluated by measuring the number of colony-forming units (CFUs) after the experimental period. Samples of activated carbon (0.2 g) were collected, plated on LB growth agar, and incubated for 72 h at 25 °C. The number of microbial colonies was then counted. Additionally, the dry weights of the cathode samples were measured to determine the number of bacteria per gram of dry weight.

2.8. Scanning electron microscopy

The membrane morphology was examined using a scanning electron microscope (SEM; TESCAN VEGA 3). Both pristine membranes and those used in MFC were prepared following the method described by Szydlowski et al. [31]. First, the samples were immersed for 12 h in a 2.5 % glutaraldehyde solution in 0.1 M phosphate-buffered saline (PBS). After washing three times with 0.1 M PBS, the samples were dehydrated using an increasing gradient of ethanol in water. Subsequently, the samples were immersed in pure hexamethyldisilazane (HMDS) and air-dried for 10 min. Finally, the samples were dried at 50 °C overnight prior to analysis.

2.9. Data processing

The experimental data were calculated and graphically visualised using OriginLab 2019. The current, power, and internal resistance were calculated according to Ohm's law.

$$R = \frac{U}{I}\ (\Omega),$$

$$P = U \times I\ (W),$$

where U – voltage (V); I – current (A); P – power (W); R – resistance (Ω)

3. Results and discussion

3.1. Pristine membranes characterisation

3.1.1. FT-IR analysis

FTIR analysis was conducted to investigate the interactions between the membrane and the biosurfactant (Fig. 1a).

All materials exhibited characteristic C–H stretching vibrations at ~ 2850 and 2950 cm^{-1}. A slight shift in these bands was observed in the modified PVDF-OH, indicating a change in the environment of the $–CH_2$ functional groups.

PVDF-OH showed a small peak at 3430 cm^{-1}, corresponding to O–H stretching, and another peak at 1713 cm^{-1} (C=O), confirming the hydroxylation of PVDF to PVDF-OH, consistent with previous studies [36]. In addition, a new, small peak at ~ 1600 cm^{-1} was observed attributed to the formation of a double bond in the PVDF-OH structure [37]. However, the intensity of this bond was low due to the minimal activity of C=C bonds in the infrared region. Furthermore, in the fingerprint region, changes in the C–F groups were noted between 1250 and 1000 cm^{-1}, aligning with literature reports [37].

The biosurfactants adsorbed on PVDF and PVDF-OH (denoted as PVDF|||biosurfactant and PVDF-OH|||biosurfactant, respectively) exhibit similar group frequency regions, with some notable differences. Broad bands in the 3800–3400 cm^{-1} range likely correspond to –OH stretching vibrations. These bands are slightly redshifted in PVDF-OH and show a significant increase in intensity. Concurrently, there is a notable decrease in the intensity of the band representing C=O stretching at 1711 cm^{-1}. This observation confirms the presence of an intermolecular hydrogen bonding network between the hydroxyl, carbonyl, and carboxylic functionalities of PVDF-OH and the

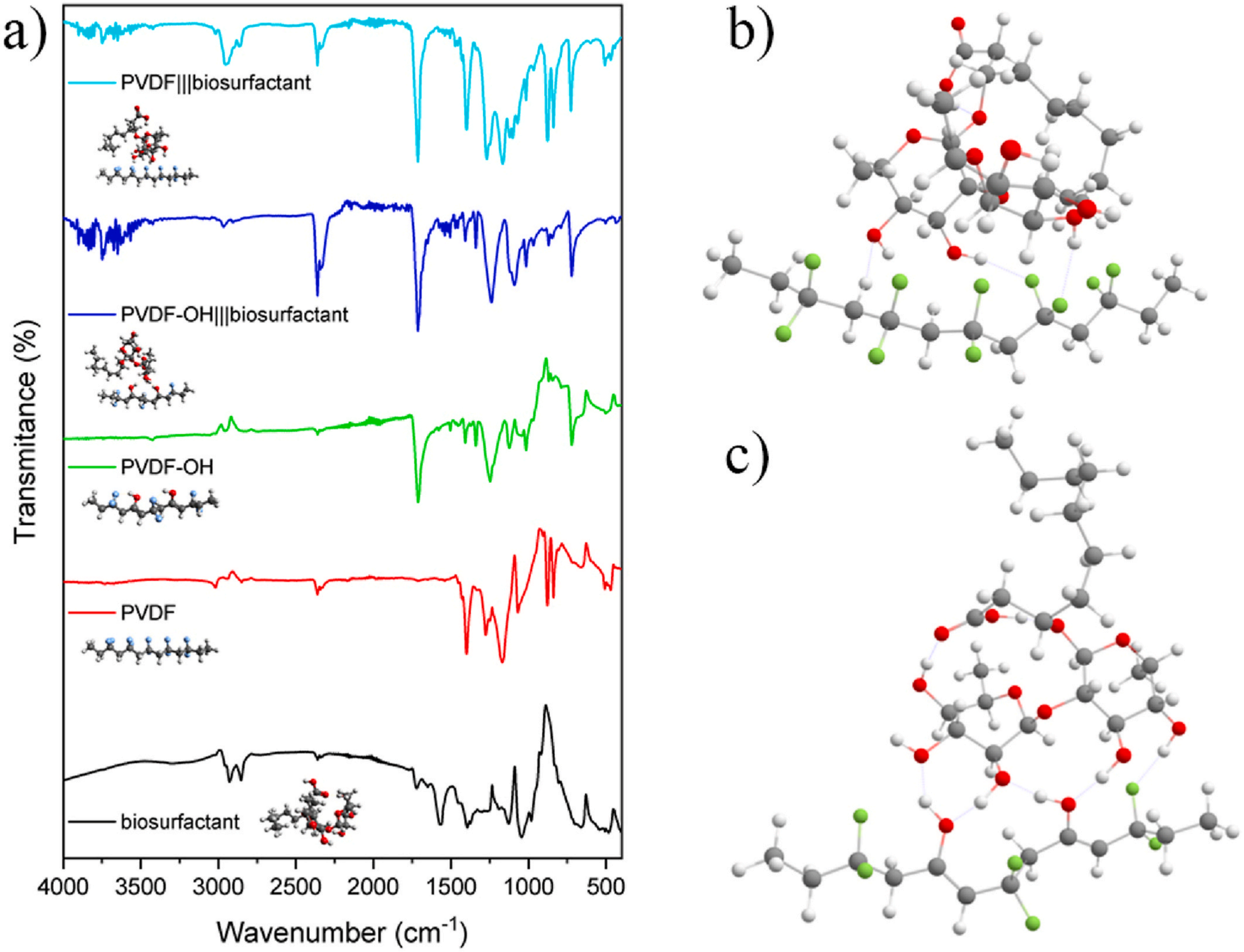

Fig. 1. a) FTIR spectra of rhamnolipids, PVDF, PVDF-OH, PVDF-OH with adsorbed biosurfactant and PVDF with adsorbed biosurfactant, b) ground state model of PVDF with adsorbed biosurfactant with visible O–H⋯F and C–H⋯O interactions and c) ground state model of PVDF-OH with adsorbed biosurfactant with visible hydrogen bonding interactions (all computations were performed in Gaussian16 [32] with functional/basis set: B3LYP/3-21G; Multiwfn software [33] was used for the elaboration of data; visualisations were made in Avogadro [34] and ChemCraft [35] and atoms are coloured: black – carbon, white – hydrogen, red – oxygen, green/blue – fluorine; double bonds were omitted). (For interpretation of the references to colour in this figure legend, the reader is referred to the Web version of this article.)

biosurfactant. This hydrogen-bonding network is further illustrated in a model studied using density functional theory (DFT; Fig. 1b and c). The interactions between PVDF-OH|||biosurfactant are visibly stronger compared to PVDF|||biosurfactant (O–H···O distance: ∼ 1.4 Å compared to O–H···F distance: ∼ 1.9 Å). The hydroxylated PVDF and biosurfactants exhibit mutually complementary and interacting binding sites, which enhances the interactions between PVDF-OH and the biosurfactant and facilitates electron transfer between the two species [38].

3.1.2. Contact angle and biosurfactants release measurements

Significant differences in contact angles were observed among the various membrane types (Fig. 2c). The pure PVDF nanofibers membrane and the alkali-treated sample (PVDF-OH) exhibited the highest hydrophobic properties, which remained stable over time. In contrast, the two-stage modified membrane (PVDF-OH/BS) demonstrated the most hydrophilic properties and displayed the most dynamic contact angle characteristics. The greatest change in surface properties was achieved by combining alkaline treatment with biosurfactant attachment. Modification with biosurfactant alone, without the –OH treatment, led to only moderate changes in membrane surface properties.

To assess the stability of the surface modification and the potential release of biosurfactants into the anolyte, PVDF/BS and PVDF-OH/BS membranes were immersed in Milli-Q water for 16 h. Fig. 2a shows the results of surface tension and UV absorption (225 nm) measurements over time. For PVDF/BS, no significant changes were observed, suggesting minimal release of biosurfactants. However, for PVDF-OH/BS, a slight decrease in surface tension and an increase in UV absorption were noted, indicating some biosurfactant release into the solution. The biosurfactants were then re-adsorbed onto the membrane, as reflected by the changes in surface tension and absorbance. This suggests that the biosurfactants on the –OH–modified nanofibers membrane can dynamically interact with other components of the MFC environment. Such interactions improve the bioavailability of substrates and enhance the hydrophilicity of the electrode surface, leading to better biofilm formation [25,39]. Even small amounts of released biosurfactants may improve the initial stage of biofilm development (Fig. 4). This observation is consistent with the electrochemical impedance spectroscopy results, where the lowest anode impedance was recorded on day 31 of operation for the Ceramic + PVDF-OH/BS membrane (Fig. 6). Additionally, the intensity of the peaks corresponding to rhamnolipids (Fig. 1a) was more pronounced in PVDF-OH/BS, suggesting higher accumulation of these compounds, likely due to stronger binding of some molecules.

Table 1 presents the water spreading area (WSA) values for each sample. The WSA analysis indicates that droplets on both PVDF and PVDF-OH membranes had reduced WSA values, meaning the droplets did not penetrate the membrane, as shown in Fig. S1. This observation aligns with the contact angle analysis results. Conversely, the membranes modified with biosurfactants (BS) exhibited excellent drop penetration. When droplets were applied to these surfaces, they spread rapidly and wetted the membranes, demonstrating that the hydrophilic properties of the BS enhanced the overall water contact angle of the membranes. Among the samples, the –OH– and BS-modified membrane exhibited the best water-spreading and drop-penetration properties.

3.2. Membranes and electrodes after MFC treatment

3.2.1. Cathode fouling and biofouling

The number of living bacteria was assessed using the colony-forming unit (CFU) technique to characterise cathode biofouling. The results indicated that all tested membranes displayed varying degrees of susceptibility to biological contamination of the cathode (Fig. 2b). The Ceramic + PVDF membrane exhibited the lowest level of cathode biofouling, consistent with the low power densities observed in this study (Fig. 4). In contrast, the Ceramic + PVDF-OH membrane showed fewer CFU than the biosurfactant (BS)-modified membranes, but had the lowest long-term power durability among the tested membranes. The highest levels of cathodic biofouling were detected for Ceramic + PVDF/BS and Ceramic + PVDF-OH/BS membranes. This observation aligns with previous study conducted by Pasternak et al. [40], which demonstrated that cathodic biofouling directly correlates with ceramic MFC performance. Similarly, our earlier research indicated that the amount of salt accumulation at the cathode was related to the MFC's long-term performance [29]. The high number of microorganisms on the cathode

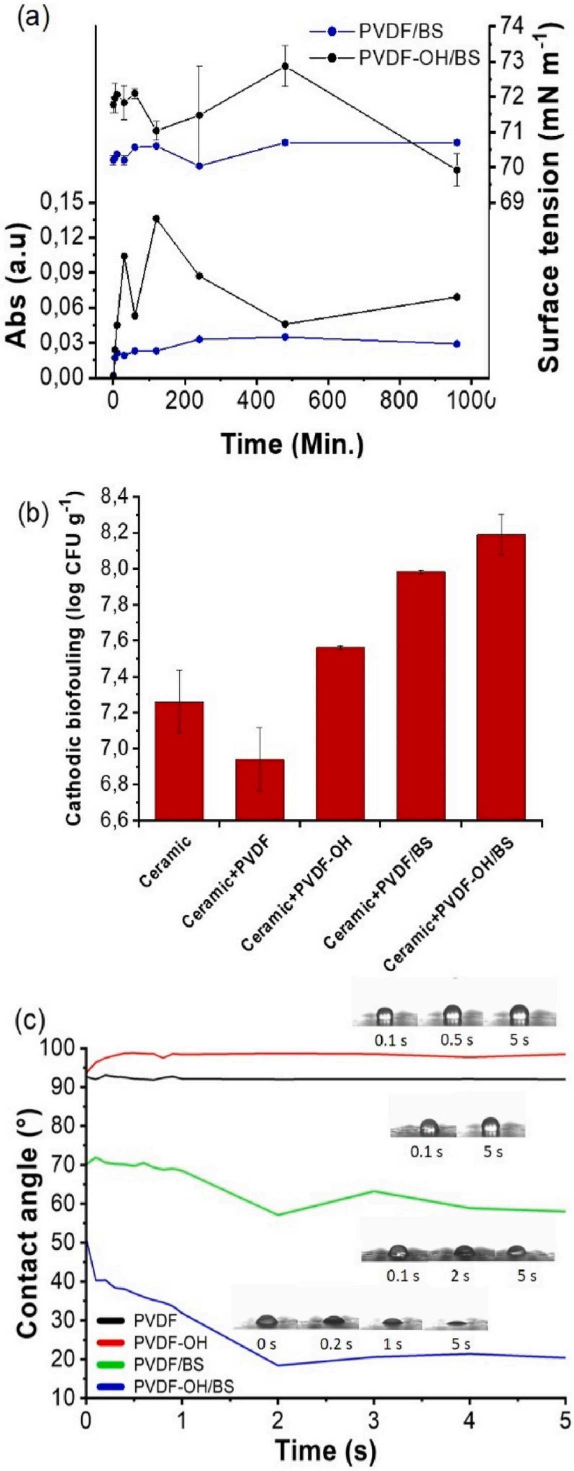

Fig. 2. Results of: (a) Biosurfactants release analysis, (b) cathodic biofouling measurements, and (c) dynamic contact angle of the investigated membrane materials.

Table 1
WSA of modified and unmodified separators.

Sample	Area of spreading in cm^2
Ceramics	0.682
PVDF	0.075
PVDF-OH	0.073
PVDF/BS	1.192
PVDF-OH/BS	3.823

electrode likely resulted from prolonged stable power generation and increased organic and inorganic compound crossover, attributed to electroosmotic drag [40,41]. The relatively low CFU count and high-power stability observed for Ceramic could be due to their diminished performance towards the end of the experiment when these data were collected.

3.2.2. *Scanning electron microscopy*

After the experimental period, the MFCs were disassembled, and the membranes were retained for surface imaging using scanning electron microscopy (SEM) (Fig. 3). All membranes displayed signs of chemical and biological fouling, although the extent varied. The control ceramic membrane exhibited a smoother surface compared to the pristine (unused) ceramic, indicating significant coverage with extracellular polymer substances (biofilm EPS) as a form of chemical fouling [17]. In contrast, the surfaces of the ceramic components in the composite membranes resembled those of the pristine ceramic, suggesting that the PVDF layer acts as a semipermeable barrier to microorganisms. This barrier limits their access to the ceramic component and improves the durability of the MFC system. SEM micrographs revealed that the ceramic component of Ceramic + PVDF was most affected by biofouling, while the lowest contamination was observed for Ceramic + PVDF/BS and Ceramic + PVDF-OH/BS. Among the PVDF components, the lowest biological contamination was recorded for Ceramic + PVDF/BS, where

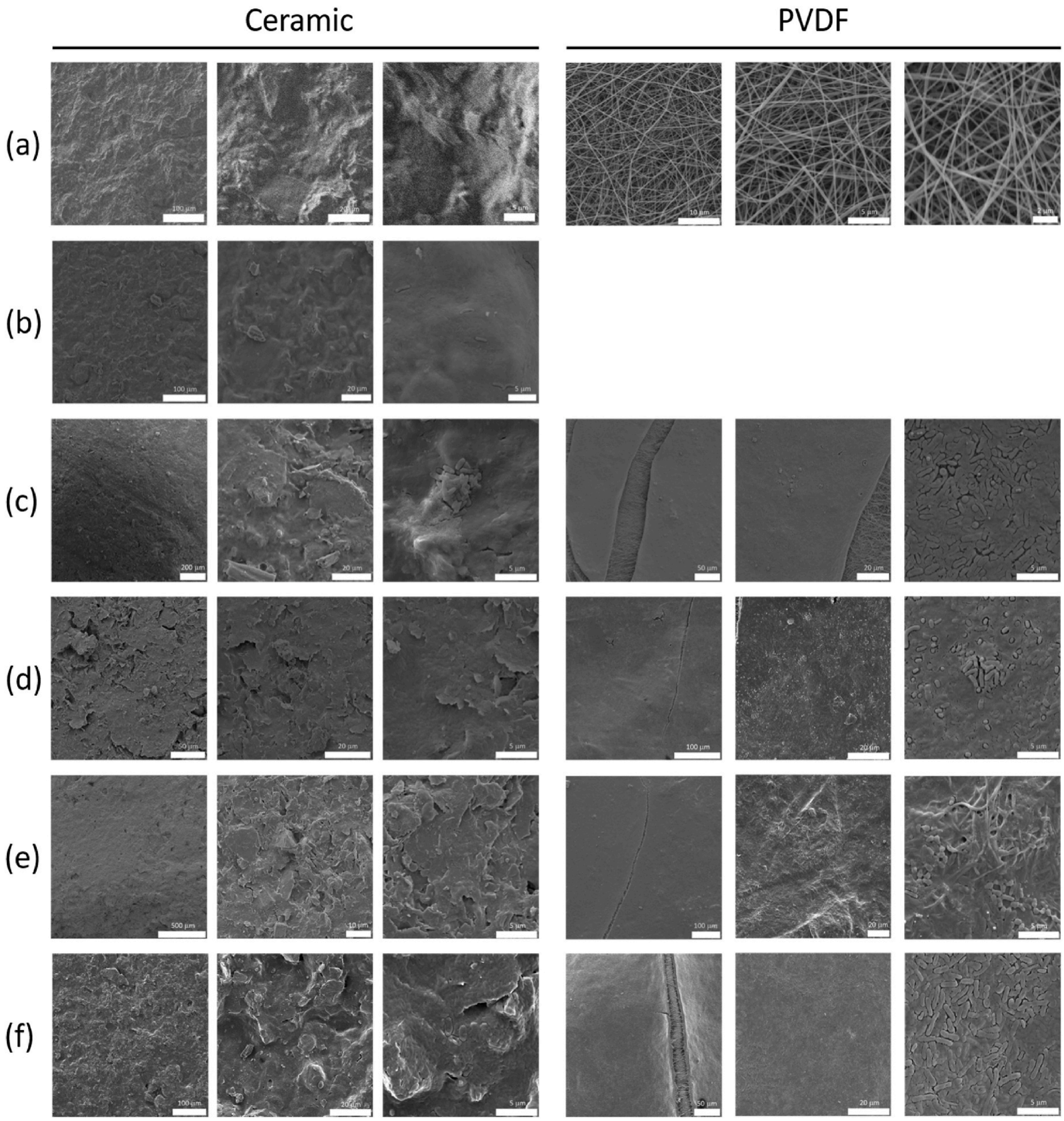

Fig. 3. (a) SEM micrographs of pristine membranes, as well as membranes after 101 days of operation, marked as: (b) Ceramic, (c) Ceramic + PVDF, (d) Ceramic + PVDF-OH, (e) Ceramic + PVDF/BS and (f) Ceramic + PVDF-OH/BS.

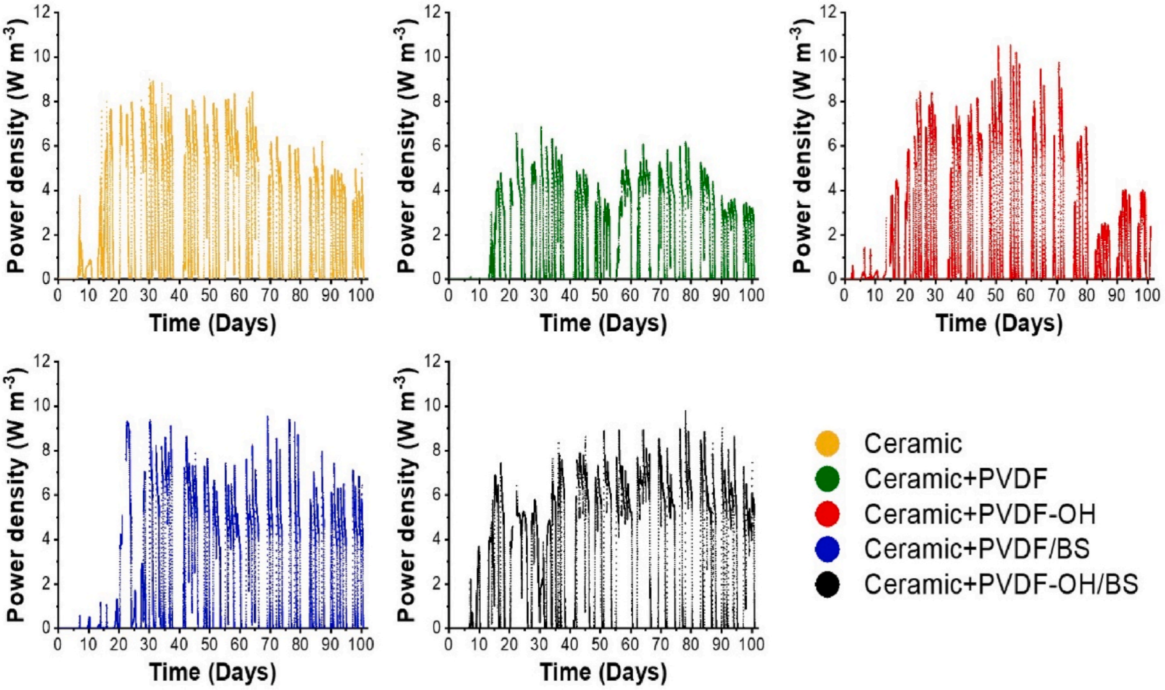

Fig. 4. Real-time monitoring of power performance.

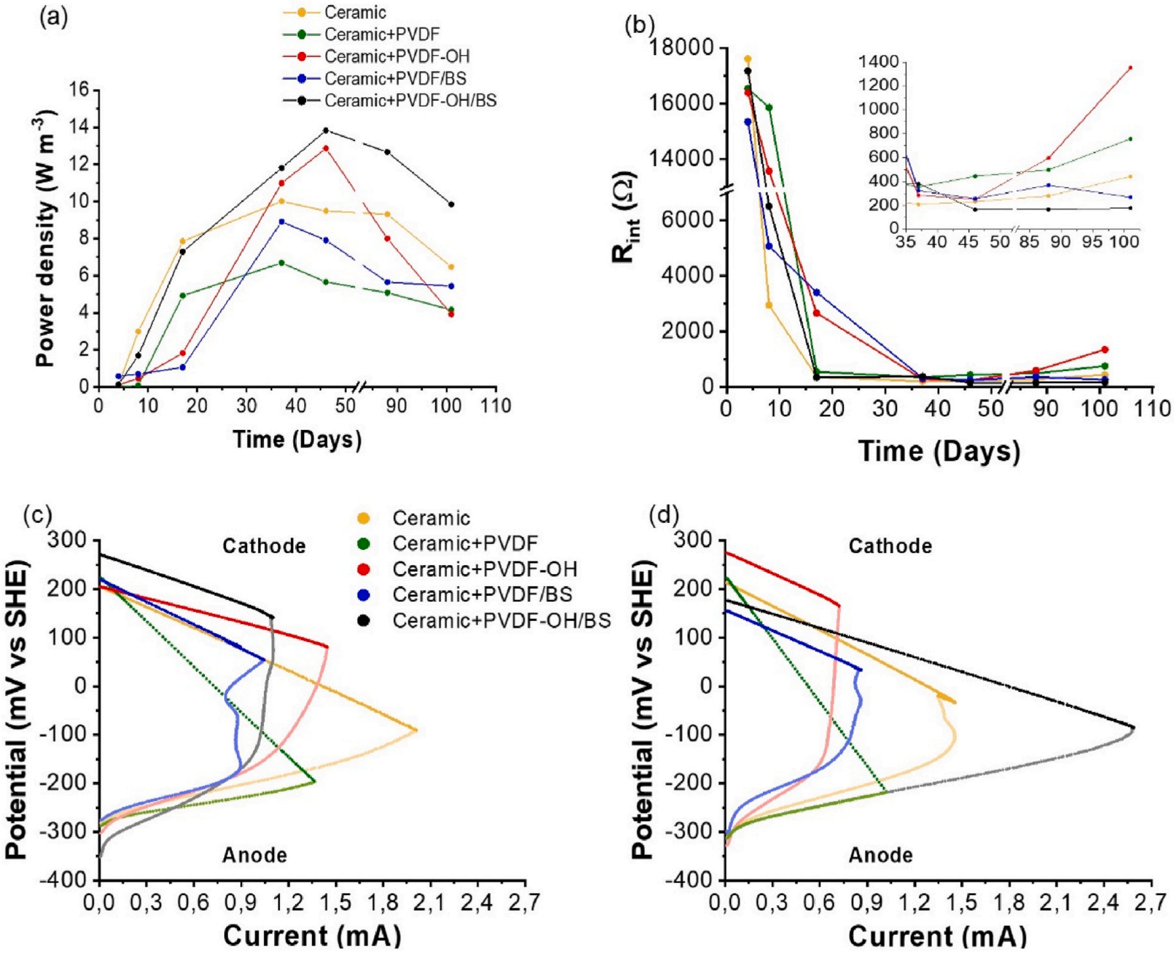

Fig. 5. (a) Changes in power density and (b) internal resistance as a function of operation time. Polarisation curves for: (c) 37th and (d) 88th day of operation.

the original nanofiber layer was visible beneath the biofilm. The remaining PVDF components exhibited a similar morphology of the biofilm on their surfaces. Hydrophilic separators tend to be less susceptible to biofouling due to reduced interactions between microorganisms and the separator surface [5]. The reduced biological contamination observed on the ceramic components of Ceramic + PVDF/BS and Ceramic + PVDF-OH/BS is likely due to the enhanced hydrophilicity of the PVDF membranes modified with biosurfactants (Fig. 2c). However, it is important to note that the membranes were collected for SEM analysis during a period when the energetic effects of biofouling were apparent in all MFCs (Figs. 4 and 5a). The PVDF and its rhamnolipids modifications create a semipermeable layer over the ceramic element, reducing microorganism access. Therefore, modifying PVDF with biosurfactants plays a crucial role in the long-term performance of ceramic composite membranes.

3.3. *Electrochemical monitoring*

3.3.1. *Real-time temporal performance*

The power densities of MFCs equipped with four different ceramic composite membranes and a control ceramic membrane were monitored in real time over 101 days of operation. The results are shown in Fig. 4. During the first 10 days, the highest increase in power was observed for Ceramic + PVDF-OH/BS. However, from day 15 onwards, a significant increase in power was recorded for all MFCs. This initial stage of operation, characterised by biofilm maturation, often limits MFC efficiency [30]. Previous studies indicated that biosurfactants significantly influence biofilm development [26]. Therefore, the highest increase in power density during this period for Ceramic + PVDF-OH/BS can be attributed to the small amount of biosurfactants released into the anolyte, as shown by the biosurfactant release analysis (Fig. 2a). On day 32, the maximum power densities for Ceramic and Ceramic + PVDF were achieved at 8.9 W m^{-3} and 6.8 W m^{-3}, respectively, while the power density for the other MFCs continued to rise. The power density obtained for the control ceramic membrane was comparable to that reported in our previous study [17]. Furthermore, this value was within the range of power densities obtained for other ceramic materials [42–44]. Nevertheless, only a short period of stable power output was observed for Ceramic, followed by a rapid drop in performance. On day 55, Ceramic + PVDF-OH reached its peak power density of 10.5 W m^{-3}, but soon after, a sharp decrease in power was noted. The low long-term stability of Ceramic and Ceramic + PVDF-OH was attributed to high membrane biofouling, as confirmed by SEM micrographs (Fig. 3). The maximum power densities for Ceramic + PVDF/BS (9.5 W m^{-3}) and Ceramic + PVDF-OH/BS (9.8 W m^{-3}) were achieved on days 70 and 79, respectively, with these modifications resulting in the smallest decrease in

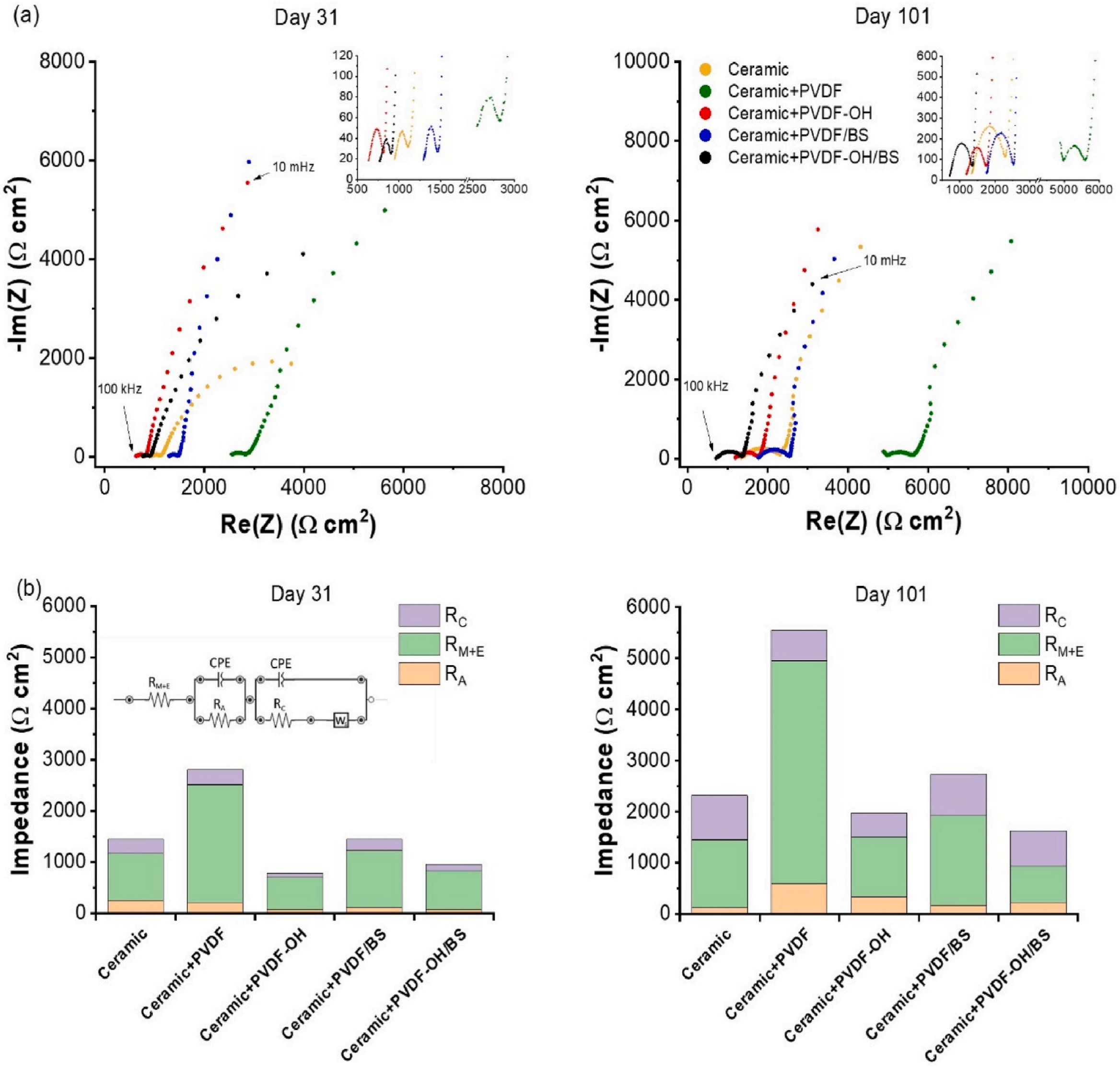

Fig. 6. (a) Nyquist plots and (b) EIS data analysis using the equivalent circuit model (ECM). The ECM is presented in the middle of plot (b).

generated power. The average of the maximum power densities of batch cycles during the last 10 days of the experiment for Ceramic + PVDF-OH/BS was equal to 7.39 ± 0.77 W m^{-3}, while for Ceramic, Ceramic + PVDF, Ceramic + PVDF-OH, and Ceramic + PVDF/BS, the value was lower by 39 %, 54 %, 55 % and 12 %, respectively. Previous studies highlight the critical role of membranes in establishing well-developed biofilms in MFCs [5]. Therefore, the superior performance stability of Ceramic + PVDF/BS and Ceramic + PVDF-OH/BS can be attributed to the enhanced antifouling properties of these modifications, as confirmed by contact angle measurements (Fig. 2c) and SEM images (Fig. 3). Despite Ceramic + PVDF-OH achieving the highest power output, its long-term stability was the lowest in this study, with the highest power stability recorded for Ceramic + PVDF-OH/BS.

3.3.2. *Long-term dynamic changes in MFC performance*

Polarisation experiments were conducted throughout the study to characterise changes in MFC performance and assess the impact of membrane modifications on MFC lifetime. Fig. 5a shows the maximum power densities obtained from LSV data. During the first 15 days, the highest increase in power density was observed for Ceramic and Ceramic + PVDF-OH/BS. After this period, the power density for Ceramic stabilised, while a continued increase was noted for Ceramic + PVDF-OH/BS. This rapid upward trend in power density for Ceramic + PVDF-OH/BS can be attributed to the efficient maturation of anodic biofilms, as observed in the real-time performance graph (Fig. 4). By day 37, the maximum power densities were recorded as 10 W m^{-3}, 6.7 W m^{-3} and 8.9 W m^{-3} for Ceramic, Ceramic + PVDF and Ceramic + PVDF/BS, respectively. On day 46, Ceramic + PVDF-OH and Ceramic + PVDF-OH/BS reached their peak power densities of 12.9 W m^{-3} and 13.8 W m^{-3}, respectively. The power density achieved by the best MFC in this study exceeded that obtained for other composite ceramic membranes under similar conditions [16,17,45]. In the subsequent period, all MFCs showed a decrease in power density, with the highest drop of 70 % recorded for Ceramic + PVDF-OH. The low performance stability of Ceramic + PVDF-OH was attributed to its high hydrophobicity (Fig. 2c) and consequently high membrane biofouling (Fig. 3). At the end of the experimental period (day 101), the power density for Ceramic + PVDF-OH/BS was 9.9 W m^{-3}, compared to lower values for Ceramic (34 % lower), Ceramic + PVDF (58 % lower), Ceramic + PVDF-OH (60 % lower), and Ceramic + PVDF/BS (45 % lower). The superior long-term stability of Ceramic + PVDF-OH/BS was due to its lower contact angle (Fig. 2c), indicating better antifouling properties and improved conductivity, as shown by FTIR analysis (Fig. 1). Therefore, PVDF modification with a biosurfactant significantly impacts the long-term operation of MFCs by ensuring excellent antifouling properties. A similar trend was observed in the changes in internal resistance (R_{int}) during operation (Fig. 5b). Initially, R_{int} for Ceramic, Ceramic + PVDF, and Ceramic + PVDF-OH/BS decreased at a similar rate, reaching comparable values by day 17, then stabilised. A slower decrease in R_{int} was observed for Ceramic + PVDF-OH and Ceramic + PVDF/BS, with stable R_{int} reached after 37 days of operation. The shortest stable R_{int} period was noted for Ceramic + PVDF-OH. The dynamic decrease in R_{int} early in operation resulted from biofilm development, which reduced electron transfer resistance and activation energy of the electrode reaction [46]. The average value of stable R_{int} for Ceramic + PVDF-OH/BS was 251.3 ± 97.4 Ω. While for Ceramic, Ceramic + PVDF, Ceramic + PVDF-OH, and Ceramic + PVDF/BS was higher by 53.1 %, 122.9 %, 240.7 % and 18.7 %, respectively. The operational stability of the MFC system is attributed to the long-term properties of the membrane, cathode, and biofilm [5,30,47]. Therefore, the lower stable R_{int} values was a result of the improved antifouling properties of the biosurfactant-modified membranes (Ceramic + PVDF-OH/BS and Ceramic + PVDF/BS), as indicated by the water spreading area test (Table 1).

The individual cathode and anode polarisation curves obtained on days 37 and 88 of operation are presented in Fig. 5c and d, respectively. On day 37, the open circuit potential of the anode (OCP_{anode}) for all MFCs reached similar values of approximately −286.9 ± 11.6 mV, except for Ceramic + PVDF-OH/BS, which had a more negative value of −351.5 mV. Subsequently, the OCP_{anode} evolved to a more negative for all MFCs, except Ceramic + PVDF-OH/BS. The evolution of the OCP_{anode} to a more positive could be attributed to excessive biofilm accumulation, which negatively impacted electron transfer resistance and substrate diffusion rate [48]. The open circuit potential of the cathode ($OCP_{cathode}$) was also similar across all MFCs, at approximately 212.7 ± 9.7 mV, except for Ceramic + PVDF-OH/BS. By day 88, a decrease in $OCP_{cathode}$ was observed for Ceramic + PVDF-OH/BS and Ceramic + PVDF/BS, whereas no significant changes were noted for Ceramic and Ceramic + PVDF. On day 88, Ceramic + PVDF-OH showed the highest $OCP_{cathode}$ value of 275.1 mV.

By analysing the polarisation curves from day 37 of operation, it was observed that the main component of the internal resistance (R_{int}) for Ceramic and Ceramic + PVDF was the ohmic resistance of the cathode (Fig. 5b), whereas for the other MFCs, performance was predominantly limited by anode concentration losses (Fig. 5c) [24,49]. On day 37, the maximum currents were 2.01 mA for Ceramic, 1.36 mA for Ceramic + PVDF, 1.45 mA for Ceramic + PVDF-OH, and 1.04 mA for Ceramic + PVDF/BS. By day 88, a decrease in the slope of the cathode polarisation curve was observed for Ceramic + PVDF/BS and Ceramic + PVDF-OH/BS (Fig. 5d). This change was likely due to the electroosmosis of inorganic salts from the anode chamber to the cathode, which can positively influence the performance of the CWZ-22 cathode, as demonstrated in our previous study [29]. For the remaining membranes, the increase in slope angle was attributed to chemical and biological fouling of the cathode [40], as well as membrane biofouling, which can decrease proton transfer and overall MFC performance [50]. An overshoot phenomenon observed in the Ceramic polarisation curves was likely caused by the blockage of pores in the activated carbon by diffusing ions, which restricted oxygen access to active sites and impeded electron flow [51]. Additionally, biofouling of the cathode and membrane further hindered proton transfer [5,17]. A significant decrease in activation, ohmic, and concentration losses was noted for Ceramic + PVDF-OH/BS, while an increase in these losses was observed for the remaining MFC types. The increase in anode losses may be due to the growth of a thick biofilm layer on the anode, which impedes substrate diffusion to deeper biofilm layers [48]. The maximum current for Ceramic + PVDF-OH/BS on day 88 was 2.58 mA.

3.3.3. *Electrochemical impedance spectroscopy*

The electrochemical impedance spectroscopy (EIS) data for the whole cell was fitted to an equivalent circuit model (ECM) as per the methodology described by Sekar and Ramasamy [52]. In this model, R_A represents the anode resistance, R_C represents the cathode resistance, and R_{M+E} represents the combined resistance of the membrane and electrolyte. The constant-phase element (CPE) models the capacitive behaviour of the electrical double layer [52], and a finite-length Warburg element (W_S) is used at the end of the ECM to account for diffusion effects [53]. The Nyquist plots from days 31 and 101 of operation are shown in Fig. 6a. Three semicircles observed in the EIS spectra allowed for the analysis of individual impedance components using the ECM (Fig. 6b) [17,54]. On day 31, the Ceramic + PVDF-OH exhibited the lowest sum of impedances and R_{M+E}, with values of 780.8 Ω cm^2 and 622.0 Ω cm^2, respectively. For Ceramic + PVDF-OH/BS, there was a 22 % higher sum of impedance and the lowest R_A observed. The impedances for Ceramic and Ceramic + PVDF/BS were similar during this period, though Ceramic + PVDF/BS showed a lower R_A. It is hypothesised that some biosurfactants bound to the membrane may have been released into the solution, aiding biofilm development on the anode and decreasing R_A [26]. The highest sum of impedances, primarily due to R_{M+E}, was recorded for Ceramic + PVDF. On day 101, the EIS results indicated an increase in the sum of impedances for all MFCs. However, significant differences were observed between the membrane types. Ceramic + PVDF-OH/BS exhibited the lowest R_{M+E} and overall sum of impedances, measured at 1625.2 Ω cm^2. For the other MFCs, impedances were 42 %, 241 %, 22 %, and 68 % higher for Ceramic, Ceramic + PVDF, Ceramic + PVDF-OH, and Ceramic + PVDF/BS, respectively. The increase in R_A was due to biofilm overgrowth, which restricts substrate diffusion to deeper biofilm layers and adversely impacts microbial activity [48]. However, the increase in R_C was associated with chemical contamination of the cathode caused by electroosmotic drag [48]. Notably, R_{M+E} for Ceramic + PVDF-OH/BS decreased by only 7 % over the 70-day period, whereas for the other membrane types, R_{M+E} increased by 45 %, 90 %, 90 %, and 58 % for Ceramic, Ceramic + PVDF, Ceramic + PVDF-OH, and Ceramic + PVDF/BS, respectively. The increase in R_{M+E} for these membranes was attributed to membrane fouling and biofouling, which negatively affected proton transfer resistance [55]. Therefore, the relatively small decrease in R_{M+E} for Ceramic + PVDF-OH/BS indicates its superior long-term condition, attributed to limited fouling effects, as corroborated by SEM micrographs (Fig. 3) and real-time MFC performance monitoring (Fig. 4).

3.4. *Coulombic efficiency and COD removal*

The COD removal ability and Coulombic Efficiency (CE) were determined after 31 days of operation to assess the substrate degradation efficiency (Table 2). The initial COD of the fresh mineral salt medium (MSM) with sodium acetate was 574 mg L^{-1}. After treatment, the COD values for all MFCs were similar, averaging 201.7 ± 17.2 mg L^{-1}. The highest COD removal rate was observed for Ceramic + PVDF-OH/BS, achieving a removal efficiency of 67.7 %. The CE values varied among the different membrane types, with Ceramic + PVDF/BS recording the highest CE at 58.7 %. This high CE was attributed to the longest duration of the batch cycle and the extended period of stable current for this MFC. The CE values for the Ceramic, Ceramic + PVDF, Ceramic + PVDF-OH, and Ceramic + PVDF-OH/BS were lower by 31 %, 30 %, 56 %, and 41 %, respectively. Notably, that COD removal and CE were assessed during the early phase of the study, before all MFCs reached their maximum performance. Nonetheless, these results reflect the overall power performance of the various membrane types during the initial maturation period of the MFC (Fig. 4). The high oxygen diffusion observed in ceramic membranes, combined with a large anode chamber volume, may lead to competitive metabolic pathways in the anolyte [44]. However, the obtained CE for Ceramic (Table 2.) was higher than those reported for other ceramic membranes in previous studies [56–58].

4. Conclusions

In this study, a two-step modification approach was employed to enhance the durability of ceramic membrane used in MFC. Initially, a polyvinylidene fluoride (PVDF) nanofibre membrane was applied for modification. Subsequently, the impact of rhamnolipid modification was evaluated. The results indicated that the application of a PVDF layer alone did not yield satisfactory outcomes. Electrochemical and surface characterisations revealed that the Ceramic + PVDF membrane exhibited the highest susceptibility to both biological and chemical fouling. However, the incorporation of biosurfactants into the PVDF nanofibers significantly improved the membranes' hydrophilicity. The modified membranes, Ceramic + PVDF/BS and Ceramic + PVDF-OH/BS, formed a semipermeable layer with enhanced antifouling properties. Among the membranes tested, the MFC equipped with the Ceramic + PVDF-OH/BS composite membrane achieved the highest power density of 13.8 W m^{-3}. Additionally, the average maximum power density of batch cycles for this MFC during the final 10 days of the experiment was 64 % higher than that of the control ceramic membrane. This study highlights the potential of using composite membranes as a promising approach for improving MFC performance. Notably, it demonstrates for the first time that naturally produced rhamnolipids can interact effectively with polymer membranes in MFCs. This interaction mitigates negative biofouling effects and enhances the long-term power performance and durability of the membranes. This study is the first to demonstrate the use of sustainable green products, such as biosurfactants, for modifying MFC membranes. Additionally, it is the first to unravel the mechanisms behind the interactions between biosurfactants and membranes.

CRediT authorship contribution statement

Aleksander de Rosset: Writing – original draft, Visualization, Methodology, Investigation, Formal analysis, Data curation. **Fatma Yalcinkaya:** Writing – original draft, Visualization, Methodology, Investigation, Formal analysis, Conceptualization. **Joanna Wolska:** Writing – original draft, Visualization, Investigation. **Stanisław Wacławek:** Writing – original draft, Visualization, Investigation, Formal analysis. **Grzegorz Pasternak:** Writing – review & editing, Supervision, Resources, Project administration, Methodology, Investigation, Funding acquisition, Formal analysis, Conceptualization.

Table 2
Comparison of the performance of ceramic membranes with membranes from this study.

		Volume	Operation time	Power density		Current density		R_{int}	CE	
Membrane type	Type of MFC	mL	Days	W m^{-3}	mW m^{-2}	A m^{-3}	A m^{-2}	Ω	%	Ref.
Ceramic	SCMFC	26	101	10.0	288.9	77.3	2.2	208	40.8[b]	This work
Ceramic + PVDF	SCMFC	26	101	6.7	193.6	52.3	1.5	354	41.4[b]	This work
Ceramic + PVDF-OH	SCMFC	26	101	12.9	372.7	55.8	1.6	252	25.5[b]	This work
Ceramic + PVDF/BS	SCMFC	26	101	8.9	257.1	40.0	1.2	256	58.7[b]	This work
Ceramic + PVDF-OH/BS	SCMFC	26	101	13.8	398.7	99.2	2.9	164	34.4[b]	This work
Ceramic coated with recycled polypropylene (PP80)	SCMFC	50	90	n.r.	81.0	~ 38.0[a]	n.r.	n.r.	11.6	[17]
Polymer derived ceramic doped with graphene oxide (GO)	DCMFC	140	45	7.2	n.r.	n.r.	~ 1.8[a]	123	28.8	[16]
Clayware	SCMFC	450	75	4.4	146.4	~ 70.0[a]	n.r.	23	10.6	[56]
Ceramic membrane modified with rice husk ash	DCMFC	2480	60	2.1	80.2	n.r.	0.4	n.r.	2.0	[59]

SCMFC – single chamber MFC; DCMFC – dual chamber MFC; CE – Coulombic efficiency; R_{int} – internal resistance; n.r. – not reported.

[a] Data taken from the plots, not available in the referenced text.

[b] Determined in the initial (31 day) period.

Declaration of competing interest

The authors declare that they have no known competing financial interests or personal relationships that could have appeared to influence the work reported in this paper.

Data availability

Data will be made available on request.

Acknowledgements

This work was financed by National Science Centre (Poland) OPUS grant (2019/33/B/NZ9/02774), Polish National Agency for Academic Exchange – Polish Returns grant (PPN/PPO/2018/1/00038), the collaboration was funded by COST Action PHOENIX: Protection, resilience, rehabilitation of damaged environment (CA19123).

Appendix A. Supplementary data

Supplementary data to this article can be found online at https://doi.org/10.1016/j.jpowsour.2024.235257.

References

[1] P. Choudhury, et al., Performance improvement of microbial fuel cells for waste water treatment along with value addition: a review on past achievements and recent perspectives, Renew. Sustain. Energy Rev. 79 (2017) 372–389, https://doi.org/10.1016/j.rser.2017.05.098. April 2016.

[2] D.A. Jadhav, et al., Scalability of microbial electrochemical technologies: applications and challenges, Bioresour. Technol. 345 (October 2021) (2022) 126498, https://doi.org/10.1016/j.biortech.2021.126498.

[3] S.M. Daud, B.H. Kim, M. Ghasemi, W.R.W. Daud, Separators used in microbial electrochemical technologies: current status and future prospects, Bioresour. Technol. 195 (2015) 170–179, https://doi.org/10.1016/j.biortech.2015.06.105.

[4] D.A. Jadhav, et al., Current outlook towards feasibility and sustainability of ceramic membranes for practical scalable applications of microbial fuel cells, Renew. Sustain. Energy Rev. 167 (July) (2022) 112769, https://doi.org/10.1016/j.rser.2022.112769.

[5] G. Pasternak, A. de Rosset, N. Tyszkiewicz, B. Widera, J. Greenman, I. Ieropoulos, Prevention and removal of membrane and separator biofouling in bioelectrochemical systems: a comprehensive review, iScience 25 (7) (2022) 104510, https://doi.org/10.1016/j.isci.2022.104510.

[6] S. Kondaveeti, R. Kakarla, H.S. Kim, B. goon Kim, B. Min, The performance and long-term stability of low-cost separators in single-chamber bottle-type microbial fuel cells, Environ. Technol. 39 (3) (2018) 288–297, https://doi.org/10.1080/09593330.2017.1299223.

[7] H. Nagar, N. Badhrachalam, V.V.B. Rao, S. Sridhar, A novel microbial fuel cell incorporated with polyvinylchloride/4A zeolite composite membrane for kitchen wastewater reclamation and power generation, Mater. Chem. Phys. 224 (2019) 175–185, https://doi.org/10.1016/j.matchemphys.2018.12.023. May 2018.

[8] D. Frattini, G. Accardo, Y. Kwon, Perovskite ceramic membrane separator with improved biofouling resistance for yeast-based microbial fuel cells, J. Membr. Sci. 599 (January) (2020) 117843, https://doi.org/10.1016/j.memsci.2020.117843.

[9] S. Angioni, L. Millia, G. Bruni, C. Tealdi, P. Mustarelli, E. Quartarone, Improving the performances of Nafion$^{\text{TM}}$-based membranes for microbial fuel cells with silica-based, organically-functionalized mesostructured fillers, J. Power Sources 334 (2016) 120–127, https://doi.org/10.1016/j.jpowsour.2016.10.014.

[10] Y. Lu, J. Jia, H. Miao, W. Ruan, X. Wang, Performance improvement and biofouling mitigation in osmotic microbial fuel cells via in situ formation of silver nanoparticles on forward osmosis membrane, Membranes 10 (6) (2020) 1–15, https://doi.org/10.3390/membranes10060122.

[11] M. Elangovan, S. Dharmalingam, A facile modification of a polysulphone based anti biofouling anion exchange membrane for microbial fuel cell application, RSC Adv. 6 (25) (2016) 20571–20581, https://doi.org/10.1039/c5ra21576e.

[12] M. Elangovan, S. Dharmalingam, Anti-biofouling anion exchange membrane using surface modified quaternized poly(ether imide) for microbial fuel cells, J. Appl. Polym. Sci. 134 (5) (2017) 1–9, https://doi.org/10.1002/app.44432.

[13] V. Yousefi, D. Mohebbi-Kalhori, A. Samimi, Ceramic-based microbial fuel cells (MFCs): a review, Int. J. Hydrogen Energy 42 (3) (2017) 1672–1690, https://doi.org/10.1016/j.ijhydene.2016.06.054.

[14] I. Das, M.M. Ghangrekar, R. Satyakam, P. Srivastava, S. Khan, H.N. Pandey, On-site sanitary wastewater treatment system using 720-L stacked microbial fuel cell: case study, J. Hazardous, Toxic, Radioact. Waste 24 (3) (2020) 1–7, https://doi.org/10.1061/(asce)hz.2153-5515.0000518.

[15] I. Das, S. Das, R. Dixit, M.M. Ghangrekar, Goethite supplemented natural clay ceramic as an alternative proton exchange membrane and its application in microbial fuel cell, Ionics 26 (6) (2020) 3061–3072, https://doi.org/10.1007/s11581-020-03472-1.

[16] V. Ahilan, et al., Microbial fuel cell performance of graphitic carbon functionalized porous polysiloxane based ceramic membranes, Bioelectrochemistry 129 (2019) 259–269, https://doi.org/10.1016/j.bioelechem.2019.06.002.

[17] G. Pasternak, N. Ormeno-Cano, P. Rutkowski, Recycled waste polypropylene composite ceramic membranes for extended lifetime of microbial fuel cells, Chem. Eng. J. (Jun. 2021) 130707, https://doi.org/10.1016/J.CEJ.2021.130707.

[18] N.K. Abd-Elrahman, N. Al-Harbi, N.M. Basfer, Y. Al-Hadeethi, A. Umar, S. Akbar, Applications of nanomaterials in microbial fuel cells: a review, Molecules 27 (21) (2022) 1–28, https://doi.org/10.3390/molecules27217483.

[19] S. Shahgaldi, et al., Performance enhancement of microbial fuel cell by PVDF/Nafion nanofibre composite proton exchange membrane, Fuel Process. Technol. 124 (2014) 290–295, https://doi.org/10.1016/j.fuproc.2014.03.015.

[20] H.-Y. Jung, S.-H. Roh, Polyvinylidene fluoride nanofiber composite membrane coated with perfluorinated sulfuric acid for microbial fuel cell application, J. Nanosci. Nanotechnol. 20 (9) (2020) 5711–5715, https://doi.org/10.1166/jnn.2020.17622.

[21] J. Xue, J. Xie, W. Liu, Y. Xia, Electrospun nanofibers: new concepts, materials, and applications, Acc. Chem. Res. 50 (8) (2017) 1976–1987, https://doi.org/10.1021/acs.accounts.7b00218.

[22] S. Agrawal, et al., Synthesis and water treatment applications of nanofibers by electrospinning, Processes 9 (10) (2021), https://doi.org/10.3390/pr9101779.

[23] I.M. Banat, R.S. Makkar, S.S. Cameotra, Potential commercial applications of microbial surfactants, Appl. Microbiol. Biotechnol. 53 (5) (2000) 495–508, https://doi.org/10.1007/s002530051648.

[24] G. Pasternak, A. de Rosset, P. Rutkowski, Horizontal microbial fuel cell system producing biosurfactants in response to current generation from waste cooking oil as a fuel, Energy Convers. Manag. 281 (March) (2023) 116807, https://doi.org/10.1016/j.enconman.2023.116807.

[25] Y. Zhang, et al., Accelerating anodic biofilms formation and electron transfer in microbial fuel cells: role of anionic biosurfactants and mechanism, Bioelectrochemistry 117 (2017) 48–56, https://doi.org/10.1016/j.bioelechem.2017.06.002.

[26] G. Pasternak, T.D. Askitosari, M.A. Rosenbaum, Biosurfactants and synthetic surfactants in bioelectrochemical systems : a mini-review influence on electron transfer 11 (March) (2020) 1–9, https://doi.org/10.3389/fmicb.2020.00358.

[27] F. Yalcinkaya, J. Hruza, Effect of laminating pressure on polymeric multilayer nanofibrous membranes for liquid filtration, Nanomaterials 8 (5) (2018), https://doi.org/10.3390/nano8050272.

[28] R. Torres-Mendieta, et al., PVDF nanofibrous membranes modified via laser-synthesized Ag nanoparticles for a cleaner oily water separation, Appl. Surf. Sci. 526 (February) (2020) 146575, https://doi.org/10.1016/j.apsusc.2020.146575.

[29] A. De Rosset, P. Rutkowski, G. Pasternak, The effect of surface and porous structure on long-term performance of carbon powder cathodes without binder , during a 300-day trial in microbial fuel cells, Sustain. Energy Technol. Assessments 58 (April) (2023) 103340, https://doi.org/10.1016/j.seta.2023.103340.

[30] G. Pasternak, J. Greenman, I. Ieropoulos, Dynamic evolution of anodic biofilm when maturing under different external resistive loads in microbial fuel cells. Electrochemical perspective, J. Power Sources 400 (August) (2018) 392–401, https://doi.org/10.1016/j.jpowsour.2018.08.031.

[31] L. Szydlowski, J. Ehlich, I. Goryanin, G. Pasternak, High-throughput 96-well bioelectrochemical platform for screening of electroactive microbial consortia, Chem. Eng. J. 427 (April 2021) (2022) 131692, https://doi.org/10.1016/j.cej.2021.131692.

[32] https://gaussian.com/citation/.".

[33] T. Lu, F. Chen, Multiwfn: a multifunctional wavefunction analyzer, J. Comput. Chem. 33 (5) (2012) 580–592, https://doi.org/10.1002/jcc.22885.

[34] M.D. Hanwell, D.E. Curtis, D.C. Lonie, T. Vandermeersch, E. Zurek, G.R. Hutchison, Avogadro: an advanced semantic chemical editor, visualization, and analysis platform, J. Cheminf. 4 (1) (2012) 17, https://doi.org/10.1186/1758-2946-4-17.

[35] Chemcraft - graphical software for visualization of quantum chemistry computations. Version 1.8, Build 682. https://www.chemcraftprog.com.

[36] A. Gebrekrstos, G. Prasanna Kar, G. Madras, A. Misra, S. Bose, Does the nature of chemically grafted polymer onto PVDF decide the extent of electroactive β-polymorph? Polymer (Guildf). 181 (August) (2019) 121764 https://doi.org/10.1016/j.polymer.2019.121764.

[37] G.J. Ross, J.F. Watts, M.P. Hill, P. Morrissey, Surface modification of poly (vinylidene fluoride) by alkaline treatment: 1. The degradation mechanism, Polymer (Guildf). 41 (5) (2000) 1685–1696, https://doi.org/10.1016/S0032-3861(99)00343-2.

[38] J.W. Steed, J.L. Atwood, Supramolecular Chemistry, John Wiley & Sons, Ltd, 2009.

[39] J.H. Hwang, K.Y. Kim, E.P. Resurreccion, W.H. Lee, Surfactant addition to enhance bioavailability of bilge water in single chamber microbial fuel cells (MFCs), J. Hazard Mater. 368 (2019) 732–738, https://doi.org/10.1016/j.jhazmat.2019.02.007. November 2018.

[40] G. Pasternak, J. Greenman, I. Ieropoulos, Regeneration of the power performance of cathodes affected by biofouling, Appl. Energy 173 (2016) 431–437, https://doi.org/10.1016/j.apenergy.2016.04.009.

[41] M. Santini, et al., Three-dimensional X-ray microcomputed tomography of carbonates and biofilm on operated cathode in single chamber microbial fuel cell, Biointerphases 10 (3) (2015) 031009, https://doi.org/10.1116/1.4930239.

[42] X.A. Walter, S. Forbes, J. Greenman, I.A. Ieropoulos, From single MFC to cascade configuration: the relationship between size, hydraulic retention time and power density, Sustain. Energy Technol. Assessments 14 (2016) 74–79, https://doi.org/10.1016/j.seta.2016.01.006.

[43] J. Winfield, L.D. Chambers, J. Rossiter, I. Ieropoulos, Comparing the short and long term stability of biodegradable, ceramic and cation exchange membranes in microbial fuel cells, Bioresour. Technol. 148 (2013) 480–486, https://doi.org/10.1016/j.biortech.2013.08.163.

[44] G. Pasternak, J. Greenman, I. Ieropoulos, Comprehensive study on ceramic membranes for low-cost microbial fuel cells, ChemSusChem 9 (1) (2016) 88–96, https://doi.org/10.1002/cssc.201501320.

[45] A. Sabina-Delgado, S.K. Kamaraj, V. Hernández-Montoya, F.J. Cervantes, Novel carbon-ceramic composite membranes with high cation exchange properties for use in microbial fuel cell and electricity generation, Int. J. Hydrogen Energy 8 (2023), https://doi.org/10.1016/j.ijhydene.2023.03.254.

[46] N.S. Malvankar, M.T. Tuominen, D.R. Lovley, Biofilm conductivity is a decisive variable for high-current-density Geobacter sulfurreducens microbial fuel cells, Energy Environ. Sci. 5 (2) (2012) 5790–5797, https://doi.org/10.1039/c2ee03388g.

[47] E.M. Klein, M.T. Knoll, J. Gescher, Microbe–Anode Interactions: comparing the impact of genetic and material engineering approaches to improve the performance of microbial electrochemical systems (MES), Microb. Biotechnol. 16 (6) (2023) 1179–1202, https://doi.org/10.1111/1751-7915.14236.

[48] J. Greenman, et al., Microbial fuel cells and their electrified biofilms, Biofilms 3 (July) (2021) 100057, https://doi.org/10.1016/j.bioflm.2021.100057.

[49] B.E. Logan, et al., Microbial fuel cells: methodology and technology, Environ. Sci. Technol. 40 (17) (2006) 5181–5192, https://doi.org/10.1021/es0605016.

[50] L. Koók, et al., Biofouling of membranes in microbial electrochemical technologies: causes, characterization methods and mitigation strategies, Bioresour. Technol. 279 (2019) 327–338, https://doi.org/10.1016/j.biortech.2019.02.001. December 2018.

[51] A.A. Kulikovsky, A. Kucernak, A.A. Kornyshev, Feeding PEM fuel cells, Electrochim. Acta 50 (6) (Jan. 2005) 1323–1333, https://doi.org/10.1016/J.ELECTACTA.2004.08.023.

[52] N. Sekar, R.P. Ramasamy, Electrochemical impedance spectroscopy for microbial fuel cell characterization, J. Microb. Biochem. Technol. 5 (SPECIALISSUE.2) (2013), https://doi.org/10.4172/1948-5948.s6-004.

[53] G. Lepage, F.O. Albernaz, G. Perrier, G. Merlin, Characterization of a microbial fuel cell with reticulated carbon foam electrodes, Bioresour. Technol. 124 (2012) 199–207, https://doi.org/10.1016/j.biortech.2012.07.067.

[54] A.P. Borole, D. Aaron, C.Y. Hamilton, C. Tsouris, Understanding long-term changes in microbial fuel cell performance using electrochemical impedance spectroscopy, Environ. Sci. Technol. 44 (7) (2010) 2740–2745, https://doi.org/10.1021/es9032937.

[55] M.J. Choi, et al., Effects of biofouling on ion transport through cation exchange membranes and microbial fuel cell performance, Bioresour. Technol. 102 (1) (2011) 298–303, https://doi.org/10.1016/j.biortech.2010.06.129.

[56] P. Chatterjee, M.M. Ghangrekar, Design of clayware separator-electrode assembly for treatment of wastewater in microbial fuel cells, Appl. Biochem. Biotechnol. 173 (2) (2014) 378–390, https://doi.org/10.1007/s12010-014-0846-x.

[57] D.A. Jadhav, A.N. Ghadge, M.M. Ghangrekar, Enhancing the power generation in microbial fuel cells with effective utilization of goethite recovered from mining mud as anodic catalyst, Bioresour. Technol. 191 (2015) 110–116, https://doi.org/10.1016/j.biortech.2015.04.109.

[58] A.N. Ghadge, D.A. Jadhav, H. Pradhan, M.M. Ghangrekar, Enhancing waste activated sludge digestion and power production using hypochlorite as catholyte in clayware microbial fuel cell, Bioresour. Technol. 182 (2015) 225–231, https://doi.org/10.1016/j.biortech.2015.02.004.

[59] A. Raychaudhuri, M. Behera, Ceramic membrane modified with rice husk ash for application in microbial fuel cells, Electrochim. Acta 363 (2020) 137261, https://doi.org/10.1016/j.electacta.2020.137261.

SUPPORTING INFORMATION

Natural rhamnolipids to increase the performance and long-term durability of PVDF-ceramic composite membranes in microbial fuel cells

Aleksander de Rosset[1], Fatma Yalcinkaya[2], Joanna Wolska[1], Stanisław Wacławek[2], Grzegorz Pasternak[1,]*

[1]Department of Process Engineering and Technology of Polymer and Carbon Materials, Faculty of Chemistry, Wroclaw University of Science and Technology, Wroclaw 50-370, Poland.

[2]Centre for Nanomaterials, Advanced Technology and Innovation, Technical University of Liberec, Studentska 1402/2, 46117, Czech Republic.

*Corresponding author: grzegorz.pasternak@pwr.edu.pl

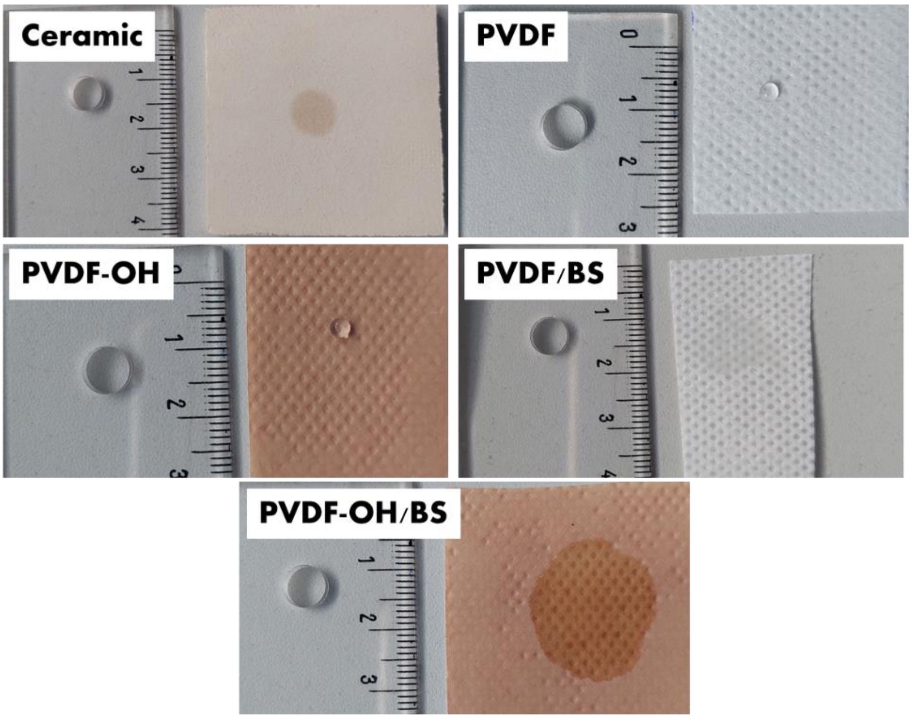

Fig. S1. Water spreading area test for modified and unmodified separators.

6. Podsumowanie i wnioski

W rozprawie wykazano, że możliwa jest jednoczesna produkcja biosurfaktantów i energii elektrycznej z odpadowych olejów roślinnych, a wydajność ich wytwarzania jest uzależniona od materiałów funkcjonalnych i konstrukcji mikrobiologicznego ogniwa paliwowego oraz składu pożywki hodowlanej. Ponadto wykazano, że biosurfaktanty mogą być wykorzystywane do modyfikacji materiałów funkcjonalnych, w celu zwiększenia wydajności energetycznej mikrobiologicznego ogniwa paliwowego. Wykorzystanie mikrobiologicznych ogniw paliwowych zasilanych olejami odpadowymi z przemysłu spożywczego do syntezy biosurfaktantów i jednoczesna produkcja energii elektrycznej może doprowadzić do zmniejszenia problemu związanego z odpadami i zwiększy ekonomiczność i konkurencyjność procesu produkcji biosurfaktantów. Ponadto technologia ta spełnia wymagania stawiane w założeniach zrównoważonego rozwoju oraz gospodarki obiegu zamkniętego.

W pierwszym rozdziale w wyniku niemal rocznego okresu funkcjonowania ogniw oceniono wydajność dwóch różnych typów węgli aktywnych jako materiałów katody powietrznej w MFC i wpływ modyfikacji nanocząstkami krzemionki na właściwości katalityczne w długim okresie eksploatacji. Wyniki wykazały najwyższą wydajność produkcji energii elektrycznej w początkowym okresie eksploatacji dla MFC wyposażonego w katodę o najbardziej mikroporowatej strukturze i największej powierzchni właściwej (CWZ-35). Jednak okres stabilnej generacji mocy dla CWZ-35 był najkrótszy spośród wszystkich testowanych materiałów. W przeciwieństwie do tych wyników, węgiel aktywny o niższej powierzchni właściwej (CWZ-22) oraz CWZ-22 modyfikowany nanocząstkami krzemionki (CWZ-22/Si) wykazały dobrą stabilność i wysoką moc wyjściową w całym eksperymencie. Charakterystyka porowatości materiałów wykazała, że rozkład wielkości porów CWZ-22, z przewagą porów poniżej 1 nm, był jednym z powodów mniejszej podatności na dezaktywację miejsc aktywnych w długim okresie eksploatacji. Ponadto analiza krzywych polaryzacji nie wykazała pozytywnego wpływu domieszkowania nanocząstkami krzemionki na wydajność energetyczną i jej długoterminowe właściwości katalityczne. W pracy wykazano, że niezmodyfikowany, tani i dostępny w handlu węgiel aktywny może być wysokowydajnym materiałem katody powietrznej, jednak rozkład wielkości porów i wynikająca z tego podatność na zanieczyszczenie chemiczne są kluczowym czynnikiem decydującym o utrzymaniu wysokiej wydajności długoterminowej konfiguracji MFC. Badania te stanowiły podstawę do doboru materiału wykorzystywanego w dalszym etapie.

W drugim rozdziale porównano skuteczność klasycznego pionowego układu MFC z układem poziomym w produkcji energii elektrycznej i biosyntezie surfaktantów z odpadowego oleju roślinnego. Obserwowana produkcja energii elektrycznej, wydajność kulombowska i rezystancja wewnętrzna wskazywały na poprawę wydajności MFC w układzie poziomym w porównaniu z układem pionowym z mieszaniem. Ponadto spadek napięcia powierzchniowego, wskazujący na obecność biosurfaktantów, zaobserwowano tylko w poziomym MFC. Wykazano, że konfiguracja pozioma poprawiła dystrybucję substratu olejowego wewnątrz komory anodowej, zwiększając biodostępność oleju dla mikroorganizmów, co bezpośrednio wpłynęło na rozwój biofilmu i degradację substratu. Co więcej, wykazano, że synteza biosurfaktantów w horyzontalnych MFC jest bezpośrednio skorelowana z wytwarzaniem energii, co może pozwolić na proste i stosunkowo tanie monitorowanie syntezy bioelektrochemicznej w stabilnym układzie biosyntezy elektrochemicznej.

W trzecim rozdziale oceniono wpływ stężenia źródła azotu w podłożu hodowlanym na wydajność produkcji biosurfaktantów i energii elektrycznej w poziomych MFC. Zaobserwowana produkcja energii elektrycznej oraz spadki napięcia powierzchniowego wskazywały na poprawę wydajności MFC wraz ze wzrostem stężenia NH_4Cl w podłożu, a maksymalną gęstość mocy oraz największy spadek napięcia powierzchniowego odnotowano dla 0.5 g L^{-1} (C/N = 2.32). Ponadto, wykazano silną ujemną korelację zmian gęstości mocy i spadku napięcia powierzchniowego jako funkcji stężenia NH_4Cl, co dowodzi, że synteza biosurfaktantów i wydajność degradacji oleju odpadowego oraz wynikająca z tego wydajność produkcji prądu elektrycznego są bezpośrednio zależne od stężenia źródła azotu. Analiza bioróżnorodności 16S wskazała na obecność dominującego szczepu *Pseudomonas aeruginosa* produkującego biosurfaktanty, wraz z innymi elektroaktywnymi gatunkami zdolnymi do biodegradacji i biosyntezy. Ich aktywność skutkowała biosyntezą jedenastu typów mono- i di-ramnolipidów. Wyniki pokazują, że stężenie źródła azotu w podłożu hodowlanym jest jednym z kluczowych czynników utrzymania wysokiej wydajności degradacji odpadowych olejów roślinnych, produkcji energii i jednoczesnej syntezy biosurfaktantów.

W ostatnim rozdziale zaprezentowano nową kompozytową membranę ceramiczną zawierającą nanowłókna polifluorku winylidenu (PVDF) oraz po raz pierwszy zastosowano modyfikację membrany za pomocą biosurfaktantów mającą na celu zwiększenie wydajności energetycznej MFC. Membranę PVDF oraz PVDF modyfikowaną ramnolipidami wykorzystano jako wewnętrzną warstwę kompozytowej membrany ceramicznej stosowanej w MFC w celu zwiększenia jej trwałości. Wyniki wykazały, że zastosowanie samej warstwy PVDF nie dało zadowalających rezultatów. Ceramiczna membrana kompozytowa z membraną PVDF wykazała najwyższą podatność na zanieczyszczenie biologiczne i chemiczne. Z drugiej strony włączenie biosurfaktantów do nanowłókien PVDF znacznie poprawiło hydrofilowość membran. W efekcie MFC wyposażone w ceramiczną membranę kompozytową z membraną PVDF modyfikowaną ramnolipidami osiągnęło najwyższą wydajność produkcji energii elektrycznej w długim okresie eksploatacji. W pracy wykazano, że membrana PVDF modyfikowana ramnolipidami utworzyła na powierzchni membrany ceramicznej półprzepuszczalną warstwę o zwiększonej odporności na zanieczyszczenia chemiczne i biologiczne i w efekcie poprawiła długoterminową wydajność energetyczną MFC i trwałość membrany ceramicznej. Wyniki te pokazują, że produkowane wewnątrz ogniwa ramnolipidy mogą stanowić nie tylko produkt, ale także czynnik zwiększający żywotność membrany MFC oraz podkreślają potencjał wykorzystania membran kompozytowych jako obiecującego podejścia do poprawy wydajności elektrycznej MFC.

7. Dorobek naukowy

PUBLIKACJE:

1. K. Kordek-Khalil, **A. de Rosset**, and P. Rutkowski, "Influence of pulsed laser ablation temperature on structure, morphology and electrocatalytic properties of cobalt-based films deposited on carbon cloth," *Appl. Surf. Sci.*, vol. 509, no. October 2019, p. 145263, 2020, doi: 10.1016/j.apsusc.2020.145263. (**IF = 6.3, 140 pkt. MNiSW**)

2. G. Pasternak, **A. de Rosset**, N. Tyszkiewicz, B. Widera, J. Greenman, and I. Ieropoulos, "Prevention and removal of membrane and separator biofouling in bioelectrochemical systems: a comprehensive review," *iScience*, vol. 25, no. 7, p. 104510, 2022, doi: 10.1016/j.isci.2022.104510. (**IF = 5.8, 20 pkt. MNiSW**)

3. G. Pasternak, **A. de Rosset**, and P. Rutkowski, "Horizontal microbial fuel cell system producing biosurfactants in response to current generation from waste cooking oil as a fuel," Energy Convers. Manag., vol. 281, no. March, p. 116807, 2023, doi: 10.1016/j.enconman.2023.116807. (**IF = 10.4, 200 pkt. MNiSW**)

4. **A. de Rosset**, P. Rutkowski, and G. Pasternak, "The effect of surface and porous structure on long-term performance of carbon powder cathodes without binder, during a 300-day trial in microbial fuel cells," Sustain. Energy Technol. Assessments, vol. 58, no. April, p. 103340, 2023, doi: 10.1016/j.seta.2023.103340. (**IF = 8.0, 140 pkt. MNiSW**)

5. **A. de Rosset**, N. Tyszkiewicz, J. Wiśniewski, N. Pudełko-Malik, P. Rutkowski, P. Młynarz, G. Pasternak, "Bioelectrochemical synthesis of rhamnolipids and energy production and its correlation with nitrogen in air-cathode microbial fuel cells," J. Environ. Manage., vol. 365, no. August, p. 121514, 2024, doi: 10.1016/j.jenvman.2024.121514. (**IF = 8.0, 200 pkt. MNiSW**)

6. **A. de Rosset**, F. Yalcinkaya, J. Wolska, S. Wacławek, and G. Pasternak, "Enhancing performance and durability of PVDF-ceramic composite membranes in microbial fuel cells using natural rhamnolipids," J. Power Sources, vol. 621, no. January, p. 235257, 2024, doi: 10.1016/j.jpowsour.2024.235257. (**IF = 8.1, 140 pkt. MNiSW**)

KONFERENCJE:

1. Chemistry & Biotechnology International Conference, online, 24-25.06.2021, Characterization and comparison of the performance of three different cathode materials for microbial fuel cells, authors: **Aleksander de Rosset**, Grzegorz Pasternak.

2. The 5th European Meeting of the International Society for Microbial Electrochemistry and Technology (ISMET), online, 13-15.09.2021, Synthesis of biosurfactants from waste vegetable oil in air-cathode microbial fuel cell, authors: **Aleksander de Rosset**, Grzegorz Pasternak.

3. Electromicrobiology 2021, Aarhus, Denmark, 3-5.11.2021, Characterisation of biosurfactant synthesis and electricity generation from waste vegetable oil in air-cathode microbial fuel cells, authors: **Aleksander de Rosset**, Grzegorz Pasternak.

4. PHOENIX COST ACTION MEETING, Rome, 19-21.01.2022, Modified Polyvinylidene Fluoride Nanofiber Membranes in Microbial Fuel Cell, authors: **Aleksander de Rosset**, Rafael Torres-Mendieta, Fatma Yalcinkaya, Grzegorz Pasternak.

5. MEEP 2022 Special Symposium on Microbial, Enzymatic & Bio-Photovoltaic Electrochemical Reactors, Fuel Cells and Electrolyser Systems, Switzerland, 6-7.07.2022, Investigation of the optimal design to produce biosurfactants and electricity from waste vegetable oil in air-cathode microbial fuel cells, authors: **Aleksander de Rosset**, Grzegorz Pasternak.

6. PANIC Summer School 2022, Poland, 30.05-3.06.2022, Long-term characterization of three different carbon cathodes in microbial fuel cell, authors: **Aleksander de Rosset**, Piotr Rutkowski, Grzegorz Pasternak.

7. ISMET8 Global Conference 2022, Greece, 19-23.09.2022, Inducing the biosurfactant synthesis and electricity generation from waste vegetable oil in air-cathode microbial fuel cell, authors: **Aleksander de Rosset**, Grzegorz Pasternak.

8. Electromicrobiology 2023, Aarhus, Denmark, 24-26.05.2023, Nitrogen controlled metabolism of waste cooking oil in air-cathode microbial fuel cells, authors: **Aleksander de Rosset**, Natalia Tyszkiewicz, Grzegorz Pasternak.

9. PHOENIX FINAL CONFERENCE, Naples, 4-5.07.2024, Rhamnolipids modified PVDF nanofibers membrane to extend the lifetime of microbial fuel cells, authors: **Aleksander de Rosset**, Fatma Yalcinkaya, Joanna Wolska, Stanisław Wacławek, Grzegorz Pasternak.

STAŻ NAUKOWY:

1. 1.09-30.09.2021 – STSM COST Action (PHOENIX), Technical University of Liberec.

UDZIAŁ W REALIZACJI GRANTÓW:

1. Wykonawca projektu „Polskie Powroty 2018”, Narodowa Agencja Wymiany Akademickiej, PPN/PPO/2018/1/00038.

   Kierownik projektu: dr hab. inż. Grzegorz Pasternak, prof.

2. Wykonawca projektu NCN OPUS „Mechanizmy bioelektrochemicznej transformacji materiałów odpadowych z przemysłu naftowego do biosurfaktantów”, 2019/33/B/NZ9/02774.

   Kierownik projektu: dr hab. inż. Grzegorz Pasternak, prof.

3. Beneficjent grantu na krótkoterminowy staż naukowy (STSM): Modyfikacja powierzchni membran z elektroprzędzonych nanowłókien dla mikrobiologicznych ogniw paliwowych, realizowanego w ramach programu badawczego COST Action PHOENIX: Protection, resilience, rehabilitation of damaged environment (CA19123).

STYPENDIUM NAUKOWE:

1. Stypendium o zwiększonej wysokości 2023/2024